



INVESTIGATING SORPTION BEHAVIOUR OF PERFLUOROALKYL SUBSTANCES TO BIOCHAR

A thesis submitted in fulfilment of the requirements for the degree of Doctor of Philosophy

Matthew Peter James Askeland

Bachelor of Environmental Science (Hons) RMIT University

School of Engineering

College of Science, Engineering and Health

RMIT University

August 2019

Declaration

I certify that except where due acknowledgement has been made, the work is that of the author alone; the work has not been submitted previously, in whole or in part, to qualify for any other academic award; the content of the thesis is the result of work which has been carried out since the official commencement date of the approved research program; any editorial work, paid or unpaid, carried out by a third party is acknowledged; and, ethics procedures and guidelines have been followed.

I acknowledge the support I have received for my research through the provision of an Australian Government Research Training Program Scholarship.

Matthew Askeland - 21 August 2019

Acknowledgements

I would like to thank my primary supervisor Jorge Paz-Ferreiro for the invaluable support and guidance he has consistently provided throughout my PhD. I extend my thanks to my secondary supervisor, Bradly Clarke, who assisted greatly not only during my PhD candidature, but in fact inspired my interest in PFAS.

I would like to extend recognition to all the scientists whom I have cited, without whose work I could not have had the basis to undertake my own.

I would like to thank my colleagues at ADE Consulting Group for their support. Notably Bruce Tehrani, Shahin Motamedi, and Ross Nefodov; for allowing me to schedule time to complete my thesis while being incredibly supportive of my self-improvement through further study.

I would like to thank my friends and my children for their understanding and accepting my word that there will be more time together in the future. To my parents, who have supported me since day one, I don't believe it possible to repay you for all you have done. I treasure you for your strength, and value the sacrifices you made to ultimately give me the privilege and resources to undertake my PhD.

Lastly, I would like to thank my beautiful wife Leanne, without your undying support I simply would never have been able to complete this task. You believed in me when I was too tired and stressed to do so myself. This is as much your accomplishment as it is mine.

Table of Contents

Abstract	1
Chapter 1 Introduction	2
1.1 Biochar	4
1.1.1 Background	4
1.1.2 Chemical Structure and Production.....	5
Biochar Structure	5
Biochar Production	5
Pyrolysis Conditions	6
Contaminants in Biochar.....	6
Biochar’s Chemistry	9
1.1.3 Applications and Guidelines.....	10
1.2 Per- and Poly - Fluorinated Substances	14
1.2.1 Background	14
1.2.2 Chemical Structure, Properties and Fate.....	16
1.2.3 Toxicity	23
1.2.4 Monitoring Programmes, Restrictions and Control.....	27
Chapter 2 PFAS-Biochar Sorption	30
2.1 Biochar as a Sorbent.....	30
2.2 PFAS Sorption to Biochar	32
2.2.1 PFAS Compound Specific Sorption Behaviour	32
2.2.2 Biochar Particle Size Influence on PFAS Sorption Behaviour.....	33
2.2.3 Electrostatic Interactions	33
2.2.4 Hydrophobic Interactions	36
2.4.5 Formation of Micelles and Layers.....	38
2.2.6 Interfering Environmental Factors.....	39
Organic Matter.....	39
Ions.....	39
pH.....	39
Temperature	40
2.3 Generalized Models and Kinetics for PFASs and Carbonaceous Sorbents	40
2.3.1 Kinetic Models.....	40
First Order Model.....	41
Pseudo-second Order Model	41

Intraparticle Diffusion Model.....	41
2.3.2 Sorption Models.....	42
Freundlich	42
Langmuir	43
Sigmoidal Langmuir Modification	43
SIPS.....	43
BET	43
Toth	44
Radke-Prusnitz	44
Redlich-Peterson.....	44
Desorption	44
2.4 Conclusion.....	45
Chapter 3 Comparative Characterization of Biochars Produced at Three Selected Pyrolysis Temperatures from Common Woody and Herbaceous Waste Streams.....	46
3.1 Abstract.....	47
3.2 Introduction	48
3.3 Materials and Methods	51
3.3.1 Raw material selection.....	51
3.3.2 Pyrolysis of raw materials	51
3.3.3 Characterization of Biochars.....	51
Chemical and Physical Characterisation	51
Contaminant Analysis	52
3.3.4 Statistics.....	53
3.4 Results and Discussion	53
3.4.1 Chemical and physical characterisation.....	53
3.4.2 Contaminant analysis.....	59
3.5 Conclusion.....	62
Chapter 4 Fast, Cost-effective, “PFAS clean” Serial Sorption Technique Coupled with Adapted High Volume Direct Aqueous Injection LCMS Method	63
4.1 Introduction.....	64
4.2 Method	64
4.2.1 Chemicals and Reagents	64
4.2.2 “PFAS Clean” Preparation of Solvents, Stocks and Standards.....	65
4.3 Sample Preparation and Sorption Experiments	66
4.3.1 Equilibrium Experimental Protocol.....	66
4.3.2 Sorption Experimental Protocol.....	66

4.3.3 Sorption Experimental Protocol.....	67
4.3.2 Sample Preparation	67
4.4 LCMS Direct Aqueous Injection Method	68
4.4.1 Calibration and Mobile Phases	68
4.4.2 Sample analysis.....	68
4.4.3 Method QA/QC	70
4.5 Method Performance	72
4.5.1 LCMS and Sample Preparation.....	72
4.5.2 Establishment of Isotherms and Sorbed Fractions	72
4.5.3 Limitations of Method	73
4.5.4 Benefits of Improved Method.....	73
Chapter 5 Examining the Sorption Behaviour of Priority PFAS onto Engineered Biochars Prepared from Waste Feedstock at Three Pyrolysis Temperatures	74
5.1 Abstract.....	75
5.2 Introduction	76
5.3 Methods.....	78
5.3.1 Biochar Preparation	78
5.3.2 Chemical Standards.....	78
Equilibrium Experiments.....	78
Sorption Experiments.....	79
Desorption Experiments	79
5.3.4 PFAS Analysis	79
5.3.5 Instrumental Analysis.....	79
5.3.6 Quality control quality assurance (QA/QC).....	80
5.3.7 Data Analysis	80
5.4 Results and Discussion	81
5.4.1 Preliminary Experiments.....	81
5.4.2 Equilibrium Experiments.....	81
5.4.3 Sorption Experiments	87
5.4.4 Desorption Experiments	96
5.5 Conclusion	98
Chapter 6 Biochar Sorption of PFOS, PFOA, PFHxS and PFHxA in Two Soils with contrasting Texture	99
6.1 Abstract.....	99
6.2 Introduction	100

6.3 Material and Methods.....	102
6.3.1 Chemicals and Reagents	102
6.3.2 Biochar	102
6.3.3 Soil Characterisation	103
6.3.4 Experimental Design	103
6.3.5 Experimental Methodology	103
6.3.6 LCMS analysis.....	104
6.3.7 Statistical Analysis.....	104
6.4. Results and Discussion	105
6.4.1 Equilibrium Experiments.....	106
6.4.2 Sorption Experiments	109
6.4.3 Desorption Experiments	112
6.5 Conclusion.....	115
Chapter 7 Conclusions	116
References	118
Appendices: Appendix A – Published Materials	142
Appendices: Appendix B – Supplementary Materials	143

List of Figures

Figure 1.1 Behaviours attributed by amphiphilia.....	20
Figure 1.2 Conceptual flowchart depicting the cycle of PFAS from production to receptors as well as their recirculation within the environment.....	22
Figure 2.1 Generalized Biochar model.....	31
Figure 2.2 Generalized PFAS model.....	33
Figure 2.3 Diagrams outlining PFAS electrostatic interactions.....	34
Figure 2.4 Examination of net negative outer charge on PFAS molecules.....	35
Figure 2.5 Electronic Double Layer Suppression.....	35
Figure 2.6 PFAS spontaneous entropy driven sorption.....	37
Figure 2.7 Diagrams representing hydrophobic interaction driven PFAS sorption Behaviour.....	37
Figure 2.8 Illustration demonstrating the formation of micellular structures.....	38
Figure 3.1 SEM Image of biochar surfaces.....	54

Figure 3.2 Composite FTIR spectra of biochars produced from straw at 350 °C, 500 °C and 750 °C.....	57
Figure 3.3 Composite FTIR spectra of biochars produced from pine at 350 °C, 500 °C and 750 °C.....	57
Figure 3.4 pH, EC and CEC of biochars, compared between feedstocks (Pine and Straw) and pyrolysis temperatures (350, 500 and 750°C).....	59
Figure 5.1 Percentage PFAS removal for Biochar versus time for PFAS biochar pairs.....	82
Figure 5.2 Intraparticle diffusion models for target compounds separated by biochar type. Displayed data for target compounds in 5 µg/L mix mode experiments.....	86
Figure 5.3 Percent target PFAS removed from solution versus application rate of biochar, separated by biochar.....	89
Figure 5.4 Maximum percentage PFAS removed from solution comparing maxima between PFAS experiments for each biochar at the highest treatment application of 100 g/L.....	90
Figure 5.5 Freundlich-Langmuir Combination sorption isotherms (Sips 1948) for target compounds separated by sorbent.....	94
Figure 5.6 Extrapolated Freundlich-Langmuir Combination sorption isotherms (SIPs) for target compounds separated by sorbent.....	95
Figure 6.1 Percentage PFAS removal by varying amendments of P750 in a loamy sand.....	109
Figure 6.2 Percentage PFAS removal by varying amendments of P750 in a sandy clay loam.....	110

List of Tables

Table 1.1 Comparison of parameters for biochars prepared at higher versus lower pyrolysis temperatures.....	8
Table 1.2 Contaminant level criteria specified by European Biochar Commission for basic and premium grade biochar classification (EBC2012).....	12
Table 1.3 Criteria specified by the International Biochar Initiative for the classification of biochars by a three tier classification system (IBI2011).....	13
Table 1.3 Primary uses of Perfluoroalkyl Substances throughout history.....	14
Table 1.4 A generalized conceptualisation of PFOS and PFOA production by Electrochemical Fluorination.....	15

Table 1.5 PFAS compounds in the present study.....	16
Table 1.6 PFSA chemical properties.....	17
Table 1.7 PFCA chemical properties.....	18
Table 1.9 Maximum PFOS and PFOA concentrations detected at 3 AFFF affected sites in Victoria, Australia.....	19
Table 1.10 Key early PFAS studies in WWTPS.....	21
Table 1.11 Key early PFAS animal studies in the environment.....	25
Table 1.12 Key PFAS guideline values from HEPA’s PFAS NEMP.....	28
Table 3.1 Literature values for biochars produced from pine or pea straw like feedstocks.....	50
Table 3.2 Summary of characteristics determined for biochars produced in study.....	56
Table 3.3 Heavy Metal concentrations detected in biochars (mg/kg).....	61
Table 3.4 PAHs concentration in biochars (mg/kg).....	61
Table 4.1 LCMS Operational Conditions.....	69
Table 4.2 LCMS Target PFAS Transitions and retention times.....	71
Table 4.3 Method Performance Data.....	72
Table 5.1 Table outlining LOQ and MDL for PFAS congeners used in biochar equilibrium, sorption and desorption experiments.....	80
Table 5.2 Assessment of equilibrium times between 8 and 48 hours for each PFAS-biochar pair carried out in triplicate by ANOVA for 100 mg biochar applications.....	83
Table 5.3 Second order experimental rate constants and R ² for each Biochar PFAS-biochar pair studied in individual mode and mix mode at 5 µg/L.....	84
Table 5.4 Minimum effective application values (g/L) for each PFAS-biochar combination at 5 µg/L.....	87
Table 5.5 Constants for Freundlich-Langmuir Model (SIPs).....	93
Table 5.6 Total desorption (%) of target PFAS from biochars after a 96-hour holding period from point of reconstitution of batch sorption tubes from sorption experiments with 5 mL distilled water.....	96
Table 6.1. Detection limits and QAQC blanks used in experiments.....	105
Table 6.2 Physiochemical parameter laboratory analysis means results for loamy sand and sandy clay loam soils used in sorption experiments.....	105
Table 6.3 ANOVA analysis of equilibrium data for mixed and individual PFAS experiments using 5 mL of PFAS spiked solution and 2.5 g of soil amended to 5% w/w P750 biochar.....	108
Table 6.4 Pseudo second order models for tested soils amended 5% w/w P750 biochar.....	108
Table 6.5 Percent (%) removal of selected PFAS to loamy sand and 5% w/w P750 biochar amended loamy sand.....	111

Table 6.6 Percent (%) removal of selected PFAS to sandy clay loam and 5% w/w P750 biochar amended sandy clay loam.....	111
Table 6.7 Percentage Desorption for loamy sand soil, control and amended with P750 Biochar at 5 % w/w.....	113
Table 6.8 Percentage Desorption for sandy clay loam soil, control and amended with P750 Biochar at 5 % w/w.....	114

Abstract

The toxicity, mobility and recalcitrant nature of the chemical class known as Perfluoroalkyl Substances (PFAS) is increasingly being demonstrated to pose a threat to human and environmental health globally. The identification of the risk posed by PFAS by numerous governments and scientific organisations has been a driver for further investigation into potential PFAS management options. Biochar has been considered as a possible sustainable approach to PFAS immobilisation due to being derived from waste biomass materials and having a demonstrated ability to sorb a variety of organic and inorganic contaminants.

This study was undertaken to determine if manipulation of biochar characteristics by varying pyrolysis conditions, such as feedstock and pyrolysis temperature, significantly impacted upon biochar PFAS sorption capacity. In addition, the influence of soil matrix was studied, accumulatively demonstrating that with further research biochar could be reverse engineered as an effective and sustainable PFAS sorbent.

It was found that by varying feedstock type, and pyrolysis temperature, a wide variety of physiochemical parameters could be manipulated. To better understand what type of physiochemical characteristic were more beneficial for PFAS sorption, a kinetic and sorption study was undertaken at environmentally relevant concentrations for a suite of biochars (pine and pea-straw feedstocks pyrolyzed at 300, 500 and 700°C). A specially developed direct aqueous injection liquid chromatography mass spectrometry method, associated sample preparation technique, and serial sorption method were developed to undertake appropriately sensitive, accurate and robust sample analysis for serial sorption biochar experiments.

Through the study of kinetic and sorption behaviour it was found that all tested biochars did not adequately sorb short chain PFAS, PFBA and PFBS. Further, low temperature biochar (350°C) sorbed far less PFAS from solution (<50 %) than its higher temperature counterparts. Sorption equilibriums were found to be reached within 0 - 96 hours to for most PFAS, with the bulk of sorption occurring in the first hour. High temperature pine biochar was demonstrated to be the most effective sorbent for PFHxA, PFHxS, PFOA and PFOS. This suggests that key characteristics for the sorption of longer chain PFAS compounds are high surface area, high aromaticity and hydrophobicity. Isotherms demonstrated complex sorption behaviour, including the formation of monolayers and micelles for some PFAS compounds. This behaviour was greatly influenced by PFAS molecular structure, primarily functional group type, and subsequently chain length. Desorption was less reversible for higher temperature biochars, with all PFAS desorbing less than 20% of sorbed fraction. Sorption behaviour was demonstrated to be impacted by intra PFAS congener interaction, with positive or negative impacts on sorption and desorption dependant on the specific biochar – PFAS congener combination.

Further investigation explored the efficacy of pine biochar produced at 750°C as a PFAS sorbent in soils. Soils used in experiments were characterised by their contrasting levels of organic matter and clay. It was found that soil type had a notable impact on biochar efficiency, with biochar being more efficient as a sorbent in soils characterised by higher clay, than in that with higher organic matter.

This work strongly suggests biochar can be employed as sustainable sorbents for PFAS. To achieve this goal, further investigation surrounding reverse engineering of biochar over a greater range of temperatures, residence times and feedstocks is required. Additionally, biochar application should be tailored to matrix type, environment type and target PFAS, for optimum performance at environmentally relevant PFAS concentrations.

Chapter 1

Introduction

Recently, increasing attention has been paid to the detection and management of Perfluoroalkyl Substances (PFAS). This is largely driven by the formal classification of certain PFAS as Persistent Organic Pollutants (POPs) under Annexure B of the Stockholm Convention on Persistent Organic Pollutants due to increasing scientific recognition of PFAS environmental persistence, mobility, ability to bioaccumulate and known toxic modes (Denyes et al. 2012; Haug et al. 2011; POPRC 2008). Prior, PFAS were believed to be environmentally inert, resulting in greater focus on previously ratified POPs, such as Polychlorinated Biphenyls (PCBs) and Polybrominated Diethers (PBDEs) (Ericson et al. 2007; Thompson et al. 2011), worldwide.

PFAS are now known to be ubiquitous in environmental matrices, humans and wildlife (D'eon & Mabury 2010; Loganathan et al. 2007; Naile et al. 2010). Temporal studies illustrate that despite the banning or restricted use of one PFAS congener, PFOS (Perfluorooctane Sulphonic Acid), under the Stockholm Convention, the concentration of total PFAS in animals has increased globally over the past 15-25 years (Houde et al. 2006). Recent studies have indicated that the shift in manufacture and use of shorter chain PFAS (Ateia et al. 2019) has seen an increasing prevalence of these in the environment (Gewurtz et al. 2019; Nakayama et al. 2019). Clarke & Smith (2011) assessed 17 classes of POPs based on overall risk and ranked PFAS as the class of greatest concern to humans and the environment due to their toxic effects, persistence and unique behavioural characteristics making them incredibly mobile in the environment.

Since the seminal article by Clarke & Smith (2011), PFAS contamination of agricultural land and potable water sources has taken center stage with an increasing body of research demonstrating PFAS migration into food products and the environment (Cao et al. 2019; Endirlik et al. 2019; EPA-Victoria 2018a; Ghisi, Vamerali & Manzetti 2019; Huset & Barry 2018). Subsequent ingestion of contaminated food has been linked to a variety of health affects (enHealth 2019; US EPA 2016b, 2017a). This has seen conservative response by regulatory bodies such as U.S.EPA through the recent release of the PFAS Action Plan which roadmaps toxicity, environmental levels, transport pathways, guidelines and management activities (US EPA 2019). In Australia, a working group consisting of the heads of the EPA Australia and New Zealand released the PFAS National Emergency Management Plan (PFAS NEMP) in January of 2018 (HEPA 2018). This has been accompanied by jurisdictional position statements adopting guidance values from the PFAS NEMP protective of human and environmental health (EPA-Victoria 2018b).

The current ever increasing understanding of the extent of PFAS contamination renders reducing environmental and human exposure of PFAS a crucial next step towards PFAS risk management. This includes the disruption of source-receptor pathways, and the containment, removal or destruction of PFAS in contaminated materials. Currently, a limited but varied number of technologies are available or under development. However, considering the mobility and subsequent extensive dispersion of PFAS contamination through the environment, many technologies are prohibitively expensive or unweildly (Kucharzyk et al. 2017; Ross et al. 2018). As such, the exploration of novel cost-effective approaches to PFAS management is essential. Minimising PFAS mobility in the environment is a critical management approach requiring further development as containing PFAS

contamination results in smaller volumes of affected material for future treatment, in addition to its major function of disrupting source-receptor pathways.

Biochar could potentially be engineered to possess the characteristics needed to address PFAS in the environment, as a cost-effective sorbent. Abdel-Fattah et al. (2015) demonstrated biochar's ability to sorb heavy metals, while Dechene et al. (2014) explored the sorption of polar organic contaminants and pesticides to biochar amended soils. Recently, Kupryianchyk et al. (2016) highlighted the sorption of PFAS to biochar, paving the way for further investigation into the potential use of biochar for the *in-situ* remediation of PFAS.

Biochar is the carbonaceous solid product resulting from the thermal decomposition of organic materials in an oxygen limited environment (IBI 2011). Biochar can be produced using waste biomass (Denyes et al. 2012; Jouiad et al. 2015), which is the largest and most sustainable energy source available, with 220 billion dry tons being produced globally each year (Azargohar et al. 2013; Das & Sarmah 2015). Consequently, biochar has been the subject of much research due to its sustainable nature and physicochemical properties lending themselves well to agriculture (soil enhancement), climate change action (carbon sequestration), environmental management (contaminated land remediation) and waste management (recycling) (Denyes et al. 2012; Heitkötter & Marschner 2015). The production of biochar is an attractive solution to a number of issues facing the environment, as the financial and environmental cost in disposing of waste materials is reduced whilst a useful product is derived (Poerschmann et al. 2015; Rehrah et al. 2014).

While a relatively limited number of studies have explored and compared PFAS sorption to biochar to other sorbents (Dalahmeh, Alziq & Ahrens 2019; Du et al. 2014; Liu et al. 2019; Xiao et al. 2017; Zhi & Liu 2018), these have not included detailed comparisons between biochars prepared under different pyrolysis conditions. Feedstock type and pyrolysis temperature could, in turn, be optimized to produce biochar having the physicochemical properties favourable for PFAS sorption. To achieve this, a better understanding of PFAS sorption to biochar in solution and in the presence of soils is required to identify the key sorption mechanisms and behaviours for selected PFAS congeners. In addition, a comprehensive approach is required to further catalogue the effect of pyrolysis temperature and feedstock type which best produce biochar optimized for PFAS sorption.

This study aims to begin addressing the above knowledge gaps through early experiments, starting with the observation of production condition impact through the characterisation of six biochars produced using 3 pyrolysis temperatures and 2 lignocellulosic feedstocks. Subsequently the prepared biochars were studied to assess PFAS sorbing qualities in solution. Considering the more recent use of short chain PFAS congeners, both short and long chain PFAS congeners were selected for experiments. Preferential sorption could then be delineated for each compound and cross referenced with physicochemical properties of the biochar as a result of its feedstock and preparation temperature. The biochar showing the greatest PFAS sorbing qualities in solution was retested in the presence of two soils, to determine the impact of soil geochemical properties upon PFAS sorption. Overall, this study collectively provides early data on PFAS-biochar sorption behaviour to the ends of guiding future works for optimised production of this renewable sorbent for the management of PFAS in the environment.

1.1 Biochar

1.1.1 Background

The International Biochar Initiative (IBI) guidelines define biochar as “a solid material obtained from the thermochemical conversion of biomass in an oxygen-limited environment” (IBI 2011). Biochar is further distinguished as different from charcoal as it is specifically produced for agronomic or environmental application (Fabbri et al. 2013). In addition, biochar is differentiated from activated carbon, which has been utilised in environmental remediation roles, as a factor of its waste biomass feedstock material and not necessarily undergoing an activation process (Denyes et al. 2012; Srinivasan & Sarmah 2015).

Biochar has its earliest record of use in the Amazon basin, dating back approximately 2000 years (Jouiad et al. 2015). Here, the residents indigenous to the region made use of biochar to improve soil fertility. These soils, known as *Terra Preta*, are characterized by its darker colour and much higher productivity than the surrounding tropical soils typical of the Amazonian region (Glaser et al. 2001). This is due to biochar application increasing soil cation exchange capacity (CEC), organic matter (OM) content and nutrient availability of the pre-*Terra Preta* soils (Glaser et al. 2000; Glaser et al. 2001; Heitkötter & Marschner 2015).

More recently biochar has seen a re-emergence in interest, with possible scope for use in environmental, agricultural and civil applications. Climate change has been a strong driver for steering biochar research towards employment as a carbon sequestration technique. Simultaneously, pressures to increase crop yields in a cost-effective manner has seen increased focus on research aiming to optimize biochar characteristics that favour biochar's utility as a soil conditioner (Abdel-Fattah et al. 2015; Lehmann 2007). Considering the above two parallel uses, biochar's ability to improve soil properties while sequestering organic carbon has rendered it an ideal vehicle for climate change action and vaulted interest in biochar as a sustainable product (Rehrah et al. 2014). The resulting pyrolysis-based research to date has primarily focused on characterization of products based on variable pyrolysis conditions (temperature, residence time, nitrogen flow rate, heating rate). However, the bulk of existing research assesses biochar unique physicochemical properties on temperature or feedstock alone, often not taking in to account the interplay between feedstock types and temperatures (Albuquerque et al. 2013; Lievens et al. 2014; Mitchell, Dalley & Helleur 2013; Peterson et al. 2012; Rehrah et al. 2014; Wiedner et al. 2013).

A growing number of studies address the novel function of biochar as an effective contaminated soil ameliorant (Denyes, Rutter & Zeeb 2013), whereby biochar is used to reduce bioavailability or immobilise contaminants (Mukherjee, Zimmerman & Harris 2011). Currently most studies are short term (4-27 weeks) with many targeting small groups of different contaminants as opposed to classes with intra- or inter- compound interactive effects (Beesley, Moreno-Jiménez & Gomez-Eyles 2010; Heitkötter & Marschner 2015).

A growing body of biochar research has contributed to the proposal of standards to assist in monitoring if biochar products are utilized in an environmentally responsible effective manner (IBI 2011; EBC 2012). This includes the provision of criteria for allowable limits of potential contaminants and characteristics of biochar's as to prevent the contamination, exacerbation of contamination or the remobilization of contaminants in the environment (Oleszczuk, Joško & Kuśmierz 2013) It has been recognised as imperative that biochar's are characterized prior to application and that this information is made available to end users and policy makers

(Albuquerque et al. 2013) as to avoid any negative impacts such as contamination or degradation of the environment through the application of biochars that are below protective standards (Lievens et al. 2014; Morales et al. 2015). Additionally, soil type must be matched with an appropriate biochar for the affliction it is destined to address (Das & Sarmah 2015; Morales et al. 2015; Qian et al. 2015). To adequately achieve this, a full understanding of contaminant-soil-biochar interaction is required.

1.1.2 Chemical Structure and Production

Biochar Structure

Biochar is chiefly composed of recalcitrant aromatic carbon ring structures, the arrangement of which attribute biochar a sheet like structure and its porosity (Al-Wabel et al. 2013). Biochar typically has a low bulk density and a high carbon fraction, oftentimes near double that found in the feedstock (Azargohar et al. 2013). In some cases, carbon fractions have been found to be as high as 90% (Jouiad et al. 2015; Ochoa-Herrera & Sierra-Alvarez 2008).

The stability of aromatic C-rings, contribute to biochars resistance to biological decay (Al-Wabel et al. 2013; Freddo, Cai & Reid 2012) as well as biochars resistance to degradation by many chemical oxidants (Mitchell, Dalley & Helleur 2013). This is notable when comparing biochar to the original feedstock's comparatively higher propensity to degrade (Thomazini et al. 2015). While values vary based on preparation method and feedstock, it has been posited that biochars may degrade at an approximate rate as low as 0.28% per annum, equating to a residence time in the environment of approximately 4000 years (Kuzyakov, Bogomolova & Glaser 2014). Due to the great variation of physiochemical properties acquired from the large variety of biomass feedstocks and production conditions used in biochar production, biochars are considered a diverse group of materials with individual batches of biochar exhibiting very different physiochemical characteristics, including degradative recalcitrance in the environment (Jouiad et al. 2015; Qian et al. 2015).

Biochar Production

Biochar is produced through a thermal decomposition process called pyrolysis, in which thermal energy is used to degrade biomass in an oxygen-limited environment which prevents combustion (Bridgwater 2003). Here degradation is the depolymerisation of biopolymers and the carbonisation of the feedstock to a more recalcitrant form through decarboxylation, dehydration, de-carbonylation, de-methylation, intermolecular derangement, condensation and aromatisation reactions (Das & Sarmah 2015; Heitkötter & Marschner 2015; Kambo & Dutta 2015). The result of this process is the conversion of less stable biomass (~17 MJ/kg) and the production of biochar (~18 MJ/kg), bio-oils (~22 MJ/kg) and syngas (~6 MJ/kg) (Azargohar et al. 2013; Das & Sarmah 2015). Here syngas is primarily composed of non-condensable volatiles such as carbon monoxide (CO), carbon dioxide (CO₂), methane (CH₄), and hydrogen (H₂) (Al-Wabel et al. 2013; Kambo & Dutta 2015).

Slow pyrolysis is the conventional carbonization method which favours the production of biochar over bio-oils or syn-gasses by employing a low heating range (300 – 750 Celsius) and a residence time of hours (Qian et al. 2015). Generally the reactors used in slow pyrolysis are stationary facilities, however the recent advent of

mobile facilities has changed the availability of feedstock as well as the cost associated with feedstock transport (Azargohar et al. 2013), in turn allowing the production of biochar on site (Denyes, MJ et al. 2012).

Pyrolysis Conditions

The pyrolysis conditions used to produce biochar are highly influential on the resultant biochar physiochemical properties because the various organic fractions intrinsic to any given feedstock decompose and transform into new compounds at different temperature ranges (Al-Wabel et al. 2013). Hemicellulose decomposition ranges <220-315°C whereas cellulose and lignin have a higher decomposition range of 315 - >400°C (Buss et al. 2015; Kambo & Dutta 2015). Generally, biochar created at higher temperatures tends to be closer in structure and composition to graphite. Those produced at lower temperatures have a structure and composition more similar to that of their original feedstock (Butnan et al. 2015; Das & Sarmah 2015). Biochars produced at higher pyrolysis temperatures typically lose most of their surface function groups but have higher surface area, whereas lower temperature biochars often have a reduced surface area due to poor development and becoming clogged with oils and tars evolved during production, but retain more surface functional groups (Das & Sarmah 2015). Pyrolysis temperature determines elemental concentration through mass loss as well as porosity based on the degassing of volatiles and subsequent fracturing during shrinkage (Das & Sarmah 2015). Thus, pyrolysis temperature plays a major role in the determination of product biochar surface area, pore size and surface functional groups (Das & Sarmah 2015). These act in tandem with the inherited chemical properties and contaminant burden specific to the feedstock (Kambo & Dutta 2015). However, pH, surface charge, thermal stability, heavy metal and organic compound concentration are all functions of the pyrolysis temperature, residence time and initial feedstock used during production (Chen et al. 2014; Heitkötter & Marschner 2015).

The above contrasts the interplay between the importance of temperature as well as feedstock during biochar production. While temperature governs many of the physiochemical characteristics of biochar, these are also heavily influenced by the choice of feedstock, ultimately determining their capacity for use in any particular application (Das & Sarmah 2015; Domene et al. 2015; Jouiad et al. 2015). The effects of temperature upon each parameter are further explored in Table 1.1.

Contaminants in Biochar

Biochar products retain several characteristics of the feedstock. This is particularly important when extended to contaminant burden. Contaminated feedstocks (metals, PAHs, dioxins, pesticides) are to be avoided as biochars produced from these will inherit these traits (Denyes et al. 2012). This is particularly the case for contaminants such as high boiling point heavy metals which are generally entirely intrinsic to the feedstock and are neither created nor volatilized during pyrolysis (Chen et al. 2014; Zielińska & Oleszczuk 2015). Due to mass loss metals increase in concentration from feedstock to the biochar product (Domene et al. 2015). Increases in heavy metal concentration of up to 4-6 fold have been observed in this manner (Freddo, Cai & Reid 2012). While most organic contaminants (pesticides) volatilize, many other organic contaminants (PAHs, pesticides, PCBs) found in the feedstock may be resilient to selected pyrolysis conditions (temperature) and therefore remain in the resultant biochar (Buss et al. 2015).

Additionally, organic compounds generated during thermochemical processing of biochars, may include PAHs, furans and dioxins (Domene et al. 2015; Oleszczuk, Joško & Kuśmierz 2013). These pyrogenic

compounds, amongst other more volatile organic compounds (VOCs) can become trapped in the micro-pore structure of biochar due to clogging or recondensation on biochar surfaces and pores of off-gases (Buss et al. 2015; Domene et al. 2015; Lievens et al. 2014).

Buss et al. (2015) detected VOCs known to be harmful to plant life up to 100 µg/g in biochar. These included naphthalene, phenanthrene and acenaphthylene (Buss et al. 2015; Chen, B & Yuan 2011; Fabbri et al. 2013). Some processes such as quenching through the addition of water have been shown to remove mobile organic contaminants (Butnan et al. 2015). Fabbri (2013) tested biochars for total PAHs evolved during the slow pyrolysis of a woody biomass and found levels of 1.2-19 µg/g, suggesting that PAH contamination may not be a major issue, as this concentration does not pose a threat at the application rates at which biochar is currently used (Fabbri et al. 2013). Conversely, Gomez-Eyles et al (2011) had found that earthworms could increase PAH bioavailability by up to 40% by fragmenting natural organic matter and releasing previously trapped contaminants. Complexation and mineralisation were suggested to be the mechanism by which these contaminants are rendered more bioavailable.

Table 1.1 Comparison of parameters for biochars prepared at higher versus lower pyrolysis temperatures

Parameter	Higher Pyrolysis Temperatures	Lower Pyrolysis Temperatures
Biochar Yield	Lesser yield (Chen et al. 2014; Kambo & Dutta 2015)	Greater yield (Chen et al. 2014; Kambo & Dutta 2015)
Carbon Stability	Higher stabilization due to higher degree of aromaticity (Al-Wabel et al. 2013; Butnan et al. 2015; Chen et al. 2014)	Greater proportion of unstable organic matter, composition closer to feedstock (Al-Wabel et al. 2013; Butnan et al. 2015; Chen et al. 2014)
Polarity and Water Affinity	Higher affinity to water, despite lower polarity (Al-Wabel et al. 2013; Chen et al. 2014; Das & Sarmah 2015)	Lower affinity to water, often due to hydrophobic surface tars (Al-Wabel et al. 2013; Chen et al. 2014; Das & Sarmah 2015)
Oxygen content	Lower O/C ratio (Abdel-Fattah et al. 2015; Hmid et al. 2014)	Higher O/C Ratio (Abdel-Fattah et al. 2015; Hmid et al. 2014)
Dissolved Organic Carbon	Lower due to volatilization (Al-Wabel et al. 2013)	Higher due to lesser volatilization (Al-Wabel et al. 2013)
Surface Area and Microstructure	Greater total surface area due to better microstructure development through outgassing (Alburquerque et al. 2013; Chen et al. 2014; Das & Sarmah 2015)	Lower surface area due to lessened micro-structure development, less carbonization and pore clogging with tars (Alburquerque et al. 2013; Chen et al. 2014; Das & Sarmah 2015)
Surface Functional Groups	Fewer surface functional groups in general and a higher proportion of basic functional groups in those that remain (Al-Wabel et al. 2013; Alburquerque et al. 2013; Butnan et al. 2015; Chen et al. 2014; Das & Sarmah 2015; Hmid et al. 2014)	Greater number of functional groups, notably: carboxylic acid, phenol, ketone, and aldehyde. A higher proportion of acidic functional groups (Al-Wabel et al. 2013; Alburquerque et al. 2013; Butnan et al. 2015; Chen et al. 2014; Das & Sarmah 2015; Hmid et al. 2014)
Cation Exchange Capacity	Lowered CEC due to functional group loss (Alburquerque et al. 2013)	-
pH	Higher pH (Al-Wabel et al. 2013; Alburquerque et al. 2013)	Lower pH (Al-Wabel et al. 2013; Alburquerque et al. 2013)
Electrical Conductivity and Salinity	Higher EC and increased salinity (Al-Wabel et al. 2013; Alburquerque et al. 2013)	Lower EC (Al-Wabel et al. 2013; Alburquerque et al. 2013)
Ash Content (C, N, P, K, Ca, and Mg)	Greater ash content, but reduction in N and H. Higher nutrient content but lower availability (Abdel-Fattah et al. 2015; Butnan et al. 2015; Al-Wabel et al. 2013; Azargohar et al. 2013; Hmid et al. 2014)	Reduced ash content. Increased nutrient holding capacity and availability (Abdel-Fattah et al. 2015; Butnan et al. 2015; Al-Wabel et al. 2013; Azargohar et al. 2013; Hmid et al. 2014)
Contaminant Burden	Lower Polycyclic Aromatic Hydrocarbons (PAHs) content but higher concentration of heavy metals due to mass loss (Domene, Enders, et al. 2015; Freddo, Cai & Reid 2012)	Higher risk of PAHs at moderate temperatures, high enough to form but low enough not to volatilize (Domene, Enders, et al. 2015; Freddo, Cai & Reid 2012)

Biochar's Chemistry

Understanding biochar physiochemistry is important not only to guide production condition decisions, but also from the perspective of the influence physiochemical properties have upon biochar suitability for selected end use. Biochars contain an ash fraction which holds a liming capacity as well as important nutrients and essential cations such as potassium (K), calcium (Ca) and magnesium (Mg) (Butnan et al. 2015; Kuzyakov, Bogomolova & Glaser 2014). Biochar surface functional groups are highly sensitive to production temperature (Qian et al. 2015). The ash fraction can be manipulated by increasing or decreasing pyrolysis temperature (Table 1.1). Similarly, pH can be manipulated in this manner, where generally biochars have a neutral to alkaline pH (Heitkötter & Marschner 2015; Kuzyakov, Bogomolova & Glaser 2014). Generally biochars made at higher temperatures tend to be more porous than those produced at lower temperatures, the latter having a greater proportion of surface functional groups (Das & Sarmah 2015). Oxygen content in biochars is manifested primarily as carbonyl, carboxyl and phenolic groups on the surface of the biochar (Abdel-Fattah et al. 2015). Functional surface groups are important as they determine by large how a biochar will interact with its environment (Mukherjee, Zimmerman & Harris 2011; Singh, Singh & Cowie 2010).

Biochar surfaces are complex, with a variety of pores and surface functional groups influencing how they interact with their environment (Mukherjee, Zimmerman & Harris 2011). The pore size exhibited by biochars can span 5 orders of magnitude and their formation is dependent upon the feedstock and production technique used (Jeffery et al. 2015). Pores are created as volatile matter escapes from the feedstock during carbonization and when the biochar fractures while cooling and shrinking after production (Abdel-Fattah et al. 2015). Macro-pores are generally inherited from the feedstock's original structure whereas smaller pores are the product of out-gassing or shrinkage (Abdel-Fattah et al. 2015; Das & Sarmah 2015). Tar formation in pores can present an anomaly in biochars made at lower temperatures as tars can result in pore clogging, however clogged oils may behave as further surface functional groups (Das & Sarmah 2015). Oxygen containing surface functional groups greatly influence the cation exchange capacity (CEC) of biochar. This occurs in tandem with any impact the ash fraction has on pH, by further increasing biochar CEC (Abdel-Fattah et al. 2015; Butnan et al. 2015). Therefore, CEC is production-method variable, based upon the ash fractions and surface functional groups being temperature dependant (Mukherjee, Zimmerman & Harris 2011).

Biochar can, based on production conditions, have a moderate affinity towards water or be hydrophobic due to low surface area, tars clogging pores, or high degree of carbonisation (Das & Sarmah 2015; Heitkötter & Marschner 2015; Jeffery et al. 2015). Biochars affinity to water is known to be strongly dependant on degree of carbonisation, surface area, pore size and the types of surface functional groups present (Das & Sarmah 2015; Jouiad et al. 2015). Over time, biochar may age, by means of oxidation of functional groups (Heitkötter & Marschner 2015), in turn changing surface chemistry and charge (Martin et al. 2012). Interestingly, surface area has been shown to increase over time due to the leaching of salts and soluble organics (Heitkötter & Marschner 2015). The sorption of dissolved organic matter to the biochar's surface is a known second mechanism of aging where the number of biochar surface functional groups may increase vicariously through the attached NOM, thereby increasing CEC (Heitkötter & Marschner 2015). Aging and pH changes are important considerations when considering surface functional groups and their interaction with the surrounding environment.

1.1.3 Applications and Guidelines

The scope for biochar usage extends from agronomic and environmental remediation applications to energy production and carbon sequestration. Many of these applications are still in their infancy and have only been seen investigation over the past decade. However, pyrolysis by-products have long served as fuel sources in the form of charcoal and syn-gas (Hmid et al. 2014). Combustion of biochar could produce ¼ more recoverable energy than the combustion of the raw biomass itself (Das & Sarmah 2015). In addition, the production of biochar, regardless of intended product application, reduces the volume of organic waste material reaching landfill. This sustainable practice is beneficial from a waste management, climate change and economic perspective (Domene, Enders, et al. 2015).

Biochar has attracted much attention as a soil amendment due to it offering a number of agronomic benefits. Agronomic benefits couple well with biochars recalcitrant nature and longevity in soils after application, which reduce the need for subsequent application (Butnan et al. 2015). It has been well established that biochar can enhance soil (chemically and structurally) in a manner that improves soil fertility (Cabrera et al. 2014; Denyes, Rutter & Zeeb 2013; Liu et al. 2012). Biochar's capability to improve soil physical structure has been demonstrated through it readily reducing bulk density and increasing water holding capacity (Al-Wabel et al. 2013; Cabrera et al. 2014; Denyes, Rutter & Zeeb 2013). These are major agronomic advantages, particularly in sandy soils with high bulk density (Butnan et al. 2015), in turn potentially improving soil fertility and the ability of seedlings to germinate and grow (Denyes, Rutter & Zeeb 2013). The chemical agronomic benefits of biochar are namely related to high biochar pH and modest liming capacity, making biochars useful soil pH and buffering capacity amendments (Butnan et al. 2015; Gomez-Eyles et al. 2011) . In addition to this, the unique surface properties of biochar (surface area, charge and charge density), result in some biochars being able to be applied to increase CEC in receiving soils (Denyes et al. 2012; Heitkötter & Marschner 2015; Hmid et al. 2014). An increase in nutrient availability (C, N, P, K, Ca, and Mg) and retention is associated with improved soil CEC and increased pH, due to increased solubility of nutrients at amended pH and the nutrient sorptive capacity of biochars (Butnan et al. 2015; Knowles et al. 2011). In addition to this, biochar itself contains a number of key macro-elements and nutrients which are introduced to the soil when applied (P, K, N and micro-elements) (Gomez-Eyles et al. 2011; Heitkötter & Marschner 2015)

Hmid et al. (2014) suggested that through biochar physiochemical improvement to soils, biochar can stimulate microbial activity as a carbon and nutrient source, which in turn influences nutrient cycling and improves soil productivity (Domene et al. 2015; Hmid et al. 2014). Increased nutrient availability to crops results in a lower demand for fertilizers and hence an improved crop yield at a lesser financial burden (Denyes, Rutter & Zeeb 2013). Further to this, biochar maintains soil health by preventing runoff and the loss of available nutrients, and as an added benefit this improves the quality of runoff water reaching waterways (Abdel-Fattah et al. 2015).

Biochars usage as a carbon capture technique has seen biochar products termed carbon neutral or carbon negative (Denyes et al. 2012; Mitchell, Dalley & Helleur 2013). This means carbon, as CO₂ or CH₄, destined to be liberated to the atmosphere through decomposition or combustion of biomass is instead trapped in pyrolysis products until use (neutral) or stored in soils (negative) (Abdel-Fattah et al. 2015; Fabbri et al. 2013). This is based upon feedstocks being considered renewable or waste biomass material (Das & Sarmah 2015). Biochar amended soil is therefore considered a sink for carbon and an attractive climate change mitigation strategy (Ojeda et al.

2015). Finally, biochar may also have the capacity to actively reduce the release of greenhouse gases such as CO₂, CH₄ and nitrogen dioxide (NO₂), from soils following its application (Liu, Y et al. 2011). Thomazini et al. (2015) and Albuquerque et al. (2013) each noted that in the realm of climate change management, not all biochars behave equally and need to be considered on a case by case basis as some degrade quicker in the environment.

Biochar aromaticity, high surface area and functionality contribute to its viability as an organic and inorganic soil contaminant remediation strategy (Hmid et al. 2014; Martin et al. 2012). This has been achieved by either sorption of contaminants to biochar and subsequent removal of 'spent' biochar for incineration or landfill. Alternatively, *in situ* remediation, which involves the sorption of contaminants to biochar to reduce their mobility in the environment and bioavailability to organisms (Lu et al. 2015; Oleszczuk, Joško & Kuśmierz 2013). An additional advantage is biochar's ability to elevate soil pH and CEC which renders a variety of toxic elements no longer bioavailable and immobile regardless of sorption to biochar itself (Gomez-Eyles et al. 2011). It has been demonstrated that the ameliorant properties of biochar could be extended beyond soils and into water and sediment remediation applications (Tang et al. 2013).

Biochar incorporation rates into soils are highly dependent on the biochar type, soil type and intended effect, however these usually range between 0.5 and 8% of soil mass w/w (Butnan et al. 2015; Fabbri et al. 2013). Unlike other soil amendments (phosphate fertilizers, lime, animal manure, biosolids), biochar's longevity in soil reduces the likelihood of contaminant accumulation associated with repeated applications (Ochoa-Herrera & Sierra-Alvarez 2008).

It follows that the improper employment of biochar can have significant implications for soils, resulting in contamination or adverse alterations to soil physiochemical properties. In the unlikely case where excessive reapplication of biochar has occurred, the result could possibly be the exceeding the allowable limits for contaminants in soils due to native soil burden (exacerbation) and inherent biochar burden (contaminant loading) (Ochoa-Herrera & Sierra-Alvarez 2008; Zielińska & Oleszczuk 2015). A direct effect on nutrient availability can be seen through changes in pH, where soils with a low buffering capacity can incur large increases in pH due to "over-liming" (Butnan et al. 2015). More acidic biochars can cause the mobilization of contaminants and nutrients as they reduce system pH, which may have further negative effects with reference to bioavailability or loss of nutrients. Interestingly, a reduction in certain pesticide effectiveness has been noted due to their sorption affinity to biochar. This results in larger pesticide applications being required (Martin et al. 2012). However, with the correct approach, the above complications can be avoided. Freddo, Cai & Reid (2012) demonstrated that with proper monitoring and application, the burdens of metals, metalloids and PAHs in biochar would be a manageable issue. Fabbri et al. (2013) reinforced this by concluding that PAH concentrations produced during pyrolysis could be almost eliminated using the appropriate pyrolysis technique.

Due to potential for misguided application, many organisations and governments are devising limits and guidelines pertaining to the concentration of contaminants and characteristics allowable in biochars destined for land application in an effort to counteract environmentally damaging effects if applied without further consideration (Domene et al. 2015; Freddo, Cai & Reid 2012; Oleszczuk, Joško & Kuśmierz 2013). The European Biochar Certificate for example sets a general metal limit of 100 mg/kg. In these guidelines there are two qualities for biochar, 'Basic' and 'Premium' (Table 1.2). There are currently no limits set for individual PAHs and PCBs in the EBC, instead a maximum allowable concentration is set for the total of all 16 United States Environmental Protection Agency (USEPA) designated PAHs (EBC 2012). Contrastingly, the IBI has 3 levels of classification

as well as requires additional parameters to be reported (IBI 2011). Level 1 is for unprocessed feedstocks only and mainly analyses biochar physical parameters not including contaminants. Processed feedstocks need to undertake Level 2 testing which includes heavy metals, boron, chlorine and sodium as well as P and K. Level 3 is optional ‘advanced testing’ which addresses porosity and surface area, but more importantly a host of possible organic contaminants (Table 1.3) (IBI 2011). In Australia there are not currently any Commonwealth or State guidance or regulations specific to biochar and its application to land, instead regulation varies case by case as per state jurisdiction (Singh, Singh & Cowie 2010). In the state of Victoria for example, biochar application is considered on a case by case basis accompanied by a formal Environmental Improvement Plan process much like that of biosolids. However, further research to support the development of biochar specific regulation has been suggested, specifically in reference to compatibility with receiving soil geochemistry and leachability of biochar contaminant fractions (EPA-Victoria 2004; Yang et al. 2018).

Table 1.2 Contaminant level criteria specified by European Biochar Commission for basic and premium grade biochar classification (EBC 2012)

Parameter	Basic Grade	Premium Grade	Unit
Cadmium	< 1.5	< 1	mg/kg (dry matter)
Chromium	< 90	< 80	mg/kg (dry matter)
Copper	< 100	< 100	mg/kg (dry matter)
Lead	< 150	< 120	mg/kg (dry matter)
Molybdenum	-	-	mg/kg (dry matter)
Mercury	1 g	1 g	mg/kg (dry matter)
Nickel	< 50	< 30	mg/kg (dry matter)
Selenium	-	-	mg/kg (dry matter)
Zinc	< 400	< 400	mg/kg (dry matter)
Total EPA 16 PAHs	<12	<4	mg/kg (dry matter)
Total PCBs	<0.2	<0.2	mg/kg (dry matter)
Dioxin	<20	<20	ng/kg (I-TEQ OMS)
Furans	<20	<20	ng/kg (I-TEQ OMS)

Table 1.3 Criteria specified by the International Biochar Initiative for the classification of biochars by a three tier classification system (IBI 2011)

Requirement	Criteria (Maximum)	Unit
Level 1 (Unprocessed feedstocks only)		
Moisture Content	Declaration	% of total mass
Total Ash	50%	% of total mass
Organic Carbon	Declaration	% of total mass
Inorganic Carbon	Declaration	% of total mass
H:C_{org}	0.7	Molar Ratio
Total N	Declaration	% of total mass
pH	Declaration	N/A
Liming	Declaration	% CaCO ₃
Particle Size Distribution	Declaration	% of total mass in each class
Earthworm Avoidance Test	Pass/ Fail	OECD methodology (1984)
Germination Inhibition Assay	Pass/Fail	OECD methodology (1984)
Level 2 (Must conform to level 1)		
Arsenic	13	mg/kg Dry Matter
Cadmium	1.4	mg/kg Dry Matter
Chromium	83	mg/kg Dry Matter
Cobalt	34	mg/kg Dry Matter
Copper	143	mg/kg Dry Matter
Lead	121	mg/kg Dry Matter
Molybdenum	5	mg/kg Dry Matter
Mercury	1.0	mg/kg Dry Matter
Nickel	47	mg/kg Dry Matter
Selenium	2	mg/kg Dry Matter
Zinc	416	mg/kg Dry Matter
Boron	Declaration	mg/kg Dry Matter
Chlorine	Declaration	mg/kg Dry Matter
Sodium	Declaration	mg/kg Dry Matter
Total P & K	Declaration	% Content
Mineral N	Declaration	mg/kg Dry Matter
Available P	Declaration	mg/kg Dry Matter
Level 3 (Must conform to level 1 & 2)		
Polychlorinated Biphenyls	0.2	mg/kg TM
Polycyclic Aromatic Hydrocarbons	6	mg EPA PAHs/kg TM
Furan	0.5	ng/kg I-TEQ OMS
Dioxin	0.5	ng/kg I-TEQ OMS
Porosity	Declaration	%
Surface Area	Declaration	m ² /g

1.2 Per- and Poly - Fluorinated Substances

1.2.1 Background

Perfluoroalkyl Substances (PFAS) are a class of synthetic fluorinated organic compounds often referred to as emerging contaminants (Gellrich, Stahl & Knepper 2012), as prior to the recent identification of their toxicity PFAS were believed to be environmentally inert (Ericson et al. 2007). Accordingly, PFAS were not strictly classed as environmental contaminants until 2010, when a growing body of evidence suggesting PFAS were toxic and environmentally persistent, saw for the first time a member of this PFAS group (PFOS) added to Annexure B of the Stockholm convention as a Persistent Organic Pollutant (POP) (Haug et al. 2010; Thompson et al. 2011). PFAS have historic and continued use in a vast number of applications and products (Table 1.4) due to a set of unique properties such as: surface activity (Milinovic et al. 2015), dispersive qualities (DoHA 2008), resistance to degradation (chemical/heat/abrasion) (Wang et al. 2013), repellence of water, oil and dirt (Naile et al. 2010).

Table 1.4 Primary uses of Perfluoroalkyl Substances throughout history

Use	Property	Reference
Adhesives	Dispersant	(Kim et al. 2013)
Aqueous Film Forming Foam (AFFF)	Foam Formation	(Kalbe et al. 2014)
Apparel and Textiles	Repellent (Oil & water)	(Thompson et al. 2011)
Carpet Coatings	Repellent (Oil & water)	(Paul, Jones & Sweetman 2008)
Chromium Plating	Dispersant, protection	(Du et al. 2014)
Cosmetics	Repellent (Oil & water)	(Kalbe et al. 2014)
Electronics	Semi-conductivity	(Zareitalabad et al. 2013)
Food Packaging	Repellent (Oil & water)	(Hradkova et al. 2010)
Lubricants	Dispersant	(Wang, P et al. 2013)
Metal protective Coating	Thermal/Chemical Resistance	(Zareitalabad et al. 2013)
Non-stick Coatings	Repellent (Oil & water)	(Wang, P et al. 2013)
Paper	Repellent (Oil & water)	(D'eon et al. 2009)
Personal Care Products	Repellent (Oil & water)	(Milinovic et al. 2015)
Pesticides	Dispersant	(Wang, P et al. 2013)
Photolithography	Dispersant	(Du et al. 2014)
Polishes and Paints	Dispersant	(Xiao et al. 2015)
Polymerization Aids	Polymerizer	(Jiang et al. 2012)

PFAS synthesis by Electrochemical Fluorination (ECF) was pioneered in 1937, where a precursor is synthesised through the reaction of an organic feedstock with hydrogen fluoride (HF) under an electric current (Wang et al. 2013) (Table 1.5). This results in the replacement of hydrogen atoms attached to the carbon backbone of the molecule with fluorine (Lau, Butenhoff & Rogers 2004). Further reaction of the precursor produces a number of PFAS with a variety of chain lengths and functional groups (Kannan, Corsolini, et al. 2002; Wang et al. 2009).

The ECF process is not completely efficient as approximately 15-30% of the PFAS produced are branched isomers, cyclic isomers or shorter in chain length (EFSA 2008). These impurities resulted in ECF being superseded by Telomerisation (Wang et al. 2009), where purities close to 99% were achieved (EFSA 2008). Telomerisation reacts iodide polymerisers (Pentafluoroethyl iodide), with a feedstock such as ethylene by free

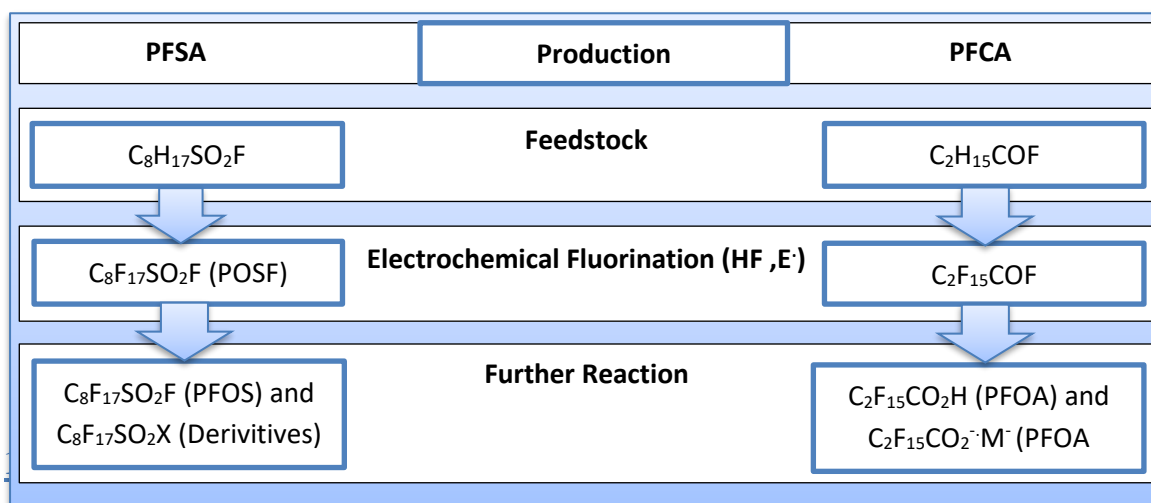
radical addition, yielding straight chained alcohols which can be further reacted to any required chain length (Lau, Butenhoff & Rogers 2004).

The production of PFAS on an industrial scale began in 1949 at 3M Laboratories (Kim et al. 2013). By the year 2000, 3M was manufacturing 78% of the PFOS precursor POSF within their two production facilities; Decatur (Alabama) and Antwerp (Belgium) (Naile et al. 2010; Paul, Jones & Sweetman 2008). However, by May of 2000, 3M announced it would voluntarily phase out the production of POSF by 2002 due to the metabolite PFOS being found to be well dispersed in environment matrices, wildlife and humans (Ericson et al. 2007; Olsen et al. 2003). 3M's study uncovered elevated concentrations of PFAS in sludge surrounding the Alabama facility reaching as high as 120 and 244 ppb for PFOS and PFOA respectively (3M 2001).

In 2002 there were 33 PFAS manufacturing facilities across the globe, notably in America (8), China (7), Europe (7), Japan (7), Russia (2) and India (1) (Prevedouros et al. 2006). Shortly after PFOS production was phased out by 3M, large scale production of PFOS began in China, with total production increasing from <50 t/year in 2004 to >200 t/year by 2006, of which approximately 50% was for export (Wang et al. 2013). Collectively the total global production of the precursor POSF was estimated to be 96,000 to 122,500 tonnes, including waste (Paul, Jones & Sweetman 2008).

The year 2010 saw the addition of PFOS, its salts and derivatives to Annexure B of the Stockholm convention (Haug et al. 2010). Currently producers make use of a shorter chain analogues such as Perfluorobutanesulfonic Acid (PFBS) in place of PFOS in their products, such as Scotchguard® in the case of 3M (Naile et al. 2012). Perfluorooctanoic Acid, PFOS's carboxylated eight carbon counterpart, still remains in production and is yet to be listed on the Stockholm Convention Annex B as a POP (UN 2015). This is too the case for PFHxS, the shorter chain (6 carbon) replacement of PFOS (UN 2017). In a similar time frame to that in which PFOS was being regulated and phased out, PFOA production was on the rise globally, with 500 t/year in 2000 growing to 1200t/year by 2004 at one facility (Tardiff et al. 2009). PFAS have never been manufactured in Australia on an industrial scale, however since PFOS was declared a POP it has been imported for speciality uses only. In 2006, 1350 kg of PFOS were imported into Australia designated for use in firefighting (Class B firefighting foam), metal plating (mist suppression), aviation (hydraulic fluid), photography and lithography (surfactants) (DoHA 2008).

Table 1.5 A generalized conceptualisation of PFOS and PFOA production by Electrochemical Fluorination



1.2.2 Chemical Structure, Properties and Fate

PFAS are a class of organofluorine compounds which can have varying chain length and do not naturally occur in the environment due to the high bond energy (approximately 110kcal/mol) required to replace alkyl chain hydrogen atoms with fluorine atoms (Du et al. 2014)(Table 1.6). The carbon bond to fluorine, the most electronegative of the halogens, renders PFAS extremely stable molecules with high resistance to biodegradation, photolysis, hydrolysis and metabolism (Naile et al. 2010; Wang et al. 2013). High C-F bond strength renders the perfluoroalkyl moiety effectively inert in the environment through weak inter/intra-molecular forces which are prevalent due to the low polarizing energy and high ionizing energy of fluorine (Müller et al. 2011). These in turn result in PFAS having a low surface tension (Lau, Butenhoff & Rogers 2004) and the fluorinated carbon chain itself, regardless of length, being both hydrophobic and oleophobic (Ericson et al. 2007) The degree of hydrophobicity typically increases with carbon chain length (Milinovic et al. 2015).

This study focuses on two major groups of PFAS, these are the Perfluoroalkyl Sulfonic Acids (PFSA) and Perfluoroalkyl Carboxylic Acids (PFCAs), in which PFOS and PFOA are considered the leading compounds with respects to the literature attributed to each (Stahl et al. 2009)(Tables 1.7 and 1.9). These two distinct PFAS subgroups are distinguished by the hydrophilic functional group they possess, either carboxylic or sulfonate groups (Labadie & Chevreuil 2011). The hydrophilic head paired with a hydrophobic and oleophobic tail give PFAS its amphiphilic chemical properties (Du et al. 2014; Lau, Butenhoff & Rogers 2004). Functional groups render PFAS molecules both polar and stable, which allows them to act as good surfactants (Müller et al. 2011). This study focuses on PFOS and PFOA, and the shorter 4 and 6 chain PFAS that have succeeded them PFBA, PFBS, PFHxA, PFHxS (Ahrens & Bundschuh 2014; Ateia et al. 2019; Wilhelm, Bergmann & Dieter 2010).

Table 1.6 PFAS Compounds in the present study

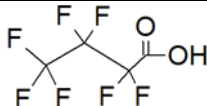
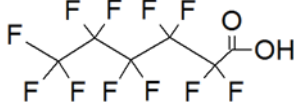
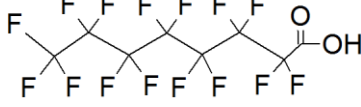
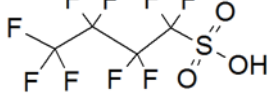

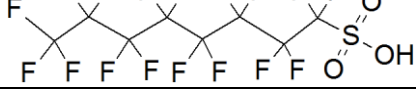
Compound	CAS and Formula	Structure
Perfluorobutanoic acid (PFBA)	375-22-4 CF ₃ (CF ₂) ₂ COOH	
Perfluorohexanoic acid (PFHxS)	307-24-4 CF ₃ (CF ₂) ₄ COOH	
Perfluorooctanoic acid (PFOA)	335-85-9 CF ₃ (CF ₂) ₆ COOH	
Perfluorobutanesulfonic acid (PFBS)	375-73-5 CF ₃ (CF ₂) ₃ SO ₃ H	
Perfluorohexanesulfonic acid (PFHxS)	355-46-4 CF ₃ (CF ₂) ₅ SO ₃ H	
Perfluorooctanesulfonic acid (PFOS)	1762-23-1 CF ₃ (CF ₂) ₇ SO ₃ H	

Table 1.7 PFSA chemical properties

Property	PFBS	PFHXS	PFOS
Appearance (25°C)	Clear liquid (NICNAS 2015b)	White Powder (NICNAS 2015a)	White powder (EFSA 2008)
Molecular Weight (g/mol)	300.10 (NICNAS 2015b)	438.20 (NICNAS 2015a)	538 g/mol (EFSA 2008)
Vapour Pressure (Pa)	631 (25°C) (U.S.EPA 2017b)	59 (25°C) (U.S.EPA 2017b)	3.31×10^{-4} (20 °C) (EFSA 2008)
Water solubility (25°C) (mg/L)	46 – 57 (U.S.EPA 2017b)	2.3 (U.S.EPA 2017b)	680 mg/L (EFSA 2008)
Melting point (°C)	76 – 84 (U.S.EPA 2017b)	58 (Concawe 2016)	>400 °C (EFSA 2008)
Boiling point (°C)	211 (U.S.EPA 2017b)	231 (Concawe 2016)	Not measurable (EFSA 2008)
Log KOW	3.9 (U.S.EPA 2017b)	5.2 (U.S.EPA 2017b)	Not measurable (EFSA 2008)
Log KOC	1 (U.S.EPA 2017b)	1.8 (U.S.EPA 2017b)	2.57 (Higgins & Luthy 2006)
Log KD	No Data	0.6 - 3.2 (U.S.EPA 2017b)	0.30-1.04 (Voogt & Sáez 2006)
Henry's Law Constant (Pa-m³/mol)	No Data	No Data	3.05×10^{-9} (EFSA 2008)
pKa	6.0 to -5.0 (U.S.EPA 2017b)	0.14 (ASTDR 2019)	-3.3 (Brooke, Footitt & Nwaogu 2004)

Table 1.8 PFCA chemical properties

Property	PFBA	PFHxA	PFOA
Appearance (25°C)	Clear Liquid (U.S.EPA 2017b)	Clear Liquid (U.S.EPA 2017b)	White powder/waxy solid (EFSA, 2008)
Molecular Weight (g/mol)	214.039 (U.S.EPA 2017b)	314.054 (U.S.EPA 2017b)	414.1 (EFSA 2008)
Vapour Pressure (25°C) (Pa)	1307 (U.S.EPA 2017b)	457 (U.S.EPA 2017b)	4.2 (EFSA 2008)
Water solubility (25°C) (mg/L)	2.14×10^5 (ASTDR 2019)	15,700 (ASTDR 2019)	9.5 g/L (EFSA 2008)
Melting point (°C)	-17.5 (ASTDR 2019)	14 (ASTDR 2019)	45-50 °C (EFSA 2008)
Boiling point (°C)	121 (ASTDR 2019)	168 (ASTDR 2019)	189-192 °C (U.S.EPA 2017b)
Log KOW	2.8 (U.S.EPA 2017b)	4.1 (U.S.EPA 2017b)	4.81 - 6.30 (3M Company, 1979)
Log KOC	1.9 (U.S.EPA 2017b)	1.9 (U.S.EPA 2017b)	2.06 (Higgins & Luthy 2006)
Log KD	No Data	No Data	1.10-1.57 (Sediment) (DuPont 2003)
Henry's Law Constant (Pa·m³/molh)	1.24 (ASTDR)	No Data	Cannot be estimated (EFSA 2008)
pKa	-0.2 to 0.7 (U.S.EPA 2017b)	-0.13 (U.S.EPA 2017b)	3.8 ± 0.1 (Prevedouros <i>et al.</i> 2006)

PFAS have two major sources to the environment; emissions generated during the manufacturing process (Prevedouros et al. 2006) and liberation during the use, disposal or leaching from products post-manufacture (Müller et al. 2011; Zareitalabad et al. 2013). Boulanger et al (2005), for example, tested common 1994 surface protection products and determined they contain 6 different PFAS compounds including PFOS and PFOA. However, is estimated that up to 80% of PFAS in the environment are present due to fluoro-polymer production (Prevedouros et al. 2006). An early example of liberation to the environment via use would be the Toronto airport fire discussed briefly in Lechner and Knapp (2011) where 48m³ of AFFF was applied to extinguish a burning aircraft, equating to an estimated release of 240 – 720 kg of PFOS salts to the environment. However, liberation of PFAS as AFFF more frequently tends to be in the case of firefighting training and maintenance for Civil, Naval, Army and Airforce purposes than for emergencies (Bräunig et al. 2019; Dauchy et al. 2019; Hale et al. 2017; Høisæter, Pfaff & Breedveld 2019). In Australia the use of PFAS containing AFFF and associated contamination has been well documented at training and emergency sites such as RAAF (Royal Australian Air Force) Base East Sale (Senversa 2017), Fiskville Country Fire Authority (CFA) Training College (Cardno-LanePiper 2014) and more recently, in the Footscray Industrial Fires (EPA-Victoria 2018a). In all cases, the leachability of PFAS from soil and sediment and subsequent transport pathways, in groundwater or surface water to sensitive receptors has been a major concern (Cardno-LanePiper 2014; Senversa 2017; EPA-Victoria 2018a). Table 1.9 outlines maximum values detected in sediment, soils, surface water and groundwater at each site.

Table 1.9 Maximum PFOS and PFOA concentrations detected at 3 AFFF affected sites in Victoria, Australia.

Site	Compound	RAAF Base East Sale (Senversa 2017)	Fiskville CFA Training College (Cardno-LanePiper 2014)	Footscray Industrial Fires (EPA-Victoria 2018a)
Soil (mg/kg)	PFOS	440*	0.258	-
	PFOA	0.84	0.0204	-
Sediment (mg/kg)	PFOS	0.881	0.79	4900
	PFOA	0.0084	0.0007	-
Surface Water (µg/L)	PFOS	0.494	28.3	4.92
	PFOA	0.009	27	0.294
Groundwater (µg/L)	PFOS	4910	-	-
	PFOA	280	-	-

*This is an uncharacteristically high result, typically PFAS contamination is in the 100 to 1000 µg/kg range around these kinds of sites. This sample was likely taken at the source.

The degradation of various PFAS precursors or unstable PFAS compounds to stable products such as PFOA (Jiang et al. 2012) and PFOS (Ericson et al. 2007; Olsen et al. 2003) through biological or chemical means could also be considered a source (Houde et al. 2006; Labadie & Chevreuil 2011; Shaw et al. 2009). Fluorotelomer alcohols are known to degrade to PFOA in the environment (Haug et al. 2011), as demonstrated by Wang et al (2005) through biodegradation of carbon-labelled 8-2 fluorotelomer alcohol (8:2 FTOH). Nowhere is degradation more evident than in Waste Water Treatment Plants (WWTPs) where influent PFOS and PFOA levels are often exceeded by those seen in the effluent (Loganathan, B. & Bommanna 2007). This results in WWTPs behaving as an intermediate source of PFAS to the environment (Lechner & Knapp 2011; Müller et al. 2011). Huset et al. (2011) observed that, in 6 landfills, leachates which contained PFAS, PFASs were the most abundant reaching

2800 ng/L, closely followed by shorter chained PFASs (2300ng/L). Table 1.10 briefly outlines key studies that support the degradation of PFAS precursors to PFOA and PFOS and their detection in WWTPs and landfills.

The mobility of PFAS in the environment is complex due to their unique amphiphilic nature (Du et al. 2014). As a consequence, they do not behave as most hydrocarbons would in the environment (Figure 1.1 and 1.2) (Labadie & Chevreuril 2011; Ericson et al. 2007). Solubility in water is solely attributed to the hydrophilic head rendering the molecule less hydrophobic than it is oleophobic (Lau, Butenhoff & Rogers 2004). PFAS with less than 8 carbons tend to have a greater water solubility (Kalbe et al. 2014). PFOS and PFOA disassociate in water, the extent of which is complete for PFOS and approximately 94% for PFOA, at environmentally relevant pH levels (EFSA 2008; Prevedouros et al. 2006). Prevedouros et al (2006) suggested that, while PFAS are short-lived in the atmosphere due to low vapour pressure, they are likely transported via oceanic aerosols within the atmosphere. Detection of various PFAS in the sera of arctic organisms, with some exceeding 3000 ng/mL, suggests that PFAS are extremely mobile and widespread in the marine environment (Houde et al. 2006).

PFAS are reported to exhibit a variety of different behaviours in water and soil solutions, including the formation of bilayers, monolayers, micelles and hemi-micelles (Du et al. 2014). Mobility in soil solutions through leaching is namely governed by PFAS functional groups, where PFCAs tend to be more mobile than PFASs in soil solutions (Gellrich, Stahl & Knepper 2012). The chemical qualities (pH, surface area, CEC, and organic carbon) of the soil play a major role in PFAS mobility and migration to groundwaters (Kalbe et al. 2014). Further, sorption behaviour in soils appears to be a factor of chain length (hydrophobicity) (Milinovic et al. 2015). Gellrich, Stahl & Knepper (2012) found longer chain PFAS displace shorter chain PFAS and groundwater tends to contain namely PFAS with <7 carbons.

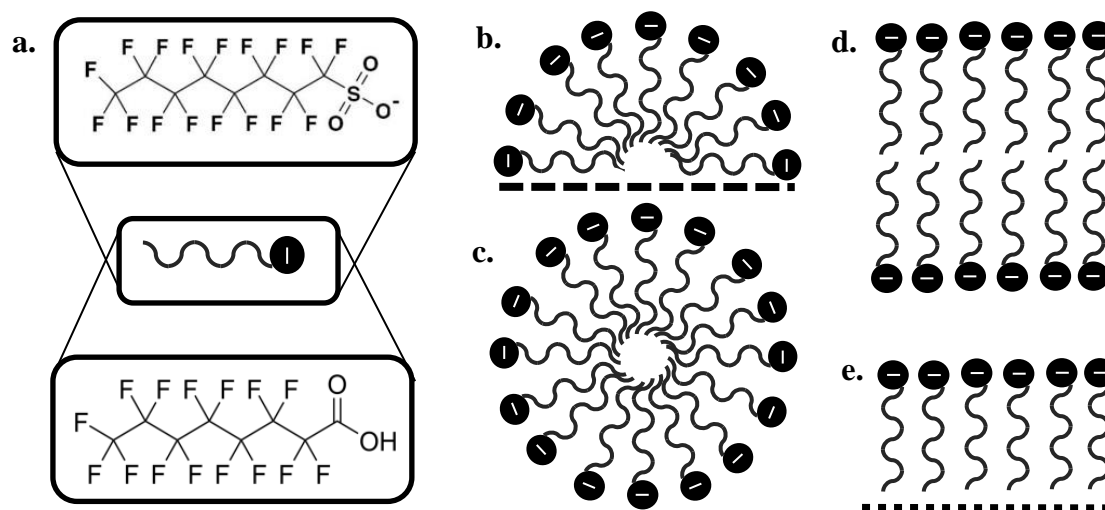


Figure 1.1 Behaviours attributed by amphiphillia: **a.** Top PFOS and Bottom PFOA demonstrating polar hydrophilic heads and hydrophobic tails. **b.** Multiple PFAS form hemi-micelle on a surface (dotted line). **c.** formation of a micelle. **d.** Formation of a bilayer. **e.** Formation of a monolayer on a surface (dotted line)

Due to their resistance to degradation, long half-life, complex behaviours, and lack of ultimate sink; PFAS are considered ubiquitous in environmental matrices (Naile et al. 2010; Zareitalabad et al. 2013). In short term, organisms, water bodies and soils can be considered temporary sinks until PFAS are remobilized or liberated. PFAS are known to bioaccumulate in organisms (Gellrich, Stahl & Knepper 2012; Naile et al. 2010). This property renders organisms a sink for PFAS until they are excreted, or the organism is consumed or decomposed. Likewise, PFAS such as PFOS often sorb onto solids, thusly sediments and sewage sludge are considered major sinks for this group of PFAS (Higgins et al. 2005; Huset et al. 2011; Labadie & Chevreuil 2011). Sewage sludge is a point of major concern, in light of their increasing popularity for land application, which may in turn render receiving soils a sink to organic matter bound PFAS (Schultz, Barofsky & Field 2006; Sepulvado et al. 2012). Table 1.10 explores key studies regarding PFAS found in WWTP sludge. Conversely, PFCAs are soluble and ultimately make their way into waterways and finally the ocean (Wang et al. 2013; Xiao et al. 2015). Thompson et al (2011) examined the fate of recalcitrant PFAS in two separate water reclamation plants in Australia, it was found that without reverse osmosis, most compounds remained at the same concentration in tap water or did not change at all.

Table 1.10 Key early PFAS studies in WWTPS

Study and Objective	Key Findings
<p>Sinclair & Kannan 2006</p> <p>Study PFAS in influent, effluent and anaerobic sludge of 6 WWTPs in New York State (USA)</p>	<ol style="list-style-type: none"> (1) PFOS in effluent ranged 3-68 ng/L (2) PFOA in effluent ranged 58 – 1050 ng/L (3) PFOS and PFOA concentration higher in effluent than anaerobic sludge (degradation of precursors) (4) Larger chain compounds preferred to partition into sludge, where the concentration of odd chain length was higher than even.
<p>Loganathan et al. 2007</p> <p>Study PFAS in influent, effluent and anaerobic sludge of 2 WWTPs (Georgia and Kentucky, USA) which had a collective treatment of 88.1 million litres per day.</p>	<ol style="list-style-type: none"> (1) PFOS ranged 2.5 – 990 ng/g dry weight in sludge and ranged 1.8 – 149 ng/L in effluent (2) PFOA ranged 7.0 – 219.0 ng/g dry weight in sludge and 1 – 334 ng/L in effluent (3) PFOSA, PFHxS, PFNA, PFDA, detected in all samples. (4) PFOS and PFOA concentration higher in effluent than anaerobic sludge (proposed degradation of precursors)
<p>Becker, Gerstmann & Frank 2008</p> <p>Study PFAS in influent, effluent and sludge of 4 WWTPS in Northern Bavaria (Germany)</p>	<ol style="list-style-type: none"> (1) Effluent PFOA concentration 20 fold higher than influent. Estimated 1/10 remains in sludge (2) Effluent PFOS concentration 3 fold higher than influent. Estimated 50% of PFOS remains in sludge
<p>Sun et al. 2011</p> <p>Study PFAS in anaerobic sludge of 20 Swiss WWTPs.</p>	<ol style="list-style-type: none"> (1) PFOS ranged 15 – 600 µg/kg dry weight in sludge (2) Total PFCAs ranged 14 – 950 µg/kg dry weight in sludge

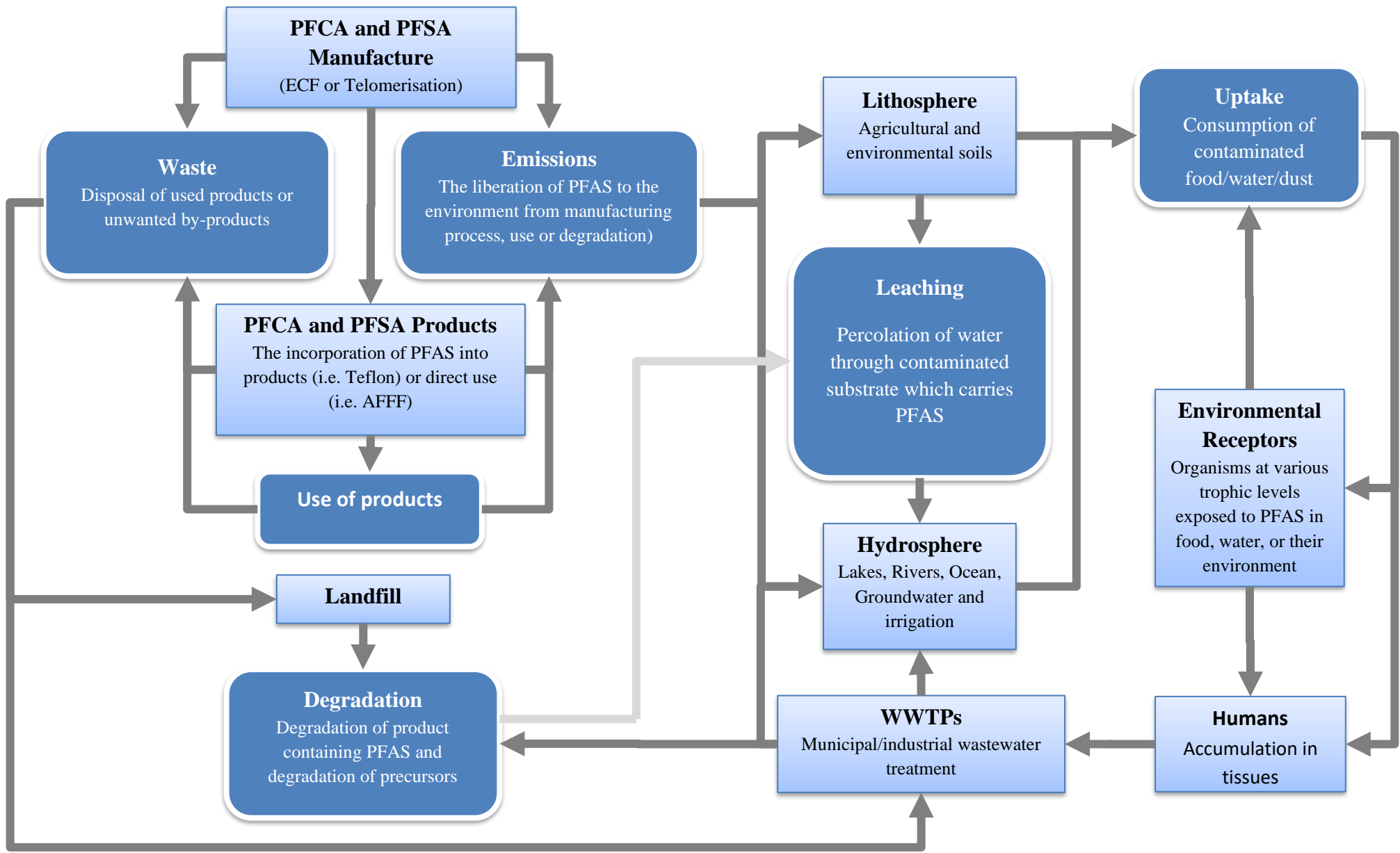


Figure 1.2 Conceptual flowchart depicting the cycle of PFAS from production to receptors as well as their recirculation within the environment

1.2.3 Toxicity

Exposure routes to PFAS are primarily by ingestion of contaminated food or water (Borg. et al. 2013). Direct contact is not believed to be an uptake route for humans (HEPA 2018), but probable for aquatic organisms including plankton (Ahrens & Bundschuh 2014). Additionally, inhalation of PFAS contaminated dust or aerosols has been found to present an additional pathway, in which dust concentrations ranging 4.6 – 5065 ng/g PFOS and 2.3 – 3700 ng/g PFOA have been detected (EFSA 2008). Haug et al (2011) suggested in a study in Norway, house dust could account for up to 50% of total PFAS uptake. In a recent Australian study, the NSW EPA concluded that exposure to PFAS in dust to on-base personnel stationed on contaminated RAAF bases could account for up to 18 % of the equivalent PFOS enHealth TDI (enHealth 2019; EPA 2017).

In consideration of the above exposure pathways, the most common route of PFAS exposure is the consumption of contaminated food and water (Haug et al. 2011). This exposure route is prevalent in humans where not only is the food itself contaminated but PFAS-containing packaging are often in direct contact with food products (D'eon & Mabury 2010). A study by Hradkova et al (2010) detected PFOS (0.7 – 12.8 µg/kg) and PFOA (1.2 to 5.1 µg/kg) in canned tuna. Contrastingly, Haug et al (2010) correlated the consumption of fish to the increased sera concentration of PFOA, Perfluoroundecanoic Acid (PFUnDA) and PFOS in his Norwegian subjects. Mak et al (2009) studied the concentrations of PFAS in tap water in the US, China, Japan, India and Canada. The study detected PFOS Perfluorohexanoic Acid (PFHxS), PFBS, Perfluorooctane Sulfonamide (PFOSA), Perfluorododecanoic Acid (PFDoDA), PFUnDA, Perfluorodecanoic Acid (PFDA), Perfluorononenoic Acid (PFNA), Perfluoroheptanoic Acid (PFHpA), Perfluorohexanoic Acid (PFHxA) and Perfluorobutanoic Acid (PFBA) in 100% of analysed samples. Recent studies in the United States have demonstrated PFAS, including concentrations above human health guidelines, are present in supermarket produce such as beef, poultry, seafood, vegetables, fruit, chocolate cake, milk and cheese (FDA 2019a, 2019b).

The study by Stahl et al (2009) highlighted the variation of PFAS uptake by various food plants, where PFAS were found to namely translocated to the vegetative parts of the plants examined. Lechner and Knapp (2011) further explored the transfer of PFOS and PFOA from soil to plant by means of calculating the transfer factor (Transfer Factor (TF) = Concentration of PFAS in plant/ Concentration PFAS in soil) for various species. Important correlations have been observed illustrating the trophic magnification of PFAS through producer and primary consumer levels. This is of great consequence to organisms higher on the food chain (Tomy et al. 2004). Recently, a number of studies have explored the transport of PFAS into plants of agricultural importance, including the increasingly encountered short chain PFAS (Ahrens & Bundschuh 2014; Ghisi, Vamerli & Manzetti 2019; Lechner & Knapp 2011; Liu et al. 2019; Stahl et al. 2009; Zhou et al. 2019; Zhu & Kannan 2019). Uptake behaviour of PFAS into many plants has been demonstrated to be higher for short chain PFAS, this is notable due to their high mobility and increased frequency of use, perhaps suggesting a higher likelihood of human exposure to short chain PFAS through food (Ahrens & Bundschuh 2014; Ghisi, Vamerli & Manzetti 2019; Zhou et al. 2019; Zhu & Kannan 2019).

Further exposure routes exist between mother and child, where children can be exposed prenatally (through blood and placenta) or postnatally through breast feeding. Kärman et al (2007) estimated, using mothers' sera levels, that through breast feeding the mother-child total PFAS transfer could be as high as 200 ng/day. This

was reinforced in Pinney et al (2014) where a similar correlation was found between mother-child PFAS transfer (specifically PFOS, PFHxS and PFOA) and the duration of breast feeding.

Using pooled serum data from the Australian population, Thompson et al (2011), observed that Australians have PFOA and PFOS sera levels similar to those seen globally. This study went further by modelling estimated exposure of Australians, finding values of $100 \pm 37 \text{ ng day}^{-1}$ and $54 \pm 15 \text{ ng day}^{-1}$ PFOS and PFOA respectively. The Australian Department of Health has set tolerable daily intake values of $0.02 \mu\text{g/kg}$ (body weight)/day and $0.16 \mu\text{g/kg}$ (body weight)/day for PFOS and PFOA respectively, as per studies commissioned to Food Standards Australia New Zealand (enHealth 2019).

PFAS resilience to degradation (particularly metabolism) and very slow elimination (including humans) (Gannon et al. 2011) results in bioaccumulation within the tissues of the organism (Naile et al. 2010). Bioaccumulation becomes more prominent when carbon chains reach a length of 6 to 7 carbons (Martin et al. 2004). It has been suggested that shorter PFAS chains and FTOHs tend to be less bioaccumulative and are therefore considered less toxic (Gellrich, Stahl & Knepper 2012; Ochoa-Herrera & Sierra-Alvarez 2008) (Martin et al., 2003). However the degradation of many PFAS compounds into more stable PFOA and PFOS has been explored as a likely drawback (Shaw et al. 2009) (Wang et al. 2009). Table 1.11 briefly explores key animal studies underpinning rates of elimination in humans and animals.

Unlike most other halogenated organic contaminants, PFAS do not accumulate in lipid based tissues as they are proteophilic instead of lipophilic (Hradkova et al. 2010). Instead PFAS accumulate in blood (binding to blood proteins) (Deon & Mabury 2010; Kim et al. 2013) and organs (liver and heart) (Hradkova et al. 2010; Xia et al. 2011). Persistence in human blood is attributed to the kidneys actively transporting PFAS back into the blood stream in place of excreting them (Gannon et al. 2011). Deon and Madbury (2010) observed very different results in rats, which could excrete PFAS, however a large time difference between males (8-30h) and females (1h) was noted. Further, PFAS are known to cross the plasma blood membrane, cross the placenta and has been found in cord blood allowing wide distribution and accumulation throughout the body (EFSA 2008).

The slow elimination of PFAS from the human body is best illustrated by the study in Hölzer et al. (2009) where 40,000 residents formerly exposed to PFOA contaminated drinking water in Sauerland (Germany) were studied. Water PFAS concentrations peaked in May 2006 ($500 - 640 \text{ ng L}^{-1}$) and were lowered to 10 ng/L by activated carbon by July 2006. Study of resident blood plasma over this time period revealed PFOA levels 4.5-8.3 times higher than the national average, where return studies determined a reduction in burden of 10% in men, 17% in mothers and 20% in children per year.

Table 1.11 Key early PFAS animal studies in the environment

Study and Objective	Key Findings
<p>(Kannan, Newsted, et al. 2002)</p> <p>Mink and otter liver PFOS, FOSA, PFHxS and PFOA concentrations studied.</p>	<ol style="list-style-type: none"> (1) Maximum otter and mink liver wet weight concentrations observed for PFOS (5140 ng/g), FOSA (590 ng/g), PFHxS (39 ng/g), and PFOA (27 ng/g), (2) PFOS and FOSA concentrations correlated. (3) PFAS concentrations increased near urbanized/industrial zones
<p>(Martin, JW et al. 2004)</p> <p>Studied 6C and higher PFCAs in the livers of various arctic mammals, fish and birds.</p>	<ol style="list-style-type: none"> (1) Odd chain length PFCAs exceeded concentration even (2) Trophic biomagnification observed
<p>(Smithwick et al. 2005)</p> <p>Analysed Polar bear livers and blood from for PFAS, in Europe and US artic.</p>	<ol style="list-style-type: none"> (1) Total PFAS ranged 435-2140 ng/g wet weight (2) Concentrations of PFAS in liver correlated in one location with PCBs 180, 153, 138 and 99 in adipose tissue. (3) PFOS con correlated with age. (4) Correlation between PFAS with adjacent chain lengths were observed (ie. C9:C10, C10:C11)
<p>(Holmström, Järnberg & Bignert 2005)</p> <p>PFOS and PFOA measured in archived Baltic Sea Guillemot eggs (1968 – 2003).</p>	<ol style="list-style-type: none"> (1) PFOS concentrations increased in the 35 years span from 1968 to 2003 from 25 to 614 ng/g, respectively (2) 30 PFOS fold increase over time period. (3) PFOA below limit of detection

In general, a vast set of impacts have been observed in animals and humans that have been contaminated with PFAS, in the lab and environment alike. However, the links between PFAS and human disease still need further establishment (enHealth 2019). Toxic effects of PFAS include those listed below:

- **Peroxisomal proliferation (liver)** Interference with a number of genes involved in lipid metabolism and utilisation, inflammation, fetal growth, hormone and immune function and possibly cancer growth (Dixon et al. 2012; Klaunig, Hocevar & Kamendulis 2012; Zhang et al. 2011). Ericson et al. (2007) had highlighted that PFOA could induce peroxisomal β -oxidation in the liver of male rats;
- **Mitochondrial injury** or dysfunction through prenatal and early life exposure (Xia et al. 2011), playing a role in apoptotic death of cell through depolarisation of plasma membrane potential and acidification (Ericson et al. 2007; Kleszczyński & Składanowski 2011);
- **Serum reductions in cholesterol and thyroid hormones** (Lau, Butenhoff & Rogers 2004);
- **Immunotoxicity** (Haug et al. 2010). PFOS and PFOA suppress cytokine secretion by immune cells in human blood cells through the modulation of transcription of a host of chemical messengers (Corsini et al. 2011);
- **Hepatotoxicity** (EFSA 2008; Lau, Butenhoff & Rogers 2004);
- **Carcinogenicity**. (EFSA 2008);
- **Endocrine disruption**. PFOA may alter female pubescent timing (Dixon et al. 2012). La Rocca et al (2012) investigated infertility in 53 couples and concluded that infertile subjects tended to have a higher serum concentration of PFOS than Italian national average; and
- **Developmental toxicity**. Kim et al (2013) showed PFAS (notably PFNA and PFuDA) to be teratogenicity and developmental toxicants through the testing of frog embryos in the lab.

1.2.4 Monitoring Programmes, Restrictions and Control

The presence of PFAS in humans was first reported by (Taves 1968). It is suggested that the PFAS most likely detected was PFOS or PFOA (Lau, Butenhoff & Rogers 2004). Forty-two years since PFAS production started PFOS alone has been added to the restrictive Annexure B of the Stockholm convention. Many countries have employed their own monitoring programs, restrictions, guidelines or outright bans of PFAS. These have been put in place both before and after 2010 listing of PFOS as a POP. Contrasting to this, many developing countries have not restricted the use or manufacture of any PFAS (Du et al. 2014).

PFOS and related compounds have been banned in the EU since 2008 (Gellrich, Stahl & Knepper 2012), and all products are required to have less than 0.005% PFAS in their final form (DoHA 2008). EU – Directive 2006/122/EC 12 December 2006 restricts the use and marketing of PFOS containing products. Regional action has been prominent in many countries. For example, Bavaria (Germany) implemented monitoring programs and guidelines for the total concentration of 11 target PFAS in 2008, allowing a maximum of 100 µg total PFAS per kilogram of sludge intended for agricultural application (Lechner & Knapp 2011). In the United States PFOA and PFOS have been nominated to be National Health and Nutrition Examination Survey (NHANES) monitored chemicals, meaning that it is now policy that PFAS are monitored in humans (Lau, Butenhoff & Rogers 2004). At the time, little data characterised the total human intake of PFAS, most countries did not have a routine drinking-water quality control management plan with respects to the control of PFAS (Xiao et al. 2015). Further data improving the scale of understanding of the health risk posed by PFAS permeating drinking water and produce from contaminated sites spurred the drafting of the US EPA's PFAS Action plan in 2019, which aims to address the long term concerns posed by PFAS contamination in the United States through a set of guidelines (USEPA, 2019). Similarly, in Australia guidelines for PFAS have been developed by the heads of the EPA's Australia New Zealand (HEPA) as the PFAS National Emergency Management Plan (NEMP). The PFAS NEMP outlines Guidelines for human health and ecological health relevant to soil, food and water (Table 1.12). It also includes allowable limits for disposal and storage in the forthcoming draft the NEMP goes further to address PFAS in waste water treatment plants (HEPA 2018).

A variety of guidelines have been proposed for PFAS intake, starting with 3M's Drinking Water Health Advisory draft lifetime exposure level of 1ppb PFOS (3M 2001). In 2008 the EFSA determined the safe Total Daily Intake (TDI) of PFOS and PFOA to be 150 ng kg⁻¹ bodyweight and 1.5 ng kg⁻¹ bodyweight respectively (EFSA 2008). Independent studies have set out drinking water equivalent levels (DWEL) with respects to cancer (testicular adenoma) undertaken in which the non-cancer level in humans was suggested to be of 0.88-2.4 µg L⁻¹ tap water (Tardiff et al. 2009). Wilhelm, Bergmann & Dieter (2010) more recently investigated shorter chain compounds and developed a lifelong expose long-term lowest maximal quality goal (general precautionary value) for total PFAS in drinking water suggesting 0.1 ng/L total PFAS appropriate. In the State of Michigan, drinking water standards have been set far lower than those seen in both the United States and Australia, and encompassed additional PFAS congeners, including PFNA (6 ng/L), PFOA (8 ng/L), PFHxA (400,000 ng/L), PFOS (16 ng/L), PFHxS (51 ng/L), PFBS (420 ng/L), and GenX (370 ng/L), testament to the growing concern over the PFAS class (EGLE 2019).

Table 1.12 Key PFAS guideline values from HEPA’s PFAS NEMP

Guideline	PFOS	PFOS + PFHxS	PFOA	
Health Based Guidance Values				
Tolerable Daily Intake (µg/kgbw/d)	0.02	0.02	0.16	
Drinking water quality value (µg/L)	0.07	0.07	0.56	
Recreational water quality value (µg/L)	0.7	0.7	5.6	
Soil Criteria for Investigation – Human Health-based Guidance Values				
Residential - garden/accessible soil (mg/kg)	0.01	0.01	0.3	
Residential with little soil access (mg/kg)	2	2	20	
Public open space (mg/kg)	1	1	10	
Industrial/ commercial (mg/kg)	20	20	50	
Soil Criteria for Investigation – Ecological Guideline Values				
Interim soil - direct exposure (mg/kg)	1	-	10	
Interim soil - indirect exposure (mg/kg)	0.01	-	-	
Terrestrial Biota Guideline Values				
Mammalian diet –aquatic biota ww (µg/kg)	4.6	4.6	-	
Avian diet –aquatic biota ww food (µg/kg)	8.2	8.2	-	
Bird egg ww µg/kg	0.2	0.2	-	
Freshwater and Marine Guideline Values				
Freshwater 99 % species protection (µg/L)	0.00023	-	19	
Freshwater 98 % species protection (µg/L)	0.13	-	220	
Freshwater 95 % species protection (µg/L)	2	-	632	
Freshwater 80 % species (µg/L)	31	-	1824	
Landfill Acceptance Criteria				
Double Lined Composite	Total (mg/kg)	50	50	50
	ASLP (ug/L)	7	7	56
Clay/single composite lined	Total (mg/kg)	50	50	50
	ASLP (µg/L)	0.7	0.7	5.6
Unlined	Total (mg/kg)	20	20	50
	ASLP (µg/L)	0.07	0.07	0.56

In consideration of the guidelines and emergency management plans instated in both Australia and the United States, it is clear that PFAS migration pathways to sensitive receptors, ecological or human, is of great concern to regulators and the public. To address this, several remediation methods for the management of PFAS are under development or in the early stages of application. Currently PFAS management falls into one of two approaches coupled to disposal or destruction; immobilisation or removal.

Immobilisation centres on obstructing contaminant-receptor pathways. This is largely achieved through the application of sorbents and physical barriers which either bind PFAS to sorbents or reduce the infiltration of water which may leach PFAS from the contaminated material. A number of sorbents have been applied to PFAS immobilisation, including activated carbons, biochars, polymers and nanoparticles (Hale et al. 2017; Kupryianchyk et al. 2016; Ross et al. 2018; Silvani et al. 2019; Zhang, Zhang & Liang 2019). Stabilization of materials using cementitious products or coatings has been successfully demonstrated to reduce PFAS mobilisation associated with the ingress of water (Söregård, Kleja & Ahrens 2019).

Removal technologies are better suited to surface, waste and ground water rather than soils due to ease of handling and contact with sorbent. PFAS have successfully been removed from solution by reverse osmosis as well as through the application of activated carbon, polymers, anion exchange resins, biochar, carbon nanotubules,

and zeolite (Horst et al. 2018; Kucharzyk et al. 2017; Kupryianchyk et al. 2016; Ross et al. 2018; Silvani et al. 2019; Tang et al. 2006; Zaggia et al. 2016; Zhang, Zhang & Liang, 2019). However, these methods have varying levels of success outside of PFOS and PFOA, depending on the type PFAS compounds present in the contaminated water (Ateia et al. 2019). Unfortunately, all the discussed treatment methods produce waste products either as PFAS contaminated sorbent or brine containing concentrated PFAS (Ateia et al. 2019). It follows that the effective application of these management strategies is largely limited by the current lack of destructive or disposal options for captured PFAS (Ross et al. 2018). Currently, disposal of contaminated soils and filter media is largely by landfill or incineration (Kucharzyk et al. 2017), however there is growing concern that PFAS contaminants will escape and re-enter the environment. Oxidative techniques are being explored (Dombrowski et al. 2018), however PFASs resistance to chemical oxidation proves a challenging task to overcome on a large scale, particularly in situ. Electrolytic and plasma arch technology have been demonstrated as applicable PFAS destruction techniques (Shangtao et al. 2018; Singh et al. 2019; Zhang et al. 2014), however this technology is expensive, power demanding and generally immobile. Lastly, bioremediation has thus far found little success for the degradation of PFAS, but bio-attenuation by constructed wetlands may be a promising approach for passive PFAS remediation (Yin et al. 2017)

The current bottleneck in PFAS management exists namely around the lack of low cost PFAS remediation options. Existing technologies are currently not at a stage of implementation which makes them sufficiently accessible to address the large scale PFAS contamination in a cost effective or practical manner (Kucharzyk et al. 2017; Ross et al. 2018). The present work aims to contribute to the interim immobilisation and capture of PFAS in a cost effective and sustainable manner, whilst effective long-term PFAS management options are further developed.

Chapter 2

PFAS-Biochar Sorption

2.1 Biochar as a Sorbent

Sorbate interactions with biochars are greatly influenced by biochar specific surface morphologies such as surface charge, surface functional groups, pore size, surface area and degree of aromatisation (Figure 2.1) (Du et al. 2014). Kinetics is the term used to explain the temporal behaviour of the sorption process, where sorption is a generalised term used to describe both the adsorption and absorption behaviours of a sorbate for a sorbent under specific environmental conditions. Adsorption refers specifically to sorbate adherence to a surface whereas sorption encompasses this process as well as partitioning (Tang, J et al. 2013). Biochar consists of an aromatic and an aliphatic fraction, where the aromatic fractions' dominant sorption mechanism is pore filling as a non-linear solute-solute competitive system (Qian et al. 2015). Comparatively, the aliphatic fraction behaves as a partitioning phase where sorption is generally linear and non-competitive (Qian et al. 2015).

Biochar surfaces, like minerals, can have permanent or temporary charges due to structurally derived charge deficits (net charges), surface functional groups or changes in solution pH affecting potential determining ions such as hydrogen (H^+) and hydroxyl (OH^-) (Martin et al. 2012; Rees, Simonnot & Morel 2014). For example, oxygenated surface functional groups (carboxyl, hydroxyl, and phenol) are binding sites for environmental contaminants such as heavy metals (Uchimiya, Chang & Klasson 2011) (Méndez et al. 2014; Qian et al. 2015) and dyes (Leng et al. 2015). The predominant electrostatic mechanisms likely to occur at oxygen containing surface functional groups are acid-base or complex redox reactions (Qian et al. 2015; Rees, Simonnot & Morel 2014; Uchimiya, Chang & Klasson 2011). Sorbates are bound to biochar surfaces through the electrostatic processes whereby the sorbate is attracted to charged surfaces or interacts with aromatic carbon double bond π -electrons (Rees, Simonnot & Morel 2014). Biochars labile fraction may in some cases result in the formation of stable metal complexes which precipitate out of solution with other mineral phases (Rees, Simonnot & Morel 2014).

Similarly, biochar has a demonstrated capability in immobilising and reducing the bioavailability of organic compounds in soils through sorption (Denyes et al. 2012; Wu et al. 2013). Examples include methyl mercury (Gomez-Eyles et al. 2013), certain PCBs (Denyes et al. 2012), pesticides (Dechene et al. 2014; Wang et al. 2010; Yu et al. 2010) and PAHs (Rakowska et al. 2014). It has been shown that the sorption capacity of biochars for organic compounds, particularly the non-polar, is largely controlled by biochar organic matter content and its degree of aromatisation (Li et al. 2014), where the predominant sorption mechanisms for organic compounds are Van De Waals forces and chemisorption (Semple et al. 2013). Sorption of organic compounds is typically fast in the initial stages, slowing in the later stages. These phases correlate with the irreversibly bound fraction, which dominates the later stages of sorption. Biochars produced at high temperature have a higher aromatic fraction, accompanied by higher surface area and porosity which render surface adsorption the dominant sorption

mechanism (Denyes et al. 2012; Qian et al. 2015; Tang et al. 2013). Partitioning to organic matter is generally relatively weak (reversible) and linear compared to adsorption to the biochar surfaces which is stronger (less reversible) and non-linear (Denyes et al. 2012). Less reversible sequestration involves the diffusion of sorbates into micropores and surfaces in which they become inaccessible (Semple et al. 2013). Biochars produced at lower temperatures have lower aromatic fractions, here organic compounds will predominantly partition into non-carbonized organic matter (Dechene et al. 2014; Qian et al. 2015; Tang et al. 2013).

Biochar is largely a heterogeneous material with varying proportions of aromatic and aliphatic fractions, as such a dual-mode sorption model is employed, as it is likely that both adsorption and partitioning are occurring simultaneously (Semple et al. 2013). In addition, the complex interplays between surface functional groups and surface area are evident in several studies outlined a review (Du et al. 2014), in which both mechanisms contribute to the sorption of sorbates. The understanding of biochar sorption mechanisms is essential to optimise biochar production conditions to be favourable of the physicochemical characteristics which drive sorption mechanisms for a target sorbate.

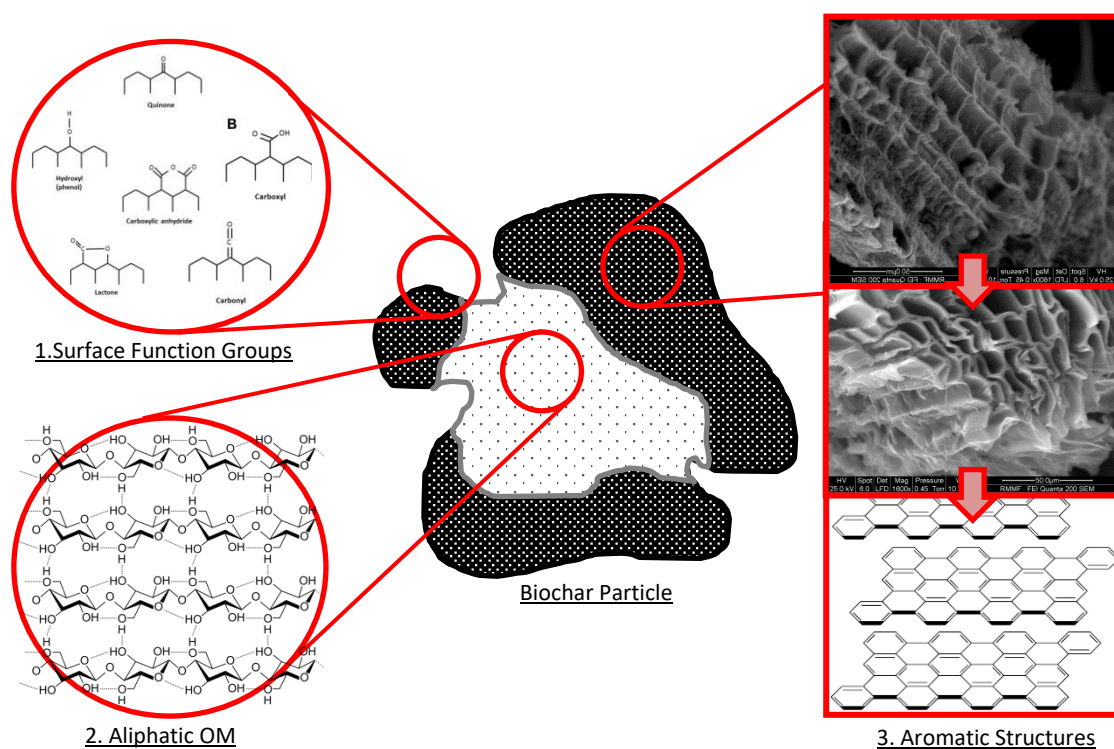


Figure 2.1 Generalized Biochar model demonstrating three notable mechanisms discussed as playing major roles in PFAS sorption: 1). Surface Functional Groups 2). Aliphatic Organic Matter 3). Aromatic Structures

2.2 PFAS Sorption to Biochar

Currently the mechanisms driving biochar as a sorbent for PFAS is poorly understood. Studies frequently compare biochar with other sorbents such as activated carbon (Du et al. 2014). Most studies suggest that hydrophobic interaction is the key driver for PFAS sorption to carbonaceous sorbents. This has been largely observed with PFAS sorption capacity being greater for sorbents with higher surface area, and sorption increasing with increasing PFAS congener carbon chain length (hydrophobicity)(Dalahmeh, Alziq & Ahrens 2019; Liu et al. 2019; Ray et al. 2019; Silvani et al. 2019; Xiao et al. 2017; Zhi & Liu 2018).

2.2.1 PFAS Compound Specific Sorption Behaviour

PFASs exist in the environment at relatively low aqueous concentrations, typically ranging from low ng/L to low mg/L in more contaminated environments (Chen et al. 2012; Hansen et al. 2010; Yu. & Hu 2011). While PFAS concentration in solution plays a major role in PFAS sorption behaviour to biochar, PFAS congener specific physiochemical attributes determine PFAS sorption behaviour overall.

Access to pores may be limited by PFAS molecule size, based on structure PFOS and PFOA are approximately 1.4 nm x 0.4 nm (Carter & Farrell 2010), allowing these molecules access into most pores, but excluding them from some primary micropores (pores <2 nm diameter)(Yu et al. 2012). Based on this size, PFOA and PFOS require an approximate 0.6 nm² of surface area per molecule for surface sorption to occur (Carter & Farrell 2010), where smaller pores may result in size restriction based exclusion of PFAS and larger pores allow the formation of aggregates and micelles (Du et al. 2014). Importantly, smaller pores result in desorption processes being less likely to occur due to limitation of access of solutions to occupied pore spaces (Carter & Farrell 2010). It is therefore likely that pore size restriction by chain length is one of many factors behind the varied sorption of PFASs from solution onto carbonaceous sorbents such as activated carbon (Hansen et al. 2010). Chularueangaksorn et al. (2014) found that PFBS entered pores more readily than larger PFAS as a factor of both its size and increased hydrophilic behaviour. This suggests that in addition to pore size exclusion, increasing chain length can manifest as an decrease in sorption due to increased hydrophobicity hindering access to pores (Zhao et al. 2011). Total surface coverage for PFOS has been estimated to be as high as 20 molecules per nm² on the basis of molecule size and assuming a normalized orientation with complete coverage (no spaces) which differs from the 0.6nm² per molecule simply as a factor of molecular orientation (parallel vs. adjacent)(Chen et al. 2012).

The chain length of the perfluorinated moiety and type of functional group each effect a given PFAS's sorption behaviour (Figure 2.2) (DME 2013). Each of these structural parameters contribute to PFAS adsorption-desorption constants (K_d). Where K_d is a constant used to demonstrate a compounds mobility in the environment with respects to its propensity to be in solution (low K_d) or sorb to solids (high K_d). Each additional PFAS CF₂ moiety results in approximately 0.5-0.6 log units higher K_d (Higgins & Luthy 2006), and sulphonate functional groups contribute an additional 0.26 log units to K_d over that of a carboxylic acid functional group (Higgins & Luthy 2006). Those compounds with lower K_d are far less likely to partition onto biochar, suggesting that order of effect in partitioning is Chain length < Sulphonate < Carboxylic Acid (Yu & Hu 2011). Structural rigidity may also limit sorption, where the inner regions of pores may find the rigid PFAS shape to be energetically unfavourable (Hansen et al. 2010). Functional groups determine the pKa of PFASs, most of which have low pKa

and therefore predominantly exist as anions in the environment (Du et al. 2014; Shin et al. 2011). PFAS sorption to carbonaceous sorbents could therefore be described as increasing with chain length, lower water solubility and increased hydrophobicity (Du et al. 2014).

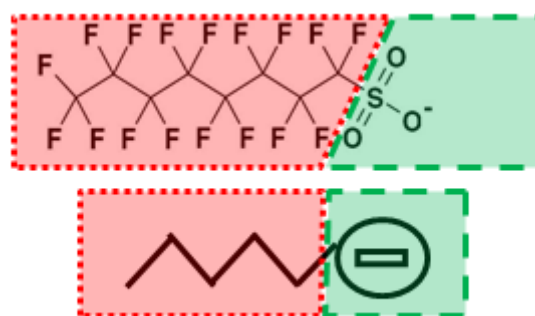


Figure 2.2 Generalized PFAS model representing PFAS in forthcoming examples by detailing hydrophobic tail (red) and hydrophilic functional group head (green). In this example the PFOS anion is depicted, though the generalized model used in forthcoming examples does not specify the number of perfluoroalkyl moieties or functional group type present.

2.2.2 Biochar Particle Size Influence on PFAS Sorption Behaviour

In addition to the sorbent qualities discussed in section 2.1, sorbent particle size is known to impact sorption behaviour, whereby smaller particles result in a greater number of exposed pores and functional groups (Hansen et al. 2010; Yu et al. 2009). Granular activated carbon (GAC) at <0.1 mm has been shown to have a higher sorption capacity for PFAS than GAC 0.9-1 mm in diameter despite having the same surface area (Du et al. 2014). Increasing the concentration of activated carbon in solution has been found to increase sorption capacity of PFOA in excess of the expected mass-based proportional increase, though the mechanism behind this has not been adequately explained (Qu et al. 2009).

2.2.3 Electrostatic Interactions

Electrostatic interactions occur due to the attraction between bodies of opposite charge, or the repulsion of bodies by the same charge (Berg, Tymoczko & Stryer 2002). PFASs can be attracted to surfaces of net positive charge due to the negative charge held by the ionic forms functional group (Figure 2.3 D). In addition to this, PFAS molecules have a net negative exterior charge with a positive region along the carbon backbone due to the electronegativity of fluorine atom drawing electrons toward outer fluorine groups and away from the alky carbons (Figure 2.2) (Du et al. 2014). These afford PFASs the ability to have weak electrostatic interactions with charged surfaces, though these predominantly originate from the charged hydrophilic functional group (Du et al. 2014). Ash fraction in biochar can infer a net positive charge to biochar, electrostatically attracting PFAS, however, in the case of low ash biochars this mechanism is unlikely (Chen et al. 2012). Dependant on charge, surface

functional groups can either repel or attract PFASs (Figure 2.3 F)(Carter & Farrell 2010). Amine and hydroxyl groups can also form weak dipole-dipole interactions (Du et al. 2014). PFASs or NOM sorbed to the surface of the sorbent may increase net surface negative charge, hence repelling other PFASs preventing sorption or effective distribution of PFAS sorbate (Figure 2.3 B&C) (Du et al. 2014). Hydrophobic CF_2 moieties repel water and therefore make hydrogen bonding to functional groups difficult, however the O in PFAS functional groups could act as proton acceptors for biochar surface functional groups ($-\text{NH}$, $-\text{OH}$ and $-\text{COOH}$). Competition with water and other molecules, for this bonding mechanism, renders it unlikely to be influential in the sorption process (Du et al. 2014).

Functional group sorption processes depend heavily on protonation, under most environmental conditions they will result in repulsion, however the OH moiety of phenol groups at neutral pH could potentially interact with the fluorine atom by hydrogen bonding (Carter & Farrell 2010). Van der Waals forces are unlikely due to PFAS molecule size as well as the interferences exerted by water (Chandler 2005; Du et al. 2014), in addition, PFAS driven π -bonding is not likely due to lack of π -electrons in most PFAS molecules (Berg, Tymoczko & Stryer 2002; Du et al. 2014). Complex interaction of PFAS molecules with biochar electronic double layer is likely to impact the mode and rate of sorption (Figure 2.5)(Carter & Farrell 2010; Du et al. 2014).

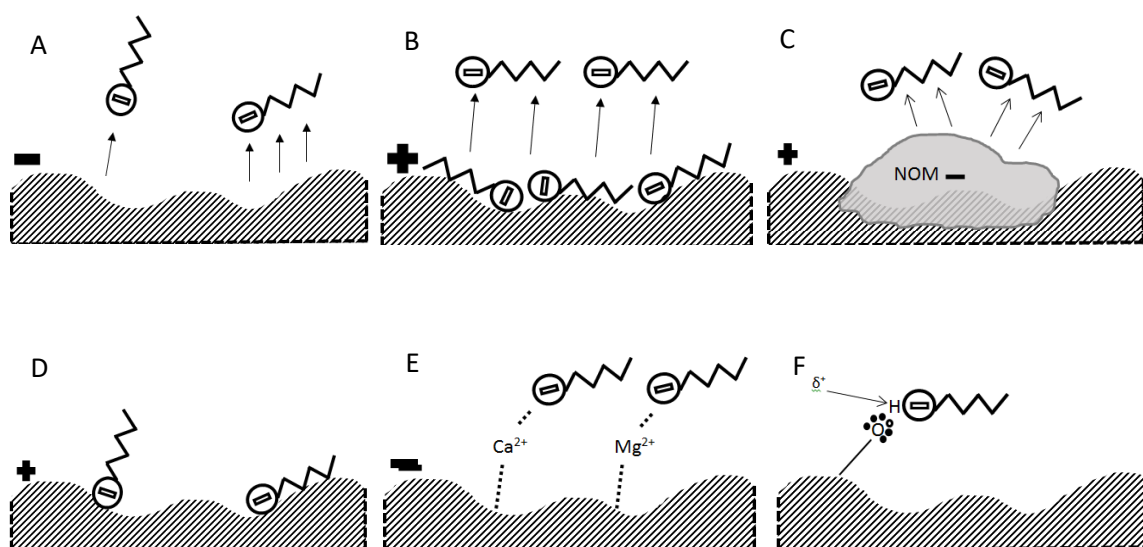


Figure 2.3 Diagrams outlining PFAS electrostatic interactions and hindrances for sorption to biochar through PFAS negative functional groups and net negative outer charge. A) Electrostatic repulsion of PFAS molecules by biochar surface with net negative charge. B) Repulsion of PFAS molecules attracted to positive biochar surface, through the negative charge of sorbed PFAS. C) PFAS molecule repulsion by negatively charged natural organic matter sorbed onto positive biochar surface. D) Electrostatic adsorption of PFAS onto positively charged biochar surface. E) Bridging of charge where divalent cations are attracted to net negative biochar surface charges, in turn acting as a bridge sorbing PFAS to neutralize charge. F) Dipole or ionic bonding between charged surface functional groups and PFAS.

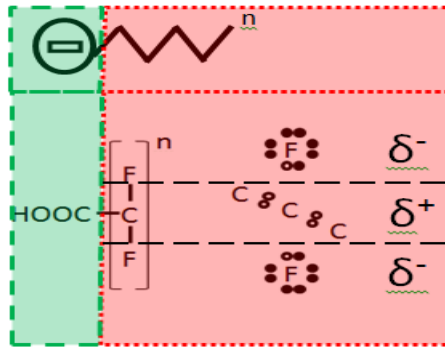


Figure 2.4 Examination of net negative outer charge on PFAS molecules, compared to generalized model. Electronegativity of fluorine atoms in PFAS molecules draw electrons further away from aryl carbons resulting in a net positive internal charge along the carbon backbone and a net negative charge on the molecules exterior. This is separate but generally less than the charge exerted by the PFAS molecules functional group.

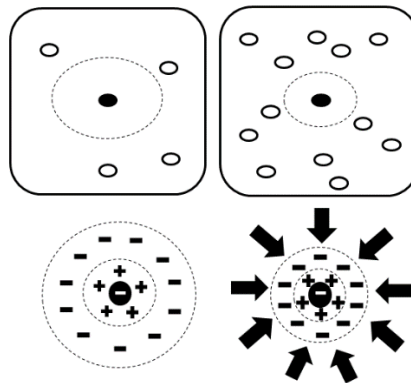


Figure 2.5 Electronic Double Layer Suppression illustrated by charged particle (black dot), surrounded by ions (white dots) and diffuse electronic layers (dotted lines). Left: A solution with a low ion concentration has a much larger, more diffuse electric double layer due to reduced external repulsion forces exerted upon it by the charges of ions (e.g. Cl^- , Na^+ , Ca^{+2}). Right: The compressed double layer caused by increased charge exerted by a greater number of ions in solution. It is likely that this behaviour will result in entropy driven coagulation and increased sorption due to the concentrated intensity of particle charge.

2.2.4 Hydrophobic Interactions

Sorption onto biochar is likely to be predominantly due to the hydrophobic nature of PFAS and associated partitioning into hydrophobic fractions of biochar (Rattanaoudom, Visvanathan & Boontanon 2012; Yang et al. 2013; Zhao et al. 2011). Structural characteristics of the biochar, such as porosity, hydrophobicity, and degree of carbonization govern sorption capacity for PFAS (Carter & Farrell 2010; Zareitalabad et al. 2013). However, it is the PFAS molecule's strong hydrophobicity that sees hydrophobic interactions overwhelm electrostatic repulsion by negatively charged surfaces (Chen et al. 2012; Du et al. 2014).

Hydrophobic sorption can be separated into partitioning and surface sorption. Partitioning relates to like-like interactions where PFAS hydrophobic tails (CF_2^n moiety) are attracted to, and seat themselves in, amorphous (aliphatic) hydrophobic organic matter due to immiscibility with water (Figure 2.7 B) (Du et al. 2014). Surface sorption is due to the hydrophobicity of PFAS tails excluding themselves from interaction with the aqueous phase (Du et al. 2014). This is through an entropy driven process which is effected by sorbent electrical double layer and particle charge, yet still strong enough to exclude PFAS from the aqueous phase, compelling it towards available surfaces (Carter & Farrell 2010; Zareitalabad et al. 2013). This is furthered by examination of Gibbs free energy at constant Gibbs pressure and temperature. The energy of the system will be at a minimum when at equilibrium. Since $\Delta G = \Delta H - T\Delta S$, the positive enthalpies of adsorption (ΔH) are required to be accompanied by an increase in entropy, this can be conceptualized as the removal of PFAS from solution to the surface of the sorbent to exclude itself from the water and its repulsion forces (Figure 2.6)(Carter & Farrell 2010).

The solvation of hydrophobic surfactant molecules, such as PFAS, requires water molecules to lose their rotational freedoms in order to maintain hydrogen bonds with other water molecules. This forms a solvation cavity around the solute that interrupts the bonding of water molecules. This is the key driving force in this entropy derived mechanism, whereby water excludes PFASs to achieve a more energetically favourable number of degrees of freedom (Carter & Farrell 2010; Du et al. 2014). The entropy driven process results in aggregation of PFASs on surfaces or each other in solution, this occurs to be less disruptive to the bonding of water molecules but appears as repulsion. In narrow spaces or regions of close contact this can result in the formation of micelles and hemi-micelles at concentrations as low as 0.001 times the PFAS critical micelle concentration (CMC) (Du et al. 2014).

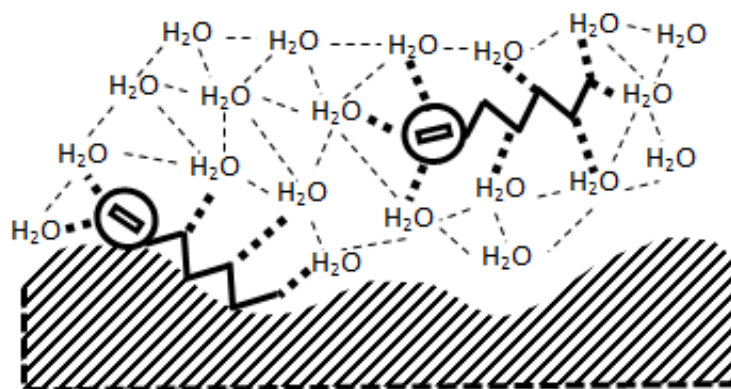


Figure 2.6 PFAS spontaneous entropy driven sorption. Hydrophobic forces drive PFAS molecules onto surface to reduce their disruption to H₂O hydrogen bond lattice. Molecule left has contact with fewer H₂O molecules and is in an energetically favoured state sorbed to the biochar surface where disruption to H₂O-H₂O bonds is minimal

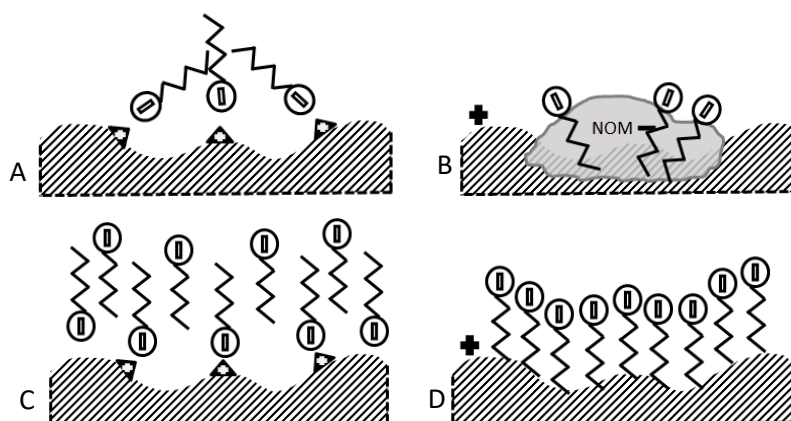


Figure 2.7 Diagrams representing hydrophobic interaction driven PFAS sorption behaviour. A) PFAS bonded to active sites, aggregation of hydrophobic portions to reduce interactions with aqueous phase. B) PFAS partitioning into natural organic matter. C) Formation of a bilayer after sufficient PFAS molecules have aggregated, formation is driven to exclude interactions with aqueous phase. D) Formation of mono-layer on charged surface, molecule orientation influenced by hydrophobic and hydrophilic portions of molecule with respect to aqueous phase.

2.2.5 Formation of Micelles and Layers

PFAS aggregate to form micelles (Figure 2.8 A&C), hemi-micelles (Figure 2.8 B) and bilayers (Figure 2.8 C), these are fluid-like structures with hydrophilic exteriors and hydrophobic interiors (Chandler 2005). Here an interface is created where water electrostatically repels PFAS to preserve its degrees of freedom with respects to its hydrogen bonds, this spontaneously results in the sorption of PFASs to surfaces (Figure 2.6). PFAS favour hydrophobic surfaces, including other PFAS, resulting in the congregation of PFAS. PFASs aggregate in a manner that their hydrophobic tails are generally grouped with their hydrophilic moiety facing the exterior of the cluster as to allow it to interaction with the aqueous phase via Van der Waals forces while excluding the aqueous phase from the interior (Chandler 2005; Paruchuri, Nguyen & Miller 2004). A dry interface is formed as the hydrogen bond network is broken around the cluster (Chandler 2005; Paruchuri, Nguyen & Miller 2004). The formation of such structures is evident in isotherms where an S shaped curvature with upward curve is present (Carter & Farrell 2010; Chen et al. 2012). This mechanism can include the formation of bilayers after sufficient PFAS have accumulated on a surface of positive charge (Figure 2.8 C) (Chen et al. 2012; U.S.EPA 2016a). Note that such clustering to form hemi-micelles is considered a monolayer (Rattanaoudom, Visvanathan & Boontanon 2012).

The formation of micelles is influenced by PFAS chain length which denote hydrophobicity as well as pose mechanical limitations based on molecule size (Chandler 2005; Hansen et al. 2010). Micelles may hinder sorption through their formation on intra-particle pores, where they can obstruct PFAS from entering further (Du et al. 2014; Yu et al. 2009). PFAS in pores and on surfaces locally increase concentration, as such they can form micelles at concentrations as low as 0.001% of typical CMCs, where this environmental condition eventuates (Xia et al. 2011; Yu et al. 2009). Typical CMCs found in literature are 15,696 mg/L for PFOA (Yu et al., 2012), 3150.8 mg/L PFOS and 411.264 mg/L PFDA (Xia et al. 2011).



Figure 2.8 Illustration demonstrating the formation of micellar structures. A) Formation of a micelle from aggregated PFAS, attached to a surface functional group by charge. B) Formation of surface hemi-micelle - by either surface charge or hydrophobic interactions resulting in sufficient aggregation. C) Free floating micelle in solution where PFAS concentration is above critical micelle concentration.

2.2.6 Interfering Environmental Factors

Competition for sorption sites is one of the many interferences that are likely to limit PFAS sorption to biochars, whether by other compounds such as organic matter, inter-PFAS competition, or PFAS solute-solute repulsion obstructing sorption directly or from nearby sorption sites (Higgins & Luthy 2006; Tang et al. 2010). Additionally, sorption environmental condition within the solution may impact sorption mechanisms and be reflected in sorption capacities and sorption rate. Key environmental factors known to influence sorbate-sorbent behaviour are further discussed below.

Organic Matter

Organic matter (OM) dissolved in the aqueous phase, such as humic acids, affects PFAS sorption through either retaining PFASs in the solution attached to OM (Du et al. 2014; Yang et al. 2013) or by restricting access to sorption sites through competition (Yu & Hu 2011). Smaller OM molecules are more with PFASs for sorption sites, whereas larger molecules tend to be responsible for the fouling and blockage of pores (Carter & Farrell 2010; Hansen et al. 2010; Yu & Hu 2011; Yu et al. 2012). Yu and Hu, 2011 saw that the addition of NOM altered equilibrium times of PFOS and PFOA to powdered activated carbon in milli-Q water from 4 hours to 72 hours. Organic matter bound to the surface of biochars can deliver a net negative surface charge, resulting in the repulsion of PFASs (Higgins & Luthy 2006; Yu et al. 2012).

Ions

Ionic strength of solutions was found to play an integral role in a number of sorption processes for PFASs to carbonaceous sorbents, these included electrical double layer compression (Figure 2.5), surface-charge neutralization, divalent cationic bridging, salting out and competitive sorption (Carter & Farrell 2010; Du et al. 2014). Ion charge and valence dictates the effect of ionic solution interferences (Chen & Yuan 2011), with cations having a greater effect at times than pH (Higgins & Luthy 2006). Cations in solution may reduce the adsorbent surface net negative charge by electrical double layer compression (Yang et al. 2013), in turn aiding sorption of anionic PFASs through reduced electrostatic repulsion (Chen & Yuan 2011). Calcium (Ca^{+2}) ions and magnesium (Mg^{+2}) ions resulted in higher sorption to OM in sediments in seawater than fresh water (Chen & Yuan 2011), specifically, higher Ca^{+2} concentrations correlate with higher PFAS sorption capacities (Higgins & Luthy 2006). Phenomena have been reported where higher pH and Ca^{+2} concentration resulted in sorbents forming more basic sites to bind divalent cations onto carboxyl, phenolic and hydroxyl group negative charges, which as a result bound more PFASs through divalent cation bridging (Figure E) (Du et al. 2014). Increasing the number of ions in solution has been shown to compress particle electrical double layer which in turn weakens both electrostatic attraction and repulsion of PFAS (Du et al. 2014).

pH

pH effects sorption behaviour by influencing speciation of sorbates (Yu et al. 2009; Zareitalabad et al. 2013). Sorption occurs at a faster rate at lower pH values due to the predominance of positive or closer to neutral charges on carbonaceous surfaces which increase electrostatic interaction with PFAS molecules (Rattanaoudom,

Visvanathan & Boontanon 2012; Yang et al. 2013). This effect is also greatest in the lower pH range (Du et al. 2014), because is closer to PFASs pKa resulting in the greatest degree of disassociation (Higgins & Luthy 2006). The same applies to sorbent surface functional groups, having higher sorption capacities for PFAS at neutral to low pH levels, but this phenomenon is poorly understood and most likely involves protonation/de-protonation as well as some of the sorbate molecules existing as neutral ions (Carter & Farrell 2010; Yu et al. 2009). Increasing pH results in a greater likelihood of negatively charged surfaces which repel PFAS (Du et al. 2014).

Temperature

No clear temperature-sorption relationship is delineated for PFAS, however increased PFAS solubility is known at higher temperatures (Qu et al. 2009). Further increased temperature increases vibrational energy, allowing PFAS to break free from surfaces (Qu et al. 2009). Current literature on influence of temperature on PFAS hydrophobic interactions is not at a state of consensus (Chandler 2005; Qu et al. 2009).

2.3 Generalized Models and Kinetics for PFASs and Carbonaceous Sorbents

2.3.1 Kinetic Models

Kinetic models assess the rate at which compounds of interest sorb to a surface and suggest limiting factors for sorption by inference of a rate determining step (Du et al. 2014). The generalized sorption process consists of three consecutive steps. Initially film/external diffusion involves the movement of sorbate from bulk solution to the surface of sorbents. Step two progresses to intra-particle diffusion whereby sorbates move to, within and between the surfaces, pores and active sites of a given particle. Lastly, equilibrium is obtained between sorbates, within particles and solution (Carter & Farrell 2010; Yu et al. 2012). The equilibrium step is considered to be slow, hence it is suggested step one and two are the most likely rate determining step (Qu et al. 2009). PFASs film diffusion stage has been observed to occur quickly (Carter & Farrell 2010), as higher initial PFAS concentration prior to sorption in solution strongly drive sorption onto sorbent boundary layer (Higgins & Luthy 2006; Yu et al. 2012). This is followed by a slower two step diffusion first into the particles internal solution, followed by sorption to active sites (Higgins & Luthy 2006). This suggests that sorption to biochar is controlled by the intra-particle diffusion rate (Du et al. 2014; Qu et al. 2009). PFAS have been found to fit a pseudo-second order model (Carter & Farrell 2010; Zhao et al. 2011), here sorption rate is proportional to the number of active sites on adsorbents (Chen et al. 2012; Qu et al. 2009; Rattanaoudom, Visvanathan & Boontanon 2012). Sorbed fraction at any measured timepoint is typically represented as Q_t (Equation 2.1), and input into experimental models used in the exploration of kinetic behaviour as described below. Q_t is calculated from experimental data, where C_0 is starting concentration of PFAS in solution ($\mu\text{g/L}$) and C_t is the remaining PFAS in solution ($\mu\text{g/L}$) at timepoint t (hours) for a given mass of sorbent m (g).

$$Q_t = \frac{(C_0 - C_t)V}{m} \quad (2.1)$$

First Order Model

Equation 2.2 represents the first order kinetic model which proposes a system where sorption is directly proportional to the concentration of PFAS in solution (linear). Where K_1 is the first order rate constant (h), C_t is the concentration of PFAS ($\mu\text{g/L}$) remaining in solution at t (hours) and C_0 is the initial concentration ($\mu\text{g/L}$) of PFAS in solution at $t = 0$. Q_t is the $\mu\text{g/g}$ PFAS sorbed at time t (hours) and Q_e is the mass PFAS sorbed per unit biochar ($\mu\text{g/g}$) at equilibrium (Equation 2.1).

$$Q_t = Q_e(1 - e^{-k_1 t}) \quad (2.2)$$

Pseudo-second Order Model

The Pseudo-second order model, an indicator of chemisorption in place of physisorption can be fitted to equilibrium data using equation 2.3. Here the rate is said to be exponentially related to the concentration of PFAS in solution and fitting suggests an excess of one reactant in solution (sorption sites). Where K_2 is the sorption rate constant ($\text{g}/(\mu\text{g h})$) for the second-order sorption.

$$\frac{t}{Q_t} = \frac{1}{K_2 Q_e^2} + \frac{t}{Q_e} \quad (2.3)$$

Intraparticle Diffusion Model

Intraparticle diffusion models are applied to delineate the varying stages of sorption described in the above passage (equation 2.4). Where the k_i ($\mu\text{g}/(\text{kg h}^{0.5})$) is the rate constant of stage i (values 1-3, where 1 is film diffusion, 2 is intraparticle diffusion, and 3 is equilibrium). C_i can be obtained from the intercept of stage i , a constant pertaining to resistance to boundary layer mass transfer. Larger C_i values suggest thicker boundary layers of greater effect. A plot of Q_t versus $t^{0.5}$ was used to obtain this data.

$$Q_i = K_i t^{0.5} + C_i \quad (2.4)$$

2.3.2 Sorption Models

Isotherms model the mode of sorption with reference to layers and mechanisms (Du et al. 2014). Langmuir and Freundlich isotherms have been commonly used to model adsorption and desorption behaviours for contaminants to biochars (Higgins & Luthy 2006; Rattanaoudom, Visvanathan & Boontanon 2012). The Langmuir isotherm assumes the formation of a monolayer and that active sites are all occupied allowing no further sorption to take place (Chen et al. 2012; Rattanaoudom, Visvanathan & Boontanon 2012). Contrastingly, the Freundlich isotherm represents multilayer sorption (Carter & Farrell 2010; Chularueangakorn et al. 2014), and has been used to model the sorption of PFAS at low concentrations to activated carbon (Higgins & Luthy 2006; Yu & Hu 2011). BET isotherms have been suggested as applicable to PFAS, as they account for aggregation of sorbates (Zhao et al. 2011), however better results may be obtained through the Temkin isotherm which takes into account sorbate-sorbate interactions (Qu et al. 2009). Generally isotherms expressing linearity describe partitioning between two phases whereas non-linearity suggests the dominance of electrostatic interactions (Chen, X et al. 2011). However non-linear isotherms can be the product of adsorption site heterogeneity, sorbate-sorbate interactions and micelle formation (Carter & Farrell 2010; Higgins & Luthy 2006; Yu et al. 2009). Sorbed fraction at equilibrium is typically represented as Q_e , and input into isotherms used in the exploration of sorption capacity as described below. Q_e is defined as sorbed mass of sorbate, per mass of sorbent at equilibrium (Equation 2.5). Q_e is calculated from experimental data, where C_0 is starting concentration of PFAS in solution ($\mu\text{g/L}$) and C_e is the remaining PFAS in solution ($\mu\text{g/L}$) at equilibrium for a given mass of sorbent m (g). The collected data is input into the following models. Models are employed in this manner to establish a relation between the solute sorbed on the surface of the biochar (per unit mass biochar) to the concentration of the solute remaining in solution.

$$Q_e = \frac{(C_0 - C_e)V}{m} \quad (2.5)$$

Freundlich

The Freundlich isotherm is applied to data in the form seen in equation 2.6. This model can be used to model sorption to non-heterogeneous surfaces as well as multilayered sorption. where Q_e is the mass of solute sorbed per mass biochar ($\mu\text{g/g}$). C_e is the mass of solute remaining in solution per litre ($\mu\text{g/L}$), K_f is the Freundlich constant related to sorption affinity, and $1/n$ a sorption intensity constant. $1/n$ values between 0 and 1 are linked to a chemisorption process, whereas values over 1 suggests cooperative sorption.

$$Q_e = K_f C_e^{1/n} \quad (2.6)$$

Langmuir

The Langmuir isotherm models data under the assumption that the adsorption of a single sorbate was on to sites upon a flat surface, where all sites are homogenous. It assumes only one molecule is sorbed per site, in a permanent manner and without further interaction with the solution or the surface. The model is described by equation 2.7, where Q_m was the maximum amount of sorbate that can be sorbed per unit of biochar ($\mu\text{g/g}$). K_L represents the Langmuir energy of adsorption ($\text{L}/\mu\text{g}$).

$$Q_e = \frac{Q_m K_L C_e}{1 + K_L C_e} \quad (2.7)$$

Sigmoidal Langmuir Modification

A modified sigmoidal Langmuir models sorption to non-heterogenous surfaces with a sigmoidal point of inflection (Equation 2.8). The point of inflection denoting two opposing forces or mechanisms of sorption that are acting against each other and are solute concentration dependant. K_L is the Langmuir adsorption energy constant which describes the strength of the sorption energy (L/g). S is a dimensionless reflection of sigmoidal behaviour. The model was applied in the form seen in equation 2.8.

$$Q_e = Q_{max} \frac{(K_L C_e)}{1 + (K_L C_e) + \left(\frac{S}{C_e}\right)} \quad (2.8)$$

SIPS

The Sips model combines Langmuir and the Freundlich models to model sorption to heterogenous surfaces at both high and low concentrations. This occurs as the model is adaptive and performs more like Langmuir in higher concentration ranges and more like the Freundlich model at lower concentrations of solute. The model is expressed in equation 2.9, where in this case K_L is the Sips isotherm constant (L/g), maximum adsorption capacity was reflected by Q_{max} ($\mu\text{g/g}$), and n is dimensionless reflection of sigmoidal behaviour.

$$Q_e = \frac{Q_m (K_L C_e)^{1/n}}{1 + (K_L C_e)^{1/n}} \quad (2.9)$$

BET

The BET model models multilayer sorption in a format similar to the Langmuir model, however, incorporates Langmuir models as layers set atop of each other. This isotherm is represented by the model at equation 2.10. Here K_{BET} represents the BET constant. Q_m the maximum BET sorption capacity ($\mu\text{g/g}$) and C_s is the BET isotherm saturation constant ($\mu\text{g/L}$).

$$Q_e = \frac{Q_m K_{BET} \left(\frac{C_e}{C_s}\right)}{\left(1 - \frac{C_e}{C_s}\right) \left(1 + (K_{BET} - 1) \frac{C_e}{C_s}\right)} \quad (2.10)$$

Toth

The Toth isotherm is another Langmuir based modelling system, similar to BET, which represents multilayer sorption, with decreasing influence based on increased Th constant. Here K_{TH} is the Toth isotherm constant ($\mu\text{g/g}$) and Th a Toth exponent ($\mu\text{g/g}$). The model was applied as equation 2.11.

$$Q_e = \frac{Q_e^\infty c_e}{(K_{TH} c_e^{Th})^{1/Th}} \quad (2.11)$$

Radke-Prausnitz

The Radke-Prausnitz isotherm performs best at low sorbate concentration. The model is outlined in equation 2.12. Where P is the Radke-Prausnitz model exponent, K is the equilibrium constant and k the Radke-Prausnitz adsorption capacity.

$$Q_e = \frac{1}{\left(\frac{1}{K_{RP} c_e}\right) + \left(\frac{1}{k_{RP} c_e^{1/P}}\right)} \quad (2.12)$$

Redlich-Peterson

The Redlich-Peterson model is represented in (Equation 2.13), where K_R is the Redlich-Peterson isotherm constant (L/g), a_R is energy of adsorption constant (L/ μg), and b is a dimensionless isotherm exponent which has a value ranging 0-1. This isotherm typically operates well across a wide range of concentrations due to the dependence on the concentration in solution and exponential function allowing it to model both heterogeneous and homogenous surfaces.

$$Q_e = \frac{K_R c_e}{1 + a_R c_e^b} \quad (2.13)$$

Desorption

Desorption is represented by equation 2.14, where desorption is calculated as a percentage (%) which represents the desorbed fraction in terms of the sorbed fraction Q_e . Where $C_{e[\text{sorp}]}$ is the concentration of PFAS in solution at equilibrium after sorption experiments ($\mu\text{g/L}$) and $C_{e[\text{desorp}]}$ is the concentration of PFAS in solution, at equilibrium, after desorption experiment ($\mu\text{g/L}$). Q_e is the sorbed fraction of PFAS from sorption experiments ($\mu\text{g/g}$).

$$\text{Desorption} = \frac{C_{e[\text{sorp}]} - C_{e[\text{desorp}]}}{Q_e} \cdot 100 \quad (2.14)$$

The models outlined above were selected as they are applicable to a range of possible sorption mechanisms. However, it is important to note that each model makes a number of mathematical assumptions, these must be taken into account on a case by case basis when assessing the data derived from any model.

2.4 Conclusion

In consideration of the content outlined in this chapter, it is evident a great diversity of sorbate-sorbent interactions are possible between biochar and PFAS. These interactions are impacted by biochar physiochemical characteristics, PFAS congener specific chemical characteristics and the nature of the environment in which sorption is taking place. While it is frequently suggested that sorption mechanisms are likely to be dominated by hydrophobic interactions, which result in greater sorption of longer chain PFAS molecules and better performance by sorbents with a greater degree of aromaticity, alternative mechanisms may be present for less hydrophobic shorter chain PFAS. An understanding of the broad PFAS-biochar sorption mechanisms, when applied to the forthcoming PFAS-biochar sorption experiments, will assist in better characterising the potential for biochar to be used as a sorbent for PFAS. Literature supports that biochars do exhibit many of the characteristics required to behave as PFAS sorbents, however the complex nature of sorption processes suggest that the suitability of any given biochar needs to be assessed on a case by case basis, taking into account biochar, target PFAS congener and environmental characteristics. Through the understanding of these requirements for effective PFAS sorption, biochars could be better reverse engineered for application as sustainable and purpose fit PFAS sorbents.

Chapter 3

Comparative Characterization of Biochars Produced at Three Selected Pyrolysis Temperatures from Common Woody and Herbaceous Waste Streams

Matthew Askeland^{1*}, Bradley Clarke², Jorge Paz-Ferreiro¹

¹ School of Engineering, RMIT University, Melbourne, Australia

² School of Science, RMIT University, Melbourne, Australia

Published work (See Appendix 1):

Askeland M, Clarke B, Paz-Ferreiro J. 2019. Comparative characterization of biochars produced at three selected pyrolysis temperatures from common woody and herbaceous waste streams. PeerJ 7:e6784 <http://doi.org/10.7717/peerj.6784>

3.1 Abstract

Biochar, the product of biomass pyrolysis, has been explored as a soil amendment and carbon capture vessel. Recent literature has aligned biochar as a novel sorbent for a host of environmental contaminants. Through the variation of pyrolysis conditions, biochars can be engineered to have qualities desirable in sorbents whilst maintaining their agronomic benefits.

This study focuses on identifying the effects that feedstock type and process temperature have on biochar characteristics which may in turn shed light on their potential environmental applications. Using this approach, six biochars were created from two waste biomasses. The biochars exhibited wide ranges of pH (5.6-11.1), surface area (16.2-397.4 m²/g), electrical conductivity (19-2826 μS/cm), fixed carbon (72-97 %), heavy metal and polycyclic aromatic hydrocarbons (PAHs). Statistically significant trends (P< 0.05) in biochar characteristics dependent upon increasing pyrolysis temperature and feedstock type were identified.

Arsenic (> 13 mg/kg), chromium (> 93 mg/kg), copper (> 143 mg/kg) and PAH (> 6 mg/kg) concentrations presented themselves as obstacles to land application in a small number of biochars with respects to International Biochar Initiative (IBI) guidelines. However, it was demonstrated that these could be eliminated through employing pyrolysis processes which encompass higher temperatures (>500 °C) and ensuring the use of contaminant-free feedstocks.

The variation in surface areas, carbonized fractions and surface functional groups achieved suggest that using the correct feedstock and process, biochar could be produced in Victoria (Australia) from common organic waste streams to the ends of acting as a sorbent, soil enhancer, and a waste management strategy.

3.2 Introduction

Biochar is the carbonaceous solid resulting from the thermochemical conversion of biomass in an oxygen-limited environment (IBI, 2011). Waste biomass is the largest and most sustainable biomass source, with 220 billion dry tons being produced globally each year (Azargohar et al. 2013). Application of biochar to soil has been demonstrated to improve soil fertility by increasing cation exchange capacity (CEC), soil organic matter content and nutrient availability of the pre-*Terra preta* soils (Glaser et al. 2000; 2001; Heitkötter and Marschner 2015).

Interest in biochar as a tool for carbon sequestration in soil (Lehmann 2007) soon developed into a focus on biochar's agronomic potential (Liu et al. 2013). Incorporation of biochar into biocomposites has expanded biochar applications further into the material sciences (Das & Sarmah 2015; Das, Sarmah & Bhattacharyya 2016). Biochar can also be used as a novel material for remediation, where contaminant sorption to biochar surfaces reduces bioavailability and mobility (Paz-Ferreiro et al. 2014; Srinivasan and Sarmah 2015). Biochar characterisation studies with respects to the effect of feedstock and temperature are imperative for adequate decision making in proceeding towards engineering the biochars of the future (Gascó et al. 2018; Lu et al. 2018).

Biochar is primarily composed of stable aromatic carbon ring structures (Al-Wabel et al. 2013), that impart resistance to degradation by oxidants (Mitchell, Dalley & Helleur 2013) and biological decay (Al-Wabel et al. 2013; Freddo, Cai & Reid 2012). Its structure gives biochars an estimated residence time in temperate environments of up to 4000 years (Kuzkayok, Bogomolova & Glaser 2014). The recalcitrance of biochar in the environment varies greatly and is influenced by pyrolysis method and choice of feedstock. Biochar includes a diverse group of materials, with each exhibiting unique physiochemical characteristics and environmental lifespans (Jouiad et al. 2015; Qian et al. 2015).

Pyrolysis temperature governs porosity of the biochar formed due to degassing of volatiles and fracturing through subsequent cooling and shrinkage (Das and Sarmah 2015). The number and types of surface functional groups present on biochar are also highly temperature dependent, due to volatility, which can result in loss or transformation at higher temperatures (Das and Sarmah 2015).

Biochar produced from contaminated feedstocks is likely to be contaminated with heavy metals, or pesticide residues (Buss et al. 2015; Denyes et al. 2012). Contaminants such as heavy metals are intrinsic to some feedstocks, such as biosolids, and are neither created nor destroyed during pyrolysis (Chen et al. 2014; Zielinska & Oleszczuk 2015). Through loss of volatiles from the feedstock, non-volatile heavy metals become more concentrated in biochar (Domene et al. 2015). Comparatively, PAHs are either native or generated during the pyrolysis process (Kambo & Dutta 2015; Domene et al. 2015; Lievens et al. 2015, Wang, Wang & Herath 2017). Heavy metals and PAHs are known toxicants to many organisms and hence could restrict the usage of derived biochars (Fredo, Cai & Reid 2012; Domene et al. 2015).

Agricultural waste has been widely researched for biochar production (Zavalloni et al. 2011). Woody and herbaceous biomass presents advantages over other agricultural waste, as it can be harvested year-round, which eliminates long-term storage. In Victoria, Australia, agriculture produces annually >1.6 million dry tonnes of waste biomass as crop stubble, stems, kernels and grain processing residues (Victoria State Government 2012a) and approximately 285,000 tons of timber wastes, including sawdust (Victoria State Government 2012b), that

could be beneficially converted to biochar materials. The generation of biochars from these wastes could potentially be an important tool for managing waste biomasses in an economical and sustainable manner. Furthermore, The State Government of Victoria has placed emphasis on the re-use of such biomass, as opposed to the practice of landfilling (Victoria State Government 2012b).

Few authors have discussed the conversion products of woody and herbaceous biomasses at different pyrolysis temperatures. A growing number of studies are available which have characterized biochars derived from various waste streams as potential waste management and reuse strategies (Cely et al. 2015; Yargicoglu et al. 2015). However, there exist very few studies which compare the effects of production temperature and studied woody and herbaceous feedstocks (Srinivasan & Sarmah 2015; Srinivasan et al. 2015) on resultant biochar characteristics at constant residence times. Table 3.1 contains comparative data for a small number of studies which have explored the characteristics to some extent for biochars derived from either pine (wood or sawdust) or straw. Table 3.1 demonstrates the current deficiency in biochar characterisation data for pine and straw feedstocks. It is also notable that there is a lack of information on trends specific to each feedstock with respects to the effect held by pyrolysis temperature on commonly measured parameters. Authors have noted the importance of such characterization studies for the optimization and designing of biochars in the future (Luo et al. 2015; Zhao et al. 2013).

In this study, six biochars were produced at three pyrolysis temperatures from two waste biomasses, pine sawdust (a softwood waste harvested all year) and pea straw (straw produced as an agricultural waste). These were chosen as they are common waste streams in Victoria, and each represents a biomass of differing structure and composition. Biochars were studied to assess the effect production temperature and feedstock specific composition had on each biochars unique characteristics. To our knowledge, this is the first study that has characterized a broad range of parameters and compared these two feedstocks and the effects pyrolysis temperature has on resultant biochars with increasing pyrolysis temperature at a constant residence time. Due to the temperature and feedstock specific nature of biochars, this work offers an important insight in the direction of “engineered biochars”.

Table 3.1 Literature values for biochars produced from pine or pea straw like feedstocks

Feedstock	T (°C)	t (min)	pH	SSA (m²/g)	FC (%)	VM (%)	Ash (%)	C (%)	H (%)	O (%)	N (%)	S (%)	Study and Location
Wheat (Straw)	368	240	10.66	-	-	-	25.1	62.8	-	-	0.83	-	Alburquerque et al. (2014) Spain
Pine (Woodchips)	428	228	8.38	-	-	-	4.4	80.0	-	-	0.37	-	
Pine (Woodchips)	450	15	7.5	288	-	-	-	83.7	-	-	0.36	-	Brennan et al. (2014)
Pine (Wood)	350	60	-	28.7	71.8	-	2.63	-	-	-	-	-	Das, Sarmah & Bhattacharyya (2016) New Zealand
Pine (Wood)	420	10	-	0.7	69.7	-	2.06	-	-	-	-	-	
Pine (Wood)	470	10	-	0.9	74.5	1.81	-	-	-	-	-	-	
Pine (Wood)	900	60	-	335.9	82.2	-	13.4	-	-	-	-	-	
Pine (Sawdust)	300	60	-	8.2	-	-	4.58	55.3	5.50	39.0	0.07	0.13	Luo et al. (2015) China
Pine (Sawdust)	500	60	-	68.4	-	-	6.91	76.0	3.54	19.8	0.15	0.47	
Pine (woodchips)	450	15	7.5	-	-	-	1.8	85.2	2.78	-	0.37	-	Moreno-Jiménez et al. (2018) Germany
Pine (Sawdust)	680	10	9.7	795	-	-	1.01	90.9	1.31	0.11	6.1	-	Srinivasan et al. (2015) New Zealand
Wheat (Straw)	500	240	10.2	33.2	63.7	17.6	18	62.9	-	-	-	-	Zhao et al. (2013) China
Pine (Sawdust)	500	240	10.5	203	72.0	17.5	9.94	75.8	-	-	-	-	

3.3. Materials and Methods

3.3.1 Raw material selection

Six biochars were prepared using pine sawdust and pea straw as feedstocks. Sawdust was obtained from pine (*Pinus radiata*), grown in several plantations ranging between Eurobin (Victoria- 36°38'18.9"S 146°51'06.2"E) to Tumut (New South Wales, Australia - 35°18'58.6"S 148°13'51.7"E) plantations. Pea straw (*Pisum sativum*) was acquired from a wholesaler (Peninsula Hay) situated in the Mornington region of South East Victoria (38°24'12.9"S 144°58'34.6"E). In this region the pea plant is used to fix nitrogen in pastures and later harvested for use as feed or mulch.

3.3.2 Pyrolysis of raw materials

Biochar was produced by tightly packing 400 g of a single feedstock into a 1 L internal volume (Radius - 7 cm; Height – 6.5 cm) stainless steel cylindrical vessel with a spring clamped lid which exerted a small downward force strong enough to prevent atmospheric exchange yet still allow evolved gases to escape under positive pressure. No inert gases were employed as oxygen was prevented from entering the vessel by the lid, any remaining oxygen existing in the vessel was either exhausted during heating or expelled through expansion during the temperature ramping process. Therefore, inside the vessel was considered an oxygen limited environment. The vessels were then placed in a furnace and the temperature ramped at 8.3°C/min to a respective 350 °C, 500 °C or 750 °C, followed by a 1-hour dwell time. These temperatures were selected as a gradient and are spread across the upper and lower as well as median thresholds for slow pyrolysis. After pyrolysis, each vessel was placed in the draft of a fume hood to allow an hour to cool before opening, to prevent ignition. The above process was carried out four times. All biochars were passed through a 1 mm sieve, homogenized and stored in polypropylene containers under standard lab conditions until analysis. Biochars were coded P (Pine Sawdust) and S (Pea Straw), and temperature groups (P350, P500, P750, S350, S500 and S750).

3.3.3 Characterization of Biochars

Chemical and Physical Characterisation

Yield of the biochar was expressed as the percentage of biochar produced after pyrolysis relative to the initial mass of feedstock. Bulk density was calculated using the mass of biochar that could be packed into a 20 mL stainless steel cylinder with minimal compression (EBC 2012). Proximate analysis was undertaken as per ASTM 1762-84:2013, however premature combustion of samples resulted in volatile matter (VM) requiring an alternate method. VM was measured using a Perkin Elmer Simultaneous Thermal Analyzer (STA) 6000, where 5

mg of sample was heated to 600°C at a rate of 30 °C/min, in a nitrogen environment. Mass loss between 105 °C and 600 °C was considered the VM fraction. Fixed carbon (FC) was calculated as the remaining mass percentage after measured VM, ash and moisture percentages had been subtracted from the total mass.

Biochar pH and electrical conductivity (EC) were determined by preparing a 1:2 biochar:deionised water slurry (20 g biochar to 40 mL of water) then pH and EC determined in accordance with US EPA 9045 (2004). The alternate solid: liquid ratio was used to ensure wetting of entire biochar sample.

Surface area analysis was undertaken by N₂ adsorption at 77 K using a Micromeritic ASAP 2400. Triplicate 10 mg samples were degassed at 100°C for 8 hours under low vacuum. Following no mass change after degassing, samples were degassed a further 12 hours under high vacuum at 200 °C and was repeated until no mass change was evident. Biochars were fitted to a BET sorption isotherm to determine surface area.

A FEI Quanta 200 Scanning Electron Microscope (SEM) was used to examine surface morphology of biochars under low vacuum at 25 kV accelerating voltage, spot size of 6 nm, and at magnifications ranging 200 – 1600x with a set working distance of 10.5.

Fourier Transform Infrared Spectroscopy (FTIR) analysis was carried out on a Perkin Elmer Spectrum 100 with single diamond/ZnSe attenuated total reflectance (ATR) module and pressure arm, as to delineate the dominant functional groups unique to each biochar.

Cation Exchange Capacity (CEC) was measured saturating the sample with a 0.5 M barium chloride solution then displacing the sorbed Ba²⁺ with a 1.0 M ammonium acetate solution (Mitchell et al. 2015). This extraction was employed to determine the sum of all cations (Mitchell et al. 2015) using inductively coupled plasma-optical emission spectrometry (ICP-OES).

Ultimate analysis was undertaken in accordance with ISO 29541:2010E and ISO 19579:2006-10E. Oxygen content was calculated using ultimate analysis data by subtracting the sum of ash, carbon, nitrogen and hydrogen as a percentage from 100 % (Enders and Lehmann 2012). Biochar thermal stability was calculated as the percentage between fixed carbon divided by the sum of fixed carbon and VM. This calculated index value estimates the degree of thermal stability of each biochar, where values closer to one suggest a more stable biochar than those closer to zero (Alburquerque et al. 2013; Chen et al. 2014).

Contaminant Analysis

Heavy metals (Cd, Cr, Cu, Pb, Hg, Ni, Zn), metalloid As and PAHs were analysed at an external certified commercial laboratory. Pseudo-total heavy metal analysis was undertaken using an adaptation of USEPA Method 3050B (1996), whereby heavy metals were extracted by refluxing of 0.1 g biochar samples in concentrated trace metals grade HNO₃ and analysed by AAS and ICP-MS.

Sixteen priority USEPA PAHs, 7,12-Dimethylbenz(a)anthracene and 3-Methylcholanthrene were determined by ultrasonic extraction of samples which were quantified by gas chromatography–mass spectrometry (GC/MS) in accordance with US EPA Method 8270D (1998). The values of heavy metals and PAHs were compared with the limits stipulated in the *Standardized Product Definition and Product testing Guidelines For Biochar That is Used In Soil* (IBI 2013).

3.3.4 Statistics

Descriptive statistics, Two-way factorial ANOVA and Pearson Correlation were carried out on IBM's SPSS Statistics 22 package. Two-way ANOVA was the key tool in verifying significant trends between biochar parameters governed by pyrolysis temperature and differences between feedstock type. Univariate factorial analysis allowed the identification of the main effect responsible for any trends observed, differentiated as temperature, feedstock or interaction. Significant results are displayed in the format ($F_{1,6} = X, p < 0.05$), where the p value is alongside the F value. F-crit values can be ascertained using F tables and the subscript numbers, the first being the degrees of freedom followed by the number of sample groups for that parameter. Pearson Correlation results are displayed as follows ($R = X, n = X, p = X$), where R is the correlation factor, n denotes the number of groups of samples sampled and the last figure corresponds to the p value.

3.4 Results and Discussion

3.4.1 Chemical and physical characterisation

Temperature was found to be the main effect influencing yield ($F_{2,18} = 12.1, p < 0.05$), with yields decreasing at higher pyrolysis temperatures for both, straw and pine feedstocks. Straw exhibited greater yields than pine at both 500 °C and 750 °C (25 % and 23 % compared to 21 % and 20 % respectively), while at 350 °C pine (34 %) produced a higher yield than straw (29 %). This is likely due to the interplay of temperature and the two feedstocks, which differ in water, lignin, cellulose and hemicellulose composition. Feedstock and temperature have been identified as the most influential parameters in the decomposition of woody and herbaceous biomasses to produce biochar (Zhao et al. 2013; Benavente et al. 2018). This is due to the variation in each feedstock with respect to their content of the biopolymers; hemicellulose, cellulose and lignin, all of which degrade at different temperature ranges (Qian et al. 2015; Kambo & Dutta 2015; Yeo et al. 2017). Comparatively the rigid structure required by trees results in a higher proportion of lignin in softwoods than in herbaceous grasses, while grasses are more cellulosic (Das and Sarmah 2015; Azargohar et al. 2013). Hemicellulose is the easiest degraded of the three major components, with complete degradation starting at 330°C (Yeo et al. 2017; Buss et al. 2015). The greatest proportion of cellulose degradation occurs at temperatures above 427°C, though degradation can begin at lower temperatures, generating much volatile matter as carbon-oxygen and carbon-hydrogen bonds are broken (Buss et al. 2015). Lignin is the most recalcitrant of these three major components, with complete degradation evident only after temperatures exceeding 607°C. This is due to lignin's structure consisting of multiple ether linkages and functional groups such as hydroxyl and methoxy (Yeo et al 2017).

A difference in surface morphology was observed using SEM in the form of cellular structure between the feedstocks, as well as, increased fracturing of structure with increased pyrolysis temperature (Figure 3.1). The cells seen in pine biochars were longer and more cylindrical than the short cuboid cells noted in straw based biochars, and the pores visible on the surface of all biochars were similar to those reported in previous literature (Shaaban et al. 2014).

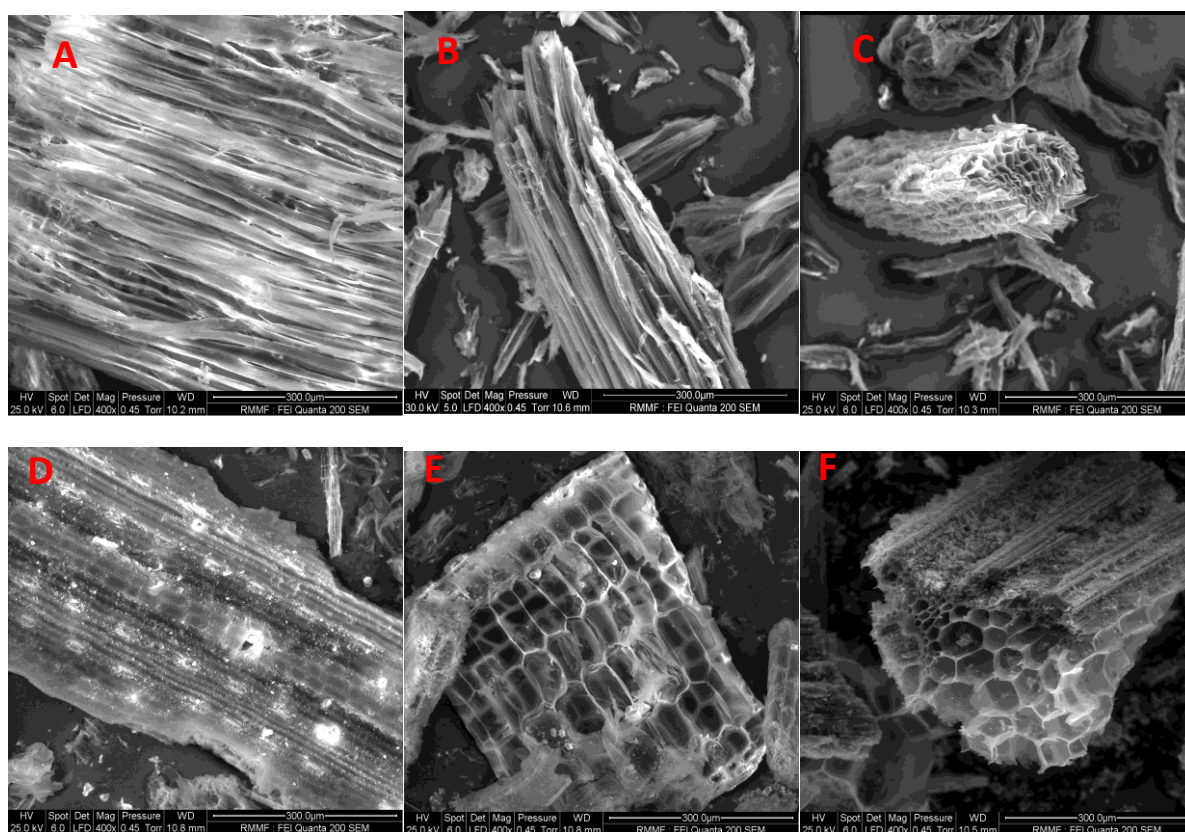


Figure 3.1 SEM Image of biochar surfaces derived from pine pyrolyzed at 350 °C, 500 °C and 750 °C (A, B and C, respectively) and straw pyrolyzed at 350 °C, 500 °C and 750 °C (D, E and F, respectively). All images obtained at 400x magnification.

Bulk density was similar across feedstocks, ranging between 0.12 – 0.17 g/cm³. Pine at 350 °C had the lowest bulk density, however at 750 °C both biochar types were matched in density (Table 3.2). This would have implications when biochars are used as soil conditioner. Thus, bulk density is of utmost importance to rainfall infiltration. Moreover, a decrease in bulk density would have ramifications, increasing soil porosity and soil aeration, and, potentially leading to a positive effect on microbial respiration.

Surface area increased in both feedstock types with higher pyrolysis temperature and large surface area differences were observed between feedstock types (Table 3.2). Feedstock ($F_{1, 11} = 529.0$, $p < 0.05$), temperature ($F_{2, 11} = 471.6$, $p < 0.05$) and their interactions ($F_{2, 11} = 132.5$, $p < 0.05$) were significant factors with respects to biochar surface area and this is consistent with similar studies, carried out in other lignocellulosic wastes (Das & Sarmah, 2015). Pine biochars had higher surface areas than straw biochars in the 500 °C ($278.0 \pm 4. \text{ cm}^2/\text{g}$) and 750 °C ($397.3 \pm 4.1 \text{ cm}^2/\text{g}$) experiments, however the depressed values at 350 °C ($16.3 \pm 5.2 \text{ cm}^2/\text{g}$) were suggested to be due to the lower temperatures resulting in the underdevelopment of pores (Abdel-Fattah et al., 2015) and clogging of pores with tars which could not volatilize (Das & Sarmah 2015). These results fit within the range expressed by in Table 3.2 for surface area.

Moisture levels ranged between 1.5 and 4.0 % in biochars produced, an increase in moisture was observed with higher pyrolysis temperature (Table 3.2). Temperature and feedstock were each found to hold significant effects over biochar moisture levels ($F_{1, 6} = 9.6$, $p < 0.05$ and $F_{1, 6} = 169.4$, $p < 0.05$, respectively). Biochars prepared

at 750 °C had the highest moisture levels, particularly P750, it is suggested that this is absorbed from the atmosphere due to the higher surface area of the material.

Temperature was found to be a main effect for VM content ($F_{2, 6} = 42.9$, $p < 0.05$), decreasing from 350 °C biochars to 750 °C biochars (Table 3.2). This is consistent with other studies (Table 3.1) as VM loss occurs as outgassing volatiles (Al-Wabel et al. 2013). Feedstock was also identified as a main effect ($F_{1, 6} = 31.4$, $p < 0.05$), exhibiting higher average VM in straw biochars than pine biochars. An interaction for both factors was present $F_{2, 6} = 8.3$, $p < 0.05$ suggesting an interplay between these two factors. Volatile matter is of importance to explain the microbial and plant responses following biochar addition to the soil, although this is a poorly understood interaction, due to the large amount of individual volatile compounds present in biochars (Spokas et al. 2011).

For ash, feedstock was determined to be a main effect ($F_{1, 6} = 219.7$, $p < 0.05$), such that ash content was significantly higher in straw biochar than pine. Ash fractions increased with higher temperature (Table 3.2), which was demonstrated to be a main effect by univariate factorial ANOVA ($F_{2, 6} = 6.6$, $p < 0.05$). This demonstrates temperature's role in forming the ash fraction, compared to feedstocks role in defining the fraction available for maximum ash formation. Further, a statistically significant interaction between feedstock and temperature was found ($F_{2, 6} = 5.3$, $p < 0.05$). Ash represents the largely inorganic fraction that cannot be volatilized or degraded by combustion, including potassium (K), calcium (Ca) magnesium (Mg), carbonates and heavy metals (Hmid et al., 2014). Ash compounds hinder the formation of aromatic structures that contribute greatly to fixed carbon content.

Fixed carbon was found to be higher in pine biochars than in straw biochars (Table 3.2). Feedstock was found to be the main effect for this difference in fixed carbon between biochars ($F_{1, 2} = 36.9$, $p < 0.05$) and is supported by literature (Zhao et al. 2013). FC values were slightly higher than those seen in literature (Table 3.2).

Fixed carbon values were in agreement with those of the thermostability index. In general, higher values of these would be indicative of a longer residence time of biochar in soil.

Thermal stability increased with pyrolysis temperature for all biochars, lower thermal stability was noted for straw biochars (Table 3.2). This suggests that pine biochars will be more recalcitrant in the environment than straw biochars (Das, Sarmah and Bhattacharyya 2016).

A reduction in oxygen and hydrogen containing functional groups, primarily carbonyl ($1690-1700\text{ cm}^{-1}$) and carboxyl groups ($1690-1760$ and $1210-1320\text{ cm}^{-1}$) between 350 °C and 500 °C, was observed through FTIR (Figures 3.2 and 3.3). In both feedstock types, FTIR suggests that at 750 °C biochars are namely comprised of C-C bonds and that most of the other functional groups and volatile components had been lost, this is similar to trends expressed in by results found for other biochars produced from woody feedstocks (Albuquerque et al. 2013; Abdel-Fattah et al. 2015). In all biochars, H and O values were comparable to literature, though slightly lower values (Table 3.2). Hydrogen content decreased with higher pyrolysis temperature and a difference was observed between feedstocks, with hydrogen in straw derived biochars being lower than in pine biochars (Table 3.2). Both feedstock and temperature significantly influenced hydrogen content ($F_{2, 2} = 250.4$, $p < 0.05$ and $F_{1, 2} = 22.9$, $p < 0.05$ respectively).

Table 3.2 Summary of characteristics determined for biochars produced in study

Biochar	P350	P500	P750	S350	S500	S750
Biochar Physiochemical Characteristics						
Surface Area (m ² /g)	16.2 ±5.2 ^{A,c}	278.0 ±4.7 ^{A,b}	397.4 ±4.1 ^{A,a}	22.2 ±3.6 ^{B,c}	46.7 ±8.9 ^{B,b}	157.7 ±4.2 ^{B,a}
Moisture (%)	1.54 ±0.01 ^{A,c}	1.73 ±0.13 ^{A,b}	3.29 ±0.06 ^{A,a}	1.72 ±0.01 ^{B,b}	1.76 ±0.03 ^{A,b}	4.01 ±0.04 ^{B,a}
Volatile Matter (%)	15.29 ±0.59 ^{A,a}	4.28 ±0.16 ^{B,b}	2.88 ±0.08 ^{B,c}	16.23 ±1.15 ^{A,a}	14.49 ±0.42 ^{A,a}	7.50 ±0.32 ^{A,b}
Ash (%)	1.16 ±0.01 ^{B,b}	1.88 ±0.01 ^{B,a}	1.92 ±0.06 ^{B,a}	15.24 ±0.17 ^{A,b}	16.21 ±1.67 ^{B,a}	23.95 ±0.29 ^{A,a}
Fixed Carbon (%)	82.01 ±2.02 ^{A,b}	92.11 ±1.97 ^{A,a}	91.91 ±3.07 ^{A,a}	66.81 ±3.18 ^{B,a}	67.54 ±2.84 ^{B,a}	64.54 ±2.98 ^{B,b}
Bulk Density (g/cm ³)	0.12 ±0.01 ^{B,c}	0.15 ±0.01 ^{A,b}	0.17 ±0.02 ^{A,a}	0.15 ±0.01 ^{A,c}	0.16 ±0.01 ^{A,b}	0.17 ±0.02 ^{A,a}
Thermal Stability	0.84 ±0.10 ^{A,c}	0.96 ±0.04 ^{A,b}	0.97 ±0.04 ^{A,a}	0.81 ±0.16 ^{A,b}	0.82 ±0.08 ^{B,b}	0.90 ±0.05 ^{B,a}
Biochar Ultimate Analysis						
Carbon (%)	75.6 ±2.1 ^{A,c}	88.0 ±1.3 ^{A,b}	93.8 ±0.9 ^{A,a}	61.3 ±2.7 ^{B,b}	64.4 ±2.5 ^{B,a}	63.9 ±2.7 ^{B,a}
Sulphur (%)	0.07 ±0.01 ^{B,a}	0.07 ±0.01 ^{B,a}	0.08 ±0.01 ^{B,a}	0.27 ±0.02 ^{A,a}	0.27 ±0.02 ^{A,a}	0.21 ±0.01 ^{A,b}
Nitrogen (%)	0.25 ±0.01 ^{B,c}	0.41 ±0.03 ^{B,b}	0.56 ±0.01 ^{B,a}	1.08 ±0.11 ^{A,a}	1.11 ±0.09 ^{A,a}	0.95 ±0.13 ^{A,a}
Hydrogen (%)	4.73 ±0.27 ^{A,a}	3.08 ±0.15 ^{A,b}	1.07 ±0.18 ^{A,c}	3.89 ±0.14 ^{B,a}	2.52 ±0.12 ^{B,b}	0.66 ±0.07 ^{B,c}
Oxygen (%)	18.26 ±2.12 ^{A,a}	6.63 ±1.31 ^{B,b}	2.65 ±0.92 ^{B,c}	18.50 ±2.71 ^{A,a}	15.76 ±3.01 ^{A,b}	10.54 ±2.72 ^{A,c}
Inorganic (%)	1.09 ±0.08 ^{A,b}	1.81 ±0.11 ^{A,a}	1.84 ±0.09 ^{A,a}	14.96 ±0.79 ^{B,c}	15.94 ±2.18 ^{B,b}	23.74 ±2.24 ^{B,a}
H:C	0.06 ±0.01 ^{A,a}	0.04 ±0.01 ^{A,b}	0.01 ±0.01 ^{A,c}	0.06 ±0.01 ^{A,a}	0.04 ±0.01 ^{A,b}	0.01 ±0.01 ^{A,c}
C:N	302.40 ±121.10 ^{A,a}	214.63 ±90.71 ^{A,b}	167.50 ±29.96 ^{A,c}	56.76 ±17.49 ^{B,a}	58.02 ±15.75 ^{B,a}	67.26 ±25.59 ^{B,b}
O:C	0.24 ±0.12 ^{B,a}	0.08 ±0.01 ^{B,b}	0.03 ±0.01 ^{B,c}	0.30 ±0.03 ^{A,a}	0.24 ±0.03 ^{A,b}	0.17 ±0.03 ^{A,c}

Statistically significant relationships (P<0.05) are denoted in table by capital letters (A, B) for feedstock and lowercase letters (a,b,c) for temperature. Values are presented as mean ± standard deviation.

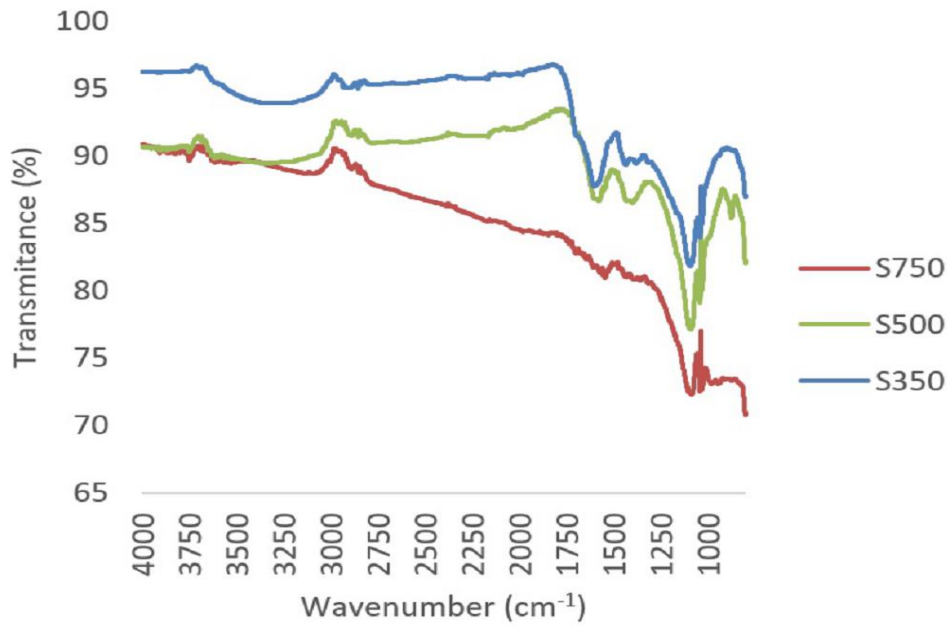


Figure 3.2 Composite FTIR spectra of biochars produced from straw at 350 °C, 500 °C and 750 °C.

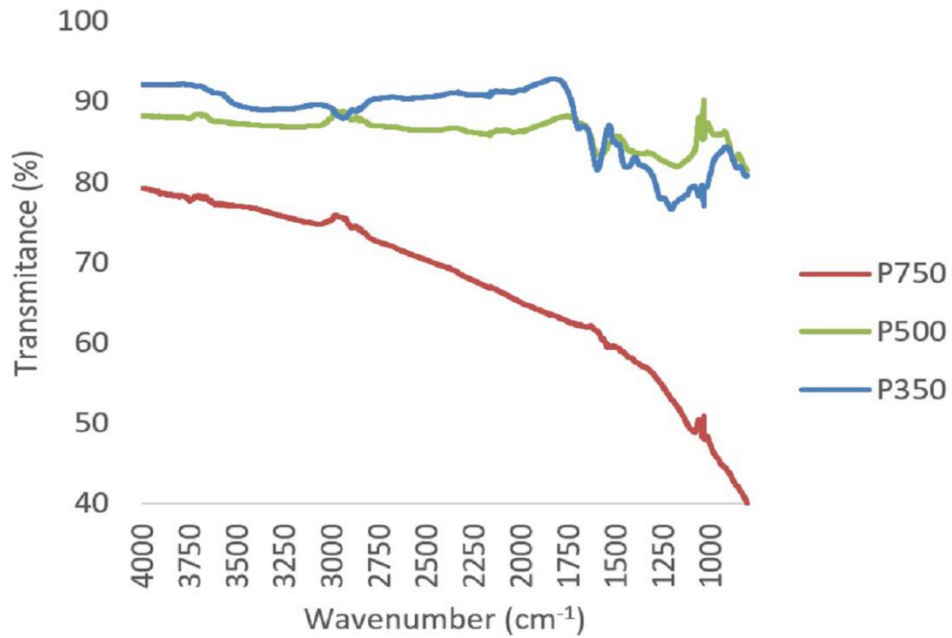


Figure 3.3 Composite FTIR spectra of biochars produced from pine at 350 °C, 500 °C and 750 °C.

Nitrogen was not affected by higher pyrolysis temperature in straw biochars, however N increased with pyrolysis temperature for pine biochars (Table 3.2). Feedstock was the main factor affecting nitrogen content ($F_{1,2} = 24.0, p < 0.05$). Similarly, feedstock was the main factor influencing percentage sulphur remaining in biochars ($F_{1,2} = 57.3, p < 0.05$). Sulphur and nitrogen values for all biochars compared well to literature values seen in Table 3.1.

H:C ratio is a measure often used to discern the degree of aromatization in biochars as increases in carbon are inversely related to hydrogen through polymerization, dehydration and volatilization. In these experiments H:C decreased in both biochar types with higher pyrolysis temperature, highlighting temperature as a main effect ($F_{2,2} = 393.1, p < 0.05$) and suggesting an increase in aromatization (Table 3.2). The loss of H is indicative of water and surface acid functional group loss, such as hydroxyl (OH) and carboxyl (COOH) through volatilization. Higher pyrolysis temperatures results in a greater loss of VM, oxygen and hydrogen as due to depolymerisation of biopolymers and the carbonisation of the feedstock to a more recalcitrant form through decarboxylation, dehydration, de-carbonylation, de-methylation, condensation and aromatisation reactions (Das & Sarmah 2015; Heitkötter et al. 2015).

Inverse relationships were observed between moisture and H:C ($R = -0.912, n = 6, p = 0.006$); bulk density and H:C ($R = -0.827, n = 6, p = 0.021$); and bulk density and yield ($R = -0.851, n = 6, p = 0.016$). The relationships between bulk density, yield, and H:C can all be understood through mass loss. Hydrogen is lost through dehydration while percentage carbon content increases through condensation and graphitization, affecting H:C. Yield decreases in proportion to H:C via mass loss, whereas bulk density increases due to the formation of graphite like structures. These are temperature dependent relationships, though the initial feedstock does play a major role in their resilience to thermal degradation. It is intuitive that moisture levels decrease from feedstock to biochar through the loss of water as steam due to the elevated temperatures used in pyrolysis. However, the increase in moisture in finished biochars as a function of temperature is surmised to be due to the hygroscopic effect exerted by their high surface area. This is further supported by the correlations seen in BET surface area relating in a negative manner to yield ($R = -0.824, n = 6, p = 0.022$), O: C ($R = -0.976, n = 6, p < 0.001$) and VM ($R = -0.964, n = 6, p = 0.001$), all of which are characteristics which decrease with higher pyrolysis temperature. This relationship highlights the impact outgassing of VM has in the formation of pores and hence a higher surface area (Das & Sarmah 2015).

Electrical conductivity (EC) and pH increased with higher pyrolysis temperature in all cases. Both pH and EC were found to be higher in straw biochars than in pine biochars (Figure 3.4). Temperature (pH: $F_{2,6} = 1706.8, p < 0.05$; and EC: $F_{2,6} = 179.5, p < 0.05$), feedstock (pH: $F_{1,6} = 4621.7, p < 0.05$; and EC: $F_{1,6} = 279.4, p < 0.05$) and their interactions (pH: $F_{2,6} = 73.5, p < 0.05$; and EC: $F_{2,6} = 103.0, p < 0.05$) were found to play a significant role in pH and EC values. This suggests the differences within feedstock groups were due to pyrolysis temperature, the different values across temperature groups were due to feedstock and the extent of the difference was due to the interaction of these two factors. Increases in EC are the result of a gain in the number of ions present through the increase in ash fraction (Albuquerque et al. 2013). Similarly, it is well-established that increasing pyrolysis temperature tends to favour the alkalinity of biochars (Yuan et al. 2011). This is partly due to an increase in inorganic carbonates (Yuan et al. 2011).

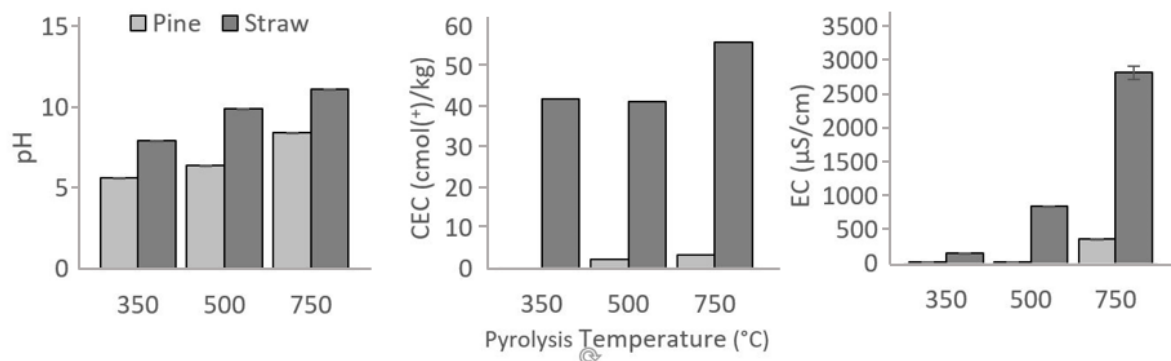


Figure 3.4 pH, EC and CEC of biochars, compared between feedstocks (Pine and Straw) and pyrolysis temperatures (350, 500 and 750°C).

CEC denotes the ability of biochar to bind cations (Hmid et al., 2014), and was found to increase with higher pyrolysis temperatures and was higher in straw derived biochars (Figure 3.4). Feedstock was the main factor influencing the differences between biochars ($F_{1,2} = 115.9$, $p < 0.05$).

Strong positive Pearson correlations were observed between pH, ash, and CEC creating a grouping of correlated parameters ($p < 0.05$). These correlations were in line with expected increases caused by pyrolysis temperature and therefore increased ash content, which result in increased pH through the concentration of ions such as K, Ca, Mg and carbonates (Kuzyakov et al., 2014, Heitkötter and Marschner, 2015). These increases in pH elevated the biochars' CEC as this parameter is pH dependent (Abdel-Fattah et al., 2015). In addition, significant positive correlations regarding sulphur ($R = 0.858$, $n = 6$, $p = 0.014$) and nitrogen ($R = 0.868$, $N = 6$, $p = 0.013$) with ash were obtained.

3.4.2 Contaminant analysis

Six of the eight heavy metals tested were detected in the biochars, with mercury and cadmium being below the limit of quantitation (<LQ) (2mg/kg) in all samples (Table 3.3). Lead, nickel and zinc were found to be below IBI guidelines in all biochars as illustrated by (Table 3.3). Similarly, arsenic, chromium and copper were below guideline levels in biochars produced from straw feedstocks.

Biochars produced from pine had elevated levels of arsenic, copper and chromium that were 1-2 orders of magnitude above IBI limits in all pine biochars excepting chromium at 750 °C. The presence of these three heavy metals at elevated concentrations was due to raw pine being milled alongside treated pine, in turn contaminating the feedstock with chromated copper arsenate. Chromated copper arsenate is the most commonly used wood preservative and treated woods typically contain chromium, copper and arsenic concentrations within the range 2.6–9.8 mg g⁻¹, 5.3–19.0 mg g⁻¹ and 5.2–16.3 mg g⁻¹ respectively (Jones & Quilliam 2014). It is likely, in Victoria and elsewhere, that timber from construction waste or wood sourced from forests, would have significant concentrations of chromated copper arsenate, which would impact the quality of the biochar. If these heavy metals are allowed to enter into the environment, through biochar application, their excessive availability could have detrimental toxic effects on local wildlife or crops (Albuquerque et al. 2013; Freddo, Cai & Reid

2012). Typically, metals measured and detected increase in concentration with higher pyrolysis temperature as found in previous work (Benavente et al., 2018). However, there are exceptions. It is likely that arsenic could be lost as volatile arsenic trioxide (As_2O_3) during pyrolysis (Jones and Quilliam 2014; Helsen and van den Bulck 2000) as it has been demonstrated that 15 – 24% of arsenic concentration can be lost during incineration at 400 – 800 °C (Yan et al. 2008). While it is possible for a fraction of arsenic to be liberated as the volatile arsenic trioxide in the presence of oxygen, it does not account for the magnitude of arsenic loss seen in this study within an oxygen limited environment at high temperature. A dissimilar trend with temperature was found for copper and chromate concentrations in pine and straw biochars. This result could be due to differences in the partition of heavy metals between the biochar and the tar. Differences in the molecular structure of the feedstocks and how contaminants are distributed in the matrix could have contributed to these results (Farrell, Rangott and Krull 2013). Further, it has been demonstrated that with respects to total heavy metals the result can be dependent on the extraction method (Enders and Lehmann 2012). Hence the term pseudo-total heavy metals must be applied, as this designates that it is the maximum that can be extracted for the method used, which is often determined by availability of lab equipment and access to materials and reagents (Beesley, Moreno-Jiménez & Gómez-Eyles 2010). In this study the remainder of the heavy metals tended to be higher in concentration in straw derived biochars than in pine. Levels for Zn were comparable to those seen for similar feedstocks for both straw and pine biochars, the same is true of Pb in pine biochars (Srinivasan & Sarmah 2015; Zhao et al. 2013), demonstrating the small pool of analogue studies from which to draw literature comparisons in this area. In Australia or in the state of Victoria, there are currently no specific biochar application guidelines and it is necessary to rely on IBI guidelines for heavy metal limits (Table 3.3). Using these criteria all straw biochars qualify as soil enhancers and all pine biochars would be unsuitable for land application due to elevated arsenic concentrations (IBI 2013). It has been demonstrated that elevated levels of arsenic, chromium and copper have a negligible effect on the determination of other parameters such as EC and pH (Jones & Quilliam 2014). Elevated metals should not interfere with ultimate analysis, proximate analysis or surface area determination.

The sixteen USEPA PAHs measured in the study were below the limit of detection (0.5 mg/kg) in most biochars with the exceptions being S500 and P350. S500 was found to contain a single PAH, 1.2 mg/kg naphthalene. Comparatively, P350 contained a total of 6 PAHs (Table 3.4), with 7,12-dimethylbenz(a)anthracene concentration dominating at 35.0 mg/kg. Out of the 6 biochars created, the PAH level in one biochar (P350) is above the suggested IBI PAH limit (6 mg/kg) (IBI 2014). PAHs are generated during biochar production through incomplete combustion of biomass. PAH concentration in biochars is feedstock-dependent (Wang et al. 2017). Naphtalene is usually the major hazardous PAH (Wang et al. 2017). In agreement with our results, it is well documented that PAH concentration in biochars diminishes with the temperature of pyrolysis (Wang et al. 2018). Oleszczuk, Joško and Kuśmierz (2013) demonstrated that in environmentally relevant applications to soil (10% rate of addition), biochar's PAH content could inhibit root growth for *Lepidium sativum* up to 92% compared to controls. Root growth inhibition started at concentrations of 5 %. Further a significant relationship was established between total PAHs, leached from biochars using water, and the mortality of a test planktonic crustacean (*Daphnia magna*). These demonstrate the threat biochars containing PAHs could pose to the environment and agricultural lands if application rates appropriate to each biochar are not determined.

Table 3.3 Heavy Metal concentrations detected in biochars (mg/kg)

Biochar	P350	P500	P750	S350	S500	S750	IBI Limits
Arsenic	1400 ±88 ^a	410 ±17 ^b	190 ±19 ^c	<LQ	<LQ	<LQ	13 - 100
Cadmium	<LQ	<LQ	<LQ	<LQ	<LQ	<LQ	1.4 - 39
Chromium	1400 ±21 ^{A,a}	180 ±19 ^{A,b}	13 ±3 ^{A,c}	2 ±1 ^{B,c}	3 ±1 ^{B,b}	13 ±2 ^{A,a}	93 - 1200
Copper	900 ±14 ^{A,a}	880 ±17 ^{A,a}	650 ±17 ^{A,b}	15 ±2 ^{B,c}	20 ±2 ^{B,b}	85 ±6 ^{B,a}	143 - 6000
Lead	2 ±1 ^{A,a}	2 ±1 ^{A,a}	2 ±1 ^{B,a}	5 ±1 ^{A,b}	3 ±1 ^{A,b}	26 ±7 ^{A,a}	121 -300
Mercury	<LQ	<LQ	<LQ	<LQ	<LQ	<LQ	1 - 17
Nickel	<LQ	<LQ	<LQ	<LQ	2 ±1 ^a	5 ±1 ^b	47 - 420
Zinc	11 ±1 ^{A,a}	10 ±1 ^{A,a}	13 ±1 ^{A,a}	39 ±1 ^{B,c}	29 ±2 ^{B,b}	120 ±5 ^{B,a}	416 - 7400

IBI Guidelines heavy metals in biochars are presented as an interval as per the original source, due to the different soil tolerance level for these elements in regulatory bodies in the US, Canada, EU and Australia. <LQ represents data points at which all samples were below the limit of quantification reporting value (2 mg/kg). Statistically significant relationships (P<0.05) are denoted by capital letters (A, B) for feedstock and lowercase letters (a, b, c) for temperature. Values are presented as average values ± standard deviation.

Table 3.4 PAHs concentration in biochars (mg/kg)

Biochar	P350	P500	P750	S350	S500	S750
Benzo(k)Fluoranthene	0.9	<LQ	<LQ	<LQ	<LQ	<LQ
7,12- Dimethylbenz(a)anthracene	35.0	<LQ	<LQ	<LQ	<LQ	<LQ
Fluoranthene	0.9	<LQ	<LQ	<LQ	<LQ	<LQ
Naphthalene	0.6	<LQ	<LQ	<LQ	1.2	<LQ
Phenanthalene	0.6	<LQ	<LQ	<LQ	<LQ	<LQ

Data only displayed for PAHs with values above detection limit in at least one biochar. IBI Guideline maximum accumulative USEPA 16 PAH concentration 6 mg/kg. “<LQ” represents data points at which all samples were below the limit of quantification (<0.2 mg/kg)

3.5 Conclusion

Six biochars of varying physiochemical properties were successfully engineered through slow pyrolysis at three selected temperatures, using waste feedstocks common in Victoria, Australia. It was found that both temperature and feedstock type were influential on the types of biochars created from selected biomasses and could in turn determine their suitability for environmental application.

All straw biochars created were compliant with IBI guidelines, with respects to contaminant burden. Pine biochars contained excessive levels of arsenic, chromium and copper due to contamination with a common wood treating agent, chromated copper arsenate. Low temperature pine biochar (350 °C) contained a number of PAHs exceeding both accumulative and individual limits, rendering them unsuited to land application; however PAHs could be eliminated by employing higher pyrolysis temperatures.

A range of different biochars with varying carbonized fractions, surface areas and functional groups were produced. The biochars created generally exhibited characteristics favourable for soil enhancement, such as elevated fixed carbon, CEC, pH and low bulk density. Our results can assist in decision making for biochars which could be engineered from pine sawdust and straw waste biomasses for specific environmental amelioration purposes, while aiding in reducing the amount of biomass reaching landfill and reducing carbon emissions.

Chapter 4

Fast, Cost-effective, “PFAS clean” Serial Sorption Technique Coupled with Adapted High Volume Direct Aqueous Injection LCMS Method

Matthew Askeland ^a, Bradley Clarke ^b and Jorge Paz-Ferreiro ^{c,*}

a Department of Environmental Engineering, RMIT University, Melbourne 3000, Australia
(E-mail: matthew.askeland@rmit.ed.au)

b School of Chemistry, University of Melbourne, Victoria 3010 Australia
(E-mail: brad.clarke@unimelb.edu.au)

c School of Engineering, RMIT University, Melbourne 3000, Australia
(E-mail: jorge.paz-ferreiro@rmit.ed.au)

Submitted for review to Chemosphere as attached Methods X paper 20st August 2019

4.1 Introduction

Per- and polyfluoroalkyl substances (PFAS) are a group of man-made chemicals attracting significant global attention due to evidence that PFAS are ubiquitous global environmental contaminants, environmental persistent, mobile, can bioaccumulate and are toxic. Consequently, increasing emphasis is placed on the immobilisation and removal of PFAS from contaminated environmental matrices such as: potable water, surface water, groundwater, wastewater, sediments and soils (Cao et al. 2019; Dauchy et al. 2017; Hepburn et al. 2019). To achieve this, development of PFAS sorbents such as powdered activated carbons, modified activated carbons, biochars, resins and nanomaterials for PFAS removal from various environmental matrices is increasingly undertaken (Du et al. 2014).

Sorption studies are used to observe the interaction of sorbent and sorbate. There are two key limitations when undertaking sorption experiments for PFAS that are (1) the experimental protocol and (2) analytical techniques. The current batch sorption methods approached recommended by OECD Guideline 106 (OECD 2000) are problematic, firstly, due to large sample numbers and PFAS specific laboratory difficulties, including near ubiquitous background PFAS contamination. Secondly, PFAS analytical techniques currently require solid-phase extraction (SPE) to be employed which is slow and expensive, prior to instrumental analysis with liquid chromatography-mass spectrometry (LC-MS). Both factors combine to make generation of PFAS sorption data difficult in a timely and cost-effective manner. As a result, a suitable alternative approach is needed to mitigate the drawbacks of current methodologies whilst catering for the high sample throughput required by benchtop trials characterising the sorption behaviour of PFAS – sorbent pairings.

The method outlined addresses the testing of sorbents capacity for PFAS sorption in an aqueous matrix, adaptable to several potential experimental conditions, in a fast and cost-effective manner. This was achieved by modifying commonly applied sorption and analytical methods (Du et al. 2014; Hepburn et al. 2019) and coupling these approaches with a high throughput LC-MS direct aqueous injection method.

4.2 Method

4.2.1 Chemicals and Reagents

EMD Millipore Hyper-grade LiChrosolv methanol (MeOH) was used as the mobile phase in LC-MS analysis, for the reconstitution of all samples in 10% MeOH and for washing pipette tips when preparing calibration standards. EMD Millipore LC-MS grade MeOH employed in sample preparation and triplicate wash of all polypropylene bottles or equipment used in experiments. All solvents were tested for PFAS content by LC-MS prior to use. Additionally, Milli-Q water (Ultrapure Millipore Synergy UV Milli-Q water system) was utilised and confirmed to be PFAS-free.

Native PFAS standards were acquired from Sigma Aldrich (Australia). These included Perfluorobutanoic acid (PFBA), Perfluorohexanoic acid (PFHxA), Perfluorooctanoic acid (PFOA), Perfluorobutanesulfonic acid (PFBS), Perfluorohexanesulfonic acid (PFHxS), and Perfluorooctanesulfonic acid (PFOS). ¹³C labelled standards for the above PFAS were obtained from Wellington Laboratories Inc. with the following labels PFBA (M3), PFHxA (M2), PFOA (M2), PFOA (M8), PFBS (M3), PFHxS (M3), PFOS (M4), PFOS (M8), where M denotes the labelled carbon number.

4.2.2 “PFAS Clean” Preparation of Solvents, Stocks and Standards

Pipette Tip Wash

Pipette tips were a known source of PFAS contamination in previous laboratory experiments. Therefore, all pipette tips were tested and confirmed to be PFAS-free prior to commencing experimental work. Furthermore, pipette tips used in experiments were washed using a two step-sequence to prevent the carryover of PFAS, or leaching of PFAS impregnated within the pipette material, into samples. Pipette tips were rinsed with MeOH three times followed by a further rinse with 10% MeOH Milli-Q water solution.

Calibration Standard and Spiking Solution Preparation

Calibration standards were prepared in Agilent Technologies 1 mL Polypropylene snap lid GC vial by serial dilution using all six native PFAS standards in a 10% by volume MeOH milli-Q water solution. Calibration standards ranged from 0.01 to 10 µg/L and included a constant concentration of 1 µg/L carbon labelled standards as PFBA (M3), PFHxA (M2), PFOA (M2), PFBS (M3), PFHxS (M3), and PFOS (M4).

A 10 µg/L Carbon labelled PFAS solution was prepared in a 50 mL polypropylene centrifuge tube using hypergrade MeOH and PFBA (M3), PFHxA (M2), PFOA (M2), PFBS (M3), PFHxS (M3), and PFOS (M4) carbon labelled standards. This solution was used for addition of surrogates to samples during sample preparation.

PFOA (M8) and PFOS (M8) were prepared in a 10% by volume MeOH milli-Q water solution to achieve a 1 µg/L concentration for injection standard.

Each target PFAS congener had a spiking solution prepared in ACS grade methanol washed 1 L polypropylene screw cap bottles using milli-Q water to achieve desired concentration. PFAS standards were dissolved in 10 mL MeOH in a polypropylene centrifuge tube before addition to a polypropylene bottle with 990 mL of milli-Q water. This bulk spiking solution was placed on a shaker for an hour before it was divided out into relevant serial experiments. 1 mL of each spiking solutions was prepared for sampling as per Section 2.3.2 and analysed by LCMS to determine exact concentration as starting concentration for experiments (C0).

In all cases, pipette tip washing mentioned in 2.2.1 was adhered to, and solutions were retained for no longer than 24 hours if not exhausted in experiments.

4.3 Sample Preparation and Sorption Experiments

4.3.1 Equilibrium Experimental Protocol

Equilibrium experiments were designed to determine the contact time required to reach a steady state (equilibrium) in a sorption system. This time value is applied to subsequent sorption/desorption experiments. In triplicate, 200 mg of sorbent (selected mass dependant on projected sorbent strength) and 5 mL of 5 µg/L PFAS spiking solution were added to pre-weighed 15 mL polypropylene centrifuge tubes. Seven (7) triplicate sets were created to be destructively sampled at their relevant timepoint, resulting in 21 samples. The samples were re-weighed and the exact mass of sorbent and PFAS spiking solution could then be determined by difference. The sample was vigorously shaken to ensure wetting of all sorbent with PFAS solution. The above was undertaken for testing the equilibrium times of each individual target PFAS – sorbent pairing resulting in the following factorial, $n = (21 \text{ samples}) * (\text{number target compounds}) * (\text{number of sorbents requiring testing})$. Samples were placed on large orbital shakers in centrifuge tube racks which were collectively secured in batches by large rubber bands and removed at time intervals of 0, 1, 2, 3, 8, 24, 48 hours for sample preparation (see section 2.3.2) and subsequent analysis (see section 2.4). Equilibrium time was determined by statistically interrogating the data using Microsoft's Excel package to determine the time point at which no statistically significant change in solution concentration was observed compared to the timepoint sampled before and after it.

4.3.2 Sorption Experimental Protocol

Sorption experiments were conducted to determine the capacity of a sorbent for a given sorbate under specific environmental conditions when the system is at equilibrium. In triplicate, various amounts of sorbent (10, 50, 75, 100, 200, 300, 400, 500 and 1000 mg – in the case of this particular experiment) were each added to individual pre-weighed 15 mL polypropylene centrifuge tubes with 5 mL of 5 µg/L PFAS spiked solution (spiked concentration experiment specific). The samples were reweighed, and by difference, the exact mass of sorbent and PFAS spiked solution could be determined. The sample was vigorously shaken to ensure wetting of all sorbent with PFAS solution. Samples were placed on large orbital shakers in centrifuge tube racks, collectively secured in batches by large rubber bands, for their relevant equilibrium times as determined in Section 2.3.1. Hereafter, samples underwent sample preparation (see section 2.3.2) before analysis by LC-MS (see section 2.4). Sorption samples in centrifuge tubes were retained, weighed, and this value used to calculate the volume of water remaining in the tube for upcoming desorption testing. The above was undertaken for each sorbent - sorbate pairing to be tested.

4.3.3 Sorption Experimental Protocol

Desorption experiments were conducted to determine the extent at which the sorbed fraction is reversible sorbed as a percentage of total sorbed fraction. This experiment employed triplicate 10, 50, 75, 100, 200, 300, 400, 500, and 1000 mg sorbent treatment samples retained from prior sorption experiments, to which 5 mL of milli-Q water was added to each tube. The samples were vigorously shaken to ensure the resuspension and adequate mixing of biochar with milli-Q water. Samples were placed on large orbital shakers in centrifuge tube racks, collectively secured in batches by large rubber bands, for their relevant equilibrium times as determined in Section 2.3.1. The samples were reweighed, and the exact mass of milli-Q water was determined by difference. Sample expected PFAS solution concentration was calculated using known PFAS concentration and remaining volume of water in tube, and exact dilution by 5 mL unspiked milli-Q addition. The difference between expected solution concentration and measured solution concentration was considered the desorbed fraction. Samples were prepared using the previously described technique (see section 2.3.2) and analysed by LC-MS (see section 2.4). Desorption was calculated as the percentage represented by the difference between expected and analytically determined solution concentration, as a factor of total sorbed fraction determined in sorption experiments (section 2.3.3).

4.3.4 Sample Preparation

All samples underwent the following preparation technique prior to LC-MS analysis. Samples for the equilibrium, sorption and desorption protocols were prepared in new Nunc™ 15 mL screw top sterile polypropylene centrifuge tubes. Samples were centrifuged at 15,000 rpm for 30 minutes and 900 µL of the supernatants decanted from each sample by washed pipette into individual pre-weighed 15 mL centrifuge tube. One hundred µL of MeOH containing 10 µg/L carbon labelled surrogates was added to the sample to result in a the 10% MeOH solution by volume with carbon labelled surrogates at a concentration of 1 µg/L. Samples were then vortexed before filtering with Terumo™ 5 mL Luer Lock polypropylene stopperless syringes and Corning™ polypropylene housed 15 mm diameter 0.2 µm cellulose syringe filters. The filtrate was delivered into a labelled polypropylene GC vial with polypropylene snap top lid and placed in a fridge at 4°C until analysis by LC-MS. Sample tubes could then be disposed of, in the case of equilibrium and desorption experiments, or retained for desorption experiments, in the case of sorption experiments.

4.4 LCMS Direct Aqueous Injection Method

4.4.1 Calibration and Mobile Phases

Calibration stock solutions were prepared in 10% MeOH milli-Q water solution at the following concentrations by serial dilution: 0.01, 0.03, 0.06, 0.09, 0.15, 0.20, 0.30, 0.50, 0.75, 1.00, 2.00, 3.00, 4.00, 6.50, 10.00 $\mu\text{g L}^{-1}$. One $\mu\text{g L}^{-1}$ carbon labelled injection standards (PFOA (M8) and PFOS (M8)) were used for “sandwich injections” to monitor instrumental method performance and replaced every 12 hours of LC-MS sampling or every 209 samples. Quantitation was achieved through isotope dilution; wherein a calibration curve was included in every new set of 209 samples.

All mobile phases were tested for PFAS contamination prior to use. Solvents were prepared in isopropyl alcohol (IPA) and MeOH washed 1 L glass Schott bottles with Teflon™ liners removed, as these were a known source of PFAS contamination.

4.4.2 Sample analysis

Samples were analysed on an Agilent 1290 Infinity II™ Liquid Chromatograph coupled to an Agilent 6495B Triple Quadrupole Mass Spectrometer. Instrument operational conditions are outlined in Table 4.1 and transitions for target compounds in Table 4.2. Sample analysis employed a “sandwich injection” in which injection standards were added to sample. This entailed the drawing of 5 μL of sample followed by 1 μL of 1 $\mu\text{g/L}$ ^{13}C injection standard, and then a further 5 μL of sample. A needle washing program was employed to prevent carry over.

Data processing and quantitation was undertaken using the Agilent Mass Hunter Suites Quantitative analysis package (Version 8). Measured PFAS concentrations were corrected in software for ^{13}C recovery, and concentrations of branched and linear isotherms quantified as a total for any PFAS congener.

Table 4.1 LCMS Operational Conditions

Item	Parameters
Sample Injection	10 μ L (5 μ L sample, 1 μ L 13 C, 5 μ L sample) Draw speed 400 μ L min ⁻¹ Ejected at 200 μ L min ⁻¹ Offset of 0.2 mm
13C Addition	1 μ L
Separation Column	Agilent EclipsePlusC18 - RRHD 1.8 μ m (2.1x50 mm)
Delay Column	Agilent EclipsePlusC18, 3.5 μ m (4.6x50mm)
Column environment	40°C
Multi-wash	1 - Needle (10 s – 90 % MeOH) 2 - Seat Backflush (10 s 50/50 MeOH) 3 - Needle and Seat Backflush (10 s start conditions)
Injection programme	1 - Needle wash (5 s) 2 - Sample draw 3 - needle wash (5 s), 4 - 13 C draw, 5 - Needle wash (5 s), 6 - Sample draw, 7 - Needle wash (5 s), 8 – Inject Time: 55 seconds
Solvents	Organic: Hypergrade MeOH Aqueous: H ₂ O with 5 mM NH ₄ acetate
Gradient	0 - 0.5 mins start condition (40 % MeOH) 0.5 - 3 mins ramp to 100 % MeOH 3 – 5.5 mins system at 100 % MeOH 5.5 mins end run
Source conditions	Gas temp: 250°C Flow: 11 l/min Nebulizer: 25 psi
Ionisation	Negative electrospray ionization
Sheath	Sheath gas 375°C Sheath gas flow 11 L/min
Capillary	Capillary pos 3500V neg
iFunnel	2500V chamber current 0.18 μ A High Pressure RF (negative) 90V Low Pressure RF (negative)100V
Detection mode	Dynamic Multiple Reaction Monitoring
Total run time:	6.5 mins per sample

4.4.3 Method QA/QC

Sample batches of ~200 samples included 15 QA/QC samples (method blanks (3), laboratory control samples (3), milli-Q solvent blank (3), MeOH solvent blank (3), and 1 µg/L QC (3)). The instrument was flushed between consecutive runs, followed by a suite of three no inject samples and two levels (high and low) of confirmatory calibration standard injections before the commencement of the following run. If no injects were found to contain target PFAS, the LCMS system was flushed using 50:50 MeOH to water for an hour, and this process repeated until non-detect PFAS no injects were attained. If either calibration standard deviated by 20 % of its previous PFAS concentration the run was stopped, and new calibration standards prepared while the system was flushed with 50:50 MeOH to water for an hour.

Method blanks were created by adding 5 mL of milli-Q water to a centrifuge tube. Laboratory control samples (LCS) were prepared in triplicate by adding 5 mL of 5 µg/L PFAS spiking solution to a centrifuge tube and processing this alongside experimental samples. These allowed the determination of any fraction of PFAS lost during storage or preparation of samples. Solvent blanks consisted of either 1 mL milli-Q water or 1 mL hyper grade methanol used in sample preparation added directly to 1 mL polypropylene GC vials with clip on polypropylene caps.

In addition, each LC-MS run included five 1 µg/L QC samples interspersed between experimental samples. A 10% RSD was allowed for 1 µg/L QC samples. Exceedance of the RSD saw the preparation and validation of a new set of calibration standards after the instrument had been flushed with 50:50 MeOH to water solution for an hour. QC samples ensured consistency in sampling and were also used to ensure no significant impact went unnoticed between solvent changes, preparation of samples and instrument running conditions for different batches.

Table 4.2 LCMS Target PFAS Transitions and retention times

Compound Name	Precursor Ion (m/z)	Product Ion (m/z)	Retention Time (min)	Delta Retention Time (min)	Fragmentor (V)	Collision Energy (V)	Cell Accelerator Voltage (V)	Polarity
PFBA	213	169	0.9	1.03	380	6	2	Negative
PFBA-13C3	216	172	2	0.5	380	8	2	Negative
PFBS	299	99	2.36	0.97	380	36	2	Negative
PFBS	299	80	2.36	0.97	380	44	2	Negative
PFBS-13C2	302	99	2.28	0.5	380	36	2	Negative
PFHxA	313	269	2.93	0.97	380	6	2	Negative
PFHxA	313	119	2.93	0.97	380	22	2	Negative
PFHxA-13C2	314.9	269.9	2.93	0.88	380	8	2	Negative
PFHxS	399	99	3.32	1.02	380	44	2	Negative
PFHxS	399	80	3.32	1.02	380	48	2	Negative
PFHxS-1C3	402	99	2.73	0.5	380	44	2	Negative
PFOA	413	368.9	3.55	1.07	380	6	2	Negative
PFOA	413	169	3.55	1.07	380	18	2	Negative
PFOA-13C8	421	376	3	0.5	380	6	2	Negative
PFOS	498.9	99	3.73	1.12	380	56	2	Negative
PFOS	498.9	80	3.73	1.12	380	56	2	Negative
PFOS - 13C4	503	99	3.27	0.5	380	48	2	Negative

4.5 Method Performance

4.5.1 LCMS and Sample Preparation

All recoveries were found to be within a 90 – 110% range, falling within the allowable 80 – 120% predetermined criteria. Method detection limits (MDL), limits of quantitation (LOQ), method precision and accuracy were calculated from experimental data and are presented in Table 4.3. Where MDL is defined as the lowest detectable concentration of any given PFAS congener for the analytical method. Comparatively LOQ represents the lowest PFAS concentration that can be accurately quantified. Precision identifies how close mean analytical results were to the true value of the sample as a percentage. Accuracy addresses variation between repeated measurements presented as a percentage deviation from the mean value. Method validation LOQs constituted a maximum of 5% of error as a fraction of 5 ppb solution concentration in experiments. Experimental replication was evident with high accuracy between samples. The method was found to be precise with quantitation demonstrating near 89.6 – 107.7% precision as a factor of actual value. RSD, for the average of 1 ppb QC samples included in a single LC-MS run was found to have a maximum value of 4.5% for any of the 6 studied compounds, well below the selected sample RSD acceptance criteria of 10%. Performance data are tabulated for each compound in Table 4.3.

Table 4.3 Method Performance Data

	PFBA	PFBS	PFHxA	PFHxS	PFOA	PFOS
MDL (ng L⁻¹)	66	31	19	70	25	72
LOQ (ng L⁻¹)	207	99	59	221	79	228
Accuracy (%)	99.3	89.6	97.5	100.4	107.5	107.7
Precision (%)	1.3	0.8	0.6	2.6	0.7	2.2

4.5.2 Establishment of Isotherms and Sorbed Fractions

The data collected from analysis were input into Freundlich and Langmuir isotherms for sorption modelling. Using the appropriate isotherm or equilibrium model, R² values of 95 - >99 % were readily achieved for compounds that adequately sorbed to tested sorbents; demonstrating that the method was fit for purpose. It was noted that PFAS-sorbent pairings with less than 40 % removal of PFAS from solution did not achieve desirable R². While suitability for isotherm input was namely determined by extent of sorption for sorbent-PFAS pairing, RSDs of <5 % were readily achieved for sorbent-sorbate pairings that resulted in high sorption.

4.5.3 Limitations of Method

Due to the low MDL and LOQ of this method, it is sensitive to PFAS contamination. This means, the highest level of PFAS clean technique needs to be applied alongside a sound QA/QC program. While this is well addressed in the sample preparation technique, the method is reliant on operator adherence to PFAS clean techniques. In addition, experimentally determined MDLs and LOQs imply an alternative method would be required to measure behaviours wherein most sample points fall in the concentration bracket 0 - 0.25 µg/L. As, such this method was not designed to measure sorption behaviour at ultra-trace (< 0.25 µg/L) concentrations. The use of a serial method as opposed to batch method generates greater control of contamination risk and identification; however, it does produce a large volume of waste in the form of centrifuge tubes, filters, syringes and pipettes. Due to the gradient and short run time employed in this high throughput method, the separation of branched and linear isomers was not possible.

4.5.4 Benefits of Improved Method

In addition to the cost and time efficiency of this method, it is suggested that the PFAS-clean aspect of the method resulted in no contamination of samples, with all blank samples presenting as non-detect for all PFAS. The experimental design as a serial method in place of a batch method removes the accumulative encumbrance of batch samples to contamination. Where in the serial method each triplicate sample is a true standalone triplicate, meaning statistical analysis is not subject to deviations of a single source, as in the case for traditional batch experiments. This method allows the high throughput of samples by batching of approximately 182 samples in a 24-hour period, not including instrument preparation, flushing and determination of equilibrium times.

Lastly, this method is flexible to be adjusted with respects to experimental parameters used, such as PFAS concentrations and congener types, mixtures thereof, sorbents, sorbent application rates, matrix environment (for example pH, Dissolved Organic Matter, EC, and temperature) and scale. This flexibility allows the application of this technique to a variety of PFAS and sorbent properties relevant to the development of more effective PFAS sorbents.

Overall, a simple cost and time effective method was developed. The method performed within the selected performance criteria during the determination of sorption qualities of selected PFAS with a given sorbent using a serial sorption technique and specially developed high throughput direct injection LCMS technique. While the method was developed for sorption studies in aqueous environmental matrices, the direct injection LCMS technique could be applied as a screening tool for PFAS in environmental surface waters, drinking water, irrigative water and wastewater effluents. Additionally, desorption of PFAS from impacted sediments or biosolids could be modelled toward risk assessment of long-term impact on PFAS mass flux from the solid matrix to the aqueous phase. This novel tool could provide fast and cost-effective quantitative assessment (qualitative if below LOQ) of PFAS in impacted matrices. It is however to be noted that the LOQs discussed in Table 4.3 are above many Australian guideline for PFAS in water (Table 1.12) (HEPA 2018).

Chapter 5

Examining the Sorption Behaviour of Priority PFAS onto Engineered Biochars Prepared from Waste Feedstock at Three Pyrolysis Temperatures

Matthew Askeland ^a, Gabriel Gascó ^b, Ana Méndez ^c, Bradley Clarke ^d and Jorge Paz-Ferreiro ^{e,*}

a Department of Environmental Engineering, RMIT University, Melbourne 3000, Australia

b Departamento de Producción Agraria, E.T.S.I. Agronómica, Alimentaria y de Biosistemas, Universidad Politécnica de Madrid, Ciudad Universitaria, 28004 Madrid, Spain

c Departamento de Ingeniería Geológica y Minera, E.T.S.I. Minas y Energía, Universidad Politécnica de Madrid, C/Ríos Rosas No. 21, 28003 Madrid, Spain

d School of Chemistry, University of Melbourne, Victoria 3010 Australia

e School of Engineering, RMIT University, Melbourne 3000, Australia

Submitted for review to Chemosphere 20th August 2019

5.1 Abstract

Biochars are produced through the thermal degradation of biomass. Recent studies have demonstrated their potential application for removal of per- and polyfluoroalkyl substances (PFAS) from water. However, little is known regarding the impact biochar production conditions have on biochar PFAS sorption behaviour. In this study, the sorption behaviour of PFAS onto biochar prepared from two feedstocks (pine wood, pea straw) at three temperature conditions (350, 500 and 750°C) was determined.

Three perfluoroalkyl carboxylic acids (PFCAs; Perflurobutanoic acid (PFBA), Perfluorohexanoic acid (PFHxA), and Perfluorooctanoic acid (PFOA)) and three perfluorosulfonic acids (PFSAs; Perfluorobutanesulfonic acid (PFBS), Perfluorohexanesulfonic acid (PFHxS), and Perfluorooctanesulfonic acid (PFOS)) were studied. Biochar characterisation and batch sorption experiments allowed for the assessment of equilibrium, sorption and desorption characteristics of studied PFAS to biochars. Experiments were carried out at PFAS concentrations emulating those observed in the environment. All biochars were found to remove < 50 % of short-chain PFAS, PFBA and PFBS, and would be unsuitable for removal of these compounds from aqueous matrices. Furthermore, biochars produced at low temperature (350 °C) removed < 50 % of all studied PFAS. In the case of the remaining PFAS-biochar combinations, equilibrium was typically reached by the 8th hour for biochar-PFAS equilibrium experiments, baring those experiments including PFHxA and PFHxS which, in many cases, required longer time periods to reach equilibrium.

Equilibrium time was found to be a factor of both congener type, and biochar production method (temperature and choice of feedstock). Pine biochar produced at 750°C exhibited favourable PFAS sorption characteristics such as a quick equilibrium time, efficacy at a comparatively low application rate, and low desorption, potentially rendering it an effective and cheap sorbent for 3 PFAS (PFHxS, PFOA, and PFOS). PFAS sorption to biochars was demonstrated to largely occur in the first 0.5- 1 hour of equilibrium experiments. The extent of sorption increased with increasing pyrolysis temperature and was higher in pine derived biochars.

PFAS functional group and chain length each affected the sorption behaviour for PFAS-biochar pairs, with functional group being of greater influence when considering PFHxS and PFOA. Biochars removed a maximum of 94 % of PFAS from solution, with a maximum desorption of 20 % following an equal desorption equilibrium period. Repeating experiments in a mixed mode resulted in little difference in PFAS-biochar specific equilibrium times. However, sorption and desorption behaviour were found to be impacted by inter-PFAS interaction. This research provides a promising first step towards the data needed for reverse engineering biochars for PFAS sorption in the aqueous environment.

Keywords: Biochar; PFAS; Perfluoroalkyl Substances; Sorption; Desorption; Remediation; Immobilization.

5.2 Introduction

Perfluoroalkyl substances (PFAS) are a class of emerging contaminant that are the focus of much recent scientific and regulatory attention due to their toxicity, ubiquity, environmental mobility and persistence (Clarke & Smith 2011; HEPA 2018). In general, PFAS molecules consist of a hydrophilic functional group attached to a hydrophobic fluorinated carbon chain of variable length (Du et al. 2014). The C-F high bond energy results in strong PFAS resistance to degradation through chemical and biological processes in the environment (Naile et al. 2010; Wang et al. 2013). PFAS anions are amphiphilic and therefore are highly mobile surfactants in the environment (Labadie & Chevreuil 2011; Olsen et al. 2005). A growing body of evidence implicates PFAS of an array of toxic modes of action, uptake pathways, and extensive dispersal throughout environmental compartments (Bengtson Nash et al. 2010; Borg et al. 2013; Rigét et al. 2019; Stahl, Thorsten, Mattern & Brunn 2011).

PFOS and its precursors were listed as an United Nations Persistent Organic Pollutants (POP) under the Stockholm Convention in 2010 (POPRC 2008) and PFOA and PFHxS were nominated to be included in 2019 (UN 2015; Wang et al. 2009). Ultimately, when released in the environment, PFAS are transported, namely by water to waterways, groundwater, soils and marine habitats (Lloyd-Smith 2016). Once in the environment PFAS can accumulate in organisms through ingestion of contaminated water, soil or dust (Haug et al. 2011). Alternatively, the consumption of contaminated organisms provides a major uptake pathway, through which biomagnification impacts apex predators, including humans (Haug et al. 2010; Stahl et al. 2009).

PFAS functional groups influence its chemical interactions within the environment. For example, PFCAs are relatively mobile in water and will sorb to a lesser extent to organic matter in the environment than PFSA of equivalent C-F chain length (Chen et al. 2012; Gellrich, Stahl & Knepper 2012; Prevedouros et al. 2006; Zareitalabad et al. 2013). Ubiquitous background detection of PFAS is considered the result of extensive PFAS use globally and subsequent dispersion throughout the environment from an array of diffuse sources [18]. In addition to ubiquitous background levels, PFAS contamination often occurs as point source contamination, where PFAS have been employed or liberated, near a transport mechanism (Prevedouros et al. 2006). Wastewater treatment plants (WWTPs) have been identified as a PFAS point source to the environment. This is due to the concentration and biotransformation of diffuse PFAS and precursors contained in influent through the wastewater treatment process, followed by their subsequent release from WWTP facilities as higher concentrations of recalcitrant PFAS molecules in effluent, recycled water or biosolids (Becker, Gerstmann & Frank 2008; Bossi et al. 2008; Eriksson, Haglund & Kärrman 2017; Ruan et al. 2015; Szabo et al. 2018; Thompson et al. 2011; Wang et al. 2005).

The need for effective removal strategies of PFAS from water is important (Zhang, Zhang, & Liang 2019), particularly to minimise further environment contamination from contaminated sites, WWTPs, or a growing list of other sources. Potentially this could be managed by addressing PFAS sources to groundwater, surface waters, and WWTPs through the capture of PFAS using sorbents, semipermeable membranes, and precursor oxidation technologies at the source, followed by subsequent destructive technologies (Kucharzyk et al. 2017; McNamara et al. 2018; Pan, Liu & Ying 2016; Ross et al. 2018). Alternatively, in the case of WWTPs, diffuse inputs to WWTPs can be addressed through capturing PFAS in the wastewater treatment process, therefore

exploiting the concentration of PFAS at this point in their transport (Appleman et al. 2014; McNamara et al. 2018; Pan, Liu & Ying 2016).

Biochar, the carbonaceous product of biomass pyrolysis, is as a potential sustainable resource for the removal of PFAS from the environment (Kupryianchyk et al. 2016). Biochars have been demonstrated to be suitable sorbents with PFAS removal efficiencies comparable to GAC in several studies (Abdel-Fattah et al. 2015; Deng et al. 2015; Du et al. 2014; Kucharzyk et al. 2017; Xiao et al. 2017), where hydrophobic biochars with high porosity and well-developed microstructure behaved as attractive sorbents for PFAS. However, focus has primarily been on PFOS and PFOA (Ray et al. 2019) with increasing attention being paid to the shorter four and six chain compounds of the perfluorocarboxylic acids (PFCAs; PFBA and PFHxA) and perfluoroalkyl sulphonic acids (PFSAs; PFBS and PFHxS) only being more recent (Glover, Quiñones & Dickenson 2018; Murray et al. 2019; Yeung, Yamashita & Falandysz 2019). Through the manipulation of biochar production parameters, such as feedstock and pyrolysis temperature, it is possible that biochars can be engineered to optimise PFAS sorption. Parameters likely to impact the affinity of PFAS for biochar may be increased the surface area, pore microstructure, degree of carbonization, and prevalence of surface functional groups (Morales et al. 2015; Tang et al. 2013; Vaughn et al. 2015; Wu et al. 2013; Xiao et al. 2017; Zhi & Liu 2018).

This study aims to examine the relationship between biochar PFAS sorption and biochar physiochemical characteristics and propose production conditions that will result in the highest PFAS removal from contaminated water. Sorption behaviour of PFAS is often heavily associated with chain length (Dalahmeh, Alziq & Ahrens 2019), selecting PFBA, PFBS, PFHxA, PFHxS, PFOA, and PFOS, allows the exploration of the effect PFAS congener chain length and functional group has on PFAS-biochar sorption behaviour for the more recalcitrant and abundant forms of PFAS. Typically surface water PFAS concentrations in the environment range from below detection limits though to hundreds of ng/L (Nakayama et al. 2019), and can reach as high as tens of µg/L at contaminated sites (Cardno-LanePiper 2014). In consideration of this, the present study undertook sorption experiments at a constant concentration reflective of that seen in the contaminated environment (surface and wastewaters). The variation of biochar mass over 3 orders of magnitude, as opposed to PFAS concentration, allowed the development of an adequately sensitive method for the quantitation of sorbed PFAS fractions at the selected low experimental PFAS concentrations. To the authors' knowledge, the present work is the first to approach a PFAS sorption study in this manner, with the current body of literature typically undertaking sorption to biochars or activated carbon within the range 0.1 – 700 mg/L (Zhang, Zhang, & Liang 2019).

5.3 Methods

5.3.1 Biochar Preparation

Six biochars were produced from pine sawdust and pea straw. Briefly, biochars were prepared at 350 °C, 500 °C and 750 °C using a heating rate of 8.3 °C min⁻¹ and a 1-hour dwell time. Biochars were coded by feedstock (pine sawdust, coded P; Pea Straw, coded S) and the respective pyrolysis temperature (P350, P500, P750, S350, S500 and S750). The production and characteristics of the six biochars studied in this experiment are detailed in a previous article [56]. Prior to batch experiments, biochars were tested for PFAS extractable in Milli-Q water. Biochars were demonstrated to be blank for all target PFAS.

5.3.2 Chemical Standards

PFAS standards for Perfluorobutanoic acid (PFBA), Perfluorohexanoic acid (PFHxA), Perfluorooctanoic acid (PFOA), Perfluorobutanesulfonic acid (PFBS), Perfluorohexanesulfonic acid (PFHxS), and Perfluorooctanesulfonic acid (PFOS) used in spiking solutions were obtained from Sigma Aldrich (Missouri, United States). ¹³C and native PFAS used in the preparation of calibration standards were purchased as individual PFBA, PFBS, PFHxA, PFHxS, PFOA and PFOS standards from Wellington Laboratories Incorporated (Ontario, Canada). Ammonium acetate was acquired from Sigma Aldrich (Missouri, United States). Hypergrade Methanol (LiSolv) was purchased from EMD Millipore (Massachusetts, United States).

5.3.3 Experimental Design

All experiments were undertaken as either an individual or mix mode, in which solutions were spiked with just one PFAS congener (individual mode) or solutions spiked with an equal concentration of each of the 6 target PFAS congeners (mix mode). All consumables and equipment were tested prior to experimental procedures and confirmed to be free from PFAS contamination.

Equilibrium Experiments

Equilibrium, sorption and desorption experiments were conducted as serial experiments carried out in 15 mL polypropylene centrifuge tubes, where 5 mL of 5 µg/L PFAS spiked solution were used in experiments. Equilibrium testing was conducted applying a constant 100 mg of each biochar to samples, which were placed on a shaker and removed for sample preparation at times 0, 1, 3, 5, 8, 24, and 48 hours. All experiments were carried out in triplicate. Sample aqueous PFAS concentrations were measured by LC-MS. Equilibrium data was fitted to first order, second order and an intraparticle diffusion models.

Sorption Experiments

In sorption experiments biochar was applied to triplicate samples over eight levels (0, 50, 75, 100, 200, 300, 400, 500 mg biochar) to achieve biochar application rates of 5, 10, 15, 20, 40, 60, 80, 100 g/L. Sorption experiments were conducted using a constant equilibrium time derived for each compound in the equilibrium experiments described previously. In addition, a constant 5 mL of 5 µg/L PFAS solution was added to each sample. Samples were prepared for LC-MS analysis after running for their relevant equilibrium time on a shaker. The volume of solution remaining in the sorption experiment centrifuge tube after sample preparations was determined by mass, and the sample was retained for desorption experiments. Experimental sorption data were then fitted to Langmuir, Freundlich, Sips, Freundlich-Langmuir, Redlich-Peterson, BET, Radke-Prausnitz, and Toth isotherms. The of best fit isother was then applied to extrapolate experimental data across the entire testing concentration range of 0 to 5 µg/L.

Desorption Experiments

Desorption experiments saw 5 mL of milli-Q water added to retained sorption experiment samples, bringing their volume to approximately 9 mL. Samples were vortexed and placed on a shaker for their relative equilibrium time before sample preparation and analysis. The exact volume of milli-Q water added, and total volume was determined by mass, allowing expected PFAS concentrations in solution (dilution) to be calculated using the known solution PFAS concentration determined in prior sorption experiments. Desorption (%) was calculated as the difference between expected solution PFAS concentration and the measured solution concentration after desorption experiment as a factor of the total amount sorbed in sorption experiments.

5.3.4 PFAS Analysis

Aqueous samples were prepared for LC-MS analysis by centrifuging samples (4000 RCF for 30 minutes) before transferring 900 µL of supernatant to a new 15 mL centrifuge tube to which 100 µL of methanol containing 10 µg/L carbon labelled PFAS standard was added to create a 10 % MeOH solution by volume containing carbon labelled standards at a concentration of 1 µg/L. Samples were vortexed and filtered (5 mL Terumo stopperless polypropylene Luer Lock syringes coupled to Corning polypropylene housed 15 mm 0.22 µm cellulose syringe filter) into 1 mL polypropylene GC vials with clip on polypropylene caps (Agilent Technologies) and stored at 6 °C until analysis.

5.3.5 Instrumental Analysis

PFAS analysis was performed on an Agilent 1290 infinity II liquid chromatograph coupled to an Agilent 6495B triple quadrupole mass spectrometer. A direct aqueous injection multiple reaction monitoring method was developed, employing Agilent EclipsePlus C18, 3.5 µm (4.6x50mm) column post solvent mixing as a PFAS delay column before the main separation column, an Agilent EclipsePlus C18 - RRHD 1.8 µm (2.1x50 mm). Each column was operated at 40°C using the solvents Hypergrade MeOH and 5mM ammonium acetate in milli-Q water at a starting condition of 40 % organic phase and ramping to 100% organic phase by 3 minutes. Organic phase

was held at 100 % for a further 2.5 minutes resulting in a total run time of 5.5 minutes. 10 μL of sample was injected as a sandwich injection, this saw 5 μL of sample collected, followed by 1 μL of injection standard (1 $\mu\text{g/L}$ carbon labelled M8PFOS and M8PFOA) and a final 5 μL of sample. The outside of the needle was washed between each needle movement and prior to the injection of the sample. Method detection limits (MDL) and limits of quantitation (LOQ) applied to experimental data were acquired using the injection of 10 LCS samples at 1 $\mu\text{g/L}$ target PFAS, dispersed throughout the experimental samples (Table 5.1) Detailed information on instrument parameters, transitions and serial sorption technique is laid out in the attached MethodsX paper (supplementary material).

Table 5.1 Table outlining LOQ and MDL for PFAS congeners used in biochar equilibrium, sorption and desorption experiments.

	PFBA	PFBS	PFHxA	PFHxS	PFOA	PFOS
MDL ($\mu\text{g L}^{-1}$)	0.043	0.031	0.019	0.030	0.025	0.038
LOQ ($\mu\text{g L}^{-1}$)	0.134	0.099	0.059	0.094	0.079	0.120
Mean Recovery (%)	99 \pm 4	92 \pm 6	97 \pm 5	100 \pm 2	102 \pm 6	101 \pm 3

5.3.6 Quality control quality assurance (QA/QC)

Quality control and quality assurance (QA/QC) samples included triplicate blanks and laboratory control samples (LCS; 1 $\mu\text{g/L}$) for all experiments. The intermingling of these QC samples with experimental samples throughout analysis and experimental process allowed for measurement and control of PFAS QA/QC as method recoveries and identification of any contamination. All data presented was collected in experimental batches which exhibited non-detect blanks and had method recoveries within the range of 80 to 120 %.

5.3.7 Data Analysis

LC-MS data was processed using Agilent Technologies Masshunter Package (version 8). Statistical analysis was undertaken using either one-way ANOVA or two-way ANOVA, using Tukey's Test as a post hoc on IBM SPSS version 25. Statistics are displayed in the format ($F_{df1, df2} = X, p < 0.05$), where X is the statistical analysis derived F-value being compared to the F-statistic for degrees of freedom between groups (df1) and within groups (df2). P values are denoted as an exact value when not statistically significant, or as $p < 0.05$ when statistically significant.

5.4 Results and Discussion

5.4.1 Preliminary Experiments

Preliminary PFAS sorption experiments to determine the suitability of the experimental design demonstrated that PFBA and PFBS sorbed poorly to all biochars (< 50 % removal) (supplementary table S1), therefore none of the studied biochars are considered adequate sorbents for the short chain PFAS; PFBA and PFBS. This was consistent with the findings of (Dalahmeh, Alziq & Ahrens 2019) and (Glover, Quiñones & Dickenson 2018). Further, experiments demonstrated that biochars created at 350°C performed weakly as sorbents for target compounds with < 50 % removal (supplementary table S1) and were not considered to be suitable sorbents for any of the studied PFAS. Consequently, the sorption behaviours of the compounds PFBA and PFBS, and the biochars P350 and S350, are not further discussed in the work below.

5.4.2 Equilibrium Experiments

Individual mode compound equilibrium experiments found the greatest proportion of sorption to biochar for PFHxS, PFOA and PFOS occurred in the first 0.5 – 1 hour of experiment for all biochars tested (Figure 5.1). This is comparable to the 1-hour value observed for PFOS and PFOA sorption to powdered activated carbon in (Qu et al., 2009). P750 attained the highest percentage removal for all compounds by the 48-hour time point in equilibrium experiments with 46 to 94 % removal of PFAS from the aqueous phase. The biochar P750 had the greatest percentage PFAS removal at each timepoint. Biochar preparation temperature influenced the PFAS removal rate with removal rates for 750°C biochars being 1.6 – 20% higher in straw biochars, and 6.3 – 90% higher in pine biochars than in 500°C biochars, in mix mode PFAS experiments. This same behaviour was observed in individual mode experiments (Figure 5.1).

In all biochars an interplay existed between PFHxS and PFOA. Initial sorption rates for PFHxS were slower than for PFOA. That was followed by a second sorption step where PFHxS removal slightly exceeded PFOA (Figure 5.1). Aside from the mid-range PFOA–PFHxA interplay, in both, individual and mix mode experiments, percentage removal in the complete period decreased following the order PFOS > PFOA > PFHxS > PFHxA. This is likely based upon C-F chain length and corresponding increasing hydrophobic nature. Ninety-four per cent removal of target PFAS was observed for PFHxS, PFOA and PFOS in P750 experiments. PFOS had the fastest rate of sorption for all biochars in the early stages of equilibrium experiments having the highest % removal by the first experimental timepoint (Figure 5.1). PFAS removal in equilibrium experiments followed an order of increasing removal; S500 < P500 < S750 < P750 (Figure 1). No difference was observed in equilibrium sorption between the biochars prepared at 500°C, based on feedstock type ($F_{2,6} = 4.14$, $p = 0.18$). Comparatively, biochars prepared at 750°C had different sorption properties depending upon the source feedstock ($F_{2,5} = 6.64$, $p < 0.05$).

Equilibrium times found that PFAS reached equilibrium for all biochars within the studied 48 hour period (Table 5.2), with the exception of PFHxA for S500 ($F_{2,2} = 27.20$, $p < 0.05$) and both, PFHxA and PFHxS, for S750 ($F_{2,2} = 36.97$, $p < 0.05$ and $F_{2,2} = 20.31$, $p < 0.05$, respectively), all of which exhibited statistical

differences in means for the final three time points tested (8, 24 and 48 hours) and were subsequently run for 96 hours to achieve equilibrium. PFOS had the same equilibrium time across all tested biochars, while PFOA, PFHxS and PFHxA varied with biochar type, demonstrating behavioural specificity of PFAS congener and biochar type combinations. P500 had the quickest equilibrium time (8 hours) for all PFAS in individual and mix mode. Equilibrium took longer than 48 hours (96 hours) only in straw derived biochars. PFHxA equilibrium was more variable and was found at 8 hours, excepting in S750 where it was only reached after 48 hours. In most cases no statistical difference was found between equilibrium times for PFAS in solutions for individual mode versus mix mode ($p < 0.05$), suggesting that inter-PFAS congener interactions did not impact sorption rate (Table 5.2). The exception to this behaviour was PFHxA in S750 experiments, where the equilibrium decreased from over 48 hours to 8 when tested in individual versus mix mode ($F_{2,5} = 8.26$, $p < 0.05$).

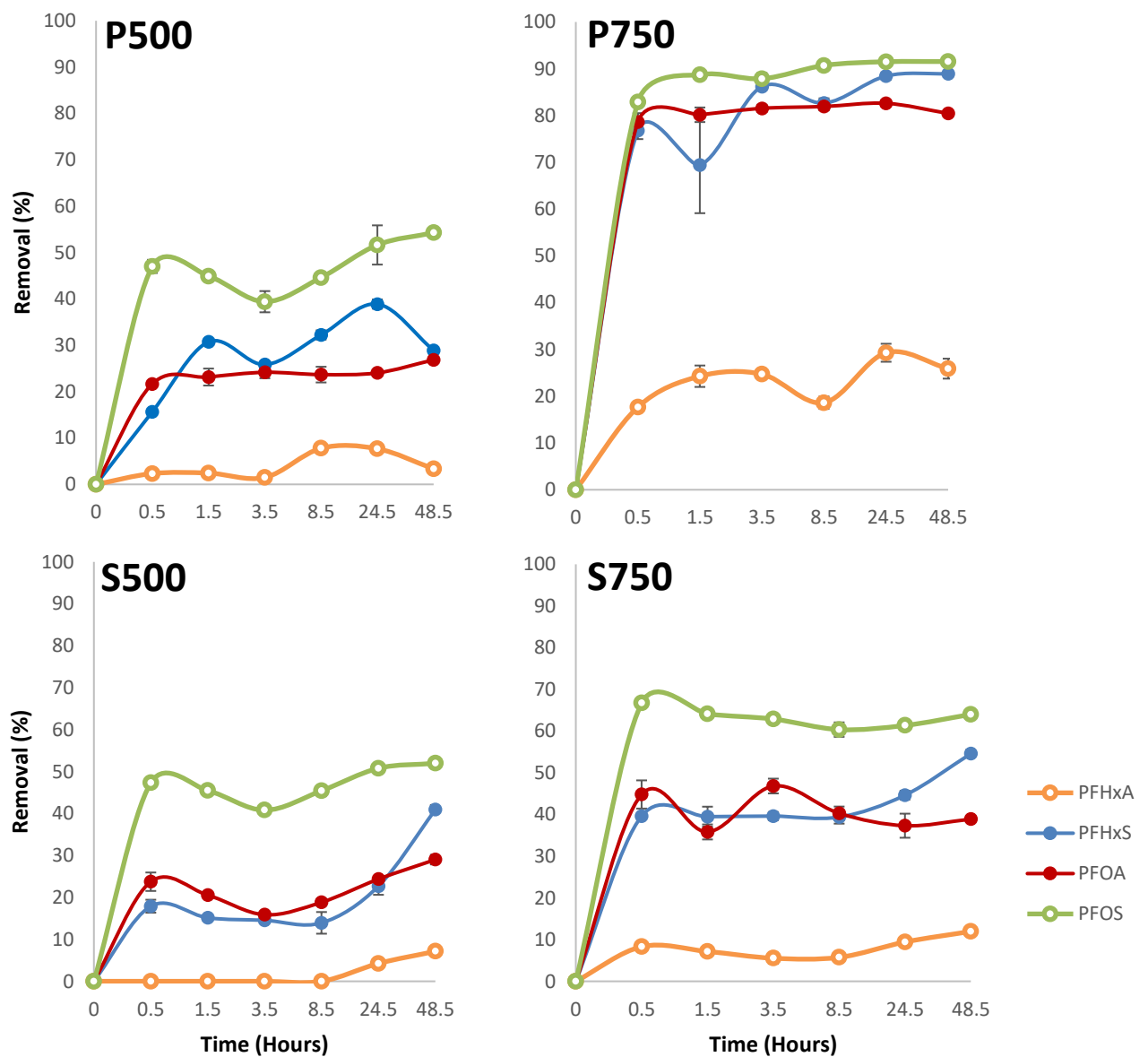


Figure 5.1 Percentage PFAS removal for Biochar versus time for PFAS biochar pairs. Note removal of biochars (S350 and P350) and PFAS Congeners (PFBA and PFBS) from study.

Table 5.2 Assessment of equilibrium times between 8 and 48 hours for each PFAS-biochar pair carried out in triplicate by ANOVA for 100 mg biochar applications.

Individual Mode																
Biochar	PFHxA				PFHxS				PFOA				PFOS			
	Eq (h)	F	F_{crit}	P	Eq (h)	F	F_{crit}	P	Eq (h)	F	F_{crit}	P	Eq (h)	F	F_{crit}	P
P500	8	0.46	5.14	0.65	8	1.41	5.14	0.31	8	1.28	5.14	0.34	8	1.97	5.14	0.22
S500	8	5.64	5.79	0.05	48 ^a	29.80	7.71	0.01	24	4.80	10.13	0.12	8	4.33	5.14	0.07
P750	8	4.46	5.14	0.06	24	0.11	10.13	0.76	8	1.12	5.79	0.40	8	0.19	5.79	0.83
S750	48 ^a	7.95	7.71	0.05	48 ^a	17.81	10.13	0.02	8	0.29	5.14	0.76	8	1.46	5.14	0.30

Mix Mode																
Biochar	PFHxA				PFHxS				PFOA				PFOS			
	Eq (h)	F	F_{crit}	P	Eq (h)	F	F_{crit}	P	Eq (h)	F	F_{crit}	P	Eq (h)	F	F_{crit}	P
P500	8	1.59	5.14	0.28	8	0.84	5.14	0.48	8	1.28	5.14	0.34	8	1.94	5.14	0.22
S500	8	2.79	5.79	0.15	48 ^a	29.29	7.71	0.01	24	4.80	10.13	0.12	8	3.80	5.14	0.09
P750	8	2.05	5.14	0.21	24	0.12	10.13	0.75	8	0.38	5.79	0.70	8	0.19	5.79	0.83
S750	8	4.91	5.79	0.07	48 ^a	18.68	10.13	0.02	8	0.29	5.14	0.76	8	1.37	5.14	0.32

a – Equilibrium not established, statistically significant difference between means at all time points (8, 24, 48 hours). Equilibrium time of 96 hours established and applied where results had p<0.05.

Table 5.3 Second order experimental rate constants and R² for each Biochar PFAS-biochar pair studied in individual mode and mix mode at 5 µg/L.

Individual Mode												
Biochar	PFHxA			PFHxS			PFOA			PFOS		
	Q_e (ug/g)	K₂ (h)	R²	Q_e (ug/g)	K₂ (h)	R²	Q_e (ug/g)	K₂ (h)	R²	Q_e (ug/g)	K₂ (h)	R²
P500	0.22	2.70	0.99	0.11	10.01	0.99	0.21	6.65	0.99	0.35	9.16	0.99
S500	0.09	18.87	0.95	0.11	2.67	0.97	0.19	2.38	0.99	0.34	6.58	0.99
P750	0.09	29.56	0.99	0.19	11.15	0.99	0.35	5.84	0.99	0.40	11.97	0.99
S750	0.06	34.25	0.99	0.11	40.86	0.99	0.20	34.09	0.99	0.36	10.38	0.99
Mix mode												
Biochar	PFHxA			PFHxS			PFOA			PFOS		
	Q_e (ug/g)	K₂ (h)	R²	Q_e (ug/g)	K₂ (h)	R²	Q_e (ug/g)	K₂ (h)	R²	Q_e (ug/g)	K₂ (h)	R²
P500	0.03	39.87	0.99	0.13	9.18	0.99	0.20	8.60	0.99	0.09	15.50	0.99
S500	0.05	2.08	0.71	0.18	0.60	0.83	0.19	13.28	0.99	0.09	17.88	0.99
P750	0.12	10.21	0.99	0.36	9.73	0.99	0.36	13.54	0.99	0.15	35.15	0.99
S750	0.06	9.25	0.99	0.23	2.47	0.99	0.23	3.42	0.99	0.11	29.63	0.99

Second order models were found to fit experimental data for individual and mix mode PFAS experiments (Table 5.3). This is in line with the observations of other studies collectively published in the review by (Du et al., 2014). First order models failed to appropriately fit the mechanism for slower sorbing PFAS-biochar relationships, namely lower temperature biochars and PFHxA and PFHxS (Table 5.3; supplementary table S4). Predicted sorption concentrations (Q_e) followed the order PFHxA > PFHxS > PFOA > PFOS. No statistically significant biochar driven effect (temperature or feedstock) on sorbed amount of PFAS at equilibrium could be established ($p > 0.05$), suggesting sorption was largely driven by PFAS compound specific attributes in individual and mix mode experiments ($p > 0.05$). However, in mix mode experiments PFOS Q_e values were significantly lower than in individual mode (Table 5.3), suggesting competition for sorption sites with other PFAS congeners ($p < 0.05$). Sorption rates (k_2) are highly dependent on biochar-PFAS congener combination (Table 5.3). Biochar-PFAS combination specific behaviour is evident through the large variation observed in sorption behaviour for each congener across the suite of tested biochars, particularly when comparing the behaviour of any one congener to each biochar. No trend could be established between PFAS sorption rate and biochar or PFAS congener alone, instead each biochar type and PFAS congener combination exhibited its own unique behaviour.

Intraparticle diffusion models were applied to the data set as per Punyapalakul et al (2013), resultant summary data are contained in supplementary tables S5 and S6. It was found that due to the rapid sorption of PFAS to biochars, only two data points fell into the first sampling bracket (film diffusion). This presented a limitation to the determination of accuracy for film diffusion representation in intraparticle diffusion models, as 2 sample points produce an R^2 of 1, suggesting a higher rate of experimental sampling would be required to capture enough data for film diffusion in early stages of sorption. The remainder of the model generated more reliable R^2 with a minimum of 3 data points per sorption phase.

Intraparticle diffusion prior to reaching equilibrium was observed for pine biochars, but not straw biochars (Figure 5.2). The lack of data resolution between 0 and 30 minutes precluded to determine if the elongated PFHxS intraparticle diffusion stage is in fact a slow film diffusion for straw biochars. The model demonstrates a very fast initial sorption, followed by a short, but slower, uptake of PFAS to reach equilibrium for all PFAS-biochar combinations. This is reflected in the equilibrium data, where the majority of PFAS is sorbed in the first 30 minutes, followed by a slow uptake over the next 3-8 hours depending on the biochar-PFAS combination (Figure 5.2).

While no trends were identified in sorption rates for biochar production conditions in second order models, intraparticle diffusion modelling reinforces that the majority of PFAS sorption to all biochars occurs in the first 30 minutes, followed by a notably different, slower mechanism (intraparticle diffusion) influencing all compounds' sorption rate when sorbing to pine biochars specifically. This both compares and opposes the trends seen in Punyapalakul et al (2013), where intraparticle diffusion was not seen in carbonaceous sorbents, whereas in the present study this depended on the biochar feedstock type. Similarly, Qu et al (2009) observed that the adsorption of PFOA onto activated carbon was largely controlled by particle diffusion. The present study demonstrated that the exhibition of this behaviour is largely dependent on biochar feedstock type. PFAS congener effects on sorption are evident through the total amount sorbed for any given biochar at equilibrium, for all biochars the order of increasing PFAS affinity followed PFHxA < PFHxS < PFOA < PFOS.

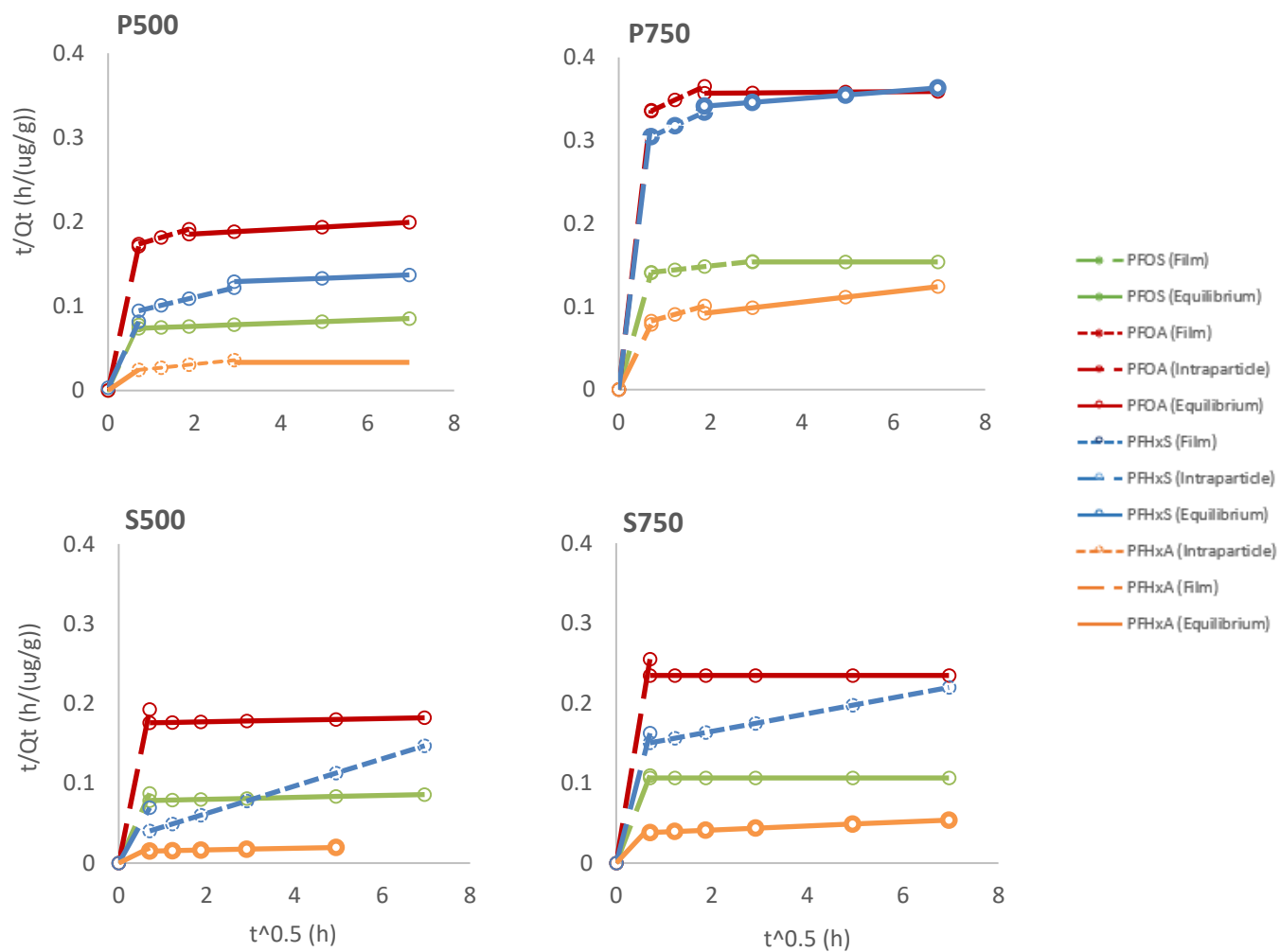


Figure 5.2 Intraparticle diffusion models for target compounds separated by biochar type. Displayed data for target compounds in 5 $\mu g/L$ mix mode experiments.

5.4.3 Sorption Experiments

Minimum effective application was defined for all compounds as the lowest measured biochar application rate beyond which the addition of further biochar to solution did not result in a statistical difference ($p < 0.05$) in PFAS removed (%) from solution. PFOS minimum effective application experiments consistently reached a minimum effective application for all biochars within the tested application range (0 – 100 g/L)(Table 5.4).

Table 5.4 Minimum effective application values (g/L) for each PFAS-biochar combination at 5 µg/L. Minimum effective applications are defined as the lowest dose at which no further statistically significant ($p < 0.05$) change in PFAS removal with further biochar application occurred.

Individual Mode					Mix Mode				
Biochar	PFHxA	PFHxS	PFOA	PFOS	Biochar	PFHxA	PFHxS	PFOA	PFOS
P500	N/A	N/A	80	60	P500	N/A	N/A	N/A	60
S500	N/A	N/A	N/A	80	S500	N/A	N/A	N/A	60
P750	N/A	60	60	40	P750	N/A	60	60	40
S750	N/A	N/A	N/A	80	S750	N/A	80	60	40

After exceeding minimum effective application rates by applying more biochar, PFAS sorption sites are in excess in solution, resulting in no further removal of PFAS from the 5 µg/L solution as the system has already reached maximum removal. This acts as a measure of removal efficiency, with reference to lower biochar application rates being more desirable. PFOS minimum effective application rate ranged 40-80 g/L dependant on biochar type. Straw biochars seldom reached a minimum effective application for tested PFAS within the experimental range (0 – 100 g/L) and would require applications exceeding the highest tested application of 100 g/L. PFOS-straw biochar combinations were an exception to this. PFHxA and PFHxS sorbed less completely to all biochars and did not achieve a minimum effective application within the tested range, excepting PFHxS for P750 which delivered a minimum effective application of 60 g/L. PFOA only reached a minimum effective application in pine biochars, ranging 60-80 g/L. It was clear that minimum effective application was reached more frequently for pine biochars, within the tested application range, than for straw biochars (Table 5.4). PFOS demonstrated lower effective application rates for high temperature pine biochars. No biochar production temperature-based difference was observed for PFOS to straw biochars with 500 and 700 °C biochars sharing a minimum effective application rate of 80 g/L (Table 5.4) ($F_{1,2} = 2.09$, $p = 12.27$). PFOA and PFHxS demonstrated biochar production temperature sensitivity, with lower application rates required to achieve minimum effective applications with higher temperature biochars. Experiments that repeated the individual mode tests as mix mode reported a lower application rate in straw biochars ($F_{1,2} = 20.55$, $p < 0.05$), while the minimum effective application rate remained the same for pine biochars ($F_{1,2} = 0.09$, $p = 11.71$).

Biochar application rate experiments are explored further in Figure 5.3, which shows P750 biochar saw quite similar behaviour for PFOS, PFOA and PFHxS. In the case of PFHxA and P750 biochars, it was observed a minimum effective application could not be reached in the tested range. Here, the slowly increasing slope demonstrates that with higher applications rate further PFHxA could be removed. This was not the case for S750,

which exhibited greater separation between compounds, with not all compounds reaching a maximum removal within the tested range. Removals were lower for S750 when compared to P750, ranging 70 - 90 % for PFOS, PFOA and PFHxS.

Overall, a sorption pattern emerged following the order PFOS > PFOA > PFHxS > PFHxA for P500, S500 and S750. This was less evident in P750 due to similar levels of removal for PFOS, PFOA and PFHxA at lower biochar applications (0 – 40 g/L). PFHxS behaved outside this pattern at the higher application rates, where PFHxS often becomes equally sorbed at levels comparable to PFOS and exceeding that of PFOA. This suggests that, in systems where more sorbent (sorption sites) exist than sorbate, there are different sorption mechanisms between the sulfonate and carboxylic PFAS groups. This suggests that PFAS functional group type had greater impact upon sorption to biochar than chain length, considering the outperformance of the 8 carbon PFOA by the 6 carbon PFHxS. Similar observations have been made in other studies, which observed greater removal of PFASs than PFCAs from water using integrated GAC methods (Glover et al., 2018). This was further evident in 500°C biochars, where a point of intersection was observed between PFOA and PFHxS at 60 g/L applications. In 750°C biochars this occurred at much lower application rates (<40 g/L), once again suggesting the influence of pyrolysis temperature, and hence a different mechanism upon this relationship.

Overall a smaller percentage of each congener was removed in mix mode compared to individual mode (Figure 5.3), however this did not decrease proportionally with number of compounds in solution, nor was it uniform for PFAS-biochar combinations. Instead the difference in sorption behaviour was a factor of application rate and was highly biochar-type sensitive, with respects to differences in removal between individual and mix mode experiments. The observed difference was more pronounced in low temperature biochars than in high temperature biochars. Overall, the major effect of a mix mode versus individual mode was slight reductions of minimum effective applications, but most notably an overall decrease in percentage PFAS removed in lower temperature biochars for the congeners PFOS, PFHxS and PFHxA. This deficit was not experienced in 750°C biochars.

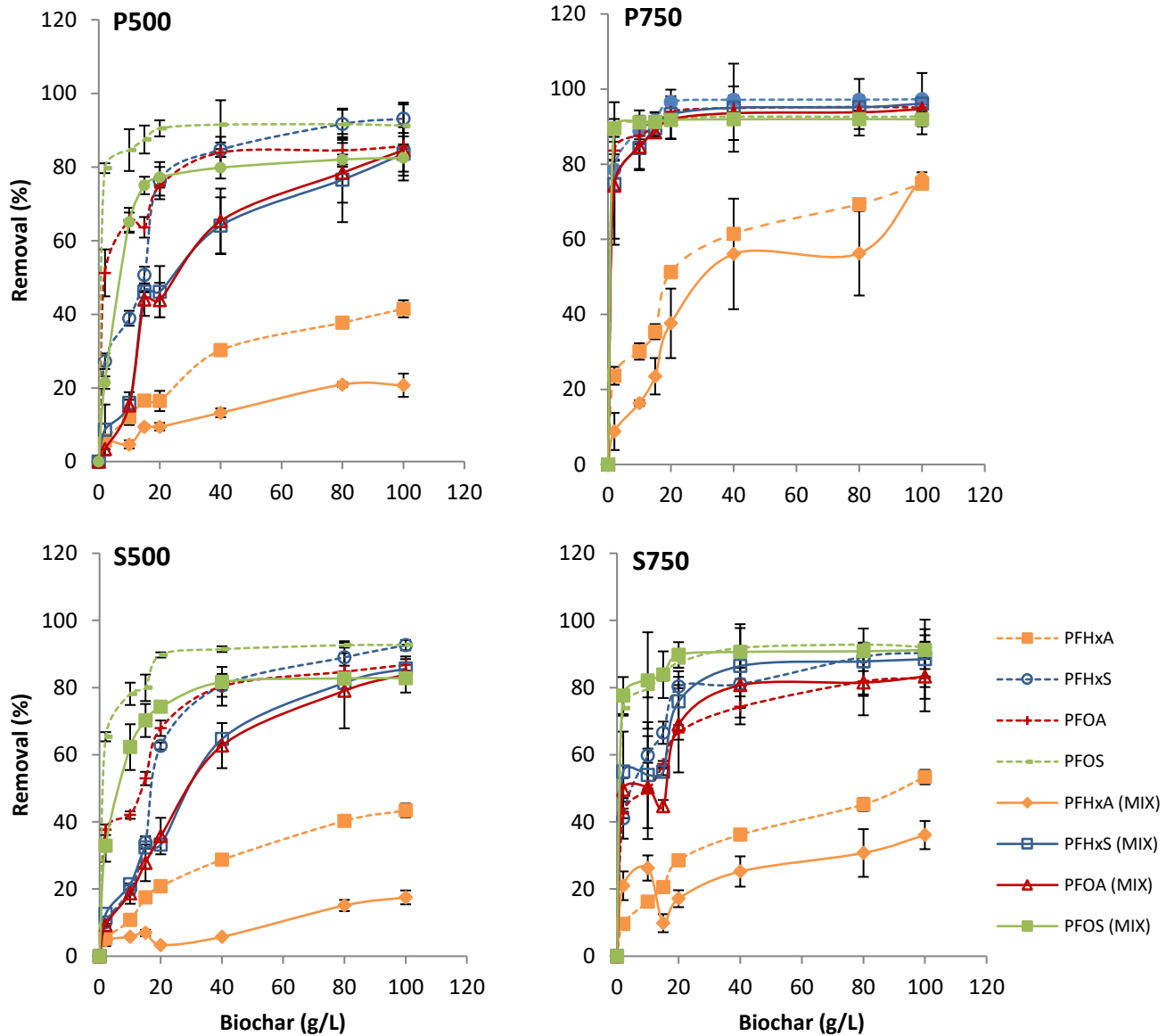


Figure 5.3 Percent target PFAS removed from solution versus application rate of biochar, separated by biochar.

Figure 5.4 highlights the maximum PFAS removal (%) achievable at the highest application studied (100 g/L) at equilibrium and does not reflect a true maximum as not all PFAS – biochar combinations reached a maximum removal across all biochars as evidenced by minimum effective applications in Table 5.4. This is too in agreement with Figure 5.3, where increasing the dose of biochar results in increases in the percentage PFAS removal for the entire tested application range for some PFAS–biochar combinations. PFHxS, PFOA and PFOS however all reached maximum removal within the studied applications for P750. PFHxA showed the greatest variance in maximum sorption at the studied levels among biochars. In conjunction with Figure 5.3, Table 5.4 suggests that maxima as witnessed in Figure 5.4 are not the ultimate measure of the effectiveness of a biochar, as some biochars reached their maximum sorption levels at far lower application rates than others, suggesting the latter measure of sorption efficiency is of greater importance.

Using the minimum effective application required to achieve maximum sorption as an index of sorption is far more effective than making assessments based on ultimate percentage removal within the studied range. Sorption followed the pattern PFOS > PFHxS > PFOA > PFHxA, with respects to maximum sorption over the studied range at equilibrium. P750 had the highest accumulative sorption, followed by S750 and with the 500°C biochars exhibiting very little difference between the two feedstock types for all tested PFAS. Assessing PFAS maximum sorption in a mix mode resulted in overall slight reductions in all PFAS compounds percent removal compared to those sorbed in individual mode, possibly suggesting competition for sorption sites. This agrees with the data in Table 5.4 which demonstrate reduced removal at various application rates across all compounds and biochars, based on the biochars being in a mix mode. Note that the total PFAS sorbed was much higher in mixed mode, even if individual mode sorption is lower in equivalent mix mode experiment when compared to individual mode. The data in Figure 4 illustrate that the removal of PFOS, PFOA and PFHxS is quite similar across all biochars with respects to maximum capacity for removal at tested concentrations and application rates. However, it is important to note this is not a measure of sorption capacity or PFAS affinity for the sorbent, which is a measure seen in sorption isotherms which model this relationship based on solution concentration versus sorbed concentration.

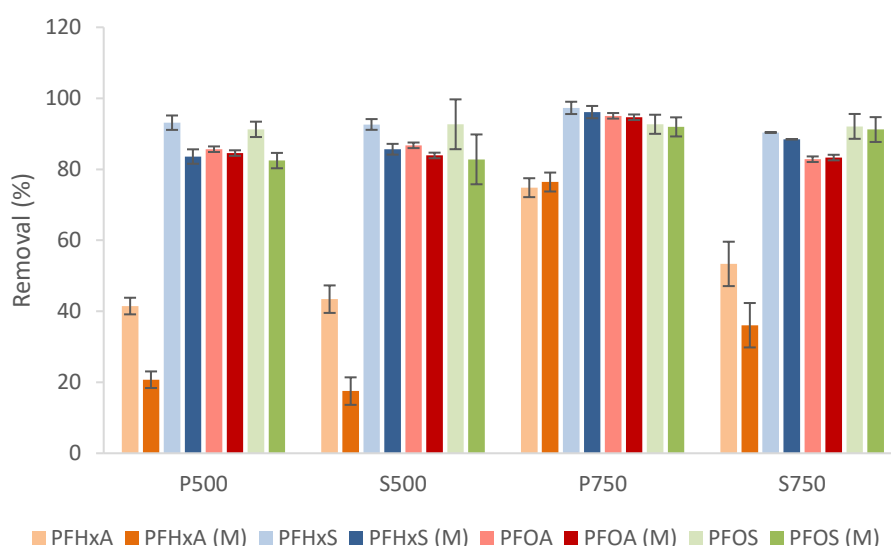


Figure 5.4 Maximum percentage PFAS removed from solution comparing maxima between PFAS experiments for each biochar at the highest treatment application of 100 g/L.

The Freundlich-Langmuir combination model (SIPs), as per equation 1, was found to provide the most consistent fit to experimental data. In this model maximum adsorption capacity is reflected by Q_{max} (ug/g), K_L represents the affinity constant (L/g), and n describes surface heterogeneity or homogeneity, with values ranging 0 to 2 and those closer to one (1) being indicative of homogenous sorption (Nethaji et al. 2013). The experimental data is shown in Freundlich-Langmuir models in Figure 5.5, with constants for all models tested contained in supplementary tables S7 and S8. Extrapolation of the experimentally selected Freundlich-Langmuir combination model was undertaken to span an entire 0-5 $\mu\text{g/L}$ range, as can be found in Figure 5.6.

Equation 1.
$$Q_e = \frac{Q_{max}(K_L C_e)^{1/n}}{1+(K_L C_e)^{1/n}}$$

Experimental data seen in Freundlich-Langmuir combination model (SIPs) plots (Figure 5.5) clearly demonstrate that sorption is affected by both, compound and sorbent type, their influence culminating in a PFAS-biochar combination specific behaviour. While sorption followed the order PFOS> PFOA> PFHxS> PFHxA at model endpoints, it is clear that an interplay between PFOA and PFHxS sorption, as seen by the intersection of models and in equilibrium modelling data, exists. This is particularly evident in pine derived biochars. The sigmoidal form exclusive to PFOS and PFOA suggest 2 modes are prevalent in sorption (monolayer versus multilayer – Type V sorption), with multilayer sorption becoming more active at the point of inflection where higher concentrations are present (smaller sorbed fraction - Q_e , higher solution concentration C_e). PFHxA and PFHxS tend to show a more traditional isothermal pattern without sigmoidal behaviour. The two mechanisms are likely hydrophobic interaction, followed by more compound specific behaviours influenced by attraction or repulsion of like congeners either with water molecules, other PFAS molecules or surface functional groups.

PFOA's isotherm was demonstrated to be less sigmoidal in straw biochars than in pine. Among all studied compounds, PFHxA exhibited the lowest affinity for any sorbent. P750 had the steepest gradient for all tested compounds, suggesting it as the sorbent with the highest PFAS affinity. This was followed by S750, and finally the 500°C biochars which were quite similar. Repeating the experiment in a mix mode resulted in little change in PFAS sorption behaviour. However, a marked increase in the sigmoidal nature of isotherms was noted in PFOS and PFOA, due to the possible increased prevalence of inter-PFAS interactions influencing multilayer sorption modes in mix mode. Additionally, this occurred alongside a reduced effect of the previously described PFOA-PFHxS interplay. Accordingly, biochar PFAS sorption affinity was slightly suppressed for most compounds in mix mode excepting PFHxS in 500°C biochars.

Extrapolated models however attempt to predict a larger concentration range using the model that had been fitted to the experimental data. Experimental C_e range does not always capture the point at which biochar sorption sites are saturated (Q_{max}). It does however reveal some new interesting behaviour at high concentrations. To this end, the broader range of PFAS-biochar combinations demonstrated PFAS in a mix mode outperforming the individual mode at higher C_e values. The behaviour exhibited by PFHxA in both individual and mix mode extrapolated isotherms was much like the isotherms in the range of C_e for experimental data. However, this was not the case for other PFAS tested. PFOS in a mix mode greatly exceeded its individual mode counterparts Q_{max} for all tested sorbents (Table 5.5). Here the higher the affinity, as indicated by the slope of initial sorption in extrapolated models (Figure 5.6), the greater the magnitude of the difference between compounds.

PFOA behaviour was similar as in experimental isotherms, except that its interactions with PFHxS were clearer than in experimental isotherms, due to the increased range of C_e . Nowhere is this better demonstrated than in the 500°C biochars where not only does 500°C mix mode PFHxS ultimately exceed PFOA, it also sees a great reduction between PFOA sorption affinity in individual versus mix mode experiments and an increase in PFHxS sorption from individual to mix mode PFAS solutions. This strongly suggests competition and opposing mechanisms, possibly linked to the functional group, resulting in preferential sorption (Li et al. 2019). The interplay between PFHxS and PFOA was illustrated by variation of the congener having a higher Q_{max} , depending on biochar type and PFAS compound combination. Previous comments are supported by PFHxS having higher Q_{max} values than PFOS in Table 5.5 for mix mode, compared to lower values in individual mode.

This hints strongly to assisted or competitive sorption. Interestingly, models predicted in individual mode tests that PFOA Q_{max} has the capacity to exceed PFOS in the 500°C biochars. Lower “n” values in extrapolated isotherms demonstrated the greater degree of sigmoidal nature in sulphonates (PFOS and PFHxS), compared to the carboxylic acids (PFOA and PFHxA). Likewise, this is more pronounced in pine rather than in straw biochars. Overall, P750 attains the highest Q_{max} values for all PFAS, in both individual and mix mode experiments. PFOS acquires most consistently the highest Q_{max} with each biochar, except in 500°C individual mode experiments where the affinity for PFOA (and Q_{max}) was higher. Nominally, P750 acquired most frequently the highest Q_{max} values, suggesting it is the most efficient at sorbing the target PFAS. This was followed by S750 and then the two 500°C lower biochars, where the sorption capacities varied based on compound behaviour.

Table 5.5 Constants for Freundlich-Langmuir Model (SIPs).

Mixed Mode																
Biochar	PFHxA				PFHxS				PFOA				PFOS			
	K_L	q_{max}	n	R²	K_L	q_{max}	n	R²	K_L	q_{max}	n	R²	K_L	q_{max}	n	R²
P500	0.14	0.02	0.47	0.59	0.12	0.39	0.70	0.93	0.31	0.15	0.31	0.73	0.29	0.52	0.27	0.97
S500	0.12	0.02	0.58	0.36	0.63	0.14	1.13	0.97	0.58	0.15	0.66	0.99	0.22	0.58	0.37	0.99
P750	5.71	0.04	0.16	0.91	1.23	0.56	0.64	0.99	3.85	0.47	0.23	0.95	5.78	10.99	0.16	0.91
S750	0.22	0.03	0.68	0.99	0.41	0.29	0.89	0.98	0.39	0.21	0.66	0.98	0.27	1.70	0.45	0.99

Individual Mode																
Biochar	PFHxA				PFHxS				PFOA				PFOS			
	K_L	q_{max}	n	R²	K_L	q_{max}	n	R²	K_L	q_{max}	n	R²	K_L	q_{max}	n	R²
P500	0.08	0.07	0.60	0.69	1.06	0.15	1.28	0.98	0.09	0.78	0.55	0.96	14.39	0.37	0.24	0.99
S500	0.13	0.06	0.56	0.76	1.23	0.10	1.90	0.99	0.11	0.64	0.92	0.96	0.74	0.51	0.65	0.98
P750	0.05	0.55	0.79	0.99	4.73	0.37	0.69	0.99	1.64	0.77	0.46	0.99	3.85	6.61	0.21	0.95
S750	0.29	0.10	1.22	0.82	1.23	0.19	0.51	0.94	4.62	0.17	7.98	0.31	0.55	0.79	0.53	0.99

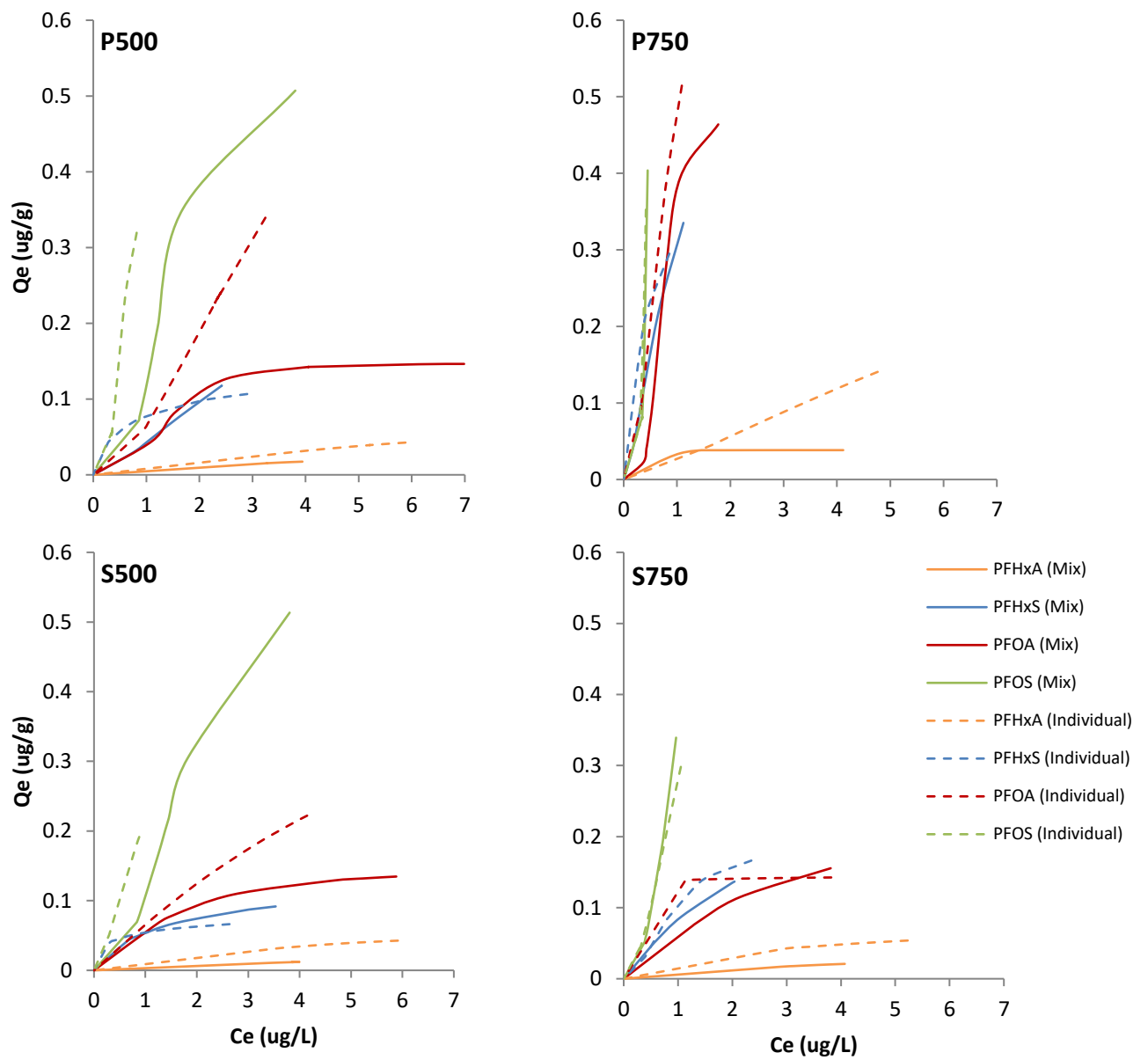


Figure 5.5 Freundlich-Langmuir Combination sorption isotherms (Sips 1948) for target compounds separated by sorbent. Data displayed as a factor of individual or mix mode. C_e range displayed as per experimental data ranges of C_e based on sorption.

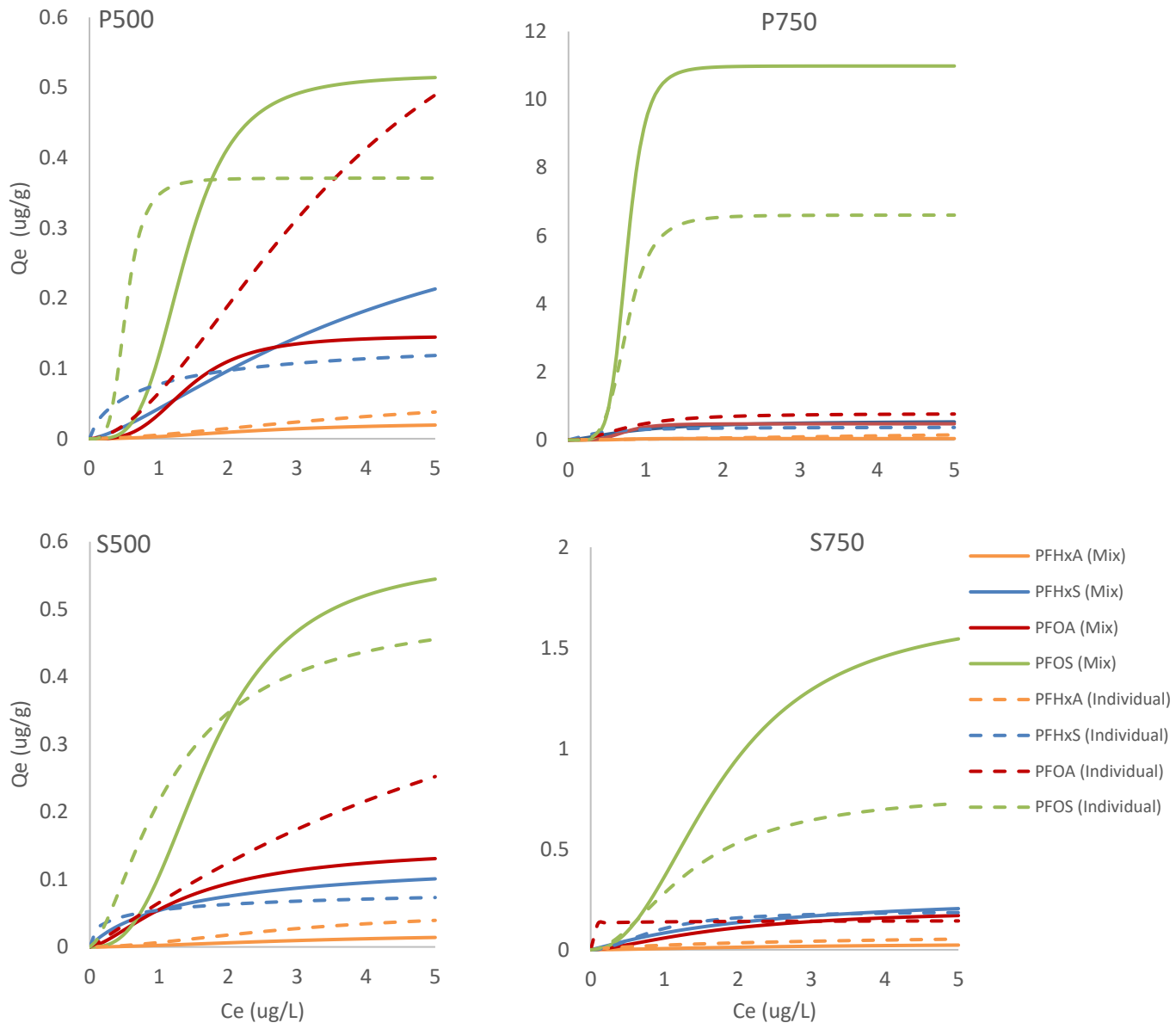


Figure 5.6 Extrapolated Freundlich-Langmuir Combination sorption isotherms (SIPs) for target compounds separated by sorbent. Data displayed as a factor of individual or mix mode experiments.

5.4.4 Desorption Experiments

PFAS desorption was observed for most biochars (Table 5.6), with values ranging from <LOQ to 92.8 %. PFOS was the only compound that did not desorb from any biochar, with desorption values for all PFOS-biochar combinations below LOQ in individual mode experiments. PFHxA sorption was highly reversible and over an order of magnitude higher from pine biochars than from straw biochars. Excepting PFHxA, all highly sorbed compounds (PFOS, PFHxS and PFOA) were found to undergo no more than 20 % desorption from all biochars.

The data strongly suggests that, while biochar characteristics were the major influencer upon sorption behaviour, compound specific behaviour was of larger influence with respect to desorption. This is evident as, despite the vast difference in the characteristics of the biochars, no desorption of PFOS is noted across all biochars. The same can be said for PFOA and PFHxS which, for the most part, do not exhibit any biochar characteristic influence-based desorption trends. Based on the data contained in Table 5.6, desorption was found to be more dependent on chain length than any other parameter in individual mode experiments. Interestingly, when the experiment was repeated as mix mode, desorption was seen for every compound across all biochars. Excepting PFHxA, all desorption was less than 20% of sorbed PFAS. Desorption was significantly greater in low temperature biochars (500°C) than in higher temp biochars (750°C) ($F_{1,2} = 33.95$, $p < 0.05$). No significant effect of feedstock type was detected ($p > 0.05$ in all cases), suggesting, once more, that strength of sorption was primarily driven by hydrophobicity.

Table 5.6 Total desorption (%) of target PFAS from biochars after a 96-hour holding period from point of reconstitution of batch sorption tubes from sorption experiments with 5 mL distilled water.

Biochar	Individual Mode				Mix Mode			
	PFHxA	PFHxS	PFOA	PFOS	PFHxA	PFHxS	PFOA	PFOS
P500	50.9 ± 1.8	15.3 ± 0.8	7.6 ± 1.1	<LOQ	92.8 ± 34.8	14.9 ± 0.9	16.3 ± 0.9	9.7 ± 0.2
S500	0.1 ± 4.2	4.2 ± 0.3	<LOQ	<LOQ	ND	10.7 ± 1.8	15.5 ± 2.8	8.5 ± 0.7
P750	20.7 ± 2.1	3.2 ± 0.1	<LOQ	<LOQ	4.7 ± 0.4	0.5 ± 0.1	0.8 ± 0.1	1.3 ± 0.1
S750	5.4 ± 2.3	5.8 ± 1.0	5.2 ± 0.2	<LOQ	8.0 ± 1.1	1.1 ± 0.1	1.5 ± 0.1	1.2 ± 0.1

Considering the above compound specific behaviours in equilibrium, sorption, and desorption, the biochar production method resultant specific physiochemical characteristics had an equally significant effect on sorption behaviour as did PFAS congener specific characteristics. This is mirrored by the findings of (Zhang et al. 2019), who suggested that, in addition to compound and sorbent specific characteristics, solution chemistry was an important consideration. In the present study, the same solution was used for all experiments except for individual versus mix mode. This meant that changes observed were a direct result of biochar addition, including its impact, on experimental solutions.

Equilibrium time was greater impacted by biochar pyrolysis temperature than by feedstock type, suggesting those biochars with a more highly carbonized nature and a higher surface area had a sorption process that occurred quicker and at a greater magnitude.

Minimum effective application trends suggest that carbon fraction and surface area are the most significant characteristics affecting application rate, demonstrating the better performance of higher pyrolysis temperatures and pine feedstock for the development of adequate surface area and a higher degree of carbonization. Similarly, correlation between carbonaceous sorbent surface area and sorption capacity were observed for PFOS, PFOA and PFHxS in (Kupryianchyk et al. 2016). It appears that the types of functional groups retained at lower temperatures, such as hydroxyl (OH) and carboxyl (COOH) (Askeland, Clarke & Paz-Ferreiro 2019), were not significantly involved in sorption. This is evidenced through poor sorption to low temperature biochars (350°C). Similarly, other characteristics that demonstrated major increases with temperature related to straw biochars, resulted in no significant change in minimum effective application (ash, pH, EC). This suggests that feedstock type was of greater influence than temperature in minimum effective application rates with pine biochars outperforming straw.

P750 performed best with respects to extrapolated Freundlich-Langmuir sorption isotherms for most tested PFAS compounds. This was seconded by S750, which in turn was followed by P500 and then S500. This suggests that in this study, pyrolysis temperature is a more important factor than the choice of feedstock with regards to increasing PFAS sorption capacity of biochars. However, it is evident in equilibrium data, in which pine feedstock biochars had an additional intraparticle diffusion sorption phase, not seen in straw biochars, that feedstock type does affect sorption behaviour within the same temperature classes. In addition, the nuances seen between PFOA and PFHxS in some biochar type combinations are likely the result of unique sorbate properties, highlighting the complexity of PFAS sorption to biochars and the need to assess sorption affinity as a factor of compound specific attributes, compound concentration, presence of other PFAS and attributes of biochar sorbent. P750 was found to be the most effective sorbent with respects to having a high sorption rate for target compounds, the greatest percentage removal and Q_{max} , the lowest dose required to reach maximum sorption and the lowest desorption. Inferentially, this suggests that the desirable characteristics for biochars for use as PFAS sorbents are high surface areas and a higher fraction of C as fixed carbon, as exhibited by P750 (Askeland, Clarke & Paz-Ferreiro 2019).

Insofar as compounds are concerned, PFOS, being the more hydrophobic PFAS congener tested (Li et al. 2019), exhibited the highest affinity and the lowest dose requirement for maximum sorption for any biochar. Overall, the minimum effective application required decreased with increasing PFAS compound carbon chain length and were lower in sulphonates than carboxylic acids. The effect of individual versus mix mode application of experiments was most evident in sorption maxima and isothermal modelling. This was due to the properties of the compounds themselves and, to a lesser extent with the physiochemical properties of the biochar surface.

Alteration of pH should have a minimal effect on PFAS sorption due to the low pKa of PFAS and to the seeming lack of sorption to surface functional groups in favour of hydrophobic sorbents. Higher ash and EC could however potentially assist with sorption due to increasing solution ionic strength which would in turn drive sorption. Testing these factors was outside the scope of this experiment.

5.5 Conclusion

Sorption behaviour at low $\mu\text{g/L}$, environmentally relevant, PFAS concentrations was successfully studied using the specially developed serial sorption technique and LC-MS method. It was found that biochars produced at 350°C from pine and straw feedstocks were inefficient sorbents for PFAS, removing $< 50\%$ from solution. Likewise, PFBA and PFBS sorbed poorly to all biochars ($< 50\%$), suggesting the biochars produced in this study are not an applicable removal technique for shorter chain PFAS molecules in water. Ultimately all 4 remaining biochars perform similarly with respect to maximum percent removal of the remaining target PFAS, but the time to equilibrium and minimum effective biochar application are vastly different among biochar and compound type combinations. The data suggests that for PFAS greater than 4 carbons long, a higher surface area and higher hydrophobicity are desirable traits for PFAS sorption. A difference was observed in percentage removal and distribution of PFAS type in individual versus mix mode experiments. This ranged based on specific PFAS - biochar type combinations. The same test applied to desorption saw an increased desorption of PFOS, which was previously strongly sorbed in individual mode experiments. Mix mode PFAS experiments had little effect on equilibrium time, however intraparticle diffusion modelling demonstrated that for pine biochars an intraparticle diffusion stage was present, which was not apparent in straw biochars.

Considering the above and the data put forward by extrapolated Freundlich-Langmuir combination models, P750, the pine biochar produced at the highest tested pyrolysis temperature, performs as the best PFAS sorbent for the PFHxA, PFHxS, PFOA and PFOS. A pyrolysis method which further optimizes temperature, and hence hydrophobicity and surface area, will have improved sorption for PFOS, PFOA, PFHxS and to a lesser extent PFHxA, in water. Further exploration of feedstocks may uncover biochars better suited for PFAS sorption. The reverse engineering of biochars for PFAS removal from water in this manner may allow for cheaper and more environmentally friendly alternative to activated carbon.

Chapter 6

Biochar Sorption of PFOS, PFOA, PFHxS and PFHxA in Two Soils with contrasting Texture

Matthew Askeland ^a, Bradley Clarke ^b, Sardar Alam Cheema ^c and Jorge Paz-Ferreiro ^{d,*}

a Department of Environmental Engineering, RMIT University, Melbourne 3000, Australia

b School of Chemistry, University of Melbourne, Victoria 3010 Australia

c Department of Agronomy, Faculty of Agriculture, University of Agriculture, Faisalabad-38040, Pakistan

d School of Engineering, RMIT University, Melbourne 3000, Australia

Submitted to Science of the Total Environment on 20th August 2019

6.1 Abstract

The ability to immobilise PFAS in soil may be an essential interim tool while technologies are developed for effective long-term treatment of PFAS contaminated soils. Biochar is a promising cost-effective and sustainable solution, which can be engineered for PFAS immobilisation. While many sorbents have been studied in solution, little is known about soil-biochar-PFAS interactions. Serial sorption experiments were undertaken using a pine derived biochar produced at 750°C (P750) and analysed by direct injection liquid chromatography mass spectrometry to determine equilibrium, sorption and desorption behaviour in an individual and mix congener experimental mode with either a loamy sand or a sandy clay loam soil. All experiments were carried out either in individual mode (solution with one PFAS at 5 µg/L) or mix mode (solution with 5 µg/L of each: PFOS, PFOA, PFHxS and PFHxA), and carried out in 2:1 water to soil solutions. Soils had biochar added in the range 0 -5 % w/w. Kinetic data were fitted to the pseudo-second order model for both amended soils, with equilibrium times ranging 0.5 to 96 hours for all congeners. PFOS sorption was 11.1 ± 4.5 % in the loamy sand compared to 69.8 ± 4.9 % in the sandy clay loam. It was demonstrated that while total sorption was higher in the unamended loamy sand than sandy clay loam for PFHxA, PFOA and PFOS, the effect of biochar amendment for each compound was found to be significantly higher in amended sandy clay loam than in amended loamy sand. Application of biochar reduced the desorbed PFAS fraction of all soils. Soil type and experimental mode played a significant role in influencing desorption. Overall, the relationship between sorbent and congener was demonstrated to be highly impacted by soil type, however the unique physiochemical properties of each PFAS congener greatly influenced its unique equilibrium, sorption and desorption behaviour for each amended soil and mode tested. Considering this, the biochar P750 had a greater effect on sorption for sandy clay loam soil compared

to loamy sand, however desorption data demonstrated comparatively greater reversibility of sorbed fraction in loamy sand soil than sandy clay loam soil. This suggests that sorption capacity should be compared with reversibility (desorption) when assessing the efficacy of biochar as a PFAS immobilisation technique in soil matrices.

6.2 Introduction

Per- and poly- fluoroalkyl substances (PFAS) are a group of anthropogenic and environmentally persistent organic compounds found to be extensively dispersed throughout environmental compartments (Bengtson Nash et al. 2010; Borg et al. 2013; Nakayama et al. 2019; Prevedouros et al. 2006; Stahl, Mattern & Brunn 2011). PFAS are receiving increasing attention in environmental and toxicological literature due to their inherent toxicity, persistence and mobility (Cai et al. 2019; Lloyd-Smith 2016; Prevedouros et al. 2006). Current treatment technologies are limited, driving demand for solutions addressing PFAS in soils, sediments, and water (ground, surface and waste)(Kucharzyk et al. 2017; Ross et al. 2018). In the interim, effective immobilisation technologies are required to prevent further PFAS migration from sources to uncontaminated environments and water sources (Brusseau 2018; Söregård, Kleja & Ahrens 2019; Xiao et al. 2015).

Biochar, created through the pyrolysis of waste biomass, has been mooted as a possible PFAS sorbent and sustainable management strategy (Kupryianchyk et al. 2016; Liu et al. 2019). However, the sorption behaviour of PFAS to biochar amended soil has not been subjected to the level of exploration with respect to soil physiochemical properties as has been undertaken for PAHs (Chen & Yuan 2011), PCBs (Denyes, Rutter & Zeeb 2013), pesticides (Cabrera et al. 2014; Dechene et al. 2014; Delwiche, Lehmann & Walter 2014) and heavy metals (Méndez et al. 2014; Uchimiya et al. 2011). To achieve this, a greater understanding of sorption behaviour is required (Du et al. 2014; Li et al. 2019), particularly with respects to PFAS immobilisation in the presence of soil matrices which are typically hard to characterise due to heterogeneity (Brusseau 2018; Campos Pereira et al. 2018; Li et al. 2019). Additionally, consideration needs to be given to the partitioning of PFAS onto sorbents in soil from the water-soil phase, in which environmental conditions such as pH and ionic strength may impact sorption (Li et al. 2019). Considering the above, equilibrium, sorption and desorption processes are greatly influenced by the duration and physicochemical properties of the sorbate, sorbent, and environment in which interaction takes place (Brusseau 2018; Li, Oliver & Kookana 2018).

PFAS sorption behaviour by solid matrices is further complicated by the molecular structure of PFAS congeners themselves (Brusseau 2018), which result in congener structure specific hydrophobic and oleophobic (Li,et al. 2019) interactions with their environment and have unique surface activity based on chain length and functional group type (Du et al. 2014; Knight et al. 2019; Li et al. 2019). Due to this complexity, a limited number of PFAS compounds, usually PFOA and PFOS, have been studied in soils (Campos Pereira et al. 2018). In light of the recent phasing out of these 2 congeners in line with the Stockholm convention sanctions (POPRC 2008; Wang et al. 2009), and their subsequent replacement with shorter 4 to 6 chain derivatives, further data are needed to model their comparative behaviours.

The current body of research largely suggests that sorption of PFAS to solid media surfaces is strongly governed by the sorbent's physicochemical properties such as organic carbon and surface functional groups. In the case of soils, organic matter (OM), metal oxides and clay content are important factors influencing sorption (Brusseau 2018; Campos Pereira et al. 2018). Currently there is little information on the interactions between PFAS and sorbent, in the presence of soil, and their relative effect upon PFAS sorption behaviours (Campos Pereira et al. 2018). The characteristic C-F hydrophobic chain moiety of PFAS molecules results in strong hydrophobicity-driven interaction with the organic matter fraction of soils (Li, Oliver & Kookana 2018). This behaviour sees organic matter frequently used as an indicator for sorption capacity when assessing PFAS fate and transport in soils or amended soils (Li et al. 2019). However, it has been demonstrated that specific fractions of OM, such as proteins, saccharides, fulvic acids and humic acids, each have their own potential impact on the sorption behaviour of various PFAS molecules to solid matrices (Campos Pereira et al. 2018). The formation of micelles and hemimicelles has been long observed in PFAS sorption studies and been demonstrated through well-fitting Freundlich type models to have strong partitioning and surface activity from the hydrophobic portion of the molecule as monolayers and bilayers. This type of hydrophobic behaviour is typically influenced by surface area, OM fraction and pore size, and in the case of biochars, degree of carbonization (Söregård, Kleja & Ahrens 2019).

However, OM alone has been shown to not be the only parameter driving PFAS sorption behaviours in complex matrices (Knight et al. 2019; Oliver et al. 2019). Electrostatic interactions have been presented as an additional likely sorption mechanism, where the negatively charged PFAS ion functional group head may interact with sorbent, surface net charges, surface functional groups, metal oxides and oxyhydroxides (Knight et al. 2019; Li et al. 2019; Li, Oliver & Kookana 2018). Surface functional groups are likely to interact with PFAS heads as generally low PFAS pKa result in a high abundance of the soluble ionised PFAS form under environmentally relevant conditions (Brusseau 2018). Ionised forms have also been demonstrated to allow interaction with Ca⁺², Mg⁺², Fe⁺³ and Al⁺³, but not monovalent cations such as Na⁺ and K⁺ (Campos Pereira et al. 2018). In addition, under environmentally relevant conditions, OM surface groups can carry a negative charge, which in the presence of multivalent cations can complex PFAS molecules by cationic bridging effects (Campos Pereira et al. 2018). This behaviour becomes more complex in soils which hold a variable pH and ionic strength dependant charge due to fluctuations of protonation of surface functional groups or net surface impacting charge bridging effects (Li, Oliver & Kookana 2018; Oliver et al. 2019). Ultimately, both soil mineral and organic matter phases may contribute to fixed and variable surface charge on soils, in turn influencing sorption behaviour (Oliver et al. 2019).

In consideration of the above, it is suggested that the influence of soil and sorbent qualities in combination with PFAS congener qualities all have a complex role in influencing the specific mechanisms, rate, extent and reversibility of PFAS sorption to sorbent amended soils (Milinovic et al. 2015). To date, many studies have examined PFAS-sorbent behaviour in aqueous solutions (Du et al. 2014; Li et al. 2019; Li et al. 2019; Zhi & Liu 2018), with varying masses of sorbent or concentrations of PFAS. Barring a small number of soil column leaching studies (Bräunig et al. 2019; Gellrich, Stahl & Knepper 2012; Høisæter, Pfaff & Breedveld 2019; Kalbe et al. 2014), the effect of the soil fraction on sorbents is seldom considered beyond brief discussion. This is particularly the case with respect to biochar. Leaching experiments are limited by poor mixing and heterogenous contact of the soil matrix with the sorbent, and sorbate with sorbents, respectively. While each experimental mode collects vital data, exploration of the direct effect of soil matrices in a well-mixed system is not well-addressed in

the literature. In addition, the comparison of PFAS behaviour as individual congeners versus in a mixture of congeners is poorly characterised. This study employed a biochar amended soil in water as a 2:1 water to soil slurry, weight per weight. This resulted in a mixable solution that overcomes the limitations common to column leaching by allowing increased mixing. In turn this allowed the study of efficiency of sorbents in amended soils for PFAS. This was achieved by the application of biochar amendments to two typical Australian soils, a loamy sand and a sandy clay loam, exhibiting contrasting characteristics. To the author's knowledge, this is the first study to observe sorbent efficiency in this manner in the presence of a soil matrix and compare PFAS sorption efficiency with soil properties. In addition, variation of these effects was studied in two experimental modes, wherein experiments were carried out with individual congeners, or in a mix mode with all four congeners in solution.

Equilibrium times, sorbed and desorbed fraction could be assessed to allow the reverse engineering and mindful application of biochar as a cost-effective interim strategy for PFAS immobilisation. This study aims to demonstrate the further need for characterisation of soil fraction and sorbent interactions and how they affect PFAS sorption in the environment. An understanding of soil–PFAS interactions and PFAS-sorbent interactions are important, however the complex soil-sorbent-PFAS interactions, likely to be determinant in the environment, are still in dire need of further detailed assessment.

6.3 Material and Methods

6.3.1 Chemicals and Reagents

Native and ¹³C PFAS standards used in the preparation of calibration standards were obtained from Wellington Laboratories Incorporated (Ontario, Canada). PFAS Salts required for preparation of 5 µg/L spiking solutions were supplied by Sigma Aldrich (Missouri, United States). Ammonium acetate used in LCMS was acquired from Sigma Aldrich (Missouri, United States) and Hypergrade Methanol (LiSolv) was purchased from EMD Millipore (Massachusetts, United States).

6.3.2 Biochar

A complete characterization, including the synthesis, of the biochar used in all experiments is available in Askeland, Clarke & Paz-Ferreiro (2019). This biochar was selected from six studied biochars in [30] due to its high surface area and high carbon content. Throughout this publication the biochar is referred to as P750, a nomenclature that denotes its production feedstock being pine, pyrolyzed at 750°C. Prior to serial experiments, PFAS analysis of P750 was undertaken to determine if PFAS were extractable in Milli-Q water over a 92-hour period.

6.3.3 Soil Characterisation

Soils used in serial experiments were selected as they had been previously characterised by a NATA accredited lab using acceptable ISO, AS and ASTM soil assessment methods. The two soils, a sandy clay loam and loamy sand, were selected due to their different physicochemical properties, particularly texture and organic matter fraction, each of which are influential factors in the sorption of PFAS (Chapter 2). Both soils exhibited similar pH, in turn isolating effects of sorption to those largely governed by soil physiochemical properties other than pH. Both soils were sampled in Mordialloc (37.9990° S, 145.0920° E), a south eastern suburb of Melbourne, Australia. Prior to batch experiments, background PFAS concentrations in soils were assessed as PFAS extractable in Milli-Q water.

6.3.4 Experimental Design

This study was set up to compare equilibrium, sorption and desorption behaviour between the two different soils (sandy clay loam and loamy sand), and soils amended with biochar. Experiments were conducted as serial experiments carried out in 15 mL polypropylene centrifuge tubes for each soil in one of two modes, individual or mix. Soils were spiked with a constant 5 mL of 5 µg/L PFAS solution containing all four selected PFAS (PFOA, PFOS, PFHxS and PFHxA), termed mix mode. Alternatively, soils were spiked with 5 mL of solution containing just one of the four selected PFAS congeners at 5 µg/L, termed individual mode. This concentration was selected to be reflective of PFAS concentrations in the contaminated soil environment (Cao et al. 2019; Seo et al. 2019; Zareitalabad et al. 2013). All experiments were carried out in the same manner for each soil, mode and individually tested PFAS congener. The PFAS selected in this study aimed to capture data for PFOS and PFOA, as well as their leading 6 carbon chain successors, PFHxA and PFHxS.

6.3.5 Experimental Methodology

Equilibrium testing was conducted for 5 % w/w applications of P750 to soil, with a total mass of 2.5 g. This was added to a 15 mL centrifuge tube containing 5 mL of 5 µg/L PFAS solution, in either individual or mix mode, and placed on a shaker for 0, 1, 3, 5, 8, 24, 48, and 96 hours. The resultant liquid to solid ratio was 2:1. In each experiment, each time point was prepared accordingly as triplicate samples for destructive sampling. Samples were prepared for LC-MS analysis and the resultant data statistically analysed prior to fitting to first order and second order models.

Sample preparation for LC-MS analysis required each sample to be centrifuged at 4000 RCF for 30 minutes and the subsequent extraction of 1 mL of supernatant to a new centrifuge tube by pipette, to which 1 mL of MeOH was added by mass to result in a 10 % MeOH w/w. Samples were vortexed prior to decanting the solution into 5 mL polypropylene stopperless Luer Lock syringes for filtration through a Corning polypropylene housed 15 mm regenerated cellulose syringe filter (0.22 µm). After filtration the prepared samples were stored in Agilent Technologies 1 mL polypropylene GC vials with clip on caps at 6 °C until analysis. Prior to experimentation, all consumables and equipment used in study were confirmed to be PFAS-free by LC-MS analysis of Milli-Q water leachable PFAS fractions over a 120-hour study period.

Sorption experiments for each soil were carried out as per equilibrium experiment methodology; however, biochar addition was incremented as % w/w for a constant 2.5 g soils sample. Treatments employed in experiments were 0, 0.5, 1, 2, 2.5, 3, 4, 5 % w/w. Equilibrium times were applied as determined in the prior equilibrium experiments, where the equilibrium time of the slowest sorbing compound were used in mixed mode experiments. All experiments were undertaken in triplicate and sample preparation for LCMS analysis was undertaken adhering to the sample preparation methodology outlined above. Triplicate experimental sorption tubes had their remaining solution volume calculated by difference in mass and were retained for desorption experiments.

In desorption experiments 5 mL of Milli-Q water was added to centrifuge tubes retained from previously described sorption experiment and placed on a shaker for their relative equilibrium time as per sorption experiments. Samples were prepared for LC-MS analysis as outlined above. Exact volumes of Milli-Q water added to each centrifuge tube were determined by mass. Desorption (%) was calculated as the difference between experimentally determined solution concentration after reconstitutions and expected solution concentration assuming dilution at a steady state as calculated by mass difference of water remaining, known starting concentration and mass of water added.

QA/QC was approached through the employment of triplicate blanks, matrix spikes and Laboratory Control Samples (LCS) samples through experiments. Blanks consisted of 5 mL of Milli-Q water in a centrifuge tube. Matrix spikes were prepared as blanks and spiked with sufficient PFAS stock solution to achieve a 5 µg/L PFAS concentration in the 5 mL solution contained in a 15 mL centrifuge tube. LCS were prepared as per blanks, with the addition of 2.5 g of 5 % w/w P750 amended soil, for each soil tested. These samples and pre-spiked 1 µg/L PFAS samples were included interspersed randomly in LCMS runs and allowed adequate measurement and control of PFAS QA/QC by method losses, recoveries, and detection of contamination.

6.3.6 LCMS analysis

All sample analysis was by direct injection LCMS using an Agilent infinity II liquid chromatograph and an Agilent 6495 triple quadrupole mass spectrometer. Briefly, the method employed Agilent EclipsePlusC18, 3.5 µm (4.6x50mm) as a delay column and an Agilent EclipsePlusC18 - RRHD 1.8 µm (2.1x50 mm) as the separation column. Separation occurred with an oven temperature of 40°C using the s Hypergrade MeOH and 5mM ammonium acetate in Milli-Q water as solvents. Supplementary tables S2 and S3 detail injection programs, solvent gradients and relevant instrument parameters. Supplementary table S1 details method performance. Table 6.1 outlines method MDL, LOQ and QC outcomes for unspiked milli-Q and solids matrix blanks. Agilent Technologies Masshunter Package (version 8) was used to process all LCMS data.

6.3.7 Statistical Analysis

Statistical analysis was undertaken for this study using IBM SPSS version 25. The software allowed the analysis and further interpretation of the data after transformation by one-way ANOVA and Tukey's Test post-hoc analysis to assess means between and across tested treatment and experimental modes.

6.4. Results and Discussion

All blanks undertaken as QC samples were returned as < MDL or less than LOQ, excepting loamy sand blank which contained small amounts of PFOS and PFOA just above the level of quantitation (Table 6.1). However, this was not leachable in the 5 % P750 amended loamy sand QC (Table 6.1). The 0.082 and 0.133 µg/L respective PFOS and PFOA leachable concentrations were deemed as native soil contamination and it was determined that, at most, this would account for 2.6 % of error considering a solution concentration of 5 µg/L in experiments. All blanks were below MDL. Analysis of soil geochemical properties revealed that soils were chemically different in CEC, TOC, OM and EC, which were found to be higher in the loamy sand soil, while the sandy clay loam soil exhibited a higher value for clay (Table 6.2). Both soils were neutral, with respect to soil pH.

Table 6.1. Detection limits and QAQC blanks used in experiments

	PFHxA (µg/L)	PFHxS (µg/L)	PFOA (µg/L)	PFOS (µg/L)
MDL	0.019	0.030	0.025	0.038
LOQ	0.059	0.094	0.079	0.120
Blank	<MDL	<MDL	<MDL	<MDL
Loamy sand blank	<LOQ	<LOQ	0.082	0.133
Sandy clay loam blank	<LOQ	<LOQ	<LOQ	<LOQ
Loamy sand + 5 % P750 Blank	<LOQ	<LOQ	<LOQ	<LOQ
Sandy clay loam+ 5 % P750 Blank	<LOQ	<LOQ	<LOQ	<LOQ

Table 6.2 Physiochemical parameter laboratory analysis means results for loamy sand and sandy clay loam soils used in sorption experiments.

Parameter	Loamy sand	Sandy clay loam
pH (CaCl₂)	6.27 ± 0.02	6.23 ± 0.02
pH Value (Dried at 40°C)	6.80 ± 0.01	6.73 ± 0.06
Electrical Conductivity (µS/cm)	728.50 ± 8.25	68.33 ± 0.24
Moisture Content (%)	3.80 ± 0.11	1.73 ± 0.10
Exchangeable Calcium (meq/100g)	12.53 ± 0.48	3.53 ± 0.12
Exchangeable Magnesium (meq/100g)	3.97 ± 0.17	0.87 ± 0.02
Exchangeable Potassium (meq/100g)	1.30 ± 0.15	0.17 ± 0.02
Exchangeable Sodium (meq/100g)	0.25 ± 0.03	0.20 ± 0.01
Cation Exchange Capacity (meq/100g)	18.40 ± 0.90	4.77 ± 0.16
Iron (%)	0.91 ± 0.06	0.64 ± 0.02
Organic Matter (%)	9.60 ± 0.16	1.50 ± 0.04
Total Organic Carbon (%)	5.53 ± 0.10	0.87 ± 0.02
Clay (%)	4.67 ± 0.62	32.00 ± 0.82

6.4.1 Equilibrium Experiments

All tested PFAS congeners had reached equilibrium after 24-hours for both experimental modes, except for PFOS in sandy clay loam in both experimental modes, PFHxS loamy sand in mix mode, and PFHxA in sandy clay loam in individual mode (Table 6.3). These exceptions had reached equilibrium by the 96th hour in the biochar amended soil solutions. In mixtures, equilibrium was faster for PFAS in sandy clay loam, excepting PFOS which was quicker in the loamy sand. In individual mode experiments were faster or equal equilibrium times were seen for all compounds in the loamy sand. PFOS always had faster sorption in loamy sand, irrespective of mix or individual mode. PFOA sorption was quicker in sandy clay loam in mix mode than in individually mode experiments, while the opposite was true in loamy sand, where individual mode PFOA sorbed faster. PFHxS sorption was always faster in loamy sand than in sandy clay loam, with faster sorption times in individual mode loamy sand experiments and slower in individual mode sandy clay loam. PFHxA was sorbed faster in sandy clay loam in mix mode, whereas sorption was slower in sandy clay loam for individual compounds. The fastest sorption for PFOS was in loamy sand. In contrast, the fastest sorption for PFHxA, PFHxS and PFOA was in sandy clay loam mix mode experiments, with equilibrium reached by 0.5 hours.

Overall equilibrium times ranged 0.5 to 96 hours across experiments, depending on the PFAS congener tested and soil type. Sorption times were highly dependent on PFAS-soil type combination, as such statistically significant relationships for sorption equilibria between individual or mix mode experiments were not detected ($p > 0.05$). PFOS exhibited a shorter equilibrium time in loamy sand than in sandy clay loam in both, mix mode (F: 39.17; p: 0.001; Fcrit: 7.71) and individual mode (F: 35.01; p: 0.001; Fcrit: 7.71) experiments.

Modelling revealed that the experimental data could not be fitted to a first order model (supplementary table S4). Kinetic behaviour was a good fit for the pseudo-second order model (Table 6.4), in line with the findings of (Li, M et al. 2019), in which the sorption of PFHxA, PFHxS, PFOA and PFOS to a powdered activated carbon was studied. The highest Q_e for PFOS was in loam sand and amended sandy clay loam. The lowest Q_e values were seen for PFHxA, particularly in the case of PFHxA in sandy clay loam mix mode experiment. In general, irrespective of matrix or mixture, Q_e followed the order PFHxA, PFOA, PFHxS, PFOS, in increasing Q_e value. Q_e values were similar between individual versus mix mode experiments in loamy sand. Q_e had a small but significant difference for PFOS (F: 12.31; p: 0.011; Fcrit: 7.71), PFHxA (F: 9.62; p: 0.001; Fcrit: 7.71), and PFHxS (F: 8.81; p: 0.029; Fcrit: 7.71) between mix and individual mode experiments for sandy clay loam, with higher Q_e in individual experiments, except for PFOA. This was not the case in loamy sand, where a statistically different mean was only seen for PFHxA (F: 13.22; p: 0.03; Fcrit: 7.71) between mix and individual modes.

K values support equilibrium data with sorption rates reflecting the compound specific equilibrium times changes between individual and mixture experiments for loamy sand versus sandy clay loam soils. PFOS K values were higher in the loamy sand compared to the than sandy clay loam. No difference was seen in amended loamy sand between mix and individual mode experiments for PFOA and PFOS, the converse was true for PHHxS and PFHxA. Comparatively large differences in congener specific K values were seen between individual and mix mode amended sandy clay loam experiments for all compounds. PFHxS had the highest K value in mixed mode sandy clay loam experiments, followed closely by PFOA for mixed mode amended sandy clay loam soils and PFOS for both mixed and individual amended loamy sand experiments. PFHxS sorption rates were higher in sandy clay loam than in loamy sand and higher for mix mode experiments.

PFOA k values were higher for sandy clay loam in mixed experiments but comparatively higher in loamy sand for individual experiments. PFHxA K values were here higher in loamy sand for mixed mode experiments but higher in sandy clay loam for individual experiments. Each congener was found to have its kinetic behaviour impacted by both soil type and experimental mode; however, the extent is dependent on congener. For example, PFOS exhibited a very large impact by soil type with very little influence of mode. Comparatively most of the congeners tested had K2 impacted by both mode and soil type. PFOA, posed different results between matrices in mixture experiment, however, similar kinetic results between matrices in individual experiments. K2 correlated well with calculated Eq values, which were also congener specific.

Table 6.3 ANOVA analysis of equilibrium data for mixed and individual PFAS experiments using 5 mL of PFAS spiked solution and 2.5 g of soil amended to 5% w/w P750 biochar. Equilibrium established as 3 consecutive points without statistical difference. Asterisked values required a 96 hours period to reach equilibrium.

	PFHxA				PFHxS				PFOA				PFOS			
	Eq (h)	F	P	Fcrit	Eq (h)	F	P	Fcrit	Eq (h)	F	P	Fcrit	Eq (h)	F	P	Fcrit
Mix loamy sand	24	0.3	0.633	10.1	48*	11.6	0.042	10.1	8	5.6	0.053	5.8	1	2.4	0.105	3.2
Mix sandy clay loam	0.5	0.4	0.872	2.8	0.5	0.4	0.866	2.8	0.5	1.3	0.321	2.8	48*	22.6	0.009	7.7
Ind loamy sand	24	2.5	0.188	7.7	3	3.1	0.091	4.1	1	2.6	0.080	3.1	1	3.1	0.053	3.2
Ind sandy clay loam	48*	32.9	0.004	7.7	1	1.9	0.168	3.2	24	9.3	0.038	7.7	48*	149.5	0.006	18.5

Table 6.4 Pseudo second order models for tested soils amended 5% w/w P750 biochar.

	PFHxA			PFHxS			PFOA			PFOS		
	Qe (µg/g)	K ₂ (h)	R	Qe (µg/g)	K ₂ (h)	R	Qe (µg/g)	K ₂ (h)	R	Qe (µg/g)	K ₂ (h)	R
Mix loamy sand	0.031	47.918	0.990	0.178	9.137	0.996	0.127	28.412	0.998	0.215	61.846	0.999
Mix sandy clay loam	0.011	11.352	0.717	0.065	158.513	0.999	0.0329	106.438	0.999	0.094	9.494	0.972
Ind loamy sand	0.090	6.181	0.987	0.187	1.158	0.934	0.139	17.476	0.995	0.223	61.405	0.999
Ind sandy clay loam	0.046	45.450	0.923	0.096	35.361	0.999	0.025	12.567	0.935	0.187	1.158	0.680

6.4.2 Sorption Experiments

Figure 6.1 explores PFAS removal percentages versus biochar application to tested soils as w/w. The origin in the x axis demonstrates PFAS sequestered by control soils. It is clear that in the loamy sand, very little further PFAS was adsorbed by the addition of biochar and increasing the application to 5 % resulted in no statistically significant increase in mean % removal beyond the initial 0.5 % application. No statistical difference was observed between mixtures and individual experiments over application ranges for loamy sand soils. The order of sorption followed the sequence PFHxA << PFHxS ~ PFOA << PFOS.

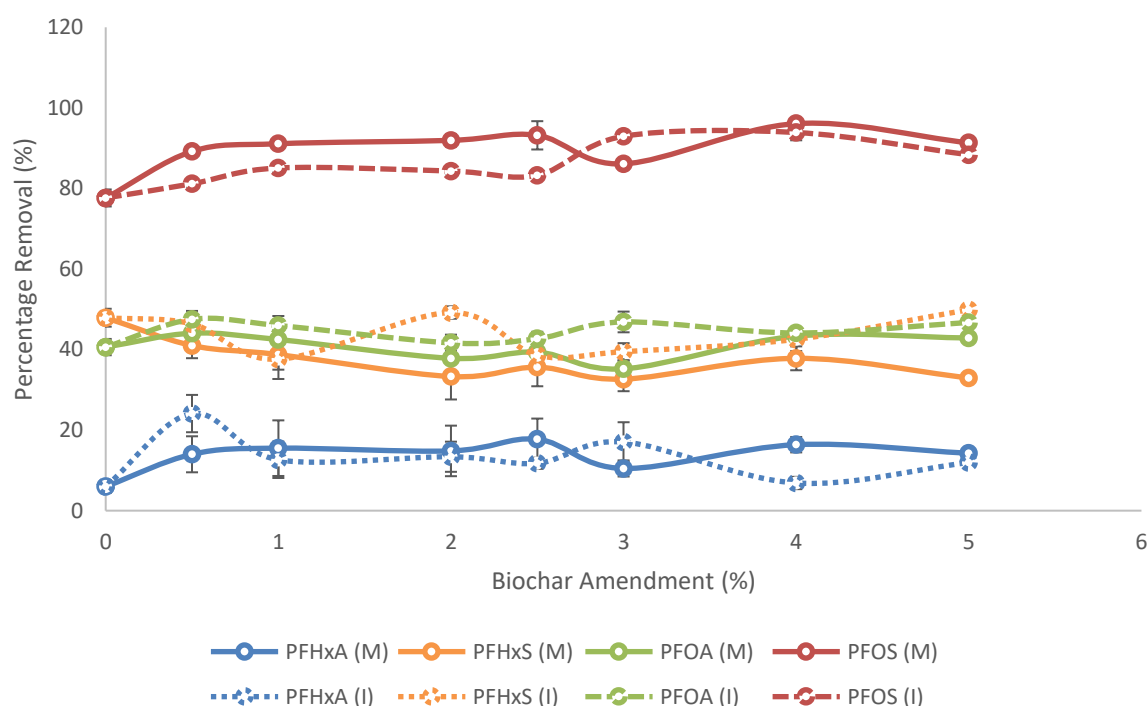


Figure 6.1 Percentage removal of selected PFAS by varying amendments of P750 in a loamy sand. Note: 0 % amendment values are representative of the fraction removed by soils.

Figure 6.2 shows removal per biochar application (%) for the sandy clay loam soil. It is evident that PFOS has a much greater increase in sorption in the amended samples compared to the control, as shown by the slope from 0 % (control) to 0.5 % w/w. This is not so obvious for the remaining compounds. However, a statistically significant gradient for PFOS ($F: 10.04$; $p: 0.027$; $F_{crit}: 7.71$) between 0.5 % and 4% demonstrates that PFAS sorption was still increasing to a measurable level with biochar addition. Similar to loamy sand, there is much variation in the data and remaining compounds all performed similarly. No statistical difference was detected between mix and individual mode experiments.

Comparing PFOS to the other tested PFAS in loamy sand experiments, the steep gradient seen between 0 and first application level in PFOS experiments demonstrates a greater effect by biochar application upon PFOS

than the other tested PFAS. In sandy clay loam the difference in percent sorption between PFHxA, PFHxS and PFOA was much less pronounced than in loamy sand experiments. PFHxA, PFOA and PFOS % removal means were higher in amended sandy clay loam soils than in loamy sand, even though the degree of sorption was still small.

Typically, laboratory experiment biochar application rates have ranged as low as 0.2 to over 10 % (W/W) equating to 7.76 and over 338 tons per hectare, respectively (Denyes et al. 2012; Domene et al. 2015). These values are calculated on the basis of a 0.3 m deep arable soil layer and an in-situ bulk density of 1.29 ton per m³ as outlined in Domene et al. 2015. While Singh et al. 2014 suggests that applications of 5-20 tons per hectare may not be agronomically feasible, higher application rates required for biochar immobilisation of PFAS as a remediation strategy, where agricultural yield is not focal, are likely to remain more cost effective or have lower inherent risk than alternative solutions such as monocell storage, activated carbon, soil washing, landfilling or thermal desorption/destruction. As such, the tested application rate of 0 to 5% w/w biochar amendment is appropriate, from an economic and feasibility standpoint, to be scaled in the future for practical real-world applications.

Isothermal sorption modelling of the data was found not to be possible due to the high impact of soil fraction on initial sorption and the lowest application of biochar reaching maximum measurable removal. This is evident in the relatively flat removal curves shown in Figure 6.1 and Figure 6.2. The exception being PFOS in sandy clay loam. However, isothermal modelling was not undertaken due to the lack of a point of comparison against the other PFAS congeners or similar observations for loamy sand experiments.

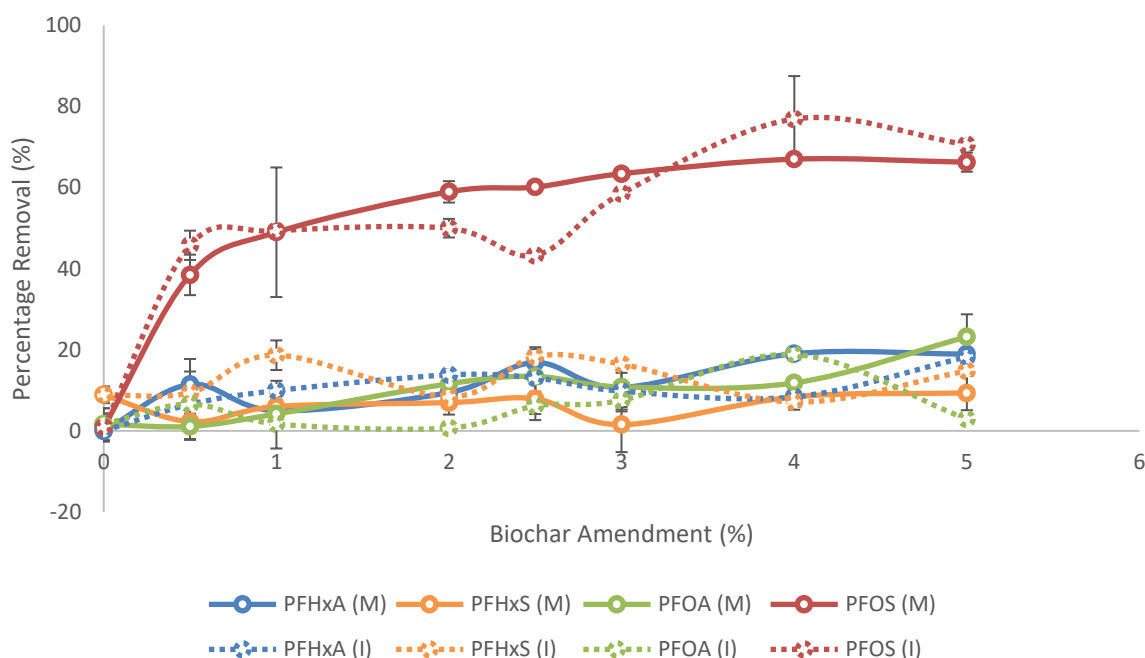


Figure 6.2 Percentage removal of selected PFAS by varying amendments of P750 in a sandy clay loam. Note: 0 % amendment values are representative of the fraction removed by soils.

Sorbed percentages of each PFAS type were different for both soil types tested, with loamy sand sorbing far greater amounts than sandy clay loam for all compounds in unamended soils (Table 6.5 and 6.6). Sorption followed, in order of increasing sorption, PFHxA, PFOA, PFHxS and PFOS for loamy sand. These results are contrary to sorption results seen in other studies which suggest sorption to carbonaceous materials follows the order of increasing chain length with compounds of equal chain length being prioritised by a sulphonate group ([15] studied this phenomenon in PFOS and PFOA). This suggests the interaction between compound and sorbent is impacted directly upon by the physiochemical properties of the soil and associated soil solution, resulting in interactions in which functional group is more of an influencing factor than chain length.

Table 6.5 Percent (%) removal of selected PFAS to loamy sand and 5% w/w P750 biochar amended loamy sand. Statistically significant differences in PFAS sorption detected by ANOVA analysis are denoted between soil, mix and individual mode biochar amended soils by capital letters (A, B, C).

	Soil (%)	Mix mode		Individual mode	
		Soil + 5 % Biochar (%)	Biochar Effect (%)	Soil + 5 % Biochar (%)	Biochar Effect (%)
PFHxA	5.9 ± 1.2 ^A	8.9 ± 4.0 ^A	3.0 ± 5.2	11.9 ± 1.3 ^B	6.0 ± 2.5
PFHxS	47.9 ± 0.8 ^A	46.2 ± 2.9 ^A	-3.7 ± 3.7	49.9 ± 2.9 ^A	2.0 ± 3.7
PFOA	40.6 ± 1.0 ^A	40.5 ± 2.7 ^A	-0.1 ± 3.7	44.1 ± 1.2 ^A	3.5 ± 2.2
PFOS	77.6 ± 2.5 ^A	88.7 ± 1.9 ^B	11.1 ± 4.5	88.4 ± 1.9 ^B	10.8 ± 4.4

In sorption experiments the highest percent removal was for PFOS, 88.7 ± 1.9 %, with a net biochar effect for mix mode loamy sand amended with P750 at 5 % w/w of 11.1 ± 4.45 (Table 6.5). The lowest observed sorption was in the mix mode test of PFHxA, where loamy sand amended with P750 at 5 % w/w saw a mere 8.9 ± 4.0 sorbed of which 3.0 ± 5.2 % was a result of biochar application. No statistically significant difference was detected between individual and mixed PFAS experiments (P>0.05), suggesting inter-PFAS interactions such as competition for active sites or increased co-sorption. The effect of biochar on sorption followed the order PFHxS < PFOA < PFHxA < PFOS. However, considered as total sorption (loamy sand and biochar), sorption followed the order PFHxA << PFHxS < PFOA < PFOS, which is closer to the results seen in (Söregård, Kleja & Ahrens 2019), where it was noted interaction with sorbent increased 11–15 % per CF₂ moiety and was 49% higher for the perfluorosulfonates than perfluorocarboxylates. Experimental data collected in the present study for individual mode experiments saw similar sorption results between PFHxS and PFOA, suggesting chain length and functional group may at times result in competing sorption mechanisms.

Table 6.6 Percent (%) removal of selected PFAS to sandy clay loam and 5% w/w P750 biochar amended sandy clay loam. Statistically significant differences in PFAS sorption detected by ANOVA analysis are denoted between soil, mix and individual mode biochar amended soils by capital letters (A, B, C).

	Soil (%)	Mix mode		Individual mode	
		Soil + 5 % Biochar (%)	Biochar Effect (%)	Soil + 5 % Biochar (%)	Biochar Effect (%)
PFHxA	-5.6 ± 0.6 ^A	13.4 ± 5.3 ^B	18.9 ± 5.9	18.2 ± 2.0 ^B	23.8 ± 2.6
PFHxS	8.9 ± 2.0 ^A	9.6 ± 5.2 ^A	0.7 ± 7.3	14.8 ± 5.1 ^A	5.9 ± 7.1
PFOA	1.6 ± 2.9 ^A	23.2 ± 1.6 ^B	21.6 ± 4.5	18.8 ± 1.4 ^B	17.2 ± 5.3
PFOS	0.8 ± 3.4 ^A	66.3 ± 2.3 ^B	65.5 ± 5.7	70.6 ± 1.4 ^B	69.8 ± 4.8

Highest removal was for individual PFOS in sandy clay loam with 5% P750 amendment w/w, which achieved a total of 70.6 ± 1.4 % removal, with biochar accounting for 69.8 ± 4.8 % of removal (Table 6.6). The lowest removal was seen in PFHxS with respects to total and effect of biochar. No statistical difference was seen between individual and mixtures tested for each compound. Total sorption followed the order PFHxS < PFHxA < PFOA < PFOS for all experiments. Effect of biochar fraction followed the same order in mix mode experiments. A similar order was followed in individual experiments, excepting no statistical difference was found between PFOA and PFHxA.

Differences between mix and individual mode experiments were common across both tested soils, suggestive of intra-PFAS competition not being a major consideration for PFAS sorption to carbonaceous materials in the presence of soil. However, the differences in soil type could suggest competitive sorption and fouling by other soil based organic substances (Zhi & Liu 2018). In addition, the effect OM and clay content presented on sorption was in line with the finding of Li, Oliver & Kookana (2018), wherein the study of PFAS sorption to soil could not be explained by any single soil property but was highly dependent on specific PFAS congener and soil geochemical property combinations. Due to the design of this experiment and complexity of the matrix, the competition of fouling agents, and effect of clay versus OM fraction could not be disambiguated, beyond demonstrating that these had a profound effect on sorption behaviour, as suggested in Li, Oliver & Kookana (2018). Likewise, the order of effectiveness for tested congeners was found to be the same between soils. However, the magnitude of effectiveness was vastly different between soils, with the lowest effectiveness in loamy sand being -3.7 ± 2.7 % and the lowest in sandy clay counterpart being 0.7 ± 7.3 %. Likewise, the highest in loam soil was found to be 11.1 ± 4.5 % for PFOS mix mode experiments whereas in sandy clay loam individual mode the highest biochar effect was 69.8 ± 4.9 %.

While total removal was often higher in loamy sand, PFHxA, PFOA and PFOS had a higher sorption effect on sorbed fraction in amended sandy clay loam than in amended loamy sand. This suggests that P750 is far more effective in the sandy slay as a sorbent, possibly due to competing organic species in the OM fraction of the loamy sand, or simply due to the larger fraction available for sorption remaining in solution for sandy slay experiments. Overall, the addition of 5 % w/w biochar greatly increased the removal of PFAS from experimental soil solutions for PFHxA (F: 28.13; p: 0.012; Fcrit: 7.71), PFOA (F: 22.72; p: 0.001; Fcrit: 7.71) and PFOS (F: 36.24; p: 0.001; Fcrit: 7.71), in mix mode. Similarly, this behaviour was observed in individual experiments between the two soils for PFHxA (F: 12.94; p: 0.013; Fcrit: 7.71), PFOA (F: 33.74; p: 0.001; Fcrit: 7.71) and PFOS (F: 29.04; p: 0.001; Fcrit: 7.71). The comparison between effectiveness highlights the need for all soils to be assessed for immobilisation on a case by case basis because of soil physicochemical properties holding significant influence on biochar sorption efficiency. PFHxS did not display any significant differences in sorption efficiency between the two soils for either experimental mode.

6.4.3 Desorption Experiments

Desorption was found to be higher in the control sandy clay loam than in loamy sand for all compounds. All desorbed fractions were in excess of 50 %, excepting PFOS in loamy sand. This suggests that the organic matter fraction or divalent metal fraction in loamy sand may be a mechanism driving less reversible sorption (Table 6.7). Comparatively, sorption to sandy clay loam soil was highly reversible. PFOS presented the lowest

desorbed fraction in the control loamy sand, whereas PFHxS presented the lowest desorption in sandy clay loam. The greatest desorption was detected for PFHxA in unamended sandy clay loam and PFOA for unamended loamy sand. In both control soils, sulphonates always had lower desorbed fractions than carboxylic acids. Desorption fraction increased in the order PFOS, PFHxS, PFHxA, PFOA in loamy sand and PFHxS, PFOS, PFOA, PFHxA in sandy clay loam.

Statistical differences ($p < 0.05$) were observed in all compounds, experimental modes and soils between the means of all amended experiments when compared to controls. This suggests that, in all cases, the addition of biochar resulted in reduction of the leachable fraction. In loamy sand, the greatest reduction for P750 amendment was seen in PFOA (41.6 ± 2.4 %) for mix mode experiments and PFHxS (37.6 ± 2.6 %) for individual mode experiments (Table 6.8). The smallest reduction in desorption was seen in PFHxA (19.3 ± 2.7 %) for mixed mode experiments and PFOS (11.1 ± 0.6 %) for individual mode experimental modes. This resulted in, in order of increasing desorbed fraction reduction, $PFHxA < PFOS < PFHxS < PFOA$ for mix mode experiments and $PFOS < PFHxA < PFOA < PFHxS$ for individual mode. Differences were only seen between individual and mix P750 effect. Loamy sand P750 desorption effect values were found to be statistically significant for all tested compounds excepting PFHxA ($F: 1.02$; $p: 0.37$; $F_{crit}: 7.71$) when comparing means between individual and mix mode experiments. This suggests that for Loamy sand experiments, desorbed fraction behaviour was very different for all tested compounds, excepting PFHxA, based on experimental mode, hinting strongly at inter-PFAS interactions. In mix experiments, the desorbed fraction itself, after P750 amendment with P750 followed the order PFHxA, PFHxS, PFOA, PFOS, with respects to decreasing desorption in a mixture. However, the same effect was not seen in individual mode experiments, where leaching was found to be greater in carboxylic acids than in sulphonates similar to the control soil, as opposed to arranged by chain length often encountered in literature (Du et al. 2014).

In sandy clay loam, the greatest reduction by biochar amendment was seen in PFOA (58.8 ± 4.3 %) for mix mode experiments and PFHxS (28.2 ± 3.2 %) for individual mode experiments. Comparatively, the smallest reductions in desorbed fraction were observed in PFHxS (26.8 ± 4.3 %) for mixed mode and PFHxA (16.8 ± 2.0 %) for individual mode experiments. Sorption order, in increasing desorption reduction followed PFHxS, PFOS, PFHxA, PFOA for mix mode experiments and PFHxA, PFOA, PFOS, PFHxA for individual experiments. Similarly, significant differences in means were observed for all PFAS, excepting PFHxS ($F: 0.75$; $p: 0.44$; $F_{crit}: 7.71$), when assessing the effect of experimental mode on P750 effect to desorption in sandy clay loam. Total desorbed unamended fraction appeared similar to loamy sand, when amended with mixed experiments, appearing to be chain length dominated and individual experiments grouped by functional group.

Table 6.7 Percentage Desorption for loamy sand soil, control and amended with P750 Biochar at 5 % w/w. Statistically significant differences in PFAS sorption detected by ANOVA analysis are denoted between soil, mix and individual mode biochar amended soils by capital letters (A, B, C).

	Soil (%)	Mix mode		Individual mode	
		Soil + 5 % Biochar (%)	Biochar Effect (%)	Soil + 5 % Biochar (%)	Biochar Effect (%)
PFHxA	63.0 ± 1.6^A	43.8 ± 1.1^B	19.2 ± 2.7	48.6 ± 1.3^B	14.4 ± 2.9
PFHxS	52.8 ± 1.3^A	24.5 ± 0.5^B	28.3 ± 1.8	15.2 ± 1.3^C	37.6 ± 2.6
PFOA	66.6 ± 0.6^A	25.1 ± 1.8^B	41.6 ± 2.4	42.7 ± 1.0^C	23.9 ± 1.6
PFOS	24.3 ± 0.3^A	4.2 ± 0.3^B	20.1 ± 0.6	13.3 ± 0.3^C	11.0 ± 0.6

Table 6.8 Percentage Desorption for sandy clay loam soil, control and amended with P750 Biochar at 5 % w/w. Statistically significant differences in PFAS desorption detected by ANOVA analysis are denoted between soil, mix and individual mode biochar amended soils by capital letters (A, B, C).

	Mix mode			Individual mode	
	Soil (%)	Soil + 5 % Biochar (%)	Biochar Effect (%)	Soil + 5 % Biochar (%)	Biochar Effect (%)
PFHXA	77.9 ± 1.0 ^A	32.5 ± 1.7 ^B	45.4 ± 2.7	61.1 ± 1.0 ^C	16.8 ± 2.0
PFHXS	54.6 ± 1.7 ^A	27.8 ± 2.6 ^B	26.8 ± 4.3	26.4 ± 1.5 ^B	28.2 ± 3.2
PFOA	72.7 ± 1.1 ^A	13.9 ± 2.1 ^B	58.8 ± 3.2	46.1 ± 1.8 ^C	26.6 ± 2.9
PFOS	56.6 ± 0.3 ^A	13.9 ± 0.4 ^B	42.7 ± 0.7	29.2 ± 0.4 ^C	27.4 ± 0.7

Comparing sandy clay loam to loamy sand experiments, the effect of biochar addition was always greater in sandy clay loam than in loamy sand with respect to reducing PFAS desorption from soil, irrespective of mix or individual experimental modes. The exception to this were PFHxS in mix mode experiments and PFHxA and PFOS in individual mode experiments, where desorption reductions were in fact higher in loamy sand than in sandy clay loam. Comparing P750 effects in sandy clay loam to loamy sand, grouped by individual or mixed mode experiments saw statistically different means of all P750 effects between soil types. The exception to this was PFHxA (F: 0.43; p: 0.54; Fcrit: 7.71) and PFOA (F: 1.24; p: 0.32; Fcrit: 7.71) in individual mode experiments, and PFHxS (F: 0.28; p: 0.62; Fcrit: 7.71) in mix mode experiments.

Desorption in all cases was compound specific; however, it was clear that for each congener, matrix type and experimental mode played a role in determining sorption behaviour. Lower desorption in loamy sand overall suggests that the retention of PFAS is potentially due to higher presence of bridging divalent ions and OM, as well as hydrophobic interaction as explored by Milinovic et al (2015), which also observed PFOS to be the least reversibly sorbed. The likely effect of electrostatic interactions in addition to more commonly explored hydrophobic interactions are mirrored in Oliver et al (2019). Oliver et al (2019) went further to highlight the importance of this electrostatic behaviour as a major contributor to changing PFAS mobility based on soil conditions, in which significant changes to soil chemistry can result in PFAS mobilisation. This needs to be considered when applying sorbents, amongst other characteristics.

Collectively, the data strongly suggest that a single soil parameter cannot be used to explain sorption behaviour across all tested congeners. This is similar to the findings of Li, Oliver & Kookana (2018), wherein sorption was seen to be a factor of PFAS congener specific attributes and soil geochemistry. Biochar has been demonstrated to be more effective for some compounds than others, with variance based on soil matrix. This includes sorption kinetics and magnitude, sorbed fraction and associated reversibility. This suggests that under certain circumstances biochars such as P750 could be effective at reducing PFAS migration from soils, Zhi & Liu (2018) suggest that engineered biochar could be near as effective as activated carbon, but more cost effective. However, soil and sorbent physiochemical compatibilities as well as stability of the environment are important considerations as to prevent changes in chemistry which may remobilise PFAS for a given soil type (Oliver et al. 2019).

6.5 Conclusion

Biochar amendments to two soils (sandy clay loam and loamy sand) resulted in varying effects on equilibrium time, sorption and desorption for the mixture and individual PFAS congeners studied. Behaviour was namely a factor of congener-soil combination and no single soil parameter could be effectively used to predict sorption behaviour of PFAS compounds as extent of sorption was largely a factor of the congener chemical properties. Equilibrium times were largely influenced between interaction of specific congeners with the soil matrix, though experimental mode had little effect on equilibrium time. Sorption to unamended loam soils was far higher for PFAS congeners tested in loamy sand than in sandy clay loam, possibly due to PFAS affinity to higher OM fraction or a greater number of cations present for bridging, in line with higher cation exchange capacity.

Biochar was found to have the highest effect on sorption for the sandy clay loam soil, however the sorption was found to be reversible, whereas desorbed fraction in loamy sand was found to be much smaller. Amendment with biochar reduced the desorbed fraction of all tested PFAS congeners for both soils and experimental modes. Overall, the effect of mixed versus individual experiments was found to be negligible, excepting in desorption studies, where mixed mode experiments desorbed far less than those conducted as individual mode. This study determined that the efficiency of biochar as an amendment is highly related to soil properties, while sorption may be more efficient in clay soils, the high reversibility is suggestive of weak sorption. This suggests the free cations and higher OM in loamy sand soils play an important role in the stronger sorption of PFAS, and that fouling by NOM is less of a barrier to sorption than expected.

Ultimately, biochar has the capacity to immobilise PFAS in soil, however the magnitude of immobilisation is strongly variable based on congener type, sorbent characteristics and soil chemistry. It is essential for adequate immobilisation in the environment that soil geochemistry, sorbent physicochemical qualities and PFAS congener type are considered to ensure PFAS are sorbed at the desired magnitude with limited reversibility, particularly in circumstances with changing environmental conditions. This is exemplified by the biochar P750 a greater effect on sorption for sandy clay loam soil compared to loamy sand, however desorption data demonstrated comparatively greater reversibility of sorbed fraction in loamy sand soil than sandy clay loam soil. This suggests that sorption capacity should be compared with reversibility (desorption) when assessing the efficacy of biochar as a PFAS immobilisation technique in soil matrices.

Chapter 7

Conclusions

The ever-growing body of research highlighting PFAS toxicity, mobility and resistance to degradation, has increasingly culminated in agreement that PFAS contamination poses a threat to human and environmental health globally. This has become a strong driver for further investigation on PFAS management mechanisms. However, the current shortage in accessible and cost-effective technologies to adequately remove or destroy PFAS in environmental matrices is generating great demand for interim solutions. The disruption of source-receptor pathways has been identified as a key PFAS management approach. This has been demonstrated to be achievable through several approaches which incorporate sorbents such as activated carbon, membranes and resins to immobilise PFAS. However, the application of most technologies to PFAS management can quickly become costly and unsustainable due to the breadth of PFAS contamination, which is often at low concentration and spread across large areas or volumes of impacted material.

In consideration of the above, biochar has been considered as a possible sustainable approach to PFAS immobilisation in the environment due to biochar being derived from waste biomass materials. Biochars have been successfully applied as sorbents for a range of organic and inorganic contaminants in the environment. Further investigation revealed that biochars characterised in literature possessed many of the physiochemical characteristics that are potentially involved in the sorption of PFAS. These characteristics include high surface area, a high degree of aromaticity, and the presence of surface functional groups. These characteristics facilitate several hydrophobic and electrostatic interactions between sorbent and PFAS molecules. However, the effect of biochar physiochemical characteristics on sorption is largely unknown and required further investigation.

In support of this, a study was undertaken to determine how biochar characteristics changed with varying pyrolysis temperature and feedstock type. It was found that by varying temperature a wide variety of physiochemical parameters could be manipulated. Increasing pyrolysis temperature resulted in higher surface areas, higher degrees of aromatisation and greater hydrophobicity. Additionally, large differences were observed between the two feedstocks tested at the same pyrolysis temperature. This demonstrated that through the variation of feedstock type, and pyrolysis temperature, biochar could be engineered with a range of physiochemical characteristics.

To better understand the type of physiochemical characteristic that are of greater benefit to PFAS sorption, a kinetic and sorption study was undertaken at environmentally relevant concentrations using a suite of biochars created at various pyrolysis temperatures (350, 500 and 750°C) from 2 different feedstocks (pine and pea straw). A specially developed direct aqueous injection liquid chromatography mass spectrometry, associated sample preparation method, and serial sorption method was developed to address near ubiquitous background PFAS contamination, high number of samples produced by experimental design and the limitations imposed by

detection limits when undertaking sorption experiments at environmentally relevant levels. The developed method was demonstrated to be adequately sensitive, accurate and robust throughout testing.

Through the study of kinetic and sorption behaviour it was found all biochars performed poorly for short chain PFAS, PFBA and PFBS. Further, low temperature biochars (> 350 °C) sorbed <50 % of PFAS from solution. Sorption was found to be fast for most PFAS, with the bulk of sorption occurring over the first hour of experiments, with all PFAS reaching equilibrium by 96 hours. Film diffusion was exhibited as the rate determining mechanism, however in the case pine biochars, a longer intraparticle diffusion step was exhibited, likely related to diffusion into pores. High temperature pine biochar was demonstrated to be the most effective sorbent for PFHxA, PFHxS, PFOA and PFOS. In turn, suggesting that high surface area, high aromaticity and hydrophobicity are important parameters to consider when aiming to increase sorption capacity for longer chain PFAS compounds. Interpretation of isotherms demonstrated complex sorption behaviour consistent with the formation of monolayers and micelles for some PFAS compounds. PFAS sorption behaviour was found to be highly influenced by PFAS molecular structure, namely functional group type, and chain length, with the former being more influential on sorption behaviour for some biochars.

Desorption was less reversible for higher temperature biochars, with all PFAS desorbing less than 20% of sorbed fraction. PFOS was the least reversible PFAS congener, with PFOS desorption being lower than detectable limits in individual mode studies. This was not the case in mixed mode experiments, where PFOS was found to be leachable. This suggests that sorption behaviour was demonstrated to be impacted by intra- PFAS congener interaction, with either positive or negative impacts on sorption and desorption dependant on the specific biochar – PFAS congener combination. As such, it was clear that PFAS sorption to any biochar needs to be considered on a case by case basis specific to solution concentration, PFAS congeners present, and the physiochemical properties of the biochar.

Further investigation was undertaken to explore the efficacy of PFAS as a sorbent in soils, as a factor of the soil environment. Pine biochar produced at 750°C was selected for this trial as it had performed well as a PFAS sorbent in the previously described studies. Soils used in experiments were characterised by their contrasting levels of organic matter and clay. It was found that soil type did have a significant impact on biochar sorption efficiency, with biochar being more efficient as a sorbent in soils characterised by higher clay than organic matter. However, desorption was found to be more reversible in the soil with finer texture than in that with higher OM. Individual versus mixed mode experiments in both soil types demonstrated that a mixture of PFAS resulted in far less desorption, suggesting intra-PFAS behaviour being reinforcing of irreversible sorption. The study demonstrated that matrix had a large effect on PFAS sorption behaviour to biochar and that the amendment of soils with biochar needs to be considered on a case by case basis to ensure adequate efficacy.

The studies undertaken in this work strongly suggest that biochar can potentially be used as a suitable and sustainable sorbent for PFAS in water and soil. Further investigation into the reverse engineering of biochar over a greater range of temperatures, residence times and feedstock varieties are required to develop biochars optimal for PFAS sorption. However, it is key that biochar application to environmental matrices need to be tailored for the matrix type, sorption environment type and PFAS congener being targeted. Inadequate consideration of these factors may result in poor sorption efficiencies, or high reversibility of sorbed PFAS fraction, each potentially posing further risk to human and environmental health.

References

- 3M 2001, 3M Environmental Laboratory: Water, Sludge, Sediment, POTW Effluent and Landfill Leachate Samples, 3M.
- Abdel-Fattah, TM, Mahmoud, ME, Ahmed, SB, Huff, MD, Lee, JW & Kumar, S 2015, 'Biochar from woody biomass for removing metal contaminants and carbon sequestration', *Journal of Industrial and Engineering Chemistry*, vol. 22, pp. 103-109.
- Ahrens, L & Bundschuh, M 2014, 'Fate and effects of poly- and perfluoroalkyl substances in the aquatic environment: A review', *Environmental Toxicology and Chemistry*, vol. 33, no. 9, pp. 1921-1929.
- Al-Wabel, MI, Al-Omran, A, El-Naggar, AH, Nadeem, M & Usman, ARA 2013, 'Pyrolysis temperature induced changes in characteristics and chemical composition of biochar produced from conocarpus wastes', *Bioresource Technology*, vol. 131, pp. 374-379.
- Alburquerque, JA, Sánchez, ME, Mora, M & Barrón, V 2013, 'Slow pyrolysis of relevant biomasses in the Mediterranean basin. Part 2. Char characterisation for carbon sequestration and agricultural uses', *Journal of Cleaner Production*, vol.120, pp. 191-197.
- Alburquerque, JA, Calero, JM, Barrón, V, Torrent, J, del Campillo, MC, Gallardo A, Villar, R 2014, 'Effects of biochars produced from different feedstocks on soil properties and sunflower growth', *Journal of Plant Nutrition and Soil Science*, vol. 177, pp. 16-25.
- Appleman, TD, Higgins, CP, Quiñones, O, Vanderford, BJ, Kolstad, C, Zeigler-Holady, JC & Dickenson, ERV 2014, 'Treatment of poly- and perfluoroalkyl substances in U.S. full-scale water treatment systems', *Water Research*, vol. 51, pp. 246-255.
- Askeland, M, Clarke, B & Paz-Ferreiro, J 2019, 'Comparative characterization of biochars produced at three selected pyrolysis temperatures from common woody and herbaceous waste streams', *PeerJ*, vol. 7, p. e6784.
- ASTDR, 2019, Toxicological Profile for Perfluoroalkyls, Agency for Toxic Substances and Disease Registry, Atlanta.
- ASTM International, 2013 Standard Test Method for Chemical Analysis of Wood Charcoal. 1762-84:2013, Pennsylvania, USA.
- Ateia, M, Maroli, A, Tharayil, N & Karanfil, T 2019, 'The overlooked short- and ultrashort-chain poly- and perfluorinated substances: A review', *Chemosphere*, vol. 220, pp. 866-882.

- Azargohar, R, Jacobson, KL, Powell, EE & Dalai, AK 2013, 'Evaluation of properties of fast pyrolysis products obtained, from Canadian waste biomass', *Journal of Analytical and Applied Pyrolysis*, vol. 104, pp. 330-340.
- Becker, AM, Gerstmann, S & Frank, H 2008, 'Perfluorooctane surfactants in waste waters, the major source of river pollution', *Chemosphere*, vol. 72, no. 1, pp. 115-121.
- Beesley, L, Moreno-Jiménez, E & Gomez-Eyles, JL 2010, 'Effects of biochar and greenwaste compost amendments on mobility, bioavailability and toxicity of inorganic and organic contaminants in a multi-element polluted soil', *Environmental Pollution*, vol. 158, no. 6, pp. 2282-2287.
- Benavente, I, Gascó, G, Plaza, C, Paz-Ferreiro, J, Méndez A, 2018, 'Choice of pyrolysis parameters for urban wastes affects soil enzymes and plant germination in a Mediterranean soil', *Science of the Total Environment*, vol. 634, pp.1308-1314.
- Bengtson Nash, S, Rintoul, SR, Kawaguchi, S, Staniland, I, Hoff, Jvd, Tierney, M & Bossi, R 2010, 'Perfluorinated compounds in the Antarctic region: Ocean circulation provides prolonged protection from distant sources', *Environmental Pollution*, vol. 158, no. 9, pp. 2985-2991.
- Berg, J, Tymoczko, J & Stryer, L 2002, *Biochemistry, Fifth Edition: International Version (hardcover)*, W. H. Freeman, <http://www.amazon.ca/exec/obidos/redirect?tag=citeulike09-20&path=ASIN/0716746840>, accessed 11/07/2018.
- Borg, D, Lund, B-O, Lindquist, N-G & Håkansson, H 2013, 'Cumulative health risk assessment of 17 perfluoroalkylated and polyfluoroalkylated substances (PFASs) in the Swedish population', *Environment international*, vol. 59, pp. 112-123.
- Borg, D, Lund, BO, Lindquist, NG & Hakansson, H 2013, 'Cumulative health risk assessment of 17 perfluoroalkylated and polyfluoroalkylated substances (PFASs) in the Swedish population', *Environ Int*, vol. 59, pp. 112-123.
- Bossi, R, Strand, J, Sortkjaer, O & Larsen, MM 2008, 'Perfluoroalkyl compounds in Danish wastewater treatment plants and aquatic environments', *Environ Int*, vol. 34, no. 4, pp. 443-450.
- Bräunig, J, Baduel, C, Barnes, CM & Mueller, JF 2019, 'Leaching and bioavailability of selected perfluoroalkyl acids (PFAAs) from soil contaminated by firefighting activities', *Science of The Total Environment*, vol. 646, pp. 471-479.
- Brennan, A, Moreno-Jiménez, E, Albuquerque, JA, Knapp, CW, Switzer, C 2014, 'Effects of biochar and activated carbon amendment on maize growth and the uptake and measured availability of polycyclic aromatic hydrocarbons (PAHs) and potentially toxic elements (PTEs)', *Environmental Pollution*, vol. 193, pp.79-87.

- Bridgwater, AV 2003, 'Renewable fuels and chemicals by thermal processing of biomass', *Chemical Engineering Journal*, vol. 91, no. 2, pp. 87-102.
- Brooke, D, Footitt, A & Nwaogu, TA 2004, Environmental Risk Evaluation Report: Perfluorooctanesulphonate (PFOS), SCHO1009BRBL-E-P, U.K Environmental Agency
https://assets.publishing.service.gov.uk/government/uploads/system/uploads/attachment_data/file/290857/scho1009brbl-e-e.pdf, accessed 18/08/2019.
- Brusseau, ML 2018, 'Assessing the potential contributions of additional retention processes to PFAS retardation in the subsurface', *Science of The Total Environment*, vol. 613-614, pp. 176-185.
- Buss, W, Mašek, O, Graham, M & Wüst, D 2015, 'Inherent organic compounds in biochar—Their content, composition and potential toxic effects', *Journal of Environmental Management*, vol. 156, pp. 150-157.
- Butnan, S, Deenik, JL, Toomsan, B, Antal, MJ & Vityakon, P 2015, 'Biochar characteristics and application rates affecting corn growth and properties of soils contrasting in texture and mineralogy', *Geoderma*, vol. 237–238, pp. 105-116.
- Cabrera, A, Cox, L, Spokas, K, Hermosín, MC, Cornejo, J & Koskinen, WC 2014, 'Influence of biochar amendments on the sorption–desorption of aminocyclopyrachlor, bentazone and pyraclostrobin pesticides to an agricultural soil', *Science of The Total Environment*, vol. 470–471, pp. 438-443.
- Cai, Y, Chen, H, Yuan, R, Wang, F, Chen, Z & Zhou, B 2019, 'Toxicity of perfluorinated compounds to soil microbial activity: Effect of carbon chain length, functional group and soil properties', *Science of The Total Environment*, vol. 690, pp. 1162 – 1169.
- Campos Pereira, H, Ullberg, M, Kleja, DB, Gustafsson, JP & Ahrens, L 2018, 'Sorption of perfluoroalkyl substances (PFASs) to an organic soil horizon – Effect of cation composition and pH', *Chemosphere*, vol. 207, pp. 183-191.
- Cao, X, Wang, C, Lu, Y, Zhang, M, Khan, K, Song, S, Wang, P & Wang, C 2019, 'Occurrence, sources and health risk of polyfluoroalkyl substances (PFASs) in soil, water and sediment from a drinking water source area', *Ecotoxicology and Environmental Safety*, vol. 174, pp. 208-217.
- Cardno-LanePiper 2014, Human Health Risk Assessment - Fiskville Community.
- Carter, KE & Farrell, J 2010, 'Removal of Perfluorooctane and Perfluorobutane Sulfonate from Water via Carbon Adsorption and Ion Exchange', *Separation Science and Technology*, vol. 45, no. 6, pp. 762-767.
- Cely, P, Gascó, G, Paz-Ferreiro, J, Méndez A 2015, 'Agronomic properties of biochars from different manure wastes', *Journal of Analytical and Applied Pyrolysis*, vol. 111, pp.173-182.

- Chandler, D 2005, 'Interfaces and the driving force of hydrophobic assembly', *Nature*, vol. 437, no. 7059, pp. 640-647.
- Chen, B & Yuan, M 2011, 'Enhanced sorption of polycyclic aromatic hydrocarbons by soil amended with biochar', *Journal of Soils and Sediments*, vol. 11, no. 1, pp. 62-71.
- Chen, H, Zhang, C, Yu, Y & Han, J 2012, 'Sorption of perfluorooctane sulfonate (PFOS) on marine sediments', *Marine Pollution Bulletin*, vol. 64, no. 5, pp. 902-906.
- Chen, T, Zhang, Y, Wang, H, Lu, W, Zhou, Z, Zhang, Y & Ren, L 2014, 'Influence of pyrolysis temperature on characteristics and heavy metal adsorptive performance of biochar derived from municipal sewage sludge', *Bioresource Technology*, vol. 164, pp. 47-54.
- Chen, X, Xia, X, Wang, X, Qiao, J & Chen, H 2011, 'A comparative study on sorption of perfluorooctane sulfonate (PFOS) by chars, ash and carbon nanotubes', *Chemosphere*, vol. 83, no. 10, pp. 1313-1319.
- Chularueangaksorn, P, Tanaka, S, Fujii, S & Kunacheva, C 2014, 'Batch and column adsorption of perfluorooctane sulfonate on anion exchange resins and granular activated carbon', *Journal of Applied Polymer Science*, vol. 131, no. 3.
- Clarke, BO & Smith, SR 2011, 'Review of 'emerging' organic contaminants in biosolids and assessment of international research priorities for the agricultural use of biosolids', *Environment International*, vol. 37, no. 1, pp. 226-247.
- Concawe 2016, Environmental fate and effects of poly and perfluoroalkyl substances (PFAS). vol. Report # 8/16., prepared by ARCADIS: T. Pancras, G. Schrauwen, T. Held, K. Baker, I. Ross, H. Slenders, Brussels, Belgium.
- Corsini, E, Avogadro, A, Galbiati, V, Dell'Agli, M, Marinovich, M, Galli, CL & Germolec, DR 2011, 'In vitro evaluation of the immunotoxic potential of perfluorinated compounds (PFCs)', *Toxicology and applied pharmacology*, vol. 250, no. 2, pp. 108-116.
- D'eon, JC & Mabury, SA 2010, 'Uptake and elimination of perfluorinated phosphonic acids in the rat', *Environmental Toxicology and Chemistry*, vol. 29, no. 6, pp. 1319-1329.
- D'eon, JC, Crozier, PW, Furdui, VI, Reiner, EJ, Libelo, EL & Mabury, SA 2009, 'Observation of a Commercial Fluorinated Material, the Polyfluoroalkyl Phosphoric Acid Diesters, in Human Sera, Wastewater Treatment Plant Sludge, and Paper Fibers', *Environmental Science & Technology*, vol. 43, no. 12, pp. 4589-4594.
- Dalahmeh, SS, Alziq, N & Ahrens, L 2019, 'Potential of biochar filters for onsite wastewater treatment: Effects of active and inactive biofilms on adsorption of per- and polyfluoroalkyl substances in laboratory column experiments', *Environmental Pollution*, vol. 247, pp. 155-164.

- Das, O & Sarmah, AK 2015, 'The love–hate relationship of pyrolysis biochar and water: A perspective', *Science of The Total Environment*, vol. 512–513, pp. 682-685.
- Das, O, Sarmah, AK, Bhattacharyya, D 2016, 'Biocomposites from waste derived biochars: Mechanical, thermal, chemical, and morphological properties', *Waste Management*, vol. 49, pp. 560-570.
- Dauchy, X, Boiteux, V, Bach, C, Colin, A, Hemard, J, Rosin, C & Munoz, J-F 2017, 'Mass flows and fate of per- and polyfluoroalkyl substances (PFASs) in the wastewater treatment plant of a fluorochemical manufacturing facility', *Science of The Total Environment*, vol. 576, pp. 549-558.
- Dauchy, X, Boiteux, V, Colin, A, Hémar, J, Bach, C, Rosin, C & Munoz, J-F 2019, 'Deep seepage of per- and polyfluoroalkyl substances through the soil of a firefighter training site and subsequent groundwater contamination', *Chemosphere*, vol. 214, pp. 729-737.
- Dechene, A, Rosendahl, I, Laabs, V & Amelung, W 2014, 'Sorption of polar herbicides and herbicide metabolites by biochar-amended soil', *Chemosphere*, vol. 109, no. 0, pp. 180-186.
- Delwiche, KB, Lehmann, J & Walter, MT 2014, 'Atrazine leaching from biochar-amended soils', *Chemosphere*, vol. 95, pp. 346-352.
- Deng, S, Nie, Y, Du, Z, Huang, Q, Meng, P, Wang, B, Huang, J & Yu, G 2015, 'Enhanced adsorption of perfluorooctane sulfonate and perfluorooctanoate by bamboo-derived granular activated carbon', *Journal of Hazardous Materials*, vol. 282, pp. 150-157.
- Denyes, Rutter, A & Zeeb, BA 2013, 'In situ application of activated carbon and biochar to PCB-contaminated soil and the effects of mixing regime', *Environmental Pollution*, vol. 182, pp. 201-208.
- Denyes, MJ, Langlois, VS, Rutter, A & Zeeb, BA 2012, 'The use of biochar to reduce soil PCB bioavailability to *Cucurbita pepo* and *Eisenia fetida*', *Science of The Total Environment*, vol. 437, pp. 76-82.
- Dixon, D, Moore, AB, E.Wallace, Hines, EP, Gibbs-Flournoy, EA, Stanko, J, Newbold, R, Jefferson, W & Fenton, SE 2012, 'P14—Histopathologic changes in the uterus, cervix and vagina of immature CD-1 mice exposed to low doses of perfluorooctanoic acid (PFOA) in the uterotrophic assay', *Reproductive Toxicology*, vol. 33, no. 4, pp. 603-604.
- DME 2013, Survey of PFOS, PFOA and other perfluoroalkyl and polyfluoroalkyl substances, The Danish Environmental Protection Agency, Denmark.
- DoHA 2008, Department of Health and Ageing: Perfluorooctane Sulfonate (PFOS) and Perfluoroalkyl Sulfonate (PFAS), National Industrial Chemicals Notification and Assessment Scheme NSW.

- Dombrowski, PM, Kakarla, P, Caldicott, W, Chin, Y, Sadeghi, V, Bogdan, D, Barajas-Rodriguez, F & Chiang, S-Y 2018, 'Technology review and evaluation of different chemical oxidation conditions on treatability of PFAS', *Remediation Journal*, vol. 28, no. 2, pp. 135-150.
- Domene, X, Enders, A, Hanley, K & Lehmann, J 2015, 'Ecotoxicological characterization of biochars: Role of feedstock and pyrolysis temperature', *Science of The Total Environment*, vol. 512–513, pp. 552-561.
- Domene, X, Hanley, K, Enders, A & Lehmann, J 2015, 'Short-term mesofauna responses to soil additions of corn stover biochar and the role of microbial biomass', *Applied Soil Ecology*, vol. 89, pp. 10-17.
- Du, Z, Deng, S, Bei, Y, Huang, Q, Wang, B, Huang, J & Yu, G 2014, 'Adsorption behavior and mechanism of perfluorinated compounds on various adsorbents—A review', *Journal of Hazardous Materials*, vol. 274, pp. 443-454.
- DuPont 2003, *Epidemiology surveillance report: Cancer incidence for Washington works site 1959-2001*, U.S. EPA AR226-1307.
- EBC 2012, *European Biochar Certificate - Guidelines for a Sustainable Production of Biochar*, European Biochar Foundation (EBC), Arbaz, Switzerland.
- EFSA 2008, 'European Food Safety Authority: Perfluorooctane sulfonate (PFOS), perfluorooctanoic acid (PFOA) and their salts', *The EFSA Journal*, vol. 653, pp. 1-131.
- EGLE 2019, *Michigan moves forward on PFAS in drinking water rules*, Michigan Department of Environment, Great Lakes and Energy, <https://www.michigan.gov/egle/0,9429,7-135-3308_3323-500772--,00.html>.
- Enders, A, Lehmann, J 2012, 'Comparison of wet-digestion and dry-ashing methods for total elemental analysis of biochar', *Communications in Soil Science and Plant Analysis*, vol. 43, pp. 1042-1052.
- Endirlik, BÜ, Bakır, E, Boşgelmez, İİ, Eken, A, Narin, İ & Gürbay, A 2019, 'Assessment of perfluoroalkyl substances levels in tap and bottled water samples from Turkey', *Chemosphere*, vol. 235, pp. 1162 – 1171.
- enHealth 2019, *enHealth Guidance Statements on per- and poly-fluoroalkyl substances*, PFAS Expert Health Panel, Australia.
- EPA-Victoria 2004, *Biosolids Land Application*, vol. 943, EPA Victoria, EPA Victoria.
- EPA-Victoria 2018a, *Industrial Fire West Footscray Community information Fact sheet – 31 August 2018*.

- EPA-Victoria 2018b, Interim position statement on PFAS, Publication 1669.2, EPA Victoria, Melbourne.
- EPA-NSW 2017, Williamstown PFAS investigations: air monitoring - Information for local residents, NSW Environment Protection Authority, NSW.
- Ericson, I, Gómez, M, Nadal, M, van Bavel, B, Lindström, G & Domingo, JL 2007, 'Perfluorinated chemicals in blood of residents in Catalonia (Spain) in relation to age and gender: a pilot study', *Environment international*, vol. 33, no. 5, pp. 616-623.
- Eriksson, U, Haglund, P & Kärrman, A 2017, 'Contribution of precursor compounds to the release of per- and polyfluoroalkyl substances (PFASs) from waste water treatment plants (WWTPs)', *Journal of Environmental Sciences*, vol. 61, pp. 80-90.
- Fabbri, D, Rombolà, AG, Torri, C & Spokas, KA 2013, 'Determination of polycyclic aromatic hydrocarbons in biochar and biochar amended soil', *Journal of Analytical and Applied Pyrolysis*, vol. 103, pp. 60-67.
- Farrell, M, Rangott, G, Krull, E 2013, 'Difficulties in using soil-based methods to assess plant availability of potentially toxic elements in biochars and their feedstocks', *Journal of Hazardous Materials*, vol. 250-251, pp.29-36.
- FDA 2019a, Analytical Results for PFAS in 2018-2019 Dairy Sampling (Parts Per Billion), <https://www.fda.gov/media/127849/download>, accessed 18/08/2019.
- FDA 2019b, Analytical Results for PFAS in 2019 Total Diet Study Sampling (Parts Per Billion), <https://www.fda.gov/media/127851/download> accessed 18/08/2019.
- Foo, KY & Hameed, BH 2010, 'Insights into the modeling of adsorption isotherm systems', *Chemical Engineering Journal*, vol. 156, no. 1, pp. 2-10.
- Freddo, A, Cai, C & Reid, BJ 2012, 'Environmental contextualisation of potential toxic elements and polycyclic aromatic hydrocarbons in biochar', *Environmental Pollution*, vol. 171, pp. 18-24.
- Gannon, SA, Johnson, T, Nabb, DL, Serex, TL, Buck, RC & Loveless, SE 2011, 'Absorption, distribution, metabolism, and excretion of [1-14 C]-perfluorohexanoate ([14 C]-PFHx) in rats and mice', *Toxicology*, vol. 283, no. 1, pp. 55-62.
- Gascó, G, Paz-Ferreiro, J, Álvarez, ML, Saa, A, Méndez, A 2018, 'Biochars and hydrochars prepared by pyrolysis and hydrothermal carbonisation of pig manure', *Waste Management*, vol. 79, pp.395-403.
- Gellrich, V, Stahl, T & Knepper, TP 2012, 'Behavior of perfluorinated compounds in soils during leaching experiments', *Chemosphere*, vol. 87, no. 9, pp. 1052-1056.

- Gewurtz, SB, Bradley, LE, Backus, S, Dove, A, McGoldrick, D, Hung, H & Dryfhout-Clark, H 2019, 'Perfluoroalkyl Acids in Great Lakes Precipitation and Surface Water (2006–2018) Indicate Response to Phase-outs, Regulatory Action, and Variability in Fate and Transport Processes', *Environmental Science & Technology*, vol. 53, pp. 8543 – 8552.
- Ghisi, R, Vamerli, T & Manzetti, S 2019, 'Accumulation of perfluorinated alkyl substances (PFAS) in agricultural plants: A review', *Environmental Research*, vol. 169, pp. 326-341.
- Giesy, JP & Kannan, K 2001, 'Global Distribution of Perfluorooctane Sulfonate in Wildlife', *Environmental Science & Technology*, vol. 35, no. 7, pp. 1339-1342.
- Glaser, B, Balashov, E, Haumaier, L, Guggenberger, G & Zech, W 2000, 'Black carbon in density fractions of anthropogenic soils of the Brazilian Amazon region', *Organic Geochemistry*, vol. 31, no. 7, pp. 669-678.
- Glaser, B, Haumaier, L, Guggenberger, G & Zech, W 2001, 'The Terra Preta phenomenon: a model for sustainable agriculture in the humid tropics', *Naturwissenschaften*, vol. 88, no. 1, pp. 37-41.
- Glover, CM, Quiñones, O & Dickenson, ERV 2018, 'Removal of perfluoroalkyl and polyfluoroalkyl substances in potable reuse systems', *Water Research*, vol. 144, pp. 454-461.
- Gomez-Eyles, JL, Sizmur, T, Collins, CD & Hodson, ME 2011, 'Effects of biochar and the earthworm *Eisenia fetida* on the bioavailability of polycyclic aromatic hydrocarbons and potentially toxic elements', *Environmental Pollution*, vol. 159, no. 2, pp. 616-622.
- Hale, SE, Arp, HPH, Slinde, GA, Wade, EJ, Bjørseth, K, Breedveld, GD, Straith, BF, Moe, KG, Jartun, M & Hoisaeter, A 2017, 'Sorbent amendment as a remediation strategy to reduce PFAS mobility and leaching in a contaminated sandy soil from a Norwegian firefighting training facility', *Chemosphere*, vol. 171, pp. 9-18.
- Hale, SE, Arp, HPH, Slinde, GA, Wade, EJ, Bjørseth, K, Breedveld, GD, Straith, BF, Moe, KG, Jartun, M & Høisaeter, Å 2017, 'Sorbent amendment as a remediation strategy to reduce PFAS mobility and leaching in a contaminated sandy soil from a Norwegian firefighting training facility', *Chemosphere*, vol. 171, pp. 9-18.
- Hansen, MC, Børresen, MH, Schlabach, M & Cornelissen, G 2010, 'Sorption of perfluorinated compounds from contaminated water to activated carbon', *Journal of Soils and Sediments*, vol. 10, no. 2, pp. 179-185.
- Haug, LS, Huber, S, Becher, G & Thomsen, C 2011, 'Characterisation of human exposure pathways to perfluorinated compounds--comparing exposure estimates with biomarkers of exposure', *Environ Int*, vol. 37, no. 4, pp. 687-693.

- Haug, LS, Huber, S, Becher, G & Thomsen, C 2011, 'Characterisation of human exposure pathways to perfluorinated compounds—comparing exposure estimates with biomarkers of exposure', *Environment International*, vol. 37, no. 4, pp. 687-693.
- Haug, LS, Thomsen, C, Brantsæter, AL, Kvaalem, HE, Haugen, M, Becher, G, Alexander, J, Meltzer, HM & Knutsen, HK 2010, 'Diet and particularly seafood are major sources of perfluorinated compounds in humans', *Environment international*, vol. 36, no. 7, pp. 772-778.
- Heitkötter, J & Marschner, B 2015, 'Interactive effects of biochar ageing in soils related to feedstock, pyrolysis temperature, and historic charcoal production', *Geoderma*, vol. 245–246, pp. 56-64.
- Helsen, L, van den Bulck, E 2000, 'Metal behavior during the low-temperature pyrolysis of chromated copper arsenate-treated wood waste', *Environmental Science and Technology*, vol. 34, pp. 2931-2938.
- HEPA 2018, PFAS National Environmental Management Plan, Heads of EPAs Australia and New Zealand, Canberra, Australia.
- Hepburn, E, Madden, C, Szabo, D, Coggan, TL, Clarke, B & Currell, M 2019, 'Contamination of groundwater with per- and polyfluoroalkyl substances (PFAS) from legacy landfills in an urban re-development precinct', *Environmental Pollution*, vol. 248, pp. 101-113.
- Higgins, CP, Field, JA, Criddle, CS & Luthy, RG 2005, 'Quantitative determination of perfluorochemicals in sediments and domestic sludge', *Environmental Science & Technology*, vol. 39, no. 11, pp. 3946-3956.
- Higgins, CP & Luthy, RG 2006, 'Sorption of perfluorinated surfactants on sediments', *Environmental Science & Technology*, vol. 40, no. 23, pp. 7251-7256.
- Hmid, A, Mondelli, D, Fiore, S, Fanizzi, FP, Al Chami, Z & Dumontet, S 2014, 'Production and characterization of biochar from three-phase olive mill waste through slow pyrolysis', *Biomass and Bioenergy*, vol. 71, pp. 330-339.
- Høisæter, Å, Pfaff, A & Breedveld, GD 2019, 'Leaching and transport of PFAS from aqueous film-forming foam (AFFF) in the unsaturated soil at a firefighting training facility under cold climatic conditions', *Journal of Contaminant Hydrology*, vol. 222, pp. 112-122.
- Holmström, KE, Järnberg, U & Bignert, A 2005, 'Temporal trends of PFOS and PFOA in guillemot eggs from the Baltic Sea, 1968-2003', *Environmental Science & Technology*, vol. 39, no. 1, pp. 80-84.
- Horst, J, McDonough, J, Ross, I, Dickson, M, Miles, J, Hurst, J & Storch, P 2018, 'Water Treatment Technologies for PFAS: The Next Generation', *Groundwater Monitoring & Remediation*, vol. 38, no. 2, pp. 13-23.

- Houde, M, Martin, JW, Letcher, RJ, Solomon, KR & Muir, DC 2006, 'Biological monitoring of polyfluoroalkyl substances: a review', *Environmental Science & Technology*, vol. 40, no. 11, pp. 3463-3473.
- Hradkova, P, Poustka, J, Hlouskova, V, Pulkrabova, J, Tomaniova, M & Hajslova, J 2010, 'Perfluorinated compounds: occurrence of emerging food contaminants in canned fish and seafood products', *Czech J Food Sci*, vol. 28, no. 4, pp. 333-342.
- Huset, CA, Barlaz, MA, Barofsky, DF & Field, JA 2011, 'Quantitative determination of fluorochemicals in municipal landfill leachates', *Chemosphere*, vol. 82, no. 10, pp. 1380-1386.
- Huset, CA & Barry, K 2018, 'Quantitative determination of perfluoroalkyl substances (PFAS) in soil, water, and home garden produce', *MethodsX*, vol. 5, pp. 697-704.
- International Biochar Initiative 2013, 'Standardized Product Definition and Product Testing Guidelines for Biochar That Is Used in Soil; IBI biochar standards', International Biochar Initiative: Victor, NY, USA.
- International Organization for Standardization 2006, 'Solid mineral fuels - Determination of sulfur by IR spectrometry – 19579', International Organization for Standardization, Geneva.
- International Organization for Standardization 2010, 'Solid mineral fuels - Determination of total carbon, hydrogen and nitrogen content - Instrumental method 29541:2010', International Organization for Standardization, Geneva.
- Jeffery, S, Meinders, MBJ, Stoof, CR, Bezemer, TM, van de Voorde, TFJ, Mommer, L & van Groenigen, JW 2015, 'Biochar application does not improve the soil hydrological function of a sandy soil', *Geoderma*, vol. 251–252, pp. 47-54.
- Jiang, Q, Lust, RM, Strynar, MJ, Dagnino, S & DeWitt, JC 2012, 'Perfluorooctanoic acid induces developmental cardiotoxicity in chicken embryos and hatchlings', *Toxicology*, vol. 293, no. 1, pp. 97-106.
- Jones, DL, Quilliam, RS 2014, 'Metal contaminated biochar and wood ash negatively affect plant growth and soil quality after land application', *Journal of Hazardous Materials*, vol. 276, pp.362-370.
- Jouiad, M, Al-Nofeli, N, Khalifa, N, Benyettou, F & Yousef, LF 2015, 'Characteristics of slow pyrolysis biochars produced from rhodes grass and fronds of edible date palm', *Journal of Analytical and Applied Pyrolysis*, vol. 111, pp. 183-190.
- Kalbe, U, Bandow, N, Bredow, A, Mathies, H & Piechotta, C 2014, 'Column leaching tests on soils containing less investigated organic pollutants', *Journal of Geochemical Exploration*, vol. 147, Part B, pp. 291-297.

- Kambo, HS & Dutta, A 2015, 'A comparative review of biochar and hydrochar in terms of production, physico-chemical properties and applications', *Renewable and Sustainable Energy Reviews*, vol. 45, pp. 359-378.
- Kannan, K, Corsolini, S, Falandysz, J, Oehme, G, Focardi, S & Giesy, JP 2002, 'Perfluorooctanesulfonate and related fluorinated hydrocarbons in marine mammals, fishes, and birds from coasts of the Baltic and the Mediterranean Seas', *Environmental Science & Technology*, vol. 36, no. 15, pp. 3210-3216.
- Kannan, K, Newsted, J, Halbrook, RS & Giesy, JP 2002, 'Perfluorooctanesulfonate and related fluorinated hydrocarbons in mink and river otters from the United States', *Environmental Science & Technology*, vol. 36, no. 12, pp. 2566-2571.
- Kim, M, Son, J, Park, MS, Ji, Y, Chae, S, Jun, C, Bae, J-S, Kwon, TK, Choo, Y-S & Yoon, H 2013, 'In vivo evaluation and comparison of developmental toxicity and teratogenicity of perfluoroalkyl compounds using *Xenopus* embryos', *Chemosphere*, vol. 93, no. 6, pp. 1153-1160.
- Klaunig, JE, Hocevar, BA & Kamendulis, LM 2012, 'Mode of action analysis of perfluorooctanoic acid (PFOA) tumorigenicity and human relevance', *Reproductive Toxicology*, vol. 33, no. 4, pp. 410-418.
- Kleszczyński, K & Składanowski, AC 2011, 'Mechanism of cytotoxic action of perfluorinated acids. III. Disturbance in Ca²⁺ homeostasis', *Toxicology and applied pharmacology*, vol. 251, no. 2, pp. 163-168.
- Knight, ER, Janik, LJ, Navarro, DA, Kookana, RS & McLaughlin, MJ 2019, 'Predicting partitioning of radiolabelled ¹⁴C-PFOA in a range of soils using diffuse reflectance infrared spectroscopy', *Science of The Total Environment*, vol. 686, pp. 505-513.
- Knowles, OA, Robinson, BH, Contangelo, A & Clucas, L 2011, 'Biochar for the mitigation of nitrate leaching from soil amended with biosolids', *Science of The Total Environment*, vol. 409, no. 17, pp. 3206-3210.
- Kucharzyk, KH, Darlington, R, Benotti, M, Deeb, R & Hawley, E 2017, 'Novel treatment technologies for PFAS compounds: A critical review', *Journal of Environmental Management*, vol. 204, pp. 757-764.
- Kucharzyk, KH, Darlington, R, Benotti, M, Deeb, R & Hawley, E 2017, 'Novel treatment technologies for PFAS compounds: A critical review', *J Environ Manage*, vol. 204, no. Pt 2, pp. 757-764.
- Kupryianchyk, D, Hale, SE, Breedveld, GD & Cornelissen, G 2016, 'Treatment of sites contaminated with perfluorinated compounds using biochar amendment', *Chemosphere*, vol. 142, pp. 35-40.
- Kuzyakov, Y, Bogomolova, I & Glaser, B 2014, 'Biochar stability in soil: Decomposition during eight years and transformation as assessed by compound-specific ¹⁴C analysis', *Soil Biology and Biochemistry*, vol. 70, pp. 229-236.

- Labadie, P & Chevreuil, M 2011, 'Partitioning behaviour of perfluorinated alkyl contaminants between water, sediment and fish in the Orge River (nearby Paris, France)', *Environmental Pollution*, vol. 159, no. 2, pp. 391-397.
- Lau, C, Butenhoff, JL & Rogers, JM 2004, 'The developmental toxicity of perfluoroalkyl acids and their derivatives', *Toxicology and applied pharmacology*, vol. 198, no. 2, pp. 231-241.
- Lechner, M & Knapp, H 2011, 'Carryover of perfluorooctanoic acid (PFOA) and perfluorooctane sulfonate (PFOS) from soil to plant and distribution to the different plant compartments studied in cultures of carrots (*Daucus carota* ssp. *Sativus*), potatoes (*Solanum tuberosum*), and cucumbers (*Cucumis Sativus*)', *Journal of agricultural and food chemistry*, vol. 59, no. 20, pp. 11011-11018.
- Lehmann, J 2007, 'A Handful of Carbon', *Nature*, vol. 447, pp. 143-144.
- Leng, L, Yuan, X, Zeng, G, Shao, J, Chen, X, Wu, Z, Wang, H & Peng, X 2015, 'Surface characterization of rice husk bio-char produced by liquefaction and application for cationic dye (Malachite green) adsorption', *Fuel*, vol. 155, pp. 77-85.
- Li, F, Fang, X, Zhou, Z, Liao, X, Zou, J, Yuan, B & Sun, W 2019, 'Adsorption of perfluorinated acids onto soils: Kinetics, isotherms, and influences of soil properties', *Science of The Total Environment*, vol. 649, pp. 504-514.
- Li, M, Sun, F, Shang, W, Zhang, X, Dong, W, Liu, T & Pang, W 2019, 'Theoretical studies of perfluorochemicals (PFCs) adsorption mechanism on the carbonaceous surface', *Chemosphere*, vol. 235, pp. 606-615.
- Li, Y, Oliver, DP & Kookana, RS 2018, 'A critical analysis of published data to discern the role of soil and sediment properties in determining sorption of per and polyfluoroalkyl substances (PFASs)', *Science of The Total Environment*, vol. 628-629, pp. 110-120.
- Lievens, C, Mourant, D, Gunawan, R, Hu, X & Wang, Y 2014, 'Organic compounds leached from fast pyrolysis mallee leaf and bark biochars', *Chemosphere*, vol. 139, pp. 659 – 664.
- Liu, J, Schulz, H, Brandl, S, Miehtke, H, Huwe, B & Glaser, B 2012, 'Short-term effect of biochar and compost on soil fertility and water status of a Dystric Cambisol in NE Germany under field conditions', *Journal of Plant Nutrition and Soil Science*, vol. 175, no. 5, pp. 698-707.
- Liu, Y, Blowes, DW, Ptacek, CJ & Groza, LG 2019, 'Removal of pharmaceutical compounds, artificial sweeteners, and perfluoroalkyl substances from water using a passive treatment system containing zero-valent iron and biochar', *Science of The Total Environment*, vol. 691.

- Liu, Y, Hou, X, Chen, W, Kong, W, Wang, D, Liu, J & Jiang, G 2019, 'Occurrences of perfluoroalkyl and polyfluoroalkyl substances in tree bark: Interspecies variability related to chain length', *Science of The Total Environment*, vol. 689.
- Liu, X, Zhan, g A, Ji, C, Joseph, S, Bian, R, Li, L, Pan, G, Paz-Ferreiro, J 2013, 'Biochar's effect on crop productivity and the dependence on experimental conditions—a meta-analysis of literature data', *Plant and Soil*, vol. 373, pp.583-594.
- Liu, Y, Yang, M, Wu, Y, Wang, H, Chen, Y & Wu, W 2011, 'Reducing CH₄ and CO₂ emissions from waterlogged paddy soil with biochar', *Journal of Soils and Sediments*, vol. 11, no. 6, pp. 930-939.
- Lloyd-Smith, MS, Rye 2016, *The Persistence and Toxicity of Perfluorinated Compounds in Australia*, National toxics Network, NSW, Australia.
- Loganathan, B & Bommanna 2007, 'Perfluoroalkyl sulfonates and perfluorocarboxylates in two wastewater treatment facilities in Kentucky and Georgia', *Water Research*, vol. 41, no. 20, pp. 4611-4620.
- Loganathan, B, Sajwan, KS, Sinclair, E, Kumar, KS & Kannan, K 2007, 'Perfluoroalkyl sulfonates and perfluorocarboxylates in two wastewater treatment facilities in Kentucky and Georgia', *Water Research*, vol. 41, no. 20, pp. 4611-4620.
- Lu, H, Li, Z, Fu, S, Méndez, A, Gascó, G & Paz-Ferreiro, J 2015, 'Combining phytoextraction and biochar addition improves soil biochemical properties in a soil contaminated with Cd', *Chemosphere*, vol. 119, pp. 209-216.
- Luo, L, Xu C, Chen, Z, Zhang, S 2015, 'Properties of biomass-derived biochars: Combined effects of operating conditions and biomass types', *Bioresource Technology*, vol. 192, pp.83-89.
- Martin, JW, Smithwick, MM, Braune, BM, Hoekstra, PF, Muir, DC & Mabury, SA 2004, 'Identification of long-chain perfluorinated acids in biota from the Canadian Arctic', *Environmental Science & Technology*, vol. 38, no. 2, pp. 373-380.
- Martin, SM, Kookana, RS, Van Zwieten, L & Krull, E 2012, 'Marked changes in herbicide sorption–desorption upon ageing of biochars in soil', *Journal of Hazardous Materials*, vol. 231–232, pp. 70-78.
- McNamara, JD, Franco, R, Mimna, R & Zappa, L 2018, 'Comparison of Activated Carbons for Removal of Perfluorinated Compounds From Drinking Water', *Journal - American Water Works Association*, vol. 110, no. 1, pp. E2-E14.
- Méndez, A, Paz-Ferreiro, J, Araujo, F & Gascó, G 2014, 'Biochar from pyrolysis of deinking paper sludge and its use in the treatment of a nickel polluted soil', *Journal of Analytical and Applied Pyrolysis*, vol. 107, pp. 46-52.

- Milinovic, J, Lacorte, S, Vidal, M & Rigol, A 2015, 'Sorption behaviour of perfluoroalkyl substances in soils', *Science of The Total Environment*, vol. 511, pp. 63-71.
- Mitchell, PJ, Dalley, TSL & Helleur, RJ 2013, 'Preliminary laboratory production and characterization of biochars from lignocellulosic municipal waste', *Journal of Analytical and Applied Pyrolysis*, vol. 99, pp. 71-78.
- Mitchell, PJ, Simpson, AJ, Soong R, Simpson, MJ 2015, 'Shifts in microbial community and water-extractable organic matter composition with biochar amendment in a temperate forest soil', *Soil Biology and Biochemistry*, vol. 81, pp.244-254.
- Moreno-Jiménez, E, Aceña-Heras, S, Fristak, V, Heinze, S, Marschner, B 2018, 'The effect of biochar amendments on phenanthrene sorption, desorption and mineralisation in different soils', *PeerJ*, vol.6, issue.5074.
- Morales, VL, Pérez-Reche, FJ, Hapca, SM, Hanley, KL, Lehmann, J & Zhang, W 2015, 'Reverse engineering of biochar', *Bioresource Technology*, vol. 183, pp. 163-174.
- Mukherjee, A, Zimmerman, AR & Harris, W 2011, 'Surface chemistry variations among a series of laboratory-produced biochars', *Geoderma*, vol. 163, no. 3-4, pp. 247-255.
- Müller, CE, Gerecke, AC, Alder, AC, Scheringer, M & Hungerbühler, K 2011, 'Identification of perfluoroalkyl acid sources in Swiss surface waters with the help of the artificial sweetener acesulfame', *Environmental Pollution*, vol. 159, no. 5, pp. 1419-1426.
- Murray, CC, Vatankhah, H, McDonough, CA, Nickerson, A, Hedtke, TT, Cath, TY, Higgins, CP & Bellona, CL 2019, 'Removal of per- and polyfluoroalkyl substances using super-fine powder activated carbon and ceramic membrane filtration', *Journal of Hazardous Materials*, vol. 366, pp. 160-168.
- Naile, J, Khim, JS, Wang, T, Chen, C, Luo, W, Kwon, B-O, Park, J, Koh, C-H, Jones, PD, Lu, Y & Giesy, JP 2010, 'Perfluorinated compounds in water, sediment, soil and biota from estuarine and coastal areas of Korea', *Environmental Pollution*, vol. 158, no. 5, pp. 1237-1244.
- Naile, J, Wiseman, S, Bachtold, K, Jones, PD & Giesy, JP 2012, 'Transcriptional effects of perfluorinated compounds in rat hepatoma cells', *Chemosphere*, vol. 86, no. 3, pp. 270-277.
- Nakayama, SF, Yoshikane, M, Onoda, Y, Nishihama, Y, Iwai-Shimada, M, Takagi, M, Kobayashi, Y & Isobe, T 2019, 'Worldwide trends in tracing poly- and perfluoroalkyl substances (PFAS) in the environment', *TrAC Trends in Analytical Chemistry*, In Press.
- Nethaji, S, Sivasamy, A & Mandal, AB 2013, 'Adsorption isotherms, kinetics and mechanism for the adsorption of cationic and anionic dyes onto carbonaceous particles prepared from *Juglans regia* shell biomass', *International Journal of Environmental Science and Technology*, vol. 10, no. 2, pp. 231-242.

- NICNAS 2015a, Direct precursors to perfluoroheptanesulfonate (PFHpS), perfluorohexanesulfonate (PFHxS) and perfluoropentanesulfonate (PFPeS): Environment tier II assessment, Australian Government.
- NICNAS 2015b, Perfluorobutanesulfonic acid and its direct precursors: Environment tier II assessment, Australian Government-Department of Health, NICNAS.
- Ochoa-Herrera, V & Sierra-Alvarez, R 2008, 'Removal of perfluorinated surfactants by sorption onto granular activated carbon, zeolite and sludge', *Chemosphere*, vol. 72, no. 10, pp. 1588-1593.
- OECD 2000, OECD 106 Guideline for The Testing of Chemicals Adsorption - Desorption Using A Batch Equilibrium Method, The Organisation for Economic Co-operation and Development.
- Ojeda, G, Mattana, S, Àvila, A, Alcañiz, JM, Volkmann, M & Bachmann, J 2015, 'Are soil-water functions affected by biochar application?', *Geoderma*, vol. 249-250, pp. 1-11.
- Oleszczuk, P, Joško, I & Kuśmierz, M 2013, 'Biochar properties regarding to contaminants content and ecotoxicological assessment', *Journal of Hazardous Materials*, vol. 260, pp. 375-382.
- Oliver, DP, Li, Y, Orr, R, Nelson, P, Barnes, M, McLaughlin, MJ & Kookana, RS 2019, 'The role of surface charge and pH changes in tropical soils on sorption behaviour of per- and polyfluoroalkyl substances (PFASs)', *Science of The Total Environment*, vol. 673, pp. 197-206.
- Olsen, G, Ehresman, D, Froehlich, J, Burris, J & Butenhoff, J 2005, 'Evaluation of the half-life (t_{1/2}) of elimination of perfluorooctanesulfonate (PFOS), perfluorohexanesulfonate (PFHS) and perfluorooctanoate (PFOA) from human serum', *International symposium on fluorinated alkyl organics in the environment. TOX017*. Available: <http://www.chem.utoronto.ca/symposium/fluoros/toxicology.htm> [accessed 11 December 2006], vol.
- Olsen, GW, Church, TR, Miller, JP, Burris, JM, Hansen, KJ, Lundberg, JK, Armitage, JB, Herron, RM, Medhdizadehkashi, Z & Nobiletti, JB 2003, 'Perfluorooctanesulfonate and other fluorochemicals in the serum of American Red Cross adult blood donors', *Environmental Health Perspectives*, vol. 111, no. 16, p. 1892.
- Pan, C-G, Liu, Y-S & Ying, G-G 2016, 'Perfluoroalkyl substances (PFASs) in wastewater treatment plants and drinking water treatment plants: Removal efficiency and exposure risk', *Water Research*, vol. 106, pp. 562-570.
- Paruchuri, VK, Nguyen, AV & Miller, JD 2004, 'Zeta-potentials of self-assembled surface micelles of ionic surfactants adsorbed at hydrophobic graphite surfaces', *Colloids and Surfaces A: Physicochemical and Engineering Aspects*, vol. 250, no. 1-3, pp. 519-526.
- Paul, AG, Jones, KC & Sweetman, AJ 2008, 'A first global production, emission, and environmental inventory for perfluorooctane sulfonate', *Environmental Science & Technology*, vol. 43, no. 2, pp. 386-392.

- Paz-Ferreiro, J, Lu, H, Fu, S, Méndez, A, Gascó, G 2014., 'Use of phytoremediation and biochar to remediate heavy metal polluted soils: a review', *Solid Earth*, vol. 5, pp. 65-75.
- Peterson, SC, Jackson, MA, Kim, S & Palmquist, DE 2012, 'Increasing biochar surface area: Optimization of ball milling parameters', *Powder Technology*, vol. 228, pp. 115-120.
- Poerschmann, J, Weiner, B, Wedwitschka, H, Zehnsdorf, A, Koehler, R & Kopinke, FD 2015, 'Characterization of biochars and dissolved organic matter phases obtained upon hydrothermal carbonization of *Elodea nuttallii*', *Bioresource Technology*, vol. 189, pp. 145-153.
- POPRC 2008, Risk management evaluation on Perfluorooctane sulfonate UN Persistent Organic Pollutants Review Committee Stockholm.
- Prevedouros, K, Cousins, IT, Buck, RC & Korzeniowski, SH 2006, 'Sources, fate and transport of perfluorocarboxylates', *Environmental Science & Technology*, vol. 40, no. 1, pp. 32-44.
- Punyapalakul, P, Suksomboon, K, Prarat, P & Khaodhiar, S 2013, 'Effects of Surface Functional Groups and Porous Structures on Adsorption and Recovery of Perfluorinated Compounds by Inorganic Porous Silicas', *Separation Science and Technology*, vol. 48, no. 5, pp. 775-788.
- Qian, K, Kumar, A, Zhang, H, Bellmer, D & Huhnke, R 2015, 'Recent advances in utilization of biochar', *Renewable and Sustainable Energy Reviews*, vol. 42, pp. 1055-1064.
- Qu, Y, Zhang, C, Li, F, Bo, X, Liu, G & Zhou, Q 2009, 'Equilibrium and kinetics study on the adsorption of perfluorooctanoic acid from aqueous solution onto powdered activated carbon', *Journal of Hazardous Materials*, vol. 169, no. 1-3, pp. 146-152.
- Rattanaoudom, R, Visvanathan, C & Boontanon, SK 2012, 'Removal of concentrated PFOS and PFOA in synthetic industrial wastewater by powder activated carbon and hydrotalcite', *J. Water Sustain.*, vol. 2, no. 4, pp. 245-258.
- Ray, JR, Shabtai, IA, Teixidó, M, Mishael, YG & Sedlak, DL 2019, 'Polymer-clay composite geomedia for sorptive removal of trace organic compounds and metals in urban stormwater', *Water Research*, vol. 157, pp. 454-462.
- Rees, F, Simonnot, MO & Morel, JL 2014, 'Short-term effects of biochar on soil heavy metal mobility are controlled by intra-particle diffusion and soil pH increase', *European Journal of Soil Science*, vol. 65, no. 1, pp. 149-161.
- Rehrah, D, Reddy, MR, Novak, JM, Bansode, RR, Schimmel, KA, Yu, J, Watts, DW & Ahmedna, M 2014, 'Production and characterization of biochars from agricultural by-products for use in soil quality enhancement', *Journal of Analytical and Applied Pyrolysis*, vol. 108, pp. 301-309.

- Rigét, F, Bignert, A, Braune, B, Dam, M, Dietz, R, Evans, M, Green, N, Gunnlaugsdóttir, H, Hoydal, KS, Kucklick, J, Letcher, R, Muir, D, Schuur, S, Sonne, C, Stern, G, Tomy, G, Vorkamp, K & Wilson, S 2019, 'Temporal trends of persistent organic pollutants in Arctic marine and freshwater biota', *Science of The Total Environment*, vol. 649, pp. 99-110.
- Ross, I, McDonough, J, Miles, J, Storch, P, Thelakkat Kochunarayanan, P, Kalve, E, Hurst, J, S. Dasgupta, S & Burdick, J 2018, 'A review of emerging technologies for remediation of PFASs', *Remediation Journal*, vol. 28, no. 2, pp. 101-126.
- Ruan, T, Lin, Y, Wang, T, Jiang, G & Wang, N 2015, 'Methodology for studying biotransformation of polyfluoroalkyl precursors in the environment', *TrAC Trends in Analytical Chemistry*, vol. 67, pp. 167-178.
- Shaaban, A, Se, S-M, Dimin, MF, Juoi, JM, Mohd Husin, MH, Mitan, NMM 2014, 'Influence of heating temperature and holding time on biochars derived from rubber wood sawdust via slow pyrolysis', *Journal of Analytical and Applied Pyrolysis*, vol. 107, pp. 31-39.
- Schultz, MM, Barofsky, DF & Field, JA 2006, 'Quantitative determination of fluorinated alkyl substances by large-volume-injection liquid chromatography tandem mass spectrometry characterization of municipal wastewaters', *Environmental Science & Technology*, vol. 40, no. 1, pp. 289-295.
- Senversa 2017, RAAF Base East Sale – Per- and Poly-fluoroalkyl Substances (PFAS) Investigations.
- Seo, S-H, Son, M-H, Shin, E-S, Choi, S-D & Chang, Y-S 2019, 'Matrix-specific distribution and compositional profiles of perfluoroalkyl substances (PFASs) in multimedia environments', *Journal of Hazardous Materials*, vol. 364, pp. 19-27.
- Sepulvado, JG, Blaine, A, Leick, B & Higgins, CP 2012, 'P39—Perfluorochemicals and perfluorochemical precursors in biosolids and biosolid-amended soils', *Reproductive Toxicology*, vol. 33, no. 4, p. 612.
- Shangtao, L, Jr., RP, Lin, H, Chiang, SY & Qingguo, H 2018, 'Electrochemical oxidation of PFOA and PFOS in concentrated waste streams', *Remediation Journal*, vol. 28, no. 2, pp. 127-134.
- Shaw, S, Berger, ML, Brenner, D, Tao, L, Wu, Q & Kannan, K 2009, 'Specific accumulation of perfluorochemicals in harbor seals (*Phoca vitulina concolor*) from the northwest Atlantic', *Chemosphere*, vol. 74, no. 8, pp. 1037-1043.
- Shin, H-M, Vieira, VM, Ryan, PB, Detwiler, R, Sanders, B, Steenland, K & Bartell, SM 2011, 'Environmental Fate and Transport Modeling for Perfluorooctanoic Acid Emitted from the Washington Works Facility in West Virginia', *Environmental Science & Technology*, vol. 45, no. 4, pp. 1435-1442.

- Silvani, L, Cornelissen, G, Smebye, AB, Zhang, Y, Okkenhaug, G, Zimmerman, AR, Thune, G, Sævarsson, H & Hale, SE 2019, 'Can biochar and designer biochar be used to remediate per- and polyfluorinated alkyl substances (PFAS) and lead and antimony contaminated soils?', *Science of The Total Environment*, vol., p. 133693.
- Singh, B, Singh, BP & Cowie, AL 2010, 'Characterisation and evaluation of biochars for their application as a soil amendment', *Soil Research*, vol. 48, no. 7, pp. 516-525.
- Singh, RK, Fernando, S, Baygi, SF, Multari, N, Thagard, SM & Holsen, TM 2019, 'Breakdown Products from Perfluorinated Alkyl Substances (PFAS) Degradation in a Plasma-Based Water Treatment Process', *Environ Sci Technol*, vol. 53, no. 5, pp. 2731-2738.
- Smithwick, M, Mabury, SA, Solomon, KR, Sonne, C, Martin, JW, Born, EW, Dietz, R, Derocher, AE, Letcher, RJ & Evans, TJ 2005, 'Circumpolar study of perfluoroalkyl contaminants in polar bears (*Ursus maritimus*)', *Environmental Science & Technology*, vol. 39, no. 15, pp. 5517-5523.
- Söregård, M, Kleja, DB & Ahrens, L 2019, 'Stabilization and solidification remediation of soil contaminated with poly- and perfluoroalkyl substances (PFASs)', *Journal of Hazardous Materials*, vol. 367, pp. 639-646.
- Spokas, A, Novak, JM, Stewart, CE, Cantrell, KB, Uchimiya, M, DuSaire, MG, Ro, KS 2011, 'Qualitative analysis of volatile organic compounds on biochar', *Chemosphere*, vol. 85, pp. 869-882
- Srinivasan, P & Sarmah, AK 2015, 'Characterisation of agricultural waste-derived biochars and their sorption potential for sulfamethoxazole in pasture soil: A spectroscopic investigation', *Science of The Total Environment*, vol. 502, pp. 471-480.
- Srinivasan, P, Sarmah, AK, Smernik, R, Das, O, Farid, M & Gao, W 2015, 'A feasibility study of agricultural and sewage biomass as biochar, bioenergy and biocomposite feedstock: Production, characterization and potential applications', *Science of The Total Environment*, vol. 512-513, pp. 495-505.
- Stahl, T, Heyn, J, Thiele, H, Hüther, J, Failing, K, Georgii, S & Brunn, H 2009, 'Carryover of perfluorooctanoic acid (PFOA) and perfluorooctane sulfonate (PFOS) from soil to plants', *Archives of environmental contamination and toxicology*, vol. 57, no. 2, pp. 289-298.
- Stahl, T, Mattern, D & Brunn, H 2011, 'Toxicology of perfluorinated compounds', *Environmental Sciences Europe*, vol. 23, no. 1, p. 38.
- Szabo, D, Coggan, TL, Robson, TC, Currell, M & Clarke, BO 2018, 'Investigating recycled water use as a diffuse source of per- and polyfluoroalkyl substances (PFASs) to groundwater in Melbourne, Australia', *Science of The Total Environment*, vol. 644, pp. 1409-1417.

- Tang, CY, Fu, QS, Robertson, AP, Criddle, CS & Leckie, JO 2006, 'Use of Reverse Osmosis Membranes to Remove Perfluorooctane Sulfonate (PFOS) from Semiconductor Wastewater', *Environmental Science & Technology*, vol. 40, no. 23, pp. 7343-7349.
- Tang, CY, Shiang Fu, Q, Gao, D, Criddle, CS & Leckie, JO 2010, 'Effect of solution chemistry on the adsorption of perfluorooctane sulfonate onto mineral surfaces', *Water Research*, vol. 44, no. 8, pp. 2654-2662.
- Tang, J, Zhu, W, Kookana, R & Katayama, A 2013, 'Characteristics of biochar and its application in remediation of contaminated soil', *Journal of Bioscience and Bioengineering*, vol. 116, no. 6, pp. 653-659.
- Tardiff, RG, Carson, ML, Sweeney, LM, Kirman, CR, Tan, Y-M, Andersen, M, Bevan, C & Gargas, ML 2009, 'Derivation of a drinking water equivalent level (DWEL) related to the maximum contaminant level goal for perfluorooctanoic acid (PFOA), a persistent water soluble compound', *Food and chemical toxicology*, vol. 47, no. 10, pp. 2557-2589.
- Taves, DR 1968, 'Evidence that there are two forms of fluoride in human serum', *Nature*, vol.217, pp. 1050 – 1051.
- Thomazini, A, Spokas, K, Hall, K, Ippolito, J, Lentz, R & Novak, J 2015, 'GHG impacts of biochar: Predictability for the same biochar', *Agriculture, Ecosystems & Environment*, vol. 207, pp. 183-191.
- Thompson, J, Eaglesham, G, Reungoat, J, Poussade, Y, Bartkow, M, Lawrence, M & Mueller, JF 2011, 'Removal of PFOS, PFOA and other perfluoroalkyl acids at water reclamation plants in South East Queensland Australia', *Chemosphere*, vol. 82, no. 1, pp. 9-17.
- Tomy, GT, Budakowski, W, Halldorson, T, Helm, PA, Stern, GA, Friesen, K, Pepper, K, Tittlemier, SA & Fisk, AT 2004, 'Fluorinated organic compounds in an eastern Arctic marine food web', *Environmental Science & Technology*, vol. 38, no. 24, pp. 6475-6481.
- USEPA 1996, 'Method 3050B: acid digestion of sediments, sludges, and soils. 3050B', United States Environmental Protection Agency, Washington D.C.
- USEPA 1998, 'Method 8270D Semivolatile Organic Compounds by Gas Chromatography/Mass Spectrometry (GCMS)', United States Environmental Protection Agency, Washington D.C.
- USEPA 2004, 'Method 9045D Soil and waste pH', United States Environmental Protection Agency, Washington D.C.
- USEPA 2016a, 'Drinking Water Health Advisory for Perfluorooctane Sulfonate (PFOS), Office of Water', United States Environmental Protection Agency, Washington D.C.

USEPA 2016b, 'Health Effects Support Document for Perfluorooctane Sulfonate (PFOS), Office of Water', United States Environmental Protection Agency, Washington D.C

USEPA 2017a, 'Health Effects Support Document for Perfluorooctanoic Acid (PFOA), Office of Water', United States Environmental Protection Agency, Washington D.C

USEPA 2017b, 'Data are calculated and updated regularly by OPERA [OPEn (quantitative) Structure-activity Relationship Application], a standalone free and open source command line application in Matlab (Version 8.2) providing QSAR models predictions. Model validation data set may be found here: <http://esc.syrres.com/interkow/EpiSuiteData.htm>.' U.S. Environmental Protection Agency (U.S. EPA): Chemistry Dashboard., <https://comptox.epa.gov/dashboard>, accessed 12/07/2019.

USEPA 2019, 'EPA's Per- and Polyfluoroalkyl Substances (PFAS) Action Plan', EPA 823R18004, United States Environmental Protection Agency, Washington D.C.

Uchimiya, M, Chang, S & Klasson, KT 2011, 'Screening biochars for heavy metal retention in soil: Role of oxygen functional groups', Journal of Hazardous Materials, vol. 190, no. 1-3, pp. 432-441.

Uchimiya, M, Klasson, KT, Wartelle, LH & Lima, IM 2011, 'Influence of soil properties on heavy metal sequestration by biochar amendment: 1. Copper sorption isotherms and the release of cations', Chemosphere, vol. 82, no. 10, pp. 1431-1437.

UN 2015, Proposal to list pentadecafluorooctanoic acid (CAS No: 335-67-1, PFOA, perfluorooctanoic acid), its salts and PFOA-related compounds in Annexes A, B and/or C to the Stockholm Convention on Persistent Organic Pollutants, UNEP/POPS/POPRC.11/5, pp. 1-18, United Nations - Stockholm Convention on Persistent Organic Pollutants, Rome.

UN 2017, Chemicals proposed for listing under the Convention United Nations - Stockholm Convention on Persistent Organic Pollutants, Stockholm Convention, <http://chm.pops.int/TheConvention/ThePOPs/ChemicalsProposedforListing/tabid/2510/Default.aspx>, Accessed 07/06/2019.

Vaughn, SF, Kenar, JA, Eller, FJ, Moser, BR, Jackson, MA & Peterson, SC 2015, 'Physical and chemical characterization of biochars produced from coppiced wood of thirteen tree species for use in horticultural substrates', Industrial Crops and Products, vol. 66, no. 0, pp. 44-51.

Victoria State Government 2012a, 'Draft Victorian Waste and Resource Recovery Policy', Department of Sustainability and Environment.

- Victoria State Government 2012b, 'Fuelled for growth: Investing in Victorias biofuels and bioenergy industries', Regional Development Victoria.
- Voogt, Pd & Sáez, M 2006, 'Analytical chemistry of perfluoroalkylated substances', *TrAC Trends in Analytical Chemistry*, vol. 25, no. 4, pp. 326-342.
- Wang, N, Szostek, B, Folsom, PW, Sulecki, LM, Capka, V, Buck, RC, Berti, WR & Gannon, JT 2005, 'Aerobic biotransformation of ¹⁴C-labeled 8-2 telomer B alcohol by activated sludge from a domestic sewage treatment plant', *Environmental Science & Technology*, vol. 39, no. 2, pp. 531-538.
- Wang, P, Wang, T, Giesy, JP & Lu, Y 2013, 'Perfluorinated compounds in soils from Liaodong Bay with concentrated fluorine industry parks in China', *Chemosphere*, vol. 91, no. 6, pp. 751-757.
- Wang, T, Wang, Y, Liao, C, Cai, Y & Jiang, G 2009, 'Perspectives on the Inclusion of Perfluorooctane Sulfonate into the Stockholm Convention on Persistent Organic Pollutants¹', *Environmental Science & Technology*, vol. 43, no. 14, pp. 5171-5175.
- Wang, C, Wang, Y, Herath, HSMK 2017, 'Polycyclic aromatic hydrocarbons (PAHs) in biochar – Their formation, occurrence and analysis: a review', *Organic Geochemistry*, vol. 114, pp. 1-11.
- Wang, J, Xia K, Waigi, MG, Gao, Y, Odinga, ES, Ling, W, Liu J 2018, 'Application of biochars to soil may result in plant contamination and human cancer risk due to exposure of polycyclic aromatic hydrocarbons', *Environment International*, vol. 121, pp. 169-177.
- Wiedner, K, Rumpel, C, Steiner, C, Pozzi, A, Maas, R & Glaser, B 2013, 'Chemical evaluation of chars produced by thermochemical conversion (gasification, pyrolysis and hydrothermal carbonization) of agro-industrial biomass on a commercial scale', *Biomass and Bioenergy*, vol. 59, pp. 264-278.
- Wilhelm, M, Bergmann, S & Dieter, HH 2010, 'Occurrence of perfluorinated compounds (PFCs) in drinking water of North Rhine-Westphalia, Germany and new approach to assess drinking water contamination by shorter-chained C4-C7 PFCs', *Int J Hyg Environ Health*, vol. 213, no. 3, pp. 224-232.
- Wu, M, Pan, B, Zhang, D, Xiao, D, Li, H, Wang, C & Ning, P 2013, 'The sorption of organic contaminants on biochars derived from sediments with high organic carbon content', *Chemosphere*, vol. 90, no. 2, pp. 782-788.
- Xia, W, Wan, Y, Li, Y-y, Zeng, H, Lv, Z, Li, G, Wei, Z & Xu, S-q 2011, 'PFOS prenatal exposure induce mitochondrial injury and gene expression change in hearts of weaned SD rats', *Toxicology*, vol. 282, no. 1, pp. 23-29.

- Xiao, F, Simcik, MF, Halbach, TR & Gulliver, JS 2015, 'Perfluorooctane sulfonate (PFOS) and perfluorooctanoate (PFOA) in soils and groundwater of a U.S. metropolitan area: Migration and implications for human exposure', *Water Research*, vol. 72, pp. 64-74.
- Xiao, X, Ulrich, BA, Chen, B & Higgins, CP 2017, 'Sorption of Poly- and Perfluoroalkyl Substances (PFASs) Relevant to Aqueous Film-Forming Foam (AFFF)-Impacted Groundwater by Biochars and Activated Carbon', *Environmental Science & Technology*, vol. 51, no. 11, pp. 6342-6351.
- Yan, X-L, Chen, T-B, Liao, X-Y, Huang, Z-C, Pan, J-R, Hu, T-D, Nie, C-J, Xie, H 2008, 'Arsenic transformation and volatilization during incineration of the hyperaccumulator *Pteris vittata* L.', *Environmental Science and Technology*, vol. 42, pp. 1479-1484.
- Yang, K-H, Lin, Y-C, Fang, M-D, Wu, C-H, Panchangam, SC, Hong, P-KA & Lin, C-F 2013, 'Sorption of Perfluorooctanoic Acid (PFOA) onto Sediment in the Presence of Dissolved Natural Organics', *Separation Science and Technology*, vol. 48, no. 10, pp. 1473-1478.
- Yang, Y, Meehan, B, Shah, K, Surapaneni, A, Hughes, J, Fouche, L & Paz-Ferreiro, J 2018, 'Physicochemical Properties of Biochars Produced from Biosolids in Victoria, Australia', *Int J Environ Res Public Health*, vol. 15, no. 7.
- Yargicoglu, EN, Sadasivam, BY, Reddy, KR, Spokas, K 2015, 'Physical and chemical characterization of waste wood derived biochars', *Waste Management*, vol. 36, pp.256-268.
- Yeung, LWY, Yamashita, N & Falandysz, J 2019, 'Legacy and emerging perfluorinated and polyfluorinated compounds: An update', *Chemosphere*, vol. 237, p. 124506.
- Yin, T, Chen, H, Reinhard, M, Yi, X, He, Y & Gin, KY-H 2017, 'Perfluoroalkyl and polyfluoroalkyl substances removal in a full-scale tropical constructed wetland system treating landfill leachate', *Water Research*, vol. 125, pp. 418-426.
- Yeo, JY, Chin, BLF, Tan, JK, Loh YS 2017, 'Comparative studies on the pyrolysis of cellulose, hemicellulose, and lignin based on combined kinetics', *Journal of the Energy Institute*, vol. 92, pp.27-37.
- Yu, J & Hu, J 2011, 'Adsorption of Perfluorinated Compounds onto Activated Carbon and Activated Sludge', *Journal of Environmental Engineering*, vol. 137, no. 10, pp. 945-951.
- Yu, J, Lv, L, Lan, P, Zhang, S, Pan, B & Zhang, W 2012, 'Effect of effluent organic matter on the adsorption of perfluorinated compounds onto activated carbon', *Journal of Hazardous Materials*, vol. 225–226, pp. 99-106.
- Yu, Q, Zhang, R, Deng, S, Huang, J & Yu, G 2009, 'Sorption of perfluorooctane sulfonate and perfluorooctanoate on activated carbons and resin: Kinetic and isotherm study', *Water Research*, vol. 43, no. 4, pp. 1150-1158.

- Yuan, J-H, Xu, R-K, Zhang, H 2011, 'The forms of alkalis in the biochar produced from crop residues at different temperatures', *Bioresource Technology*, vol. 102, pp. 3488-97.
- Zaggia, A, Conte, L, Falletti, L, Fant, M & Chiorboli, A 2016, 'Use of strong anion exchange resins for the removal of perfluoroalkylated substances from contaminated drinking water in batch and continuous pilot plants', *Water Research*, vol. 91, pp. 137-146.
- Zareitalabad, P, Siemens, J, Hamer, M & Amelung, W 2013, 'Perfluorooctanoic acid (PFOA) and perfluorooctanesulfonic acid (PFOS) in surface waters, sediments, soils and wastewater – A review on concentrations and distribution coefficients', *Chemosphere*, vol. 91, no. 6, pp. 725-732.
- Zavalloni, C, Alberti, G, Biasiol, S, Vedove, GD, Fornasier, F, Liu, J, Peressotti, A 2011, 'Microbial mineralization of biochar and wheat straw mixture in soil: A short-term study', *Applied Soil Ecology*, vol.50, pp. 45-51.
- Zhang, C, Peng, Y, Ning, K, Niu, X, Tan, S & Su, P 2014, 'Remediation of Perfluoroalkyl Substances in Landfill Leachates by Electrocoagulation', *CLEAN – Soil, Air, Water*, vol. 42, no. 12, pp. 1740-1743.
- Zhang, DQ, Zhang, WL & Liang, YN 2019, 'Adsorption of perfluoroalkyl and polyfluoroalkyl substances (PFASs) from aqueous solution - A review', *Science of The Total Environment*, vol. 694, p. 133606.
- Zhang, J, Wan, Y, Li, Y, Zhang, Q, Xu, S, Zhu, H & Shu, B 2011, 'A rapid and high-throughput quantum dots bioassay for monitoring of perfluorooctane sulfonate in environmental water samples', *Environmental Pollution*, vol. 159, no. 5, pp. 1348-1353.
- Zhang, W, Zhang, D & Liang, Y 2019, 'Nanotechnology in remediation of water contaminated by poly- and perfluoroalkyl substances: A review', *Environmental Pollution*, vol. 247, pp. 266-276.
- Zhao, D, Cheng, J, Vecitis, CD & Hoffmann, MR 2011, 'Sorption of Perfluorochemicals to Granular Activated Carbon in the Presence of Ultrasound', *The Journal of Physical Chemistry A*, vol. 115, no. 11, pp. 2250-2257.
- Zhao, L, Cao, X, Mašek, O & Zimmerman, A 2013, 'Heterogeneity of biochar properties as a function of feedstock sources and production temperatures', *Journal of Hazardous Materials*, vol. 256-257, pp. 1-9.
- Zhi, Y & Liu, J 2018, 'Sorption and desorption of anionic, cationic and zwitterionic polyfluoroalkyl substances by soil organic matter and pyrogenic carbonaceous materials', *Chemical Engineering Journal*, vol. 346, pp. 682-691.
- Zhou, Y, Lian, Y, Sun, X, Fu, L, Duan, S, Shang, C, Jia, X, Wu, Y & Wang, M 2019, 'Determination of 20 perfluoroalkyl substances in greenhouse vegetables with a modified one-step pretreatment approach coupled with ultra performance liquid chromatography tandem mass spectrometry(UPLC-MS-MS)', *Chemosphere*, vol. 227, pp. 470-479.

Zhu, H & Kannan, K 2019, 'Distribution and partitioning of perfluoroalkyl carboxylic acids in surface soil, plants, and earthworms at a contaminated site', *Science of The Total Environment*, vol. 647, pp. 954-961.

Zielińska, A & Oleszczuk, P 2015, 'The conversion of sewage sludge into biochar reduces polycyclic aromatic hydrocarbon content and ecotoxicity but increases trace metal content', *Biomass and Bioenergy*, vol. 75, pp. 235-244.

Appendices:

Appendix A – Published Materials

Appendices:

Appendix B – Supplementary Materials

Table S1 Table demonstrating maximum removals of PFAS in 200 mg mix mode PFAS sorption experiments to al biochars over a 48-hour period.

	PFBA (%)	PFBS (%)	PFHxA (%)	PFHxS (%)	PFOA (%)	PFOS (%)
S350	20 ± 1	20 ± 3	19 ± 4	22 ± 4	28 ± 4	57 ± 4
P350	26 ± 1	28 ± 1	28 ± 1	29 ± 1	33 ± 1	49 ± 1
S500	28 ± 7	34 ± 7	32 ± 7	56 ± 5	58 ± 5	94 ± 1
P500	15 ± 4	23 ± 3	23 ± 3	52 ± 3	58 ± 2	93 ± 1
S750	26 ± 2	35 ± 2	34 ± 1	67 ± 2	65 ± 2	95 ± 1
P750	34 ± 5	35 ± 4	46 ± 4	89 ± 1	91 ± 1	99 ± 1

Table S2 Relevant LC MS/MS Operational Conditions and Parameters

Item	Parameters
Sample Injection	10 μ L (5 μ L sample, 1 μ L 13 C, 5 μ L sample) Draw speed 400 μ L min ⁻¹ Ejected at 200 μ L min ⁻¹ Offset of 0.2 mm
13C Addition	1 μ L
Separation Column	Agilent EclipsePlusC18 - RRHD 1.8 μ m (2.1x50 mm)
Delay Column	Agilent EclipsePlusC18, 3.5 μ m (4.6x50mm)
Column environment	40°C
Multi-wash	1 - Needle (10 s – 90 % MeOH) 2 - Seat Backflush (10 s 50/50 MeOH) 3 - Needle and Seat Backflush (10 s start conditions)
Injection programme	1 - Needle wash (5 s) 2 - Sample draw 3 - needle wash (5 s), 4 - 13 C draw, 5 - Needle wash (5 s), 6 - Sample draw, 7 - Needle wash (5 s), 8 – Inject Time: 55 seconds
Solvents	Organic: Hypergrade MeOH Aqueous: H ₂ O with 5 mM NH ₄ acetate
Gradient	0 - 0.5 mins start condition (40 % MeOH) 0.5 - 3 mins ramp to 100 % MeOH 3 – 5.5 mins system at 100 % MeOH 5.5 mins end run
Source conditions	Gas temp: 250°C Flow: 11 l/min Nebulizer: 25 psi
Ionisation	Negative electrospray ionization
Sheath	Sheath gas 375°C Sheath gas flow 11 L/min
Capillary	Capillary pos 3500V neg
iFunnel	2500V chamber current 0.18 μ A High Pressure RF (negative) 90V Low Pressure RF (negative)100V
Detection mode	Dynamic Multiple Reaction Monitoring
Total run time:	6.5 mins per sample

Table S3 Transitions and retention times for selected ¹³C and native PFAS used in experiment by LC MS/MS operational conditions and parameters outlined in Table S1

Compound Name	ISTD?	Precursor Ion	Product Ion	Threshold	Ret Time (min)	Delta Ret Time	Fragment or	Collision Energy	Cell Accelerator Voltage	Polarity
PFBA-13C3	TRUE	216	172	10734	2	0.5	380	8	2	Negative
PFBS	FALSE	299	99	3828	2.36	0.97	380	36	2	Negative
PFBS	FALSE	299	83	481	2.36	0.97	380	32	2	Negative
PFBS	FALSE	299	80	8811	2.36	0.97	380	44	2	Negative
PFBS-13C2	TRUE	302	99	12702	2.28	0.5	380	36	2	Negative
PFHxA	FALSE	313	269	15050	2.93	0.97	380	6	2	Negative
PFHxA	FALSE	313	119	700	2.93	0.97	380	22	2	Negative
PFHxA-13C2	TRUE	314.9	269.9	5145	2.93	0.88	380	8	2	Negative
PFHxS	FALSE	399	119	623	3.32	1.02	380	44	2	Negative
PFHxS	FALSE	399	99	2879	3.32	1.02	380	44	2	Negative
PFHxS	FALSE	399	80	4771	3.32	1.02	380	48	2	Negative
PFHxS-13C3	TRUE	402	99	895	2.73	0.5	380	44	2	Negative
PFOA	FALSE	413	368.9	12641	3.55	1.07	380	6	2	Negative
PFOA	FALSE	413	169	2279	3.55	1.07	380	18	2	Negative
PFOA-13C8	TRUE	421	376	3825	3	0.5	380	6	2	Negative
PFOS	FALSE	498.9	99	2011	3.73	1.12	380	56	2	Negative
PFOS	FALSE	498.9	80	4548	3.73	1.12	380	56	2	Negative
PFOS - 13C4	TRUE	503	99	12702	3.27	0.5	380	48	2	Negative
PFBA	FALSE	213	169	12702	0.9	1.03	380	6	2	Negative

Table S4 First Order experimental rate constants and R² for each Biochar PFAS-biochar pair studied in individual and mix mode at 5 µg/L.

Individual Mode												
Biochar	PFHxA			PFHxS			PFOA			PFOS		
	Q_e (ug/g)	K₁ (h)	R²	Q_e (ug/g)	K₁ (h)	R²	Q_e (ug/g)	K₁ (h)	R²	Q_e (ug/g)	K₁ (h)	R²
P500	0.06	3.72	0.93	0.09	2.22	0.94	0.19	2.42	0.96	0.34	3.68	0.98
S500	0.05	41.83	0.00	0.07	4.81	0.74	0.14	5.31	0.83	0.31	4.83	0.97
P750	0.09	39.38	0.98	0.18	3.99	0.97	0.31	31.89	0.96	0.37	34.37	0.97
S750	0.06	25.80	0.96	0.11	3.89	0.99	0.20	5.30	0.99	0.33	5.10	0.99

Mix mode												
Biochar	PFHxA			PFHxS			PFOA			PFOS		
	Q_e (ug/g)	K₁ (h)	R²	Q_e (ug/g)	K₁ (h)	R²	Q_e (ug/g)	K₁ (h)	R²	Q_e (ug/g)	K₁ (h)	R²
P500	0.03	3.23	0.87	0.13	2.06	0.92	0.19	4.53	0.99	0.08	8.41	0.97
S500	0.02	3.13	0.39	0.17	0.05	0.60	0.18	29.63	0.98	0.08	14.31	0.96
P750	0.11	2.64	0.86	0.34	5.99	0.96	0.36	5.82	0.99	0.15	5.36	0.99
S750	0.04	8.22	0.85	0.18	4.61	0.87	0.23	21.31	0.98	0.11	19.17	0.99

Table S5 Constants for Intraparticle Diffusion models for each PFAS-biochar pair studied in individual mode in 5 µg/L PFAS solutions over timepoints ranging 0 - 48 hours.

	Biochar	Film Diffusion			Intra Particle Diffusion			Equilibrium		
		K ₁ (h ^{0.5})	C ₁	R ²	K ₁ (h ^{0.5})	C ₂	R ²	K ₁ (h ^{0.5})	C ₃	R ²
PFHxA	P500	0.04	0.00	1.00	0.00	0.03	0.45	0.01	0.02	0.52
	S500	0.03	0.00	1.00	-	-	-	0.00	0.01	0.61
	P750	0.11	0.00	1.00	-	-	-	0.02	0.04	0.79
	S750	0.06	0.00	1.00	-	-	-	0.00	0.05	0.85
PFHxS	S500	0.10	0.00	1.00	-	-	-	0.02	0.03	0.78
	P500	0.11	0.00	1.00	0.00	0.12	0.55	0.01	0.09	0.62
	S750	0.23	0.00	1.00	-	-	-	0.01	0.14	0.90
	P750	0.46	0.00	1.00	0.00	0.33	0.98	0.03	0.29	0.70
PFOA	S500	0.27	0.00	1.00	-	-	-	0.00	0.18	0.05
	P500	0.16	0.02	1.00	0.00	0.18	0.54	0.02	0.16	0.88
	S750	0.36	0.00	1.00	-	-	-	0.00	0.23	0.88
	P750	0.48	0.00	1.00	0.00	0.36	0.98	0.03	0.32	0.99
PFOS	S500	0.12	0.00	1.00	-	-	-	0.00	0.08	0.14
	P500	0.11	0.00	1.00	-	-	-	0.00	0.07	0.72
	S750	0.15	0.00	1.00	-	-	-	0.00	0.11	0.95
	P750	0.20	0.00	1.00	0.00	0.15	0.99	0.01	0.14	0.99

Table S6 Constants for Intraparticle Diffusion models for each PFAS-biochar pair studied in 5 µg/L PFAS mix mode experiments, over timepoints ranging 0 - 48 hours.

	Biochar	Film Diffusion			Intra Particle Diffusion			Equilibrium		
		K ₁ (h ^{0.5})	C ₁	R ²	K ₂ (h ^{0.5})	C ₂	R ²	K ₃ (h ^{0.5})	C ₃	R ²
PFHxA	P500	0.04	0.00	1.00	0.01	0.02	0.52	0.00	0.03	0.45
	S500	0.03	0.00	1.00	-	-	-	0.00	0.01	0.61
	P750	0.11	0.00	1.00	-	-	-	0.02	0.04	0.79
	S750	0.06	0.00	1.00	-	-	-	0.00	0.05	0.85
PFHxS	S500	0.10	0.00	1.00	-	-	-	0.02	0.03	0.78
	P500	0.11	0.00	1.00	0.01	0.09	0.62	0.00	0.12	0.55
	S750	0.23	0.00	1.00	-	-	-	0.01	0.14	0.90
	P750	0.46	0.00	1.00	0.03	0.29	0.70	0.00	0.33	0.98
PFOA	S500	0.27	0.00	1.00	-	-	-	0.00	0.18	0.05
	P500	0.16	0.02	1.00	0.02	0.16	0.88	0.00	0.18	0.54
	S750	0.36	0.00	1.00	-	-	-	0.00	0.23	0.88
	P750	0.48	0.00	1.00	0.03	0.32	0.99	0.00	0.36	0.98
PFOS	S500	0.12	0.00	1.00	-	-	-	0.01	0.08	0.14
	P500	0.11	0.00	1.00	-	-	-	0.01	0.07	0.72
	S750	0.15	0.00	1.00	-	-	-	0.00	0.11	0.95
	P750	0.20	0.00	1.00	0.01	0.14	0.99	0.00	0.15	0.99

Table S7 Isotherm constants for fitted individual mode PFAS experimental data.

	PFHxA				PFHxS				PFOA				PFOS			
Freundlich	1/n	K _f	-	R ²	1/n	K _f	-	R ²	1/n	K _f	-	R ²	1/n	K _f	-	R ²
P500	0.12	0.03	-	0.58	0.36	0.07	-	0.97	1.34	0.07	-	0.96	1.83	0.49	-	0.95
S500	0.31	0.02	-	0.74	0.24	0.05	-	0.99	0.86	0.07	-	0.97	1.20	0.23	-	0.98
P750	0.10	0.08	-	0.56	0.71	0.35	-	0.96	1.32	0.48	-	0.98	4.67	21.02	-	0.95
S750	0.73	0.02	-	0.87	0.73	0.09	-	0.90	1.43	0.04	-	0.98	1.49	0.28	-	0.99
Langmuir	q _{max}	K _L	-	R ²	q _{max}	K _L	-	R ²	q _{max}	K _L	-	R ²	q _{max}	K _L	-	R ²
P500	0.05	0.83	-	0.61	0.13	1.73	-	0.98	0.79	0.16	-	0.84	0.26	2.22	-	0.47
S500	0.05	0.82	-	0.73	0.07	3.61	-	1.00	0.36	0.31	-	0.92	0.26	1.47	-	0.81
P750	0.19	0.33	-	0.86	0.81	0.73	-	0.97	2.22	0.23	-	0.90	0.32	2.67	-	0.31
S750	0.08	0.36	-	0.81	0.39	0.34	-	0.92	0.18	1.50	-	0.50	0.24	2.07	-	0.58
Sigmoidal	q _{max}	K _L	S	R ²	q _{max}	K _L	S	R ²	q _{max}	K _L	S	R ²	q _{max}	K _L	S	R ²
P500	0.04	9.37	10.43	0.59	0.13	1.77	0.00	0.98	1.60	0.15	2.35	0.96	1.85	5.32	15.34	0.96
S500	0.04	9.35	10.45	0.71	0.07	3.61	0.00	1.00	0.40	0.39	1.22	0.94	0.56	0.95	0.54	0.98
P750	0.42	0.13	1.31	0.98	0.42	3.21	0.12	0.99	0.93	14.37	12.44	0.99	6.86	3.70	17.41	0.66
S750	0.10	0.31	1.11	0.86	0.21	4.46	3.50	0.94	0.34	2.32	13.69	0.90	1.38	0.65	1.56	0.99
SIPs	K _L	q _{max}	n	R ²	K _L	q _{max}	n	R ²	K _L	q _{max}	n	R ²	K _L	q _{max}	n	R ²
P500	0.08	0.07	0.60	0.69	1.06	0.15	1.28	0.98	0.09	0.78	0.55	0.96	14.39	0.37	0.24	0.99
S500	0.13	0.06	0.56	0.76	1.23	0.10	1.90	0.99	0.11	0.64	0.92	0.96	0.74	0.51	0.65	0.98
P750	0.05	0.55	0.79	0.99	4.73	0.37	0.69	0.99	1.64	0.77	0.46	0.99	3.85	6.61	0.21	0.95
S750	0.29	0.10	1.22	0.82	1.23	0.19	0.51	0.94	4.62	0.17	7.98	0.31	0.55	0.79	0.53	0.99

BET	q_{\max}	K_{BET}	C_s	R^2	q_{\max}	K_{BET}	C_s	R^2	q_{\max}	K_{BET}	C_s	R^2	q_{\max}	K_{BET}	C_s	R^2
P500	0.04	9.09	22.55	0.68	0.09	32.48	11.02	0.97	1.12	0.68	11.06	0.96	0.99	0.57	2.56	0.90
S500	0.04	9.07	22.52	0.76	0.06	28.69	11.24	0.90	0.30	4.63	18.00	0.97	0.66	0.90	3.64	0.98
P750	0.06	7.13	7.64	0.99	0.32	10.13	3.97	0.97	2.42	3.17	16.36	0.93	3.32	2.22	16.43	0.44
S750	0.06	1.66	11.68	0.95	0.25	8.81	15.99	0.91	0.38	3.64	17.50	0.91	1.70	2.63	17.54	0.92
Toth	$Q_{e^{\infty}}$	K_{th}	Th	R^2	$Q_{e^{\infty}}$	K_{th}	Th	R^2	$Q_{e^{\infty}}$	K_{th}	Th	R^2	$Q_{e^{\infty}}$	K_{th}	Th	R^2
P500	0.04	10.00	10.00	0.55	0.15	0.58	0.74	0.98	0.26	14.10	3.31	0.77	0.37	27.39	22.72	0.79
S500	0.04	10.00	10.00	0.69	0.08	0.30	0.63	1.00	0.19	13.82	3.59	0.84	0.27	23.81	12.66	0.97
P750	0.83	14.45	0.86	0.97	0.32	0.17	3.08	0.98	0.52	31.28	24.80	0.94	0.62	11.00	7.70	0.44
S750	0.05	102.56	63.95	0.67	0.38	3.75	1.13	0.92	0.20	13.51	3.52	0.67	0.29	38.83	23.73	0.92
Radke-Prausnitz	K_{rp}	k_{rp}	p	R^2	K_{rp}	k_{rp}	p	R^2	K_{rp}	k_{rp}	p	R^2	K_{rp}	k_{rp}	p	R^2
P500	0.00	2.03	1.23	N/A	0.00	0.00	1.85	N/A	0.00	0.00	1.84	N/A	0.40	220.46	0.13	0.99
S500	0.00	4.86	0.04	N/A	0.00	0.00	1.73	N/A	0.00	0.00	2.19	N/A	0.44	0.46	0.73	0.97
P750	0.00	480.95	4021.50	N/A	0.72	0.60	6718.99	0.97	0.47	3929.35	0.11	1.00	30.06	22.76	0.21	0.94
S750	0.00	0.23	1.25	N/A	0.00	0.00	1.53	N/A	0.00	0.00	2.06	N/A	0.49	0.66	0.51	0.99
Redlich-Peterson	K_r	a_r	beta	R^2	K_r	a_r	beta	R^2	K_r	a_r	beta	R^2	K_r	a_r	beta	R^2
P500	0.02	2.15	0.00	0.70	0.20	1.49	1.05	0.98	0.24	1.50	0.00	0.92	0.58	0.80	0.00	0.79
S500	0.03	1.03	0.54	0.76	0.19	2.23	1.14	1.00	0.18	1.70	0.21	0.97	0.37	0.77	0.00	0.97
P750	0.09	1.97	0.00	0.99	0.57	0.95	2.36	0.98	0.68	0.53	0.00	0.94	0.45	0.00	0.03	0.44
S750	0.03	1.32	0.09	0.92	0.10	0.00	6.29	0.98	0.18	1.72	0.00	0.94	0.48	0.93	0.00	0.92

Note: Where units are $K_r: (\text{ug/g})/(\text{ug/L})^{1/n}$, $q_{\max}: \text{ug/g}$, $K_L: \text{L/ug}$, $b: \text{L/ug}$, $K_L: \text{L/ug}$, $C_s: \text{ug/L}$, $Q_{e^{\infty}}: \text{ug/g}$, $K^{\text{th}}: (\text{ug/l})^{\text{Th}}$, $K_{\text{rp}}: K_{\text{rp}}$, $k_{\text{rp}}: (\text{ug/g})/(\text{ug/L})^{(1/p)}$, $K_r: \text{L/ug}$, $a_r: \text{L/ug}$

Table S8 Isotherm constants for fitted 5 µg/L mix mode experimental data.

	PFHxA				PFHxS				PFOA				PFOS			
Freundlich	1/n	K _f	-	R ²	1/n	K _f	-	R ²	1/n	K _f	-	R ²	1/n	K _f	-	R ²
P500	1.20	0.00	-	0.65	1.17	0.04	-	0.94	0.32	0.08	-	0.60	1.01	0.14	-	0.88
S500	0.50	0.01	-	0.35	0.45	0.05	-	0.96	0.42	0.07	-	0.97	1.08	0.13	-	0.94
P750	0.16	0.03	-	0.95	1.02	0.31	-	0.99	1.79	0.22	-	0.83	6.16	55.48	-	0.91
S750	0.09	0.02	-	0.94	0.76	0.08	-	0.98	0.67	0.07	-	0.96	1.98	0.37	-	0.99
Langmuir	q _{max}	K _L	-	R ²	q _{max}	K _L	-	R ²	q _{max}	K _L	-	R ²	q _{max}	K _L	-	R ²
P500	0.02	9.73	-	0.50	0.09	4.82	-	0.52	0.13	3.83	-	0.54	0.88	0.23	-	0.79
S500	0.07	0.06	-	0.36	0.13	0.76	-	0.97	0.18	0.49	-	0.98	1.06	0.18	-	0.86
P750	0.04	9.59	-	0.92	0.35	2.01	-	0.78	1.54	0.22	-	0.91	2.41	0.18	-	0.32
S750	0.03	0.49	-	0.97	0.38	0.28	-	0.98	0.34	0.23	-	0.97	1.41	0.21	-	0.76
Sigmoidal	q _{max}	K _L	S	R ²	q _{max}	K _L	S	R ²	q _{max}	K _L	S	R ²	q _{max}	K _L	S	R ²
P500	0.02	9.04	10.71	0.53	0.22	3.17	13.86	0.92	0.16	6.68	11.82	0.71	0.71	3.56	14.04	0.93
S500	0.01	9.11	10.65	0.34	0.09	15.22	8.83	0.96	0.14	7.08	11.64	0.98	0.75	2.84	14.17	0.98
P750	0.04	3.92	0.24	0.94	0.74	0.96	0.33	1.00	0.79	8.89	12.53	1.00	6.13	3.46	18.15	0.50
S750	0.04	0.43	1.12	0.99	0.38	0.28	0.00	0.98	0.22	0.80	1.25	0.98	2.54	2.69	15.83	0.98
SIPs	K _L	q _{max}	n	R ²	K _L	q _{max}	n	R ²	K _L	q _{max}	n	R ²	K _L	q _{max}	n	R ²
P500	0.14	0.02	0.47	0.59	0.12	0.39	0.70	0.93	0.31	0.15	0.31	0.73	0.29	0.52	0.27	0.97
S500	0.12	0.02	0.58	0.36	0.63	0.14	1.13	0.97	0.58	0.15	0.66	0.99	0.22	0.58	0.37	0.99
P750	5.71	0.04	0.16	0.91	1.23	0.56	0.64	0.99	3.85	0.47	0.23	0.95	5.78	10.99	0.16	0.91
S750	0.22	0.03	0.68	0.99	0.41	0.29	0.89	0.98	0.39	0.21	0.66	0.98	0.27	1.70	0.45	0.99

BET	q_{max}	K_{BET}	C_s	R²	q_{max}	K_{BET}	C_s	R²	q_{max}	K_{BET}	C_s	R²	q_{max}	K_{BET}	C_s	R²
P500	0.02	8.49	18.05	0.59	0.25	3.78	16.94	0.92	0.16	81.70	87.45	0.64	0.90	2.63	15.92	0.87
S500	0.01	8.58	18.37	0.36	0.10	12.71	16.29	0.94	0.13	14.72	22.32	0.96	0.85	3.07	17.80	0.93
P750	0.26	1.08	25.27	0.27	1.51	3.52	16.32	0.98	3.15	0.95	11.78	0.96	15.84	0.00	0.57	0.88
S750	0.74	0.63	89.55	0.99	0.23	7.58	15.98	0.98	0.64	1.05	17.97	0.76	1.41	0.61	4.19	0.90
Toth	Q_{e[∞]}	K_{th}	Th	R²	Q_{e[∞]}	K_{th}	Th	R²	Q_{e[∞]}	K_{th}	Th	R²	Q_{e[∞]}	K_{th}	Th	R²
P500	0.02	10.00	10.00	0.50	0.13	11.01	3.12	0.86	0.17	1.12	0.95	0.65	2.64	71.74	1.48	0.88
S500	0.01	10.00	10.00	0.34	0.13	1.26	0.93	0.97	0.27	1.27	0.56	0.98	0.95	15.28	1.52	0.91
P750	0.04	5.85	15.65	0.91	0.37	5.41	10.98	0.99	0.56	13.86	4.33	0.94	0.51	10.39	10.48	0.33
S750	0.09	56.16	1.47	1.00	0.14	12.80	5.43	0.98	1.33	2.54	0.42	0.96	0.34	15.75	12.58	0.81
Radke-Prausnitz	K_{rp}	k_{rp}	p	R²	K_{rp}	k_{rp}	p	R²	K_{rp}	k_{rp}	p	R²	K_{rp}	k_{rp}	p	R²
P500	0.05	0.00	3.57	N/A	0.00	2.04	1.16	N/A	0.00	2.02	1.24	N/A	0.15	2.20	1.10	0.85
S500	0.00	4.86	0.04	N/A	0.00	0.00	2.08	N/A	0.00	4.86	0.04	N/A	0.14	4.86	0.04	0.99
P750	0.00	0.00	2.19	N/A	0.31	0.00	ND	N/A	0.29	ND	3998	0.95	0.41	482.54	4021.50	0.23
S750	0.00	0.15	1.34	N/A	0.44	0.00	1.11	N/A	0.00	0.12	1.32	N/A	1.51	0.48	0.46	0.98
Redlich-Peterson	K_r	a_r	beta	R²	K_r	a_r	beta	R²	K_r	a_r	beta	R²	K_r	a_r	beta	R²
P500	0.01	2.12	0.00	0.63	0.14	1.84	0.00	0.93	0.05	0.00	4.20	0.88	0.33	1.36	0.00	0.88
S500	0.01	1.03	0.00	0.37	0.14	1.58	0.80	0.97	0.11	0.75	0.88	0.98	0.24	0.74	0.00	0.94
P750	0.05	0.78	1.15	0.91	0.50	0.62	0.00	0.99	0.47	0.63	0.00	0.96	0.64	0.57	0.00	0.33
S750	0.01	1.32	0.23	1.00	0.16	0.96	0.48	0.98	0.13	1.01	0.54	0.96	0.52	0.91	0.00	0.81

Note: Where units are $K_F: (\text{ug/g})/(\text{ug/L})^{1/n}$, $q_{\text{max}}: \text{ug/g}$, $K_L: \text{L/ug}$, $b: \text{L/ug}$, $K_L: \text{L/ug}$, $C_s: \text{ug/L}$, $Q_e^\infty: \text{ug/g}$, $K^{\text{th}}: (\text{ug/l})^{\text{th}}$, $K_{rp}: K_{rp}$, $k_{rp}: (\text{ug/g})/(\text{ug/L})^{(1/p)}$, $K_r: \text{L/ug}$, $a_r: \text{L/ug}$